Protein particles for structuring in very low fat mayonnaise

By

Peter William Young

A thesis submitted to

The University of Birmingham

For the degree of

DOCTOR OF PHILOSOPHY

Department of Chemical Engineering

College of Physical and Engineering Sciences

The University of Birmingham

July 2020

Abstract

This thesis aims to further understanding of protein fluid gels and their potential for use in reduced fat products. Previous research on fluid gels has shown their potential for fat replacement in semi-solid foods, and protein fluid gels have been used for the stabilization of foams. This thesis will investigate processing methods for and the influence of pH on the production of protein fluid gels, determining how this influences the fluid gel properties.

Initially, protein fluid gels produced from egg white were compared with those produced from WPI as protein fluid gels have been produced previously from WPI. These were produced through heating under shear. Rheology and soft tribology were used to investigate the properties of these fluid gels. As proteins have different net charges at different pH levels relative to the isoelectric point (pI), the influence of pH on fluid gel properties was investigated. Fluid gels produced at the pI were shown to produce aggregated particles of less than 1 μm diameter. These systems produced at the pI demonstrated greater friction values in the mixed and boundary regimes of lubrication. Egg fluid gels offer a new functional ingredient for food products, in particular products such as mayonnaises and dressings in which egg is already an ingredient.

Following on from this, dry protein fluid gel particles were produced from WPI through spray drying, and the properties of suspensions for these particles were investigated. To further understand the potential of these systems for use in reduced fat products, properties of emulsions stabilized by these particles were investigated and compared with a full fat mayonnaise and an emulsion stabilized by commercially available Simplesse™.

The greatest loss of solubility through processing of WPI was observed at pH 3.5. At pH 3.5, particles with an average size of 22.9 ± 2.0 μm upon dispersion were produced. Addition of

salts after particle production showed no effect on suspension rheology, demonstrating the potential for use in reduced fat dressings or mayonnaises in which salt is an ingredient.

Both the particles and soluble protein were shown to be surface active. Emulsions stabilized by 20% spray-dried WPI in the aqueous phase were stable and showed similar rheology with increasing oil contents with oil droplets shown to contribute to the structuring of suspensions. Protein particles are shown to contribute to the structure of reduced fat emulsions.

Acknowledgements

I would like to thank my supervisors Prof. Ian Norton and Dr Tom Mills for their support and guidance throughout my project, helping me to develop as a researcher.

I thank Bakkavor salads for funding this project and allowing the publication of results in peer-reviewed journals, in particular, Debbie Park, Sue Feuerhelm and Sarah Dawson for discussions throughout my project.

Special thanks to everyone within the Microstructure group, Department of Chemical Engineering, University of Birmingham, for making the PhD experience; it would not have been the same without you.

I would like to thank my parents for supporting me in all of my endeavours. Thank you to Bex for her support throughout.

Table of contents

List of figures

List of tables

List of abbreviations

ALR – atomization gas–liquid–mass ratio

BSA – Bovine serum albumin

DIC – Differential interference contrast

DNA – Deoxyribonucleic acid

DSC – Differential scanning calorimetry

EHL – Elasto-hydrodynamic lubrication

FTIR – Fourier transform infrared

HLB – Hydrophilic–lipophilic balance

HLD – Hydrophile–lipophile deviation

Hz – Hertz

kDa – Kilodaltons

LVR – Linear viscoelastic region

mMol – Millimolar

MTM – Mini traction machine

mV – Millivolts

NMR – Nuclear magnetic resonance

O/W – Oil in water

PDMS – polydimethylsiloxane

pI – Isoelectric point

PTFE – Polytetrafluoroethylene

SEM – Scanning electron microscopy

SLS – Static light scattering

SRR – Slide–roll ratio

UV – Ultraviolet

W/O – Water in oil

W/O/W – Water in oil in water

WPI – Whey protein isolate

Symbols

Symbol	Definition	Unit
A_a	Apparent area of contact	m^2
A_r	Real area of contact	m^2
D(4,3)	Volume weighted mean	μm
ΔG_u	Free energy of unfolding	Joules
E_{det}	Energy of detachment	Joules
F_t	Tangential friction force	N
γ	Interfacial tension	mN m^{-1}
g	Acceleration due to gravity	m s^{-2}
η	Viscosity	Pa.s
η_c	Continuous phase viscosity	Pa.s
N_{so}	Sommerfield number	-
P	Viscosity ratio	-
pKa	Acid dissociation constant	pH
Φ	Phase volume	-
Φ_m	Maximum phase volume	-
Θ	Contact angle	^{o}
U	Speed	m s^{-1}
W	Load	N

CHAPTER 1.
Introduction

1.1. Background

Fats are an important component in many foods, and they contribute to the desirable creamy textures and structure of these foods (Norton and Norton, 2010). However, with increasing consumer awareness of health and increasing obesity levels throughout the world, food manufacturers are coming under pressure from governments to reduce the calorie content of foods. There is further pressure for this to be achieved using natural ingredients. The introduction of taxes on unhealthy foods was first implemented in Hungary with a tax on sugary foods, followed by other countries after its success achieving a sustained reduction in consumption of target products (World Health Organization, 2015). In the UK, the government implemented its own 'health tax' in 2018 with the introduction of the 'sugar tax' for soft drinks with high sugar contents. With the success shown in Hungary of taxing unhealthy foods, further government regulations for high-calorie-content foods, such as mayonnaises, can be expected. However, whilst there is pressure to make foods healthier, consumers still want these products to maintain the textural properties of their full fat counterparts.

Maintaining the desirable texture of these products whilst reducing fat requires a structural approach combining both formulation and processing techniques (Norton and Norton, 2010). An example of combining processing and formulation for the replacement of fat in emulsions is fluid gels. These are suspensions of soft gelled particles produced by gelation in a shear field (Norton *et al.*, 1998). The properties of these systems can be manipulated through changes in processing (shear rates and temperature rates) and formulation (gelling material, co-solutes and cross-linkers) (Fernández Farrés and Norton, 2015; Garrec *et al.*, 2013). These systems have been engineered to behave in a similar manner to emulsions. They have similar rheology to full fat mayonnaises, exhibiting yield stress and shear thinning behaviour (Norton

et al., 2013), and behave as a solid at rest but flow under shear. These soft gelled particles act to lubricate during oral processing, contributing to a desirable creamy texture (Malone *et al*., 2003a).

Fluid gels have been successfully produced from whey protein isolate (WPI) (Lazidis *et al*., 2016). WPI is available in commercial fat replacers also, for example *Simplesse*® (CP Kelco) and *Dairy Lo*® (Pfizer). *Simplesse*® is WPI particles of diameter 0.1–3μm produced through rapid heating of WPI at pH 2 in the presence of lecithin or other aggregation-blocking agents in a high shear field to reduce the aggregation of particles of denatured protein. Discrete particles of egg white have also been produced through the desalting of salted eggs; these particles also showed potential for the replacement of oil in mayonnaises (Wang *et al*., 2015).

Proteins offer advantages in the replacement of fats with their desirable nutritional contribution to final products. However, proteins are sensitive to pH: the net charge of proteins is influenced by pH as the charge of individual amino acid residues changes. Mayonnaises have an acidic pH, and thus this pH dependence of proteins is important for use in these products.

1.2. Industrial relevance

Bakkavor salads is the industrial sponsor of this project. Bakkavor was founded in 1986 in Iceland by the Gudmundsson brothers. They now have more than 18,000 employees working in freshly prepared food, mainly based in the UK, USA and China, producing ready meals, soups, sauces, prepared salads, dips and sandwiches. Dips, condiments and coleslaws based on mayonnaise have a high fat content. With increasing levels of obesity and associated health conditions, there is increased pressure from both governments and consumers to provide healthier alternatives.

These convenience foods are becoming increasingly popular (Bruner *et al*., 2010). However, these foods contribute to high levels of fats, salt and sugar in diets. These ingredients have been linked to the increasing rates of obesity and the associated health conditions worldwide, including high blood pressure, type 2 diabetes mellitus and cardiovascular disease. Owing to these factors, producers are under pressure to produce reduced fat alternatives. However, reduced fat foods come with negative connotations associated with inferior taste and texture (Hamilton *et al*., 2000).

There is increasing consumer pressure for this fat reduction to be achieved using 'clean label' ingredients. As proteins are an essential part of a balanced diet and naturally occur, they offer a promising clean label ingredient.

Ultimately, as producers of high fat convenience foods and as increasing government and consumer pressure demands healthier foods without compromising flavour and texture, the development of new systems for fat replacement is beneficial to Bakkavor. Embracing the change in consumer demand for healthier convenience foods will enable the company to develop with the changing trends.

1.3. Objectives

Given the nutritional advantage proteins offer for the replacement of oil and the potential shown for the use of fluid gels in low fat foods protein fluid gels offer an exciting option for fat reduction. However, the influence of pH on these systems and the potential for their use in acidic products requires further investigation. This thesis aims to develop understanding of the potential for protein fluid gels in low fat foods and methods for the production of dry fluid gel powders.

To achieve this, fluid gels were produced from egg white and WPI at different pH using traditional sheared gelation methods. WPI was then used to develop an alternative technique for the production of dry fluid gel particles using spray drying. These suspensions were analysed by various analytical techniques, including rheology and soft tribology.

Further to this, the influence of salts on particle formation and suspension properties of particles produced by spray drying was investigated. Understanding of the influence of salts on these particles is important; salt is in an ingredient in these foods, and calcium ions are also found in hard water.

A full fat mayonnaise and Simplesse® were used to represent a full fat product and commercially available protein particulate thickener, respectively, for comparison. The rheology and tribology of emulsions stabilized by the dry particles produced in this thesis were compared with these systems.

1.4. Thesis layout

This thesis is presented with each chapter standing as its own body of work reading similar to a research paper. Instead of a single materials and methods chapter, each chapter has its own material and methods section. Each experimental chapter has a short introduction to the body of work and explains how it follows on from the previous chapter.

Chapter 2 is a literature review, reviewing the relevant literature on soft particles as fat mimetics and the methods used to relate texture to sensory properties during oral processing, justifying the use of soft tribology throughout this thesis.

Chapter 3 is the first of the results chapters and looks at the potential for production of fluid gels from egg white proteins. This is compared with the previously characterized systems of WPI fluid gels. The influence of pH on the textural properties of these fluid gels is investigated using rheology and tribology to further understand the textures of these fluid gels.

Chapter 4 follows on from the potential that WPI fluid gels showed in Chapter 3 for use as a fat mimetic. In this chapter, a new method for the production of dry protein particles is investigated using spray drying. How pH and salts can be used to manipulate this process is investigated. The advantage of a dry protein particle powder is that it can be dispersed in current manufacturing facilities without the requirement for heating and cooling in shear, which is required for traditional preparation of protein fluid gels.

Chapter 5 further investigates the emulsion-stabilizing properties of WPI particles produced by spray drying and the properties of emulsions produced are investigated. These emulsions are then compared with full fat mayonnaise and commercially available WPI particles.

Chapter 6 is a short chapter briefly touching on the scale-up potential of egg white fluid gel production and production of WPI particles.

Chapter 7 presents the conclusions of this thesis and recommendations for future work.

1.5. Presentations and publications

Publication

- Young, P. W., Mills, T. B. & Norton, I. T. 2020. Influence of pH on fluid gels produced from egg and whey protein isolate. Food Hydrocolloids 111, 106108

Poster presentation

- Young, P. W., Mills, T. B. & Norton, I. T. 2019. The influence of pH on egg white fluid gels. 8th International Symposium on Food Rheology and Structuring (ISFRS), Zurich, 2019

1.6. References

BRUNNER, T.A., VAN DER HORST, K. and SIEGRIST, M., 2010. Convenience food products. Drivers for consumption. *Appetite, 55*(3), pp.498-506.

FERNÁNDEZ FARRÉS, I. & NORTON, I. T. 2015. The influence of co-solutes on tribology of agar fluid gels. *Food Hydrocolloids,* 45**,** 186-195.

GARREC, D. A., GUTHRIE, B. & NORTON, I. T. 2013. Kappa carrageenan fluid gel material properties. Part 1: Rheology. *Food Hydrocolloids,* 33**,** 151-159.

HAMILTON, J., KNOX, B., HILL, D. & PARR, H. 2000. Reduced fat products–Consumer perceptions and preferences. *British Food Journal,* 102, 494-506.

LAZIDIS, A., HANCOCKS, R. D., SPYROPOULOS, F., KREUß, M., BERROCAL, R. & NORTON, I. T. 2016. Whey protein fluid gels for the stabilisation of foams. *Food Hydrocolloids,* 53**,** 209-217.

MALONE, M. E., APPELQVIST, I. A. M. & NORTON, I. T. 2003. Oral behaviour of food hydrocolloids and emulsions. Part 1. Lubrication and deposition considerations. *Food Hydrocolloids,* 17**,** 763-773

NORTON, I., FOSTER, T. & BROWN, R. 1998. The science and technology of fluid gels. *SPECIAL PUBLICATION-ROYAL SOCIETY OF CHEMISTRY,* 218**,** 259-268.

NORTON, J. & NORTON, I. J. S. M. 2010. Designer colloids—towards healthy everyday foods? 6**,** 3735-3742.

SULLO, A., WATSON, R. L., NORTON, I. T. J. G. & STABILISERS FOR THE FOOD INDUSTRY: CHANGING THE FACE OF FOOD MANUFACTURE: THE ROLE OF HYDROCOLLOIDS-17, R. S. O. C., CAMBRIDGE, UK 2014. Design of colloidal foods for healthier diets. 289-299.

142 WANG, Y., ZHENG, H., LI, Y., LI, B. & CHEN, Y. 2015. One step procedure for desalting
143 salty egg white and preparing fat analogue and its application in mayonnaise. *Food*
144 *Hydrocolloids,* 45**,** 317-326.
145 WORLD HEALTH ORGANIZATION. 2015. Assessment of the impact of a public health
146 product tax: final report.

147

1

CHAPTER 2.
Literature review

2.1. Introduction

This chapter aims to give an overview of the literature relevant to topics discussed throughout this thesis. It begins with an introduction to the proteins investigated throughout this thesis, then protein gelation and fluid gel production. Justification of the use of soft tribology throughout this thesis and its relevance to oral perception is discussed before the lubrication of fluid gels and emulsions. An overview of spray drying as a technique for the drying of materials is presented.

2.2. Proteins

Proteins are polypeptides composed of repeating units of amino acids. There are 21 different amino acids found in proteins, with the order of these making up the primary structure of the protein. The amino acids are linked together into polymers by peptide bonds. The amino acids can have different functional groups, some polar, some non-polar and with varying charges. The charges of some of these groups are influenced by their environment (Nelson *et al*., 2008). Proteins fold into regular structures in the form of helices and sheets, which are stabilized by hydrogen bonding. These structures make up the secondary structure of the protein. The formation of these structures is driven by the lowest conformational energy of the primary structure (Pauling *et al*., 1951). These secondary structures order spatially to a thermodynamically more favourable state by burying hydrophobic residues in the core of the protein and exposing hydrophilic residues to water; this three-dimensional ordering is the tertiary structure of the protein. Tertiary structure is primarily stabilized by hydrophobic interactions, hydrogen bonding and disulphide bridges. This folding is further contributed to by non-protein or other protein molecules, such as ions, sugars or lipids, in the quaternary structure (Zhu *et al*., 1994). Ions interact with charged and polar amino acids.

There are four common types of protein: globular, fibrous, disordered and membrane proteins. Globular proteins are generally soluble in water, with hydrophobic residues buried within the protein core and hydrophobic residues on the outer surface. Fibrous proteins are made up of long chains running in parallel to each other. Disordered proteins inherently have no fixed three-dimensional structure, and they often interact with other proteins or deoxyribonucleic acid (DNA) to function within cells. Membrane proteins occur in the phospholipid bilayer of cells; these can be integral to the membrane or temporarily attached.

2.3. Whey protein isolate (WPI)

Whey proteins are a by-product of the production of cheese and casein (Federation, 1998). Whey protein isolates are defined as having a protein content of >90%. Purification of proteins from the whey produced during cheese production can be performed by filtration techniques. To produce whey protein isolates with higher protein concentrations, ion-exchange chromatography and gel filtration are used (Tovar Jiménez *et al*., 2012; Etzel, 2004b).

2.3.1. Composition and protein structure

Whey protein contains several different proteins. Within this, α-lactalbumin and β-lactoglobulin are the two major proteins representing 65–70% of the total protein content of whey. Other proteins include bovine serum albumin (BSA), lactoferrin and a selection of immunoglobulins (Etzel, 2004b; Madureira *et al*., 2007). The molecular weight and isoelectric point (pI) of these are presented in Table 2.1.

Table 2. 1. Fractions of whey proteins and their molecular weight and pI (Etzel, 2004a; Madureira et al., 2007).

Protein	**Content in WPI (%)**	**Molecular weight (kDa)**	**pI (pH)**
β-Lactoglobulin	35	18	5.4
α-Lactalbumin	32	14	4.4
Bovine serum albumin	9	66	5.1
Immunoglobulins	21	150	5–8
Lactoferrin	3	77	7.9

2.4. Egg white

For the purpose of this literature review, chicken eggs will be discussed as they are used throughout this thesis. Eggs are made up of three major components: yolk, white (albumen) and shell. The yolk contains the majority of lipids in whole egg and carotenoids that give it its yellow colour (Kovacs-Nolan *et al*., 2005).

Egg white is predominantly made up of water, accounting for ~ 88% of the egg white. Protein accounts for ~11% of the egg albumen, with the final 1% being lipids, ash and carbohydrates. The major proteins of egg albumen are considered to be ovalbumin, ovotransferrin, ovomucoid, lysozyme and ovomucin. Minor proteins include avidin, cystatin, ovomacroglobulin, ovoflavoprotein, ovoglycoprotein and ovoinhibitor. The properties of these proteins are represented in Table 2.2.

Table 2. 2. Fractions of protein in egg albumen with their molecular weight and pI.

Protein	**Content in egg white (%)**	**Molecular weight (kDa)**	**pI (pH)**	**References**
Ovalbumin	54	45	4.5	(Kovacs-Nolan *et al*., 2005)
Ovotransferrin	12	76	6	(Stadelman *et al*., 2017)
Ovomucoid	11	28	4.1	(Kovacs-Nolan *et al*., 2005)
Lysozyme	3.5	14.4	10.7	(Huopalahti *et al*., 2007; Wan *et al*., 2006)
Ovomucin	3.5	8.3 220–270	4.5–5	(Omana *et al*., 2010)
Ovoinhibitor	1.5	46.5	4.9–5.3	(Tomimatsu *et al*., 1966, 1991)
Ovoglycoprotein	1	24.4	3.9	(Ketterer, 1965)
Ovoflavoprotein	0.8	32	4	(Awadé and Efstathiou, 1999)
Ovomacroglobulin	0.5	640	4.5–4.7	(Li-Chan, 1989)
Cystatin	0.05	12	5.1	(Anastasi *et al*., 1983)
Avidin	0.05	68.3	10	(Pugliese *et al*., 1994)

2.5. Protein gelation

In this section, gelation of globular proteins induced by heating was looked into, including mechanisms and the effects of extrinsic factors on the gel properties and gelation of globular proteins.

Barbu *et al*. (1954) showed using electron microscopy that the mechanism of gelation for proteins in horse serum and egg albumen was one of globular proteins polymerizing not by total denaturation of the protein structure. Koseki *et al*. (1989) used far-ultraviolet (UV) circular dichroism spectroscopy and transmission electron microscopy to investigate the mechanism of gelation for ovalbumin. Far-UV circular dichroism spectroscopy showed a permanent change in the microenvironment of aromatic amino acid residues upon heating, showing that, although the globular nature of the protein was not broken down, some rearrangement of structure was occurring. This was shown to produce linear polymers by transition electron microscopy. This is explained as a molten globule structure on denaturation of ovalbumin in which partial denaturation exposes hydrophobic regions; these hydrophobic regions aggregate together, forming linear polymers of globular proteins. Hydrophobic interactions are the main driver of protein aggregation (Campbell *et al*., 2003).

The ordering of polymers during the aggregation step of gelation controls the final structure and properties of gels. This is controlled by ionic strength and pH (Croguennec *et al*., 2002; Holt *et al*., 1984; Verheul and Roefs, 1998). Gels produced at ionic concentrations >0.1 M have been shown to have a mixed structure with a combination of strands and aggregates, while those produced at ionic concentrations <0.1 M have a fine-stranded structure (Foegeding *et al*., 1995). This change in structure was shown to be due to favouring of aggregation of protein molecules below their denaturation temperature.

pH also affects the properties of gels: proteins have little net charge at a pH around their pI, which reduces electrostatic repulsion between proteins during aggregation. This has been shown by electron microscopy of β-lactoglobulin gels produced around the pI (Langton and Hermansson, 1992), with gels produced closer to the pI showing a globular aggregated structure while those produced further away from the pI produce particles embedded in a continuous fine-stranded network. This same trend in structure of protein gels with pH has been shown by Handa *et al*. (1998) for egg albumen gels.

2.6. Fluid gels

Fluid gels are suspensions of soft gelled particles dispersed in a non-gelled continuous phase (Cassin *et al*., 2000); these are produced by sheared gelation of biopolymers. These soft particles can be used to emulate textural properties of oil droplets within an emulsion. Fluid gels were originally produced by cooling of cold gelling biopolymers in shear (Norton *et al*., 1999; Garrec and Norton, 2012). However, in recent years, heat gelling of proteins (Moakes *et al*., 2015a; Lazidis *et al*., 2016) and salt gelling of hydrocolloids have also been used (Farrés and Norton, 2014; Fernández Farrés *et al*., 2013).

The formation of particles in shear has been shown to be via nucleation and growth (Norton *et al*., 1999), by which nuclei form and aggregate together at the gelation temperature of the polymer being used. The final size of the aggregated nuclei is controlled by the shear field present, with final particle size being an equilibrium between aggregation and breakdown of aggregates. This equilibrium can be shifted by changing shear rates and the rates of cooling used during production (Gabriele *et al*., 2009). Increased shear rates also decrease the phase volume occupied by the gelled phase in fluid gels.

The shear disruption during gelation has been proposed to disrupt coil formation at the surfaces of particles, leading to reduced density of the gelled network at particle surfaces as the coil helix transition is disrupted. This has been investigated by differential scanning calorimetry (DSC), through comparisons of melting enthalpies for fluid gels with that of their quiescent gels. In agarose fluid gels, no change in enthalpy of melting was observed for fluid gels and quiescently gelled systems (Norton *et al*., 1999). However, an enthalpy change between the melting of fluid gels and quiescent gels was observed by Garrec *et al.* (2012) for κ-carrageenan fluid gels. This had been attributed to the different gelling rates of the biopolymers and the rate of ordering relative to the shear rates being used. The rate of molecular ordering in agarose is two to three times greater than that of κ-carrageenan (Norton *et al*., 1986). Disruption of molecular ordering at the particle surface explains the observed difference in melting enthalpy. The extent of this disruption is influenced by the shear rate relative to the rate of gelation. Norton (2016) observed no change in melting enthalpy between quiescently set gels and fluid gels produced from κ-carrageenan and κ-carrageenan–gellan gum mixed systems.

Frith *et al*. (2002) compared the properties of agarose fluid gels with agar microgels produced by the reverse emulsion technique detailed by Adams *et al*. (2004). For microgel formation, a water in oil (W/O) emulsion of hot agarose solution is formed then cooled with agitation to prevent droplet aggregation. These gelled emulsions then centrifuged and washed in distilled water repeatedly to remove oil and surfactant. This produces spherical monodisperse gelled particles that are made up of the same components as agarose fluid gels, so observed changes in their properties can be attributed to the shape and structure of fluid gel particles. Agarose microgels were shown to have a maximum packing fraction of ~0.64, which correlates with Einstein's calculations for the random maximum packing fraction of hard monodisperse spheres (Einstein, 1906). For microgels, a large increase in elastic modulus was observed at this

maximum packing fraction. For fluid gel particles, an increased elastic modulus is shown over a wide range of phase volumes. The anisotropic nature of the fluid gel particles allows formation of a percolated network at reduced volume fractions showing elastic behaviour across a broad range of phase volumes (Φ) (Adams *et al*., 2004).

2.7. Tribology

Tribology is the study of friction, lubrication wear and thin film rheology. Traditionally, tribology has been used to study mechanical components of machines to study wear of moving components. It is used for increasing efficiency of moving parts and increasing their lifespan by reducing wear.

Recently, tribology has been used to study foods and cosmetic products to further understand how their textures are perceived (Dowson, 1996; Shewan *et al.*, 2020). Cosmetic products (for example, skin creams) are perceived in thin films between the skin and the fingers as they are applied. For foods, they are perceived between the tongue and palate in thin films. Understanding this part of processing is vital in understanding sensory perception of such products.

During oral processing, bulk rheology is initially perceived as a bite or mouthful of food is taken into the mouth; through chewing and mixing with saliva further breakdown occurs. This broken-down food is then perceived in thin layers within the mouth (de Wijk and Prinz, 2005; de Wijk *et al*., 2003). In these thin layers, the lubricating properties of the film formed is detected by mechanical receptors within the mouth as the tongue slides past the palate and the teeth (Malone *et al*., 2003a).

2.7.1. Friction

Friction was first described as the force resisting sliding motion between two contacting objects.

In 1699, Amontons developed two laws of friction (shown below) through studying friction of dry sliding contacts.

1st law: $F_t \propto W$, tangential friction force is directly proportional to the applied load

2nd law: Friction is independent of apparent area of contact (A_a)

Amontons' laws were later confirmed by Coulomb (1785). Coulomb showed that these surfaces were not perfectly smooth but that they had peaks and troughs in the surface. He proposed that friction was as a result of these asperities interlocking.

Bowden and Tabor (1964) further developed on Coulomb's theories, proposing that friction was caused by intermolecular adhesion at these touching asperities. Thus, the real area of contact was smaller than the apparent area of contact ($A_r < A_a$) as only asperities from each surface were in contact.

At a similar time, Archard proposed that the linear relationship observed between F_t and W was the nature of the contact, an asperity contact being present owing to roughness of the surfaces. The number of asperities in contact increased linearly with increased normal force. This has since been confirmed theoretically and practically by Greenwood and Williamson (1966).

2.7.2. Contact mechanics

The contact in the ball on disc tribometer can be modelled as a sphere on a flat surface using the equation devised by Hertz (1881); this is described by Equation 2.1. The Hertz theory corresponds to the area of contact between two contacts in a single asperity contact; single asperity contacts have been observed using the steel ball on silicone elastomer disc used in this project.

$$a = \left(\frac{3WR^*}{4E^*}\right)^{\frac{1}{3}} \quad (2.1a)$$

$$\frac{1}{R^*} = \frac{1}{R_1} + \frac{1}{R_2} \quad (2.1b)$$

$$\frac{1}{E^*} = \left(\frac{1 - V_1^2}{E_1} + \frac{1 - V_2^2}{E_2}\right) \quad (2.1c)$$

W is the normal force applied, R_1 is the radius of the ball and $R_2 = \infty$ as the disk is a flat surface of infinite radius. V values represent the Poisson's ratio of the ball and disc, and E values represent the Young's modulus of these surfaces. a is the radius of the contact area; a circular contact is produced by the sphere on the disc, and thus the area of contact is given by $A = a\pi^2$. It follows that if the contact follows Hertz law, an $F_t \propto W^{2/3}$ relationship is observed with varying normal force in this compliant contact.

Atomic force microscopy has been used to confirm that true single asperity contacts follow Hertz law, while for 'real' asperity contacts Archard's first law is still obeyed. This has been shown using silicone-based surfaces that deform, giving a single asperity contact (Izabela *et al*., 2008).

2.7.3. Lubricants

Friction between two surfaces is also affected by the presence of lubricant between the surfaces, as well as the nature of the surfaces. In oral processing, this is contributed to by both the lubricating nature of saliva and the food mixing together.

Richard Stribeck first presented three regimes of lubrication in his work on bearings in 1902, which showed that increasing entrainment speed did not simply increase lubrication, friction was initially constant before decreasing to a minimum and then increasing again (Stribeck,

1902). This work was presented by plotting friction values against the dimensionless value defined as the Sommerfield number. The Sommerfield number is calculated as shown in Equation 2.2.

$$N_{so} = \frac{\eta U}{W} \tag{2.2}$$

The phenomenon presented by Stribeck showed three regimes of lubrication of these systems; these are presented in Figure 2.1.

Boundary lubrication — this is observed at low speeds when friction is independent of increasing speed; at these low speeds, lubricant is not being entrained into the contact, so friction is controlled by the contact of the two surfaces. Boundary regime lubrication is of importance in machines to reduce wear of moving parts in start-up and shutdown, in which the speed of the moving parts is not great enough to entrain lubricant separating the surfaces. This can be manipulated by modifying the properties of the surfaces as has been shown using graphite and polytetrafluoroethylene (PTFE) (Williams, 2005).

Mixed lubrication — as speed is increased, the lubrication transitions into the mixed lubrication regime, in which friction decreases with increasing entrainment speed. Lubricant begins to be entrained into the gap, separating the surfaces. Throughout this regime, friction is a combination of lubricant properties and surface properties. With increasing speed, pressure of lubricant in the gap increases, separating the surfaces and reducing the contribution of contacting asperities to friction values observed.

Hydrodynamic lubrication — this is observed as the two surfaces are fully separated. Friction increases with increasing speed as gap size increases and more lubricant is present in the gap.

In this regime, surface properties do not contribute towards observed friction as they are completely separate. Bulk rheology is being observed in the hydrodynamic lubrication regime.

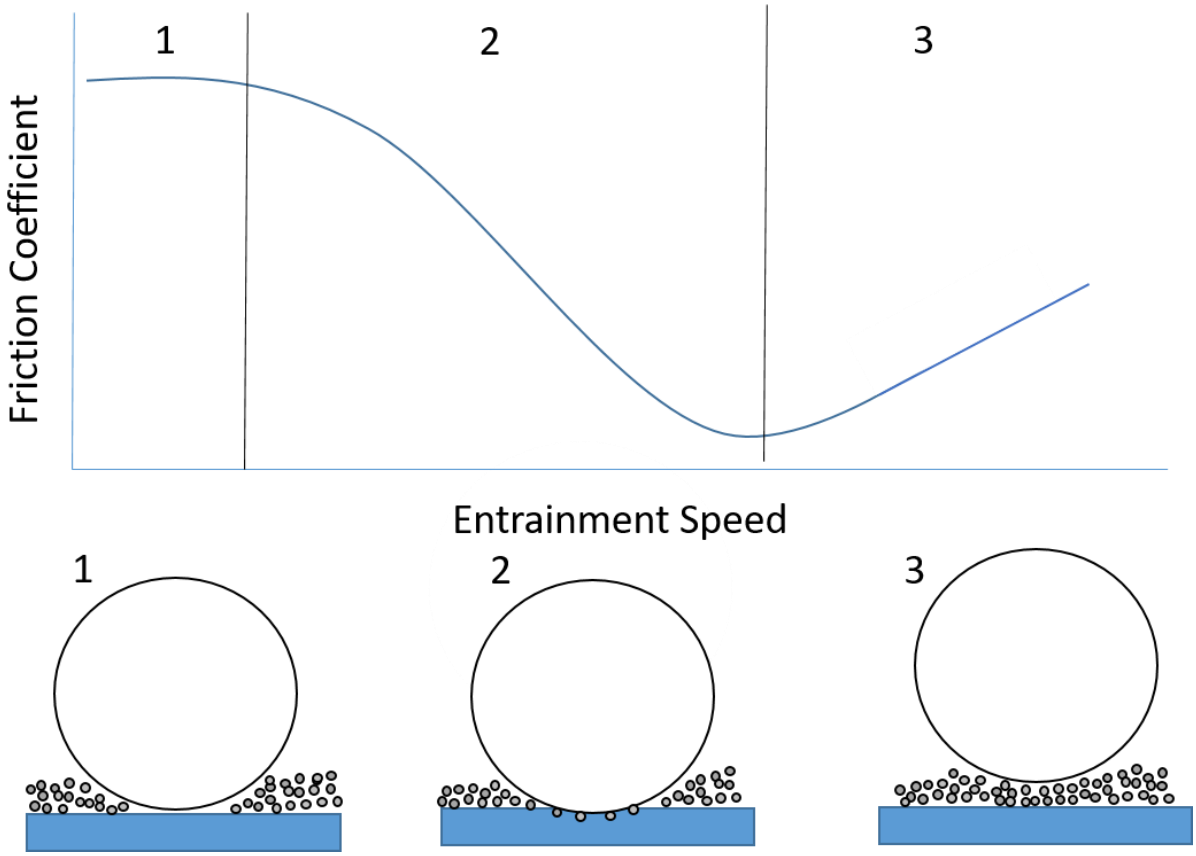

Figure 2. 1. Schematic showing the three regimes of lubrication. 1) Boundary regime of lubrication, 2) mixed regime of lubrication and 3) hydrodynamic regime of lubrication.

2.7.3.1. Fluid gel lubrication

For fluid gels like those studied in this work, a different shape of Stribeck curve has been observed, with two peaks in friction (Gabriele *et al.*, 2010). An initial decrease in friction is observed, followed by an increase in friction as the systems transition between boundary and mixed lubrication. This has been proposed to be as a result of entrainment of the continuous phase into the contact, increasing lubrication. An increase in friction is then observed as the gap size becomes large enough for particle entrainment to occur; the rolling and sliding of particles

in a monolayer between the surfaces is attributed to the increase in friction. As the gap size increases, multilayers of particles can enter the gap, reducing friction further (Mills *et al*., 2013).

This peak in friction was not shown by Garrec and Norton (2013) investigating the tribology of κ-carrageenan fluid gels with particle sizes <1 μm. This was proposed to be as a result of the particles being small enough to fit within the asperities of the surfaces used and thus entrained at all entrainment speeds. This was further confirmed by phase volume and particle properties affecting friction in the boundary regime, giving friction values below that of the linear polymer of the continuous phase. This effect of phase volume on the lubrication in the boundary regime of lubrication showed a decrease in friction with increasing Φ <0.3. A plateau region is then observed between 0.3 and 0.6 Φ, and further reduction in friction is shown at Φ >0.7. Using agarose fluid gels, Gabriele *et al*. (2010) showed a difference in lubrication in the mixed regime dependent on whether entrainment speed was ramping up or down. This was attributed to exclusion of particles from the contact. In the ramp up, the ball starts stationary with no lubricant in the contact; in the down ramp, particles are already entrained into the gap, providing a smooth curve of lubrication without the peak observed as particles are entrained. This supports that for this system with an average particle size ~90 μm, particle entrainment does not occur in the boundary regime.

However, it has been shown by breaking down the contributions of the particles and the continuous phase that particle entrainment is observed at all speeds for agar fluid gels of particle size >100 μm (Fernández Farrés and Norton, 2015).

Increasing friction has been observed with increasing particle size in fluid gel systems by Gabriele *et al*. (2010); this relationship of increasing particle size and increasing friction has also been observed in custard systems (de Wijk and Prinz, 2005).

2.7.3.2. Emulsion lubrication

The effects of oil concentration on the lubrication of emulsions was investigated by Malone *et al*. (2003a); guar gum was used to thicken the continuous phase of these emulsions to normalize the bulk viscosity of the emulsions tested. The Stribeck curve produced for 1% oil superimposed onto the curve of water in the boundary and mixed regimes, while curves of emulsions of oil concentrations >20% overlaid pure oil in the boundary and mixed regimes.

De Vicente *et al.* (2006) went on to investigate the effects of the viscosity ratio (p) between the oil and the continuous phase. Glycerol was used to give a $p = 1$ ratio for emulsions with different oil phase volumes. For the ratio $p = 1$, all Stribeck curves were shown to overlay in the boundary and mixed regimes of lubrication for 0–100% oil. Further investigation was carried out by the same team into the viscosity ratio of emulsions, using 20% oil and manipulating the viscosity of the continuous phase. Through doing this it was shown that curves of different viscosity ratios could be overlaid by multiplying entrainment speed by the droplet viscosity for $p > 4$ and multiplying by continuous phase viscosity for $p < 4$. This is attributed to the droplets not being forced to the surfaces in systems with $p > 4$. Owing to the low viscosity of the oil phase, the oil droplets will be deformed by stress in the contact and thus will not contact with the surfaces (de Vicente *et al*., 2006). It is noteworthy that no surfactant was added in these emulsion systems.

This proposal of oil pooling in the contact enhancing lubrication was further supported by work from Dresselhuis *et al*. (2007), who showed reduced friction for emulsions showing greater coalescence.

2.8. Spray drying

Spray drying was first introduced in 1872 by Samuel R. Peroy as a novel drying technique. "Spray drying is the transformation of feed from a fluid state into a dried particulate form by spraying the feed into a hot air drying environment" (Masters and Ela, 1991). The spray-

drying process can be broken down into four steps (Anandharamakrishnan, 2015). The first step is atomization: this involves disruption of the fluid into droplets in the air. Atomization is important for the drying process as this increases the surface area for evaporation and reduces the distance water must travel from the centre of droplets. There are two major types of atomizer: a rotary atomizer and a pressure nozzle. A rotary atomizer uses centrifugal energy to disrupt the liquid. This disruption is controlled by the speed of the atomizer, with increasing speed increasing atomization energy. In a pressure nozzle, liquid is forced through an orifice, breaking it up into small particles. Droplet size has been shown to be directly proportional to feed rate through the pressure nozzle. The pressure nozzle produces less homogeneous droplets than the rotary atomizer.

The second step is the contact with hot gas. There are two different styles of spray dryer available: the co-current and counter-current flow type. In the co-current spray dryer, the hot gas flows in the top in the same direction as the droplets through the drying chamber. In counter-current flow, the gas flows through the spray dryer in the opposite direction to the flow of droplets. Counter-current spray dryers offer slower drying with greater maximum particle temperature, as gas is coldest at the point where the droplets enter the spray dryer. As the gas flows through the dryer, it cools. However, for co-current spray dryers, the gas is hottest at its initial interaction with droplets. Thus, greatest cooling occurs initially when heat is transferred to the particles at their coldest point.

The third step is evaporation of moisture or drying. As the hot gas meets the droplets initially, the droplets are not heated owing to evaporation of water dissipating heat away from the droplets. This leads to a plateau in particle temperature. Once particles are dry, they then heat up until they reach equilibrium with the outlet gas temperature.

Crust formation occurs at the droplet surface as water initially evaporates from the surface of droplets. The maximum temperature the particle reaches is controlled by the falling period, as this will limit the time for heat transfer. If the maximum temperature of the particle gets too high during the falling period, a bubble can form in the centre as the remaining water evaporates; this can lead to irregularities in the shape of the particles (Anandharamakrishnan, 2015).

The final step is the separation of particles. This is done by a cyclone in which the particles are pushed to the outside by the airflow spiralling through a cylinder.

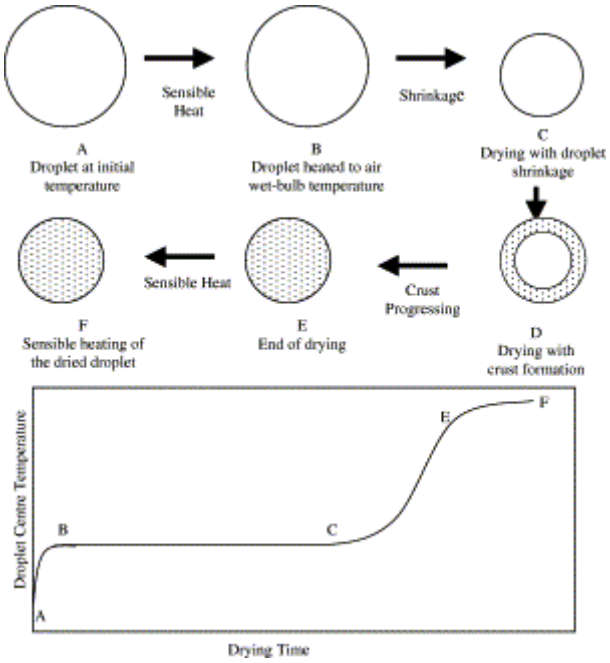

Figure 2. 2. Schematic of predicted droplet structure and core temperature through spray drying. Taken from Farid (2003).

Figure 2.2 shows the expected structure and respective core temperature of a droplet during falling in the drying chamber of a spray dryer. An initial increase in droplet core temperature is observed as the droplet is sprayed into the hot air. This temperature will then plateau at the wet bulb temperature as the water evaporates and the droplet shrinks. As the droplet surface begins to dry, a crust will form. Once this crust has formed, droplet temperature can increase

again as evaporation is slowed. The expected temperatures for particles in a co-current spray dryer are relatively low owing to the loss of temperature of the air as heat is transferred to the particles.

The use of spray drying in the production of particulate thickeners for use as fat replacers has been previously patented by Gidley and Hedges (1998) who spray dried hot solutions of hydrocolloids. This method produced particles that upon rehydration in cold water had a size <100 μm.

Production of insoluble WPI aggregates through spray drying has been previously observed by Anandharamakrishnan *et al*. (2008). However, no information on the properties, morphology or nature of these aggregates was given in this study.

Influence of spray-drying parameters on the emulsifying properties has been investigated by Bernard *et al.* (2011). They showed that with increasing inlet temperature an increase in loss of solubility through spray drying was observed for whey protein concentrate. The greatest loss of solubility observed through this was 8.3%; loss of solubility can be assumed to be particle production, so only 8.3% of the total protein produced particles. Increased temperature of processing and loss of solubility was shown to decrease droplet sizes of emulsions produced. This decreased droplet size was attributed to the denaturation of the β-lactoglobulin component of the WPC denaturing not the formation of particles. Similar observations of increased spray-drying inlet temperature enhancing the foam stabilization for whey products has been shown by Relkin *et al.* (2007) and Bernard *et al.* (2011). In this work, protein aggregates were shown to form through spray drying of whey obtained from filtration of skimmed milk.

2.9. Protein particles

Owing to their demonstrated use in fat replacement, protein particles are of significant interest. Several protein particulate systems have been patented.

Micro-particulate whey is currently commercially produced as a fat replacer under the brand *Simplesse*®. These are spherical particles of denatured WPI ranging between 0.1 and 3 μm in size. They are produced by adjusting the pH of whey between pH 3.5 and 4.5, then heating to 80–130ºC under shear. The temperature of heating affects the time required for heating, with heating times of 5 minutes required at 80ºC and heating times of 5 seconds suitable at 120ºC. This heating process was carried out in a pressurized vessel to limit water evaporation during the heating process (Anandharamakrishnan, 2015).

A method for production of a whey precipitate that can be dried and then re-suspended has been patented. Aggregates of whey that precipitate out are produced by adjusting the pH of acid whey to more alkaline pH. This method produces particles of 10 μm; the precipitated aggregates are then washed by resuspension before further centrifugation in water. The particles can then be dried by rotary drying, oven drying or spray drying. These precipitates can be further stabilized by divalent cations (Shah and Luksas, 1980).

For both of the processes discussed above, particles are produced and then dried, with spray drying being an option for the drying technique but not a processing method for the particle production.

2.10. Influence of pH on proteins

pH contributes to protein solubility and aggregation kinetics owing to the influence of charge on protein folding and solubility. At pH greater than the pI of a protein, the protein will have a positive net charge, at the pI the protein will have a neutral net charge and the protein will

have a negative net charge at a pH below the pI. Net charge contributes to protein aggregation kinetics, with the least intermolecular electrostatic repulsion at the pI. However, the influence of pH on protein aggregation is not as simple as just that of net charge (Pace *et al*., 2009).

2.10.1. Intramolecular stability

Ionizable side chains make up on average 29% of the amino acids in proteins (Jordan *et al*., 2005). The charge of these residues is dependent on pH and the local environment of the residue. These amino acids each have an individual pK_a (the pH at which their net charge is neutral). Thus, changing the pH causes the charge distribution within the protein molecule to change (Pelegrine and Gasparetto, 2005). There are two mechanisms of protein instability with changing residue charges: specific and non-specific. Non-specific protein instability is due to electrostatic repulsion between residues of the same charge. Specific interactions are due to the formation of salt bridges as a result of ion pairing. Unlike non-specific interactions, increasing charge can increase the stability of specific interactions, potentially favouring specific protein conformations at different pH (Dill, 1990; Strop and Mayo, 2000; Grimsley, 1999).

pH influences the free energy of protein unfolding; calculation of this is shown in Equation 2.3. The free energy of unfolding is calculated as a combination of the enthalpy change of unfolding, the temperature and the entropy change due to unfolding. Calculation of ΔG_u is complex owing to influences of protein environment as well as the environment of the individual amino acid residues within the folded protein. Mutagenesis and other techniques have been used to investigate the enthalpy of unfolding of specific residues within proteins. ΔG_u is influenced by changes in pH owing to favourable and unfavourable interactions between residues as residue charges change. However, owing to the contributions of desolvation of residues (Tollinger *et al*., 2003) and interactions with polar neutrally charged

residues, predictions of true ΔG_u changes with pH are challenging. With changing pH, the free energy of protein unfolding will change. This change is a sum of the effects of pH on all of the amino acid residues in the folded and unfolded state.

$$\Delta G_u = \Delta H - T\Delta S \quad (2.3)$$

2.10.2. Intermolecular stability

As the charges of individual amino acid residues of the protein change with changing pH, so too does the net charge of the molecule. This was first presented in a model by Tanford and Kirkwood (1957), who showed that proteins have point charges on their surface. Before this, proteins were treated as impenetrable spheres with a uniform charge distribution, but this uniform charge distribution did not explain the clear aggregation observed at pI for proteins. Changes in the net charge of proteins influence the electrostatic interactions between molecules.

Proteins have a net charge at pH away from the pI, which leads to intermolecular electrostatic repulsion, making aggregation unfavourable (Chi *et al*., 2003a; Ip *et al*., 1995; Mulkerrin and Wetzel, 1989; Tsai *et al*., 1998). The precipitation of proteins at their pI has been well documented and is used as a method of protein purification (Boye *et al*., 2010; Karaca *et al*., 2011a; Becktel and Schellman, 1987; Kakalis and Regenstein, 1986; Mann and Malik, 1996; De Wit, 1989; Hall, 1996; Wong *et al*., 1996). This technique is based on the reduced net charge of proteins at pH near to their pI. This reduced net charge reduces intermolecular repulsion between protein molecules, thus favouring aggregation. Owing to the anisotropic nature of proteins, dipoles are still present at a neutral net charge, and thus these opposite charges on protein surfaces attract favouring intermolecular aggregation (Chi *et al*., 2003a; Striolo *et al*., 2002).

406 2.10.3. Gel structure

407 These changes in intermolecular and intramolecular interactions with pH influence the
408 structure of protein gels. This aggregated structure observed around the pI is the result of the
409 reduced net charge of the protein molecules reducing intermolecular repulsion. Thus,
410 reduction in intermolecular repulsion increases the rate of aggregation. As the rate of
411 aggregation increases, the rate of protein denaturation becomes the rate-limiting step of
412 gelation (Renkema *et al.,* 2002; Renkema *et al.,* 2000). This means that during gelation
413 protein molecules do not have time to orientate within the gel structure, and thus they
414 aggregate, giving the particulate structure observed. As the pH moves away from the pI, a
415 mixed structure of strands and particulates is observed. Figure 2.3 shows scanning electron
416 microscopy (SEM) images of β-lactoglobulin gels with changing pH. At pH 5.5 (pI), the gel
417 has an aggregated particulate nature with regular size particles and voids (Langton *et al.,*
418 1992). At pH 4.5, the structure appears to be a combination of the particulate structure and a
419 fine-stranded structure. At pH 4, sheets are seen; these sheets are the fine-stranded structure
420 expected for gels produced away from the pI.

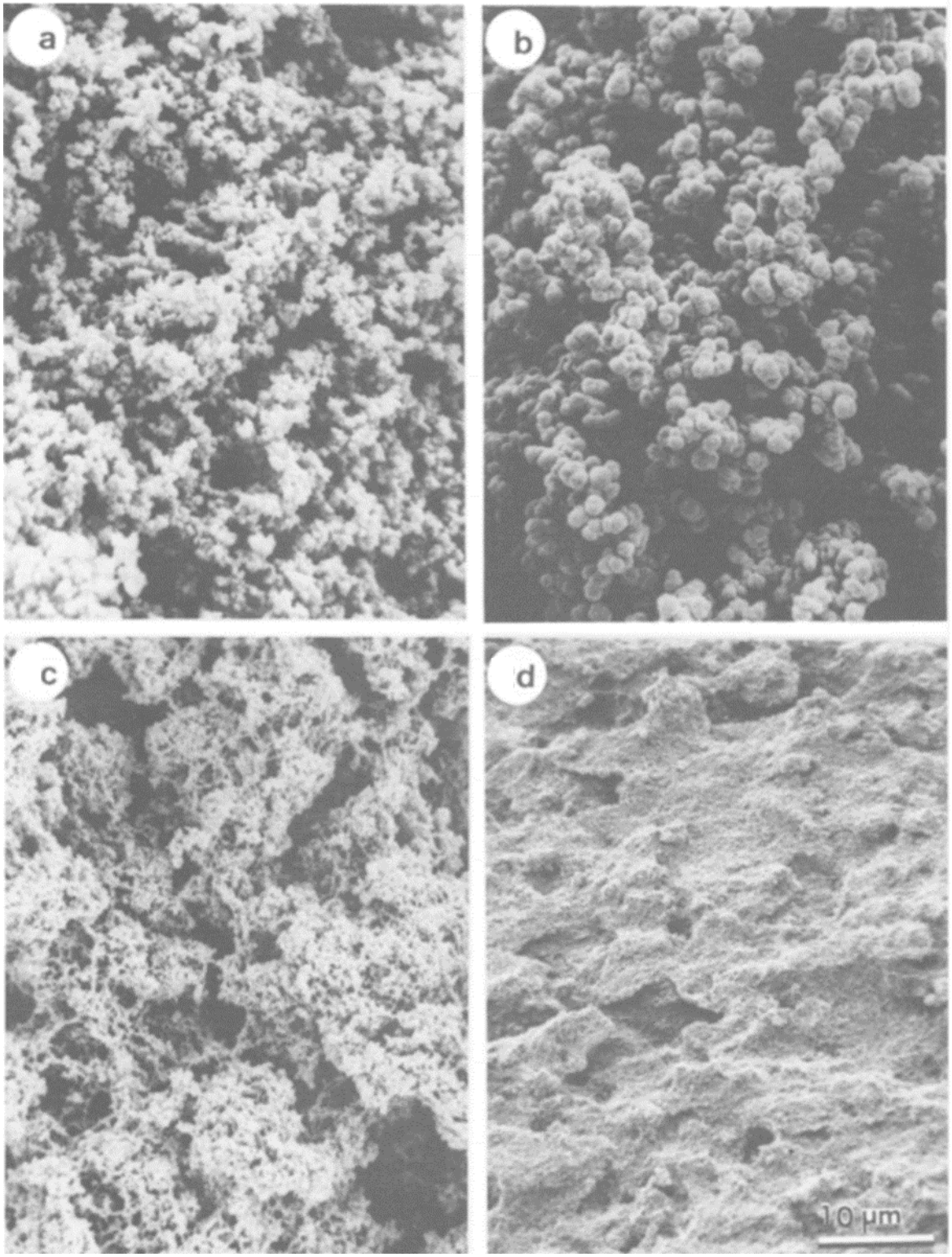

Figure 2. 3. SEM micrographs at low magnification of β-lactoglobulin gels formed at (a) pH 6, (b) pH 5.5, (c) pH 4.5 and (d) pH 4. Taken from Langton and Hermansson (1992).

2.11. Effect of salts on proteins

Several factors contribute to the folding, unfolding and segregation of proteins. The simplest of these is electrostatic shielding with increasing salt concentration. Electrostatic shielding is the damping of electrostatic forces by mobile charged molecules. This damping reduces the Debye length (Debye and Hückel, 1923). The Debye length defines the distance over which electrostatic forces occur. Reduction in the distance electrostatic effects are effective over reduces repulsion and attraction owing to charged molecules (Chi *et al*., 2003b).

In 1888, Franz Hofmeister observed that different concentrations of different salts were required to salt out proteins. In this work, the concentrations of different salts required for the sedimentation of egg proteins was investigated (Hofmeister, 1888). It was shown that some salts had a stabilizing effect on proteins, salting them in (kosmotropic). Thus, a series is presented in which salts are ordered by their salting out capability (Figure 2.4). Since this initial publication, there has been much research into the factors influencing this series. Ion polarizability (Conway and Ayranci, 1999), Gibbs free energy of hydration (Ganea *et al*., 1999) and charge density (Nucci and Vanderkooi, 2008) have all been shown to contribute to the observed trends.

$$Citrate^{3-} > Sulfate^{2-} > Phosphate^{2-} > F^- > Cl^- > Br^- > I^- > NO_3^- > ClO_4^-$$

$$N(CH_3)_4^+ > NH_4^+ > Cs^+ > Rb^+ > K^+ > Na^+ > H^+ > Ca^{2+} > Mg^{2+} > Al^{3+}$$

Chaotropic **Kosmotropic**

Salt out **Salt in**

Figure 2. 4. Order of the salting out potential of anions (top panel) and cations (bottom panel) according to the Hofmeister series.

There are also specific binding effects of ions. WPI is known to specifically bind to divalent ions (Zhu and Damodaran, 1994). This is via a crosslinking interaction with anionic charged residues on the protein surface. These interactions can promote protein aggregation behaviour (Kuhn and Foegeding, 1991). Ions can also bind to the peptide bond owing to the dipole across the bond that is caused by the partial charges on the carboxyl and amino groups.

These mechanisms of salt influence the stability of proteins by a combination of stabilizing and destabilizing effects, with promotion of unfolding and aggregation possible. These effects of salts are pH dependent, with protein charges being influenced by changing pH.

2.12. Emulsions

Emulsions are mixtures of two or more immiscible liquids. Emulsions are commonly found in foods. Oil in water (O/W) emulsions are found in mayonnaises, salad dressings and ice creams. W/O emulsions are found in spreads and margarines. Duplex emulsions (water in oil in water; W/O/W) have been used for encapsulation and fat reduction (Dickinson, 2011; Shimizu *et al*., 1995). Emulsions are inherently unstable systems because it is thermodynamically favourable for the system to separate into two phases, reducing the contact area between the two phases. Through the formation of droplets during emulsification this surface area is increased. Some of the mechanisms responsible for this instability are now discussed.

2.12.1. Emulsion stability

2.12.1.1 Aggregation

Within an emulsion, droplets move owing to Brownian motion, mechanical agitation and gravity; this leads to collisions between droplets. When these droplets come into contact, they can either aggregate or separate again. There are two main types of aggregation: coalescence

and flocculation. Coalescence is when two droplets come together and combine to form a single larger droplet. Flocculation is when these droplets stay in contact with each other but the structure of the individual droplets does not breakdown; these flocs can be difficult to disrupt (strong flocs) or are easily disrupted (weak flocs).

2.12.1.1.1. Coalescence

Coalescence is when a larger droplet is formed from smaller droplets merging. This occurs when external forces overcome the Laplace pressure of the droplets, flattening their surfaces, resulting in the rupture of the film of continuous phase between the two droplets. Eventually this progression will lead to oiling off. This process is self-accelerating, as larger droplets have a lower Laplace pressure making coalescence easier. This can be overcome by using an emulsifier with better coverage. If a thick film is formed at the interface, it will not rupture as easily.

2.12.1.1.2. Flocculation

Flocculation is the aggregation of droplets into clusters. Within these clusters, the individual droplets maintain their structure. Flocculation can promote gravitational separation or hinder it depending on the concentration of dispersed phase in the system. For dilute systems, flocculation promotes creaming; however, in more concentrated emulsions, flocculation of droplets interferes with the movement of droplets due to gravity. These structures are represented in Figure 2. 5. Schematic showing structures formed by flocculation in A) dilute emulsion and B) concentrated emulsion..

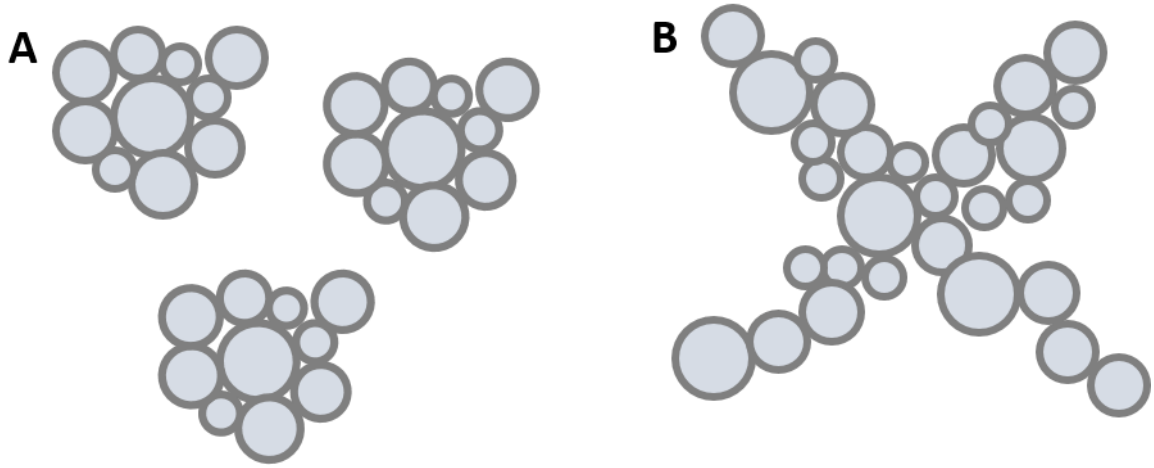

Figure 2. 5. Schematic showing structures formed by flocculation in A) dilute emulsion and B) concentrated emulsion.

2.12.1.2. Ostwald ripening

Another mechanism by which overall droplet size increases is Ostwald ripening: one droplet's size increases at the expense of the other. However, this is not due to the two droplets coming together but through the mass transfer of soluble dispersed phase through the continuous phase from the smaller droplet to the larger droplet. This process can occur without the integrity of the interface between the two phases being compromised. This is driven by the difference in vapour pressure between smaller droplets and larger droplets, owing to the increased surface area relative to the volume in smaller droplets.

2.12.1.3. Creaming and sedimentation

Creaming and sedimentation are forms of gravitational separation; these are due to the density difference between the two phases, which leads to oil floating on water. This can be tackled by using weighting agents in the oil phase (for example, bromo vegetable oil, ester gum and damar gum), which reduces the density difference. Another technique for reducing the gravitational effects on an emulsion is to increase the viscosity of the continuous phase, thus making it harder for droplets to migrate through it. Thick layers formed on the surface of droplets also reduce the density difference. Stokes' law can be used to calculate the rate at

which creaming or sedimentation will occur. However, this equation oversimplifies the process by making assumptions that cannot be applied to food emulsions: it assumes droplets to be solid and all droplets to be the same size. Furthermore, Stokes' equation (Equation 2.4) does not account for high solid contents in emulsions and how these influence the rate of creaming or sedimentation.

$$v = \frac{2}{9}\frac{(\rho_c - \rho_d)}{\eta} g r^2 \quad (2.4)$$

Where r is the radius of droplets, g is the acceleration due to gravity, ρ is the density of phases and η is the viscosity.

2.12.1.4. Biological destabilization

Enzyme hydrolysis and lipid oxidation are both processes by which the molecules of the oil phase are broken down. Enzyme hydrolysis breaks down the esters in fats; this can be caused by enzymes present in other ingredients in foods. Break down of esters leads to hydrolytic rancidity and can potentially produce toxic products. Ester hydrolysis can also occur in hot moist conditions without enzymes. Lipid oxidation is the oxidation of the lipid molecules; this is caused by water soluble initiators. Meta-ions and low pH accelerate this process owing to the charged nature of the initiators. Low levels of lipid oxidation can enhance aroma, but high levels lead to a putrid smell and taste.

2.12.2. Emulsifiers

Emulsifiers act to stabilize emulsions and can be split into three categories: surfactants, proteins and particles.

2.12.2.1. Surfactant

Surfactants are small surface-active molecules. These are amphiphilic, which enables them to adsorb at interfaces and reduce the interfacial tension. Adsorption of surfactants to the

interface is favourable because it reduces the caging of water molecules at the interface, reducing the interfacial tension. It also reduces the unfavourable interactions between the immiscible liquids and the reduction in the unfavourable interactions between the region of the amphiphilic molecule that is insoluble in the bulk phase. There are several types of surfactant. Non-ionic surfactants are commonly used in foods and include Tweens (sorbitan esters) and Spans (Rosen and Kunjappu, 2012; Kralova *et al*., 2009). Cationic surfactants are molecules that carry a positive charge; there are very few food-grade cationic surfactants, and lauric arginate is one of these. Anionic surfactants are molecules that carry a negative charge, for example, fatty acid salts. Zwitterionic surfactants have both positive and negative charges, giving no net charge, for example lecithins. Ionic surfactants give oil droplets a surface charge, and droplets with the same charge repel each other.

Methods of classifying surfactants have been developed over the years in an attempt to rationalize surfactant selection. Three main methods have been presented, all of them based on similar principles. Bancroft's rule is based on the solubility of a surfactant in oil or water. The hydrophilic–lipophilic balance (HLB) is the ratio of hydrophilic groups to lipophilic groups. The hydrophile–lipophile deviation (HLD) is based on the relative affinity of a surfactant for oil and water. All of these classification methods are based on the hydrophilic and hydrophobic natures of the surfactants.

Bancroft's rule was first presented by Davis (1994). Bancroft's rule states that the phase in which the surfactant preferentially resides will be the continuous phase of the emulsion. Thus, a surfactant that favoured the aqueous phase would form an O/W emulsion and a surfactant that favours the oil phase would produce a W/O emulsion. There are limitations to this rule, and through appropriate processing conditions the continuous phase of emulsions can be

tailored. This rule offers little insight into the stability of the emulsions formed, but it is a good rule of thumb.

HLB was first presented by Griffin (1949) as a classification method for whether surfactants favour the aqueous or oil phase. The HLB of a surfactant can be calculated by Equation 2.5 (Sjoblom, 2001; McClements, 2015). Surfactants with a lower HLB value (3–6) are more lipophilic, meaning they favour the oil phase. The phase in which most of the surfactant resides is the phase that favours being the continuous phase. Thus, a surfactant with a low HLB favours W/O emulsions. Surfactants with an intermediate value (7–9) favour neither the oil nor the aqueous phase. Surfactants with a high HLB (10–18) cannot be readily dispersed in oil and favour water as the continuous phase. A great example of HLB influencing properties is in mayonnaises, which are 80% volume oil but remain water continuous as a result of the high HLB of egg yolk proteins used to stabilize them (Depree and Savage, 2001).

$$HLB = 7 + \sum(hydrophillic\ group\ numbers) - \sum(lipophillic\ group\ numbers) \qquad (2.5)$$

Group numbers are predetermined in literature for many chemical groups. By entering these numbers into Equation 2.5, the HLB number of any molecule can be calculated.

The HLB does not account for temperature or changes in environment. The properties of surfactants are heavily influenced by these, and thus the group numbers of molecules must be corrected for the conditions used (Pasquali *et al*., 2008).

2.12.2.2. Proteins as emulsifiers

Amino acid residues can be hydrophobic, hydrophilic or amphiphilic; thus, the functionality of proteins depends on the nature of the amino acids it is made up of and the order in which they occur. Protein size and native structure also contribute to the surface activity of proteins. Proteins generally bury hydrophobic residues within their core to shelter them from

574 unfavourable interactions with water at the protein surface. Surface hydrophobicity of
575 proteins is a contributor to the surface activity of proteins (Kim *et al*., 2005).

576 Proteins adsorb to the interface much slower than low molecular weight surfactants owing to
577 their size. Solubility of proteins is an important factor in emulsion stability: if proteins are not
578 readily soluble in water, they favour protein–protein interactions, leading to large aggregates
579 that cannot readily diffuse to the interface (Karaca *et al*., 2011b). More polar proteins are
580 more soluble in water.

581 Protein net charge can contribute to the stability of protein-stabilized emulsions. If proteins
582 give all droplets the same surface charge, there will be electrostatic repulsion between
583 droplets (Richmond, 1990; Magdassi, 1996). This charge is influenced by pH and the
584 contribution of the charge by the ionic environment (Dickinson, 2003; Lam and Nickerson,
585 2013). Around the pI of the protein there is a neutral net charge; this reduces electrostatic
586 repulsion, leading to protein aggregation and in turn promoting flocculation of droplets
587 (Foegeding and Davis, 2011).

588 At the interface, proteins experience a degree of conformational re-orientation and/or
589 unfolding (Walstra, 2002). This is to position hydrophilic residues in the aqueous phase and
590 hydrophobic residues in the oil phase. For smaller proteins with no tertiary structure, for
591 example, casein, this unfolding can readily occur at the interface (Bohin *et al*., 2012). For
592 globular proteins (egg ovalbumin, BSA and β-lactoglobulin), conformational changes are
593 much slower, owing to restraints in restructuring (Baier *et al*., 2005; Najbar *et al*., 2003;
594 Malmsten, 1998).

595 pH influences the ability of proteins to adsorb at interfaces. As pH changes, so too do the
596 charges on amino acid residues. These may play important roles in the conformation of the

proteins. As these change with increasing and decreasing pH, the protein may begin to unfold. This unfolding can expose hydrophobic residues that are buried in the core of the protein, increasing surface activity. These unfolded proteins are more easily able to undergo conformational changes at the interface to reduce the number of unfavourable interactions (McClements, 2015; Tcholakova *et al*., 2006).

Unfolding of proteins at the interface can expose sulfhydryl groups previously buried in the core of the protein. This can lead to the formation of disulphide bonds at the interface. The formation of these disulphide bonds can contribute to increased viscoelasticity of these interfaces, increasing emulsion stability (Dickinson, 1992). However, if the disulphide bonds form between the proteins making up the interfaces on separate droplets, disulphide bond formation can contribute to droplet coalescence (Joshi *et al*., 2012).

The contribution of proteins to interface rheology is important to consider. The contribution of interfacial rheology has been studied in crayfish protein isolate (Romero *et al*., 2011). Through this study it was shown that with changing pH little change in interfacial tension was observed; however, changes in the elasticity of the interface were shown. Increased interface elasticity produced more stable emulsions. Changes in interface rheology have been shown to influence the bulk viscoelasticity of creams (Mackie *et al*., 2007).

2.12.2.3. Particles

Particles can aggregate at oil–water interfaces and form a mechanical barrier to coalescence. Emulsions stabilized by colloidal particles were first presented by Ramsden (1904) and Pickering (1907). These emulsions stabilized by particles have been coined Pickering emulsions. Unlike for surfactants, particles act as a mechanical barrier to coalescence and flocculation with limited reductions in interfacial tension (Hunter *et al*., 2008). This stability is instead caused by a mechanical barrier forming at the interface preventing coalescence of

droplets. This method has been shown to produce very stable emulsions (Binks and Lumsdon, 1999; Aveyard *et al*., 2003). The large energy required for the desorption of particles from the interface makes adsorption of particles to the interface effectively irreversible (Tambe *et al*., 1994). This is different to for surfactants that are in a dynamic equilibrium between the interface and solution. Particle properties influence the stability of emulsions and are now discussed.

2.12.2.3.1. Wettability

Particles were shown to form a densely packed layer at the interface between two immiscible fluids. Particles will provide greater stability to emulsions in which they favour wetting of the continuous phase. This is because the particle's position in the interface is determined by the particle wettability. For particles with a contact angle of water <90º, the majority of the particle will reside in the aqueous phase. A particle with a contact angle for water and of 90º will favour neither the aqueous nor lipid phase. Particles with contact angle for water >90º will reside predominantly in the lipid phase. Unlike for surfactants in which HLB is used, for particles contact angle is used to predict the phase that will be favoured as the dispersed phase in the emulsion (Aveyard *et al*., 2003).

Particles with a contact angle of water <90º will reside predominantly in the aqueous phase; thus, the equator of the particle is in the aqueous phase, producing a monolayer that curves around the lipid phase.

$$E_{det} = \pi r^2 \gamma_{ow} (1 \pm \cos\theta)^2 \qquad (2.6)$$

Equation 2.6 relates the energy of detachment of a particle from the interface to particle properties. The particle radius is represented by r, γ_{ow} is the interfacial tension between the aqueous and lipid phase, and θ represents the contact angle of the particle. From this equation

644 it can be determined that when the contact angle for water of the particle is 90º, the energy of
645 detachment from the interface is greatest (Schmitt *et al*., 2014).

646 Equation 2.6 assumes spherical particles with a uniform surface. However, particles with
647 distinct hydrophobic and hydrophilic surface regions have been investigated and are coined
648 Janus particles. Janus particles have been shown to produce emulsions with greater stability
649 than particles with homogeneous wettability properties (Binks and Fletcher, 2001).

650 *2.12.2.3.2. Size*
651 Particle size contributes to the adsorption and desorption of particles from the interface, with
652 larger particles having slower adsorption and desorption rates. Pickering particles are
653 generally orders of magnitude larger than surfactants, and thus they diffuse much slower. This
654 slow diffusion and absorption to the interface is important during emulsification. Droplets are
655 broken up, increasing the area of interface. The slower rate of adsorption of particles to the
656 interface will leave a greater surface area of the newly formed interface uncovered, leaving it
657 susceptible to coalescence (Niknafs *et al*., 2011; Pichot *et al*., 2009). This often leads to
658 formation of coarser emulsions.

659 In Equation 2.6 for calculating the detachment energy of particles from the interface, particle
660 radius squared is present. From this it is shown that with decreasing particle diameter the
661 energy of detachment from the interface of the particle decreases. It can therefore be observed
662 that particle size is a balance between absorption rates and energy of detachment from the
663 interface.

664 *2.12.2.3.3. Shape*
665 The influence of particle shape on emulsion stability has been investigated by Madivala *et al*.
666 (2009a). It was shown that changing aspect ratio of ellipsoidal particles influenced interface
667 rheology and emulsion stability (Madivala *et al*., 2009b), showing that particles with a higher

aspect ratio could stabilize emulsions that particles of a lower aspect ratio with similar wettability could not. Further studies have shown ellipsoidal particles to stabilize emulsions at lower concentrations than spherical particles (Kralchevsky *et al*., 2005; Vella *et al*., 2004).

2.12.2.3.4. Food-grade Pickering particles

A selection of food-grade particles has been used for the stabilization of emulsions. Solid fat crystals are essential in the stabilization of spreads and margarines, which are W/O emulsions (Hodge and Rousseau, 2005). These include modified starches (Rayner *et al*., 2012; Yusoff and Murray, 2011; Timgren *et al*., 2011), celluloses (Kargar *et al*., 2012; Kalashnikova *et al*., 2011; Melzer *et al*., 2003), protein particles (Paunov *et al*., 2007; de Folter *et al*., 2012), flavonoids (Luo *et al*., 2011; Luo *et al*., 2012) and wax particles (Binks *et al*., 2009).

2.12.2.3.5. Protein particles as Pickering particles

WPI nanoparticles have been used for stabilizing emulsions (Wu *et al*., 2015). These were produced through heating of a W/O emulsion with WPI in the aqueous phase. These particles were shown to produce stable emulsions with good wetting properties at pH above or below pI and low salt concentrations (10 mMol). Soft WPI particles have been produced through gelation then homogenization (Destribats *et al*., 2014).

Alternative protein sources have also been used for the production of protein particles, including pea proteins (Shao and Tang, 2016), peanut protein isolate (Jiao *et al*., 2018) and soy nanoparticles (Liu *et al*., 2013; Liu and Tang, 2016a; Liu and Tang, 2016b)

2.12.3. Emulsion rheology

Flow properties are important in emulsion products and how they are perceived, with high viscosity being shown to contribute to the creamy perception of these products (Kokini, 1987). In mayonnaises, a shear thinning product exhibiting yield stress is expected. Below this yield stress these systems behave as a solid, above this yield stress they will flow. Shear

thinning is observed in high internal phase emulsions. In this section, some of the factors that influence the rheology of emulsions are briefly discussed.

With increasing dispersed phase volume for emulsions, an increase in viscosity is observed; changes in shear thinning and thickening behaviour are also observed. Changes in emulsion droplet packing with increasing dispersed phase concentration have been outlined in previous work (Pal, 2011; Quemada *et al*., 2002; Stickel and Powell, 2005). This work looked at monodisperse emulsions, showing that at low concentrations the droplets do not interact with each other. With increasing concentration, increased spatial confinement of particles is observed, with systems of phase volume >0.58 having solid-like characteristics. Above the maximum random packing fraction of 0.64 for monodisperse spheres, droplets are expected to deform, allowing higher phase volumes to be achieved.

$$\eta_r = \eta_c \left(1 - \frac{\Phi}{\Phi_m}\right)^{-2} \tag{2.7}$$

A simplified model for dispersion rheology (Krieger and Dougherty, 1959b; Barnes, 1994) is presented in Equation 2.7. η_c represents the continuous phase viscosity, Φ represents the phase volume and Φ_m represents the maximum phase volume. From this equation several key factors in emulsion rheology can be observed. The influence of continuous phase viscosity is important (η_c). Increasing the viscosity of the continuous phase will increase the emulsion viscosity. This technique has been used in the development of reduced fat dressings and sauces by the addition of thickeners and gelling agents to the continuous phase, which increases the viscosity of reduced fat emulsions (Sikora *et al*., 2008; Ma *et al*., 2013).

Another factor that influences the viscosity of emulsions is the maximum random packing fraction. For hard monodisperse spheres, the maximum random packing fraction was

calculated by Einstein (1911) to be 0.64. However, if a bi-disperse system with two different sizes of sphere is used, the phase volume of the maximum packing fraction will increase, thus decreasing the viscosity. This has been investigated with mixtures of several different size spheres (Chong *et al*., 1971). For suspensions with a broad size distribution, a larger Φ_m will occur.

Particle shape also contributes to the maximum packing fraction, with particles of higher aspect ratio packing together more tightly than spheres. In emulsions, the change in shape of droplets in laminar flow may contribute

Dispersed phase rheology is generally not important because of the layer formed around droplets by surfactants; however, for high internal phase emulsions like mayonnaises, internal phase rheology is relevant (Derkach, 2009).

2.13. References

ADAMS, S., FRITH, W. J. & STOKES, J. R. 2004. Influence of particle modulus on the rheological properties of agar microgel suspensions. *Journal of Rheology,* 48**,** 1195-1213.

ANANDHARAMAKRISHNAN, C. 2015. *Spray drying techniques for food ingredient encapsulation*, John Wiley & Sons.

ANANDHARAMAKRISHNAN, C., RIELLY, C. D. & STAPLEY, A. G. F. 2008. Loss of solubility of α-lactalbumin and β-lactoglobulin during the spray drying of whey proteins. *LWT - Food Science and Technology,* 41**,** 270-277.

ANASTASI, A., BROWN, M. A., KEMBHAVI, A. A., NICKLIN, M. J. H., SAYERS, C. A., SUNTER, D. C. & BARRETT, A. J. 1983. Cystatin, a protein inhibitor of cysteine proteinases. Improved purification from egg white, characterization, and detection in chicken serum. *Biochemical Journal,* 211**,** 129-138.

AVEYARD, R., BINKS, B. P., CLINT, J. H. J. A. I. C. & SCIENCE, I. 2003. Emulsions stabilised solely by colloidal particles. 100**,** 503-546.

AWADÉ, A. C. & EFSTATHIOU, T. 1999. Comparison of three liquid chromatographic methods for egg-white protein analysis. *Journal of Chromatography B: Biomedical Sciences and Applications,* 723**,** 69-74.

BAIER, S. K., MCCLEMENTS, D. J. J. C. R. I. F. S. & SAFETY, F. 2005. Influence of cosolvent systems on the gelation mechanism of globular protein: thermodynamic, kinetic, and structural aspects of globular protein gelation. 4**,** 43-54.

BARBU, E., BASSET, J. & JOLY, M. 1954. * ACTION DES HAUTES PRESSIONS SUR LA SERUM-ALBUMINE DE CHEVAL-ETUDE PAR LA BIREFRINGENCE

749 DECOULEMENT. *BULLETIN DE LA SOCIETE DE CHIMIE BIOLOGIQUE,* 36**,**
750 323-333.
751 BARNES, H. A. 1994. Rheology of emulsions — a review. *Colloids and Surfaces A:*
752 *Physicochemical and Engineering Aspects,* 91**,** 89-95.
753 BECKTEL, W. J. & SCHELLMAN, J. A. 1987. Protein stability curves. *Biopolymers,* 26**,**
754 1859-1877.
755 BELITZ, H.-D., GROSCH, W. & SCHIEBERLE, P. J. F. C. 2009. Food additives. 429-466.
756 BERNARD, C., BROYART, B., VASSEUR, J., GRANDA, P. and RELKIN, P., 2008.
757 Enhancement of protein structure-forming properties in liquid foams by spray drying.
758 Dairy science & technology, 88(1), pp.65-80.
759 BERNARD, C., REGNAULT, S., GENDREAU, S., CHARBONNEAU, S. and RELKIN, P.,
760 2011. Enhancement of emulsifying properties of whey proteins by controlling spray-
761 drying parameters. Food Hydrocolloids, 25(4), pp.758-763.
762 BINKS, B. & LUMSDON, S. J. P. C. C. P. 1999. Stability of oil-in-water emulsions
763 stabilised by silica particles. 1**,** 3007-3016.
764 BINKS, B. P. & FLETCHER, P. D. I. 2001. Particles Adsorbed at the Oil−Water Interface: A
765 Theoretical Comparison between Spheres of Uniform Wettability and "Janus"
766 Particles. *Langmuir,* 17**,** 4708-4710.
767 BINKS, B.P. and ROCHER, A., 2009. Effects of temperature on water-in-oil emulsions
768 stabilised solely by wax microparticles. Journal of colloid and interface science,
769 335(1), pp.94-104.
770 BOHIN, M. C., VINCKEN, J.-P., VAN DER HIJDEN, H. T., GRUPPEN, H. J. J. O. A. &
771 CHEMISTRY, F. 2012. Efficacy of food proteins as carriers for flavonoids. 60**,** 4136-
772 4143.

BOWDEN, F. P. & TABOR, D. 1964. *The friction and lubrication of solids. Vol. 2*, OUP.

BOYE, J. I., AKSAY, S., ROUFIK, S., RIBÉREAU, S., MONDOR, M., FARNWORTH, E. & RAJAMOHAMED, S. H. 2010. Comparison of the functional properties of pea, chickpea and lentil protein concentrates processed using ultrafiltration and isoelectric precipitation techniques. *Food Research International,* 43**,** 537-546.

BRUGGER, B., ROSEN, B. A. & RICHTERING, W. J. L. 2008. Microgels as stimuli-responsive stabilizers for emulsions. 24**,** 12202-12208.

CAMPBELL, L., RAIKOS, V. & EUSTON, S. R. 2003. Modification of functional properties of egg-white proteins. *Food / Nahrung,* 47**,** 369-376.

CASSIN, G., APPELQVIST, I., NORMAND, V. & NORTON, I. 2000. Stress-induced compaction of concentrated dispersions of gel particles. *Colloid and Polymer Science,* 278**,** 777-782.

CHI, E. Y., KRISHNAN, S., KENDRICK, B. S., CHANG, B. S., CARPENTER, J. F. & RANDOLPH, T. W. 2003a. Roles of conformational stability and colloidal stability in the aggregation of recombinant human granulocyte colony-stimulating factor. *Protein Science,* 12**,** 903-913.

CHI, E. Y., KRISHNAN, S., RANDOLPH, T. W. & CARPENTER, J. F. 2003b. Physical Stability of Proteins in Aqueous Solution: Mechanism and Driving Forces in Nonnative Protein Aggregation. *Pharmaceutical Research,* 20**,** 1325-1336.

CHONG, J. S., CHRISTIANSEN, E. B. & BAER, A. D. 1971. Rheology of concentrated suspensions. 15**,** 2007-2021.

CONWAY, B. E. & AYRANCI, E. 1999. Effective Ionic Radii and Hydration Volumes for Evaluation of Solution Properties and Ionic Adsorption. *Journal of Solution Chemistry,* 28**,** 163-192.

797 COULOMB, C. 1785. The theory of simple machines. *Mem. Math. Phys. Acad. Sci,* 10**,** 4.
798 CROGUENNEC, T., NAU, F. & BRULÉ, G. 2002. Influence of pH and Salts on Egg White
799 Gelation. *Journal of Food Science,* 67**,** 608-614.
800 DAMODARAN, S. J. F. S. F. C. 2008. Amino acids, peptides and proteins. 4**,** 217-329.
801 DAVIS, H. T. 1994. Factors determining emulsion type: Hydrophile—lipophile balance and
802 beyond. *Colloids and Surfaces A: Physicochemical and Engineering Aspects,* 91**,** 9-
803 24.
804 DE FOLTER, J. W., VAN RUIJVEN, M. W. & VELIKOV, K. P. 2012. Oil-in-water
805 Pickering emulsions stabilized by colloidal particles from the water-insoluble protein
806 zein. *Soft Matter,* 8**,** 6807-6815.
807 DE VICENTE, J., SPIKES, H. A. & STOKES, J. R. 2006. Viscosity Ratio Effect in the
808 Emulsion Lubrication of Soft EHL Contact. *Journal of Tribology,* 128**,** 795-800.
809 DE WIJK, R. A. & PRINZ, J. F. 2005. The role of friction in perceived oral texture. *Food*
810 *Quality and Preference,* 16**,** 121-129.
811 DE WIJK, R. A., VAN GEMERT, L. J., TERPSTRA, M. E. J. & WILKINSON, C. L. 2003.
812 Texture of semi-solids; sensory and instrumental measurements on vanilla custard
813 desserts. *Food Quality and Preference,* 14**,** 305-317.
814 DE WIT, J. 1989. The milk protein system, Functional properties of whey proteins.
815 *Developments in Dairy Chemistry-4*.
816 DEBYE, P. & HÜCKEL, E. 1923. De la theorie des electrolytes. I. abaissement du point de
817 congelation et phenomenes associes. *Physikalische Zeitschrift,* 24**,** 185-206.
818 DEPREE, J. A. & SAVAGE, G. P. 2001. Physical and flavour stability of mayonnaise.
819 *Trends in Food Science & Technology,* 12**,** 157-163.

DERKACH, S. R. 2009. Rheology of emulsions. *Advances in Colloid and Interface Science,* 151**,** 1-23.

DESTRIBATS, M., ROUVET, M., GEHIN-DELVAL, C., SCHMITT, C. & BINKS, B. P. J. S. M. 2014. Emulsions stabilised by whey protein microgel particles: towards food-grade Pickering emulsions. 10**,** 6941-6954.

DICKINSON, E. 1992. *Introduction to food colloids,* Oxford University Press.

DICKINSON, E. & PARKINSON, E. L. 2004. Heat-induced aggregation of milk protein-stabilized emulsions: sensitivity to processing and composition. *International Dairy Journal,* 14**,** 635-645.

DICKINSON, E. J. F. B. 2011. Double emulsions stabilized by food biopolymers. 6**,** 1-11.

DICKINSON, E. J. F. H. 2003. Hydrocolloids at interfaces and the influence on the properties of dispersed systems. 17**,** 25-39.

DILL, K. A. 1990. Dominant forces in protein folding. *Biochemistry,* 29**,** 7133-7155.

Dowson, D., 1996. Tribology and the skin surface. Bioengineering of the skin: Skin surface imaging and analysis, pp.159-179.

DRESSELHUIS, D. M., KLOK, H. J., STUART, M. A. C., DE VRIES, R. J., VAN AKEN, G. A. & DE HOOG, E. H. A. 2007. Tribology of o/w Emulsions Under Mouth-like Conditions: Determinants of Friction. *Food Biophysics,* 2**,** 158-171.

EINSTEIN, A. 1906. A new determination of molecular dimensions. *Ann. Phys.,* 19**,** 289-306.

EINSTEIN, A. J. A. D. P. 1911. Berichtigung zu meiner Arbeit:„Eine neue Bestimmung der Moleküldimensionen" . 339**,** 591-592.

ETZEL, M. R. 2004a. Manufacture and Use of Dairy Protein Fractions. *The Journal of Nutrition,* 134**,** 996S-1002S.

ETZEL, M. R. J. T. J. O. N. 2004b. Manufacture and use of dairy protein fractions. 134**,** 996S-1002S.

FARID, M. 2003. A new approach to modelling of single droplet drying. *Chemical Engineering Science,* 58**,** 2985-2993.

FARRÉS, I. F. & NORTON, I. 2014. Formation kinetics and rheology of alginate fluid gels produced by in-situ calcium release. *Food Hydrocolloids,* 40**,** 76-84.

FEDERATION, I. D. 1998. *The World Dairy Situation*, IDF General Secretariat.

FERNÁNDEZ FARRÉS, I., DOUAIRE, M. & NORTON, I. T. 2013. Rheology and tribological properties of Ca-alginate fluid gels produced by diffusion-controlled method. *Food Hydrocolloids,* 32**,** 115-122.

FERNÁNDEZ FARRÉS, I. & NORTON, I. T. 2015. The influence of co-solutes on tribology of agar fluid gels. *Food Hydrocolloids,* 45**,** 186-195.

FOEGEDING, E. A., BOWLAND, E. L. & HARDIN, C. C. 1995. Factors that determine the fracture properties and microstructure of globular protein gels. *Food Hydrocolloids,* 9**,** 237-249.

FOEGEDING, E. A. & DAVIS, J. P. J. F. H. 2011. Food protein functionality: A comprehensive approach. 25**,** 1853-1864.

FRITH, W., GARIJO, X., FOSTER, T. & NORTON, I. 2002. Microstructural origins of the rheology of fluid gels. *Special Publication-royal Society of Chemistry,* 278**,** 95-103.

G. MULKERRIN, M. & WETZEL, R. 1989. *pH dependence of the reversible and irreversible thermal denaturation of γ interferons*.

GABRIELE, A., SPYROPOULOS, F. & NORTON, I. 2010. A conceptual model for fluid gel lubrication. *Soft Matter,* 6**,** 4205-4213.

GABRIELE, A., SPYROPOULOS, F. & NORTON, I. T. 2009. Kinetic study of fluid gel formation and viscoelastic response with kappa-carrageenan. *Food Hydrocolloids,* 23**,** 2054-2061.

GANEA, C., BABES, A., LÜPFERT, C., GRELL, E., FENDLER, K. & CLARKE, R. J. 1999. Hofmeister Effects of Anions on the Kinetics of Partial Reactions of the Na+,K+-ATPase. *Biophysical Journal,* 77**,** 267-281.

GARREC, D. A. & NORTON, I. T. 2012. Understanding fluid gel formation and properties. *Journal of Food Engineering,* 112**,** 175-182.

GARREC, D. A. & NORTON, I. T. 2013. Kappa carrageenan fluid gel material properties. Part 2: Tribology. *Food Hydrocolloids,* 33**,** 160-167.

GIDLEY, M. J. & HEDGES, N. D. 1998. Suspensions of gelled biopolymers. Google Patents.

GREENWOOD, J. & WILLIAMSON, J. P. Contact of nominally flat surfaces. Proceedings of the Royal Society of London A: Mathematical, Physical and Engineering Sciences, 1966. The Royal Society, 300-319.

GRIFFIN, W. C. J. J. S. C. C. 1949. Classification of surface-active agents by" HLB". 1**,** 311-326.

GRIMSLEY, G. 1999. *Increasing protein stability by altering long-range coulombic interactions*.

HALL, G. M. 1996. *Methods of testing protein functionality,* Springer Science & Business Media.

HANDA, A., TAKAHASHI, K., KURODA, N. & FRONING, G. W. 1998. Heat-induced Egg White Gels as Affected by pH. *Journal of Food Science,* 63**,** 403-407.

HERTZ, H. 1881. On the contact of elastic solids. *Z. Reine Angew. Mathematik,* 92**,** 156-171.

889 HODGE, S. & ROUSSEAU, D. 2005. Continuous-phase fat crystals strongly influence water-
890 in-oil emulsion stability. *Journal of the American Oil Chemists' Society,* 82**,** 159-164.
891 HOFMEISTER, F. 1888. Zur lehre von der wirkung der salze. *Archiv für experimentelle*
892 *Pathologie und Pharmakologie,* 25**,** 1-30.
893 HOLT, D. L., WATSON, M. A., DILL, C. W., ALFORD, E. S., EDWARDS, R. L., DIEHL,
894 K. C. & GARDNER, F. A. 1984. Correlation of the Rheological Behavior of Egg
895 Albumen to Temperature, pH, and NaCl Concentration. *Journal of Food Science,* 49**,**
896 137-141.
897 HUNTER, T. N., PUGH, R. J., FRANKS, G. V., JAMESON, G. J. J. A. I. C. & SCIENCE, I.
898 2008. The role of particles in stabilising foams and emulsions. 137**,** 57-81.
899 HUOPALAHTI, R., ANTON, M., LÓPEZ-FANDIÑO, R. & SCHADE, R. 2007. *Bioactive*
900 *egg compounds,* Springer.
901 IP, A., ARAKAWA, T., SILVERS, H., M. RANSONE, C. & W. NIVEN, R. 1995. *Stability*
902 *of recombinant consensus interferon to air-jet and ultrasonic nebulization*.
903 IZABELA, S., MICHAEL, C. & ROBERT, W. C. 2008. Recent advances in single-asperity
904 nanotribology. *Journal of Physics D: Applied Physics,* 41**,** 123001.
905 JIAO, B., SHI, A., WANG, Q. & BINKS, B. P. 2018. High-Internal-Phase Pickering
906 Emulsions Stabilized Solely by Peanut-Protein-Isolate Microgel Particles with
907 Multiple Potential Applications. 57**,** 9274-9278.
908 JORDAN, I. K., KONDRASHOV, F. A., ADZHUBEI, I. A., WOLF, Y. I., KOONIN, E. V.,
909 KONDRASHOV, A. S. & SUNYAEV, S. 2005. A universal trend of amino acid gain
910 and loss in protein evolution. *Nature,* 433**,** 633.

JOSHI, M., ADHIKARI, B., ALDRED, P., PANOZZO, J., KASAPIS, S. & BARROW, C. J. F. C. 2012. Interfacial and emulsifying properties of lentil protein isolate. 134**,** 1343-1353.

KAKALIS, L. T. & REGENSTEIN, J. M. 1986. Effect of pH and salts on the solubility of egg white protein. *Journal of Food Science,* 51**,** 1445-1447.

KALASHNIKOVA, I., BIZOT, H., CATHALA, B. & CAPRON, I. 2011. New Pickering emulsions stabilized by bacterial cellulose nanocrystals. *Langmuir*, 27**,** 7471-7479.

KARACA, A. C., LOW, N. & NICKERSON, M. 2011a. Emulsifying properties of chickpea, faba bean, lentil and pea proteins produced by isoelectric precipitation and salt extraction. *Food Research International*, 44**,** 2742-2750.

KARACA, A. C., LOW, N. & NICKERSON, M. J. F. R. I. 2011b. Emulsifying properties of chickpea, faba bean, lentil and pea proteins produced by isoelectric precipitation and salt extraction. 44**,** 2742-2750.

KARGAR, M., FAYAZMANESH, K., ALAVI, M., SPYROPOULOS, F. & NORTON, I. T. 2012. Investigation into the potential ability of Pickering emulsions (food-grade particles) to enhance the oxidative stability of oil-in-water emulsions. *Journal of colloid and interface science,* 366**,** 209-215.

KETTERER, B. 1965. Ovoglycoprotein, a protein of hen's-egg white. *The Biochemical journal*, 96**,** 372-376.

KIM, H., DECKER, E. & MCCLEMENTS, D. J. L. 2005. Influence of protein concentration and order of addition on thermal stability of β-lactoglobulin stabilized n-hexadecane oil-in-water emulsions at neutral pH. 21**,** 134-139.

KOKINI, J. L. 1987. The physical basis of liquid food texture and texture-taste interactions. *Journal of Food Engineering,* 6**,** 51-81.

KOSEKI, T., KITABATAKE, N. & DOI, E. 1989. Irreversible thermal denaturation and formation of linear aggregates of ovalbumin. *Food Hydrocolloids,* 3**,** 123-134.

KOVACS-NOLAN, J., PHILLIPS, M., MINE, Y. J. J. O. A. & CHEMISTRY, F. 2005. Advances in the value of eggs and egg components for human health. 53**,** 8421-8431.

KRALCHEVSKY, P., IVANOV, I., ANANTHAPADMANABHAN, K. & LIPS, A. J. L. 2005. On the thermodynamics of particle-stabilized emulsions: curvature effects and catastrophic phase inversion. 21**,** 50-63.

KRALOVA, I., SJÖBLOM, J. J. J. O. D. S. & TECHNOLOGY 2009. Surfactants used in food industry: a review. 30**,** 1363-1383.

KRIEGER, I. M. & DOUGHERTY, T. J. J. T. O. T. S. O. R. 1959. A mechanism for non-Newtonian flow in suspensions of rigid spheres. 3**,** 137-152.

KUHN, P. R. & FOEGEDING, E. A. 1991. Factors Influencing Whey Protein Gel Rheology: Dialysis and Calcium Chelation. *Journal of Food Science,* 56**,** 789-791.

LAM, R. S. & NICKERSON, M. T. J. F. C. 2013. Food proteins: a review on their emulsifying properties using a structure–function approach. 141**,** 975-984.

LANGTON, M. & HERMANSSON, A.-M. 1992. Fine-stranded and particulate gels of β-lactoglobulin and whey protein at varying pH. *Food Hydrocolloids,* 5**,** 523-539.

LAZIDIS, A., HANCOCKS, R. D., SPYROPOULOS, F., KREUß, M., BERROCAL, R. & NORTON, I. T. 2016. Whey protein fluid gels for the stabilisation of foams. *Food Hydrocolloids,* 53**,** 209-217.

LI-CHAN, E. J. C. C. R. P. B. 1989. Biochemical basis for the properties of egg white. 2**,** 21-58.

LIU, F. & TANG, C.-H. 2016a. Soy glycinin as food-grade Pickering stabilizers: Part. II. Improvement of emulsification and interfacial adsorption by electrostatic screening. *Food Hydrocolloids,* 60**,** 620-630.

LIU, F. & TANG, C.-H. 2016b. Soy glycinin as food-grade Pickering stabilizers: Part. III. Fabrication of gel-like emulsions and their potential as sustained-release delivery systems for β-carotene. *Food Hydrocolloids,* 56**,** 434-444.

LIU, F., TANG, C.-H. J. J. O. A. & CHEMISTRY, F. 2013. Soy protein nanoparticle aggregates as Pickering stabilizers for oil-in-water emulsions. 61**,** 8888-8898.

LUO, Z., MURRAY, B. S., ROSS, A.-L., POVEY, M. J. W., MORGAN, M. R. A. & DAY, A. J. 2012. Effects of pH on the ability of flavonoids to act as Pickering emulsion stabilizers. *Colloids and Surfaces B: Biointerfaces,* 92**,** 84-90.

LUO, Z., MURRAY, B. S., YUSOFF, A., MORGAN, M. R. A., POVEY, M. J. W. & DAY, A. J. 2011. Particle-Stabilizing Effects of Flavonoids at the Oil−Water Interface. *Journal of Agricultural and Food Chemistry,* 59**,** 2636-2645.

MA, Z., BOYE, J. I. J. F. & TECHNOLOGY, B. 2013. Advances in the design and production of reduced-fat and reduced-cholesterol salad dressing and mayonnaise: a review. 6**,** 648-670.

MACKIE, A. R., RIDOUT, M. J., MOATES, G., HUSBAND, F. A., WILDE, P. J. J. J. O. A. & CHEMISTRY, F. 2007. Effect of the interfacial layer composition on the properties of emulsion creams. 55**,** 5611-5619.

MADIVALA, B., FRANSAER, J. & VERMANT, J. J. L. 2009a. Self-assembly and rheology of ellipsoidal particles at interfaces. 25**,** 2718-2728.

MADIVALA, B., VANDEBRIL, S., FRANSAER, J. & VERMANT, J. J. S. M. 2009b. Exploiting particle shape in solid stabilized emulsions. 5**,** 1717-1727.

MADUREIRA, A. R., PEREIRA, C. I., GOMES, A. M., PINTADO, M. E. & MALCATA, F. X. J. F. R. I. 2007. Bovine whey proteins–Overview on their main biological properties. 40**,** 1197-1211.

MAGDASSI, S. 1996. *Surface activity of proteins: chemical and physicochemical modifications*, Crc Press.

MALMSTEN, M. 1998. *Biopolymers at interfaces*, CRC Press.

MALONE, M. E., APPELQVIST, I. A. M. & NORTON, I. T. 2003. Oral behaviour of food hydrocolloids and emulsions. Part 1. Lubrication and deposition considerations. *Food Hydrocolloids,* 17**,** 763-773.

MANN, B. & MALIK, R. 1996. Studies on some functional characteristics of whey protein-polysaccharide complex.

MASTERS, G. M. & ELA, W. P. 1991. *Introduction to environmental engineering and science*, Prentice Hall Englewood Cliffs, NJ.

MCCLEMENTS, D. Food Emulsions: Principles, Practice, and Techniques. CRC series in contemporary food science. 2005. Boca Raton: CRC Press.

MCCLEMENTS, D. J. 2015. *Food emulsions: principles, practices, and techniques*, CRC press.

MELZER, E., KREUTER, J. & DANIELS, R. 2003. Ethylcellulose: a new type of emulsion stabilizer. *European Journal of Pharmaceutics and Biopharmaceutics,* 56**,** 23-27.

MILLS, T., KOAY, A. & NORTON, I. T. 2013. Fluid gel lubrication as a function of solvent quality. *Food Hydrocolloids,* 32**,** 172-177.

MOAKES, R. J. A., SULLO, A. & NORTON, I. T. 2015. Preparation and characterisation of whey protein fluid gels: The effects of shear and thermal history. *Food Hydrocolloids,* 45**,** 227-235.

NAJBAR, L. V., CONSIDINE, R. F. & DRUMMOND, C. J. J. L. 2003. Heat-induced aggregation of a globular egg-white protein in aqueous solution: investigation by atomic force microscope imaging and surface force mapping modalities. 19**,** 2880-2887.

NELSON, D. L., LEHNINGER, A. L. & COX, M. M. 2008. *Lehninger principles of biochemistry*, Macmillan.

NGAI, T., AUWETER, H. & BEHRENS, S. H. J. M. 2006. Environmental responsiveness of microgel particles and particle-stabilized emulsions. 39**,** 8171-8177.

NIKNAFS, N., SPYROPOULOS, F. & NORTON, I. T. J. J. O. F. E. 2011. Development of a new reflectance technique to investigate the mechanism of emulsification. 104**,** 603-611.

NORTON, A. B. 2016. *Microstructural understanding of hydrocolloid and mixed hydrocolloid systems for biomedical applications.* University of Birmingham.

NORTON, I., GOODALL, D., AUSTEN, K., MORRIS, E. & REES, D. 1986. Dynamics of molecular organization in agarose sulphate. *Biopolymers,* 25**,** 1009-1029.

NORTON, I. T., JARVIS, D. A. & FOSTER, T. J. 1999. A molecular model for the formation and properties of fluid gels. *International Journal of Biological Macromolecules,* 26**,** 255-261.

NUCCI, N. V. & VANDERKOOI, J. M. 2008. Effects of Salts of the Hofmeister Series on the Hydrogen Bond Network of Water. *Journal of molecular liquids,* 143**,** 160-170.

OMANA, D. A., WANG, J. & WU, J. J. J. O. C. B. 2010. Co-extraction of egg white proteins using ion-exchange chromatography from ovomucin-removed egg whites. 878**,** 1771-1776.

PACE, C. N., GRIMSLEY, G. R. & SCHOLTZ, J. M. 2009. Protein ionizable groups: pK values and their contribution to protein stability and solubility. *Journal of Biological Chemistry,* 284**,** 13285-13289.

PAL, R. 2011. Rheology of simple and multiple emulsions. *Current Opinion in Colloid & Interface Science* 16**,** 41-60.

PASQUALI, R. C., TAUROZZI, M. P. & BREGNI, C. J. I. J. O. P. 2008. Some considerations about the hydrophilic–lipophilic balance system. 356**,** 44-51.

PAULING, L., COREY, R. B. & BRANSON, H. R. J. P. O. T. N. A. O. S. 1951. The structure of proteins: two hydrogen-bonded helical configurations of the polypeptide chain. 37**,** 205-211.

PAUNOV, V. N., CAYRE, O. J., NOBLE, P. F., STOYANOV, S. D., VELIKOV, K. P. & GOLDING, M. 2007. Emulsions stabilised by food colloid particles: Role of particle adsorption and wettability at the liquid interface. *Journal of colloid and interface science,* 312**,** 381-389.

PELEGRINE, D. H. G. & GASPARETTO, C. A. 2005. Whey proteins solubility as function of temperature and pH. *LWT - Food Science and Technology,* 38**,** 77-80.

PICHOT, R., SPYROPOULOS, F., NORTON, I. J. J. O. C. & SCIENCE, I. 2009. Mixed-emulsifier stabilised emulsions: Investigation of the effect of monoolein and hydrophilic silica particle mixtures on the stability against coalescence. 329**,** 284-291.

PICKERING, S. U. 1907. CXCVI.-Emulsions. *Journal of the Chemical Society, Transactions,* 91**,** 2001-2021.

PUGLIESE, L., MALCOVATI, M., CODA, A. & BOLOGNESI, M. 1994. Crystal structure of apo-avidin from hen egg-white. *Journal of Molecular Biology,* 235**,** 42-46.

QUEMADA, D., BERLI, C. J. A. I. C. & SCIENCE, I. 2002. Energy of interaction in colloids and its implications in rheological modeling. 98**,** 51-85.

RAMSDEN, W. J. P. O. T. R. S. O. L. 1904. Separation of solids in the surface-layers of solutions and 'suspensions'(observations on surface-membranes, bubbles, emulsions, and mechanical coagulation).—Preliminary account. 72**,** 156-164.

RAYNER, M., TIMGREN, A., SJÖÖ, M. & DEJMEK, P. 2012. Quinoa starch granules: a candidate for stabilising food-grade Pickering emulsions. *Journal of the Science of Food and Agriculture,* 92**,** 1841-1847.

RELKIN, P., BERNARD, C., MEYLHEUC, T., VASSEUR, J. and COURTOIS, F., 2007. Production of whey protein aggregates with controlled end-use properties. Le lait, 87(4-5), pp.337-348.

RENKEMA, J.M., GRUPPEN, H. and VAN VLIET, T., 2002. Influence of pH and ionic strength on heat-induced formation and rheological properties of soy protein gels in relation to denaturation and their protein compositions. Journal of Agricultural and Food Chemistry, 50(21), pp.6064-6071.

RENKEMA, J.M., GRUPPEN, H. and VAN VLIET, T., 2002. Influence of pH and ionic strength on heat-induced formation and rheological properties of soy protein gels in relation to denaturation and their protein compositions. Journal of Agricultural and Food Chemistry, 50(21), pp.6064-6071.

RICHMOND, J. 1990. *Cationic surfactants: organic chemistry,* CRC Press.

ROMERO, A., BEAUMAL, V., DAVID-BRIAND, E., CORDOBÉS, F., ANTON, M., GUERRERO, A. J. L.-F. S. & TECHNOLOGY 2011. Interfacial and emulsifying behaviour of crayfish protein isolate. 44**,** 1603-1610.

ROSEN, M. J. & KUNJAPPU, J. T. 2012. *Surfactants and interfacial phenomena*, John Wiley & Sons.

SCHMITT, V., DESTRIBATS, M. & BACKOV, R. J. C. R. P. 2014. Colloidal particles as liquid dispersion stabilizer: Pickering emulsions and materials thereof. 15**,** 761-774.

SHAH, S. M. & LUKSAS, A. J. 1980. Food composition containing whey colloidal precipitate. Google Patents.

SHAO, Y. & TANG, C.-H. 2016. Gel-like pea protein Pickering emulsions at pH3.0 as a potential intestine-targeted and sustained-release delivery system for β-carotene. *Food Research International,* 79**,** 64-72.

SHEWAN, H.M., PRADAL, C. and STOKES, J.R., 2020. Tribology and its growing use toward the study of food oral processing and sensory perception. Journal of Texture Studies, 51(1), pp.7-22.

SHIMIZU, M., NAKANE, Y. J. B., BIOTECHNOLOGY, & BIOCHEMISTRY 1995. Encapsulation of biologically active proteins in a multiple emulsion. 59**,** 492-496.

SIKORA, M., BADRIE, N., DEISINGH, A. K., KOWALSKI, S. J. C. R. I. F. S. & NUTRITION 2008. Sauces and dressings: a review of properties and applications. 48**,** 50-77.

SJOBLOM, J. 2001. *Encyclopedic handbook of emulsion technology*, CRC press.

STADELMAN, W. J., NEWKIRK, D. & NEWBY, L. 2017. *Egg science and technology*, CRC Press.

STEVENS, L. 1991. *Genetics and Evolution of the Domestic Fowl.* Cambridge: Cambridge University Press.

STICKEL, J. J. & POWELL, R. L. J. A. R. F. M. 2005. Fluid mechanics and rheology of dense suspensions. 37**,** 129-149.

STRIBECK, R. 1902. Die wesentlichen eigenschaften der gleit-und rollenlager. *Zeitschrift des Vereines Deutscher Ingenieure,* 46**,** 1341-1348, 1432-1438, 1463-1470.

STRIOLO, A., BRATKO, D., WU, J. Z., ELVASSORE, N., BLANCH, H. W. & PRAUSNITZ, J. M. 2002. Forces between aqueous nonuniformly charged colloids from molecular simulation. *The Journal of Chemical Physics,* 116**,** 7733-7743.

STROP, P. & MAYO, S. L. 2000. Contribution of Surface Salt Bridges to Protein Stability. *Biochemistry,* 39**,** 1251-1255.

TAMBE, D. E., SHARMA, M. M. J. A. I. C. & SCIENCE, I. 1994. The effect of colloidal particles on fluid-fluid interfacial properties and emulsion stability. 52**,** 1-63.

TANFORD, C. & KIRKWOOD, J. G. 1957. Theory of Protein Titration Curves. I. General Equations for Impenetrable Spheres. *Journal of the American Chemical Society,* 79**,** 5333-5339.

TCHOLAKOVA, S., DENKOV, N. D., IVANOV, I. B., CAMPBELL, B. J. A. I. C. & SCIENCE, I. 2006. Coalescence stability of emulsions containing globular milk proteins. 123**,** 259-293.

TIMGREN, A., RAYNER, M., SJÖÖ, M. & DEJMEK, P. 2011. Starch particles for food based Pickering emulsions. *Procedia Food Science,* 1**,** 95-103.

TOLLINGER, M., CROWHURST, K. A., KAY, L. E. & FORMAN-KAY, J. D. 2003. Site-specific contributions to the pH dependence of protein stability. *Proceedings of the National Academy of Sciences,* 100**,** 4545-4550.

TOMIMATSU, Y., CLARY, J. J. & BARTULOVICH, J. J. 1966. Physical characterization of ovoinhibitor, a trypsin and chymotrypsin inhibitor from chicken egg white. *Archives of Biochemistry and Biophysics,* 115**,** 536-544.

TOVAR JIMÉNEZ, X., ARANA CUENCA, A., TÉLLEZ JURADO, A., ABREU CORONA, A. & MURO URISTA, C. R. J. J. O. T. M. C. S. 2012. Traditional methods for whey protein isolation and concentration: effects on nutritional properties and biological activity. 56**,** 369-377.

TSAI, A. M., VAN ZANTEN, J. H. & BETENBAUGH, M. J. 1998. II. Electrostatic effect in the aggregation of heat-denatured RNase A and implications for protein additive design. *Biotechnology and Bioengineering,* 59**,** 281-285.

VELLA, D., AUSSILLOUS, P. & MAHADEVAN, L. J. E. 2004. Elasticity of an interfacial particle raft. 68**,** 212.

VERHEUL, M. & ROEFS, S. P. F. M. 1998. Structure of Particulate Whey Protein Gels: Effect of NaCl Concentration, pH, Heating Temperature, and Protein Composition. *Journal of Agricultural and Food Chemistry,* 46**,** 4909-4916.

WALSTRA, P. 2002. *Physical chemistry of foods*, CRC Press.

WAN, Y., LU, J., CUI, Z. J. S. & TECHNOLOGY, P. 2006. Separation of lysozyme from chicken egg white using ultrafiltration. 48**,** 133-142.

WILLIAMS, J. 2005. *Engineering tribology*, Cambridge University Press.

WONG, D. W., CAMIRAND, W. M., PAVLATH, A. E., PARRIS, N. & FRIEDMAN, M. 1996. Structures and functionalities of milk proteins. *Critical Reviews in Food Science & Nutrition,* 36**,** 807-844.

WU, J., SHI, M., LI, W., ZHAO, L., WANG, Z., YAN, X., NORDE, W. & LI, Y. 2015. Pickering emulsions stabilized by whey protein nanoparticles prepared by thermal cross-linking. *Colloids and Surfaces B: Biointerfaces,* 127**,** 96-104.

YUSOFF, A. & MURRAY, B. S. 2011. Modified starch granules as particle-stabilizers of oil-in-water emulsions. *Food Hydrocolloids,* 25**,** 42-55.

ZHU, H. & DAMODARAN, S. 1994. Effects of calcium and magnesium ions on aggregation of whey protein isolate and its effect on foaming properties. *Journal of Agricultural and Food Chemistry*, 42**,** 856-862.

ZHU, H., DAMODARAN, S. J. J. O. A. & CHEMISTRY, F. 1994. Effects of calcium and magnesium ions on aggregation of whey protein isolate and its effect on foaming properties. 42**,** 856-862.

CHAPTER 3.
Influence of pH on protein fluid gels

3.1. Introduction

In this chapter, the potential for egg white proteins and WPI for the production of fluid gels is investigated. As highlighted in Chapter 2, protein fluid gels show potential for use in reduced fat semisolid foods. Proteins are a clean label ingredient with a positive perception by consumers deemed to be nutritionally desirable. The influence of pH on the properties of these fluid gels is investigated. Understanding how pH influences these systems is important if they are to be used in mayonnaises and other acidic products. The net charge of protein will change as pH changes relative to the pI of the protein.

3.2. Materials

3.2.1. WPI

WPI (Davisco) was used. Protein (89.4%), ash (3.0%), moisture (0.4%) and lactose (0.3%).

3.2.2. Egg white

Chicken eggs were purchased from a supermarket (Tesco) and separated by hand.

3.2.3. Acetic acid

2M acetic acid was purchased from Sigma Aldrich (UK).

3.3. Methods

3.3.1. Solution preparation

3.3.1.1. WPI

A stock solution of 15% w/w was produced by gradual addition of WPI powder to distilled water gently stirred by means of a magnetic stirrer for 12 hours at 6ºC. 0.01% sodium azide was added to this stock solution to prevent bacterial growth. Stock solution was stored in a fridge at 6ºC until use, for a maximum of 30 days. Solutions for fluid gel production were prepared from this stock solution by mixing with 2 M acetic acid to the desired pH. The solution was then made up to the appropriate volume with distilled water to give a final

concentration of 12% w/w and further mixed for 10 minutes. Three different pH solutions were prepared.

- pH_{Native}: the pH of the WPI solution dispersed in distilled water was not adjusted. For WPI, this was pH 8. This was used as it is above the pI, so the protein is expected to have a net negative charge.
- pI: this is well documented as pH 4.9 for WPI (Demetriades *et al*., 1997). This was used as at the pI the protein is expected to have a net neutral charge.
- pH 3.5: this pH was used as it is below the pI, so the protein is expected to have a net positive charge.

A concentration of 12% was chosen for WPI fluid gels as this is the concentration that was used previously by Lazidis *et al.* (2016) for the production of WPI fluid gels.

3.3.1.2. Egg white

The egg whites were heated to 65°C and held at this temperature for 10 minutes while stirring gently. The resultant solution was then passed through a 1 mm sieve. This process removed ovomucoid and ovotransferrin from the egg white; ovotransferrin is the second most prevalent protein in egg white after ovoalbumin. Ovotransferrin was shown to inhibit fluid gel formation as discussed later in section 3.3.1.2. This treated egg white was then stored in a fridge for no longer than 1 week before use. The treated egg white was mixed with 2 M acetic acid to the desired pH before being made up to a final dilution of 75% w/w with distilled water. Three different pH solutions were prepared.

- pH_{Native}: the pH of the solution was not adjusted. For the treated egg white, this pH was 7.5. This was used as it is above the pI of ovoalbumin, so the protein is expected to have a net negative charge.

- pI: the pH solution was prepared at pH 4.5 as this is documented as the pI for ovoalbumin, the main protein in egg white (Stevens, 1991). This was used as at the pI of ovalbumin the protein is expected to have a net neutral charge.
- pH 3.5: this pH was used as it is below the pI of ovoalbumin, so the protein is expected to have a net positive charge.

Final protein concentration in the egg white sample post heat treatment and dilution was estimated using absorbance at 280 nm in line with methods outlined by Ross (1991). The final protein concentration was calculated to be between 6.9 and 7.6% w/w.

This regime of heat treatment and concentration of egg white was determined experimentally. A concentration of 75% was used as initial experiments showed 100% concentration to gel around the vane geometry in the rheometer and not form a homogeneous sample, producing particles between the cylinder of gel formed around the vane and the cup geometry. A concentration of 50% was shown to foam out of the geometry. Heat treatment for the removal of ovotransferrin was used. As in preliminary experiments, ovotransferrin was shown not to produce distinct particles within the cup and vane geometry of the rheometer. This was shown by performing fluid gel preparation experiments up to different maximum temperatures. Samples prepared at a maximum temperature of 65ºC separated into a gel phase and a yellow translucent liquid phase. The translucent nature of the liquid phase indicated that there were no particles dispersed within this phase, which was confirmed with light microscopy.

3.3.2. Fluid gel preparation

A vane and cup geometry was used on a Malvern Kinexus Rheometer. The vane and cup geometry was used as this geometry produces the largest volume of sample. The solutions were allowed to equilibrate to 40°C for 10 minutes. A constant shear rate of 500 s^{-1} was

applied. Samples were heated while sheared from 40 to 90°C at a rate of 2°C min^{-1}. They were then held at 90°C for 2 minutes while remaining under shear, followed by a cooling step from 90°C to 5°C at a rate of 4°C min^{-1}. A film of sample formed around the top of the cup for all samples produced. Samples were then stored in a fridge for 24 hours before testing. The heating and cooling rates used correlate closely with those used previously in pin-stirrers for larger scale production of WPI fluid gels (Lazidis *et al*., 2016). The hold at 90°C was used to observe any time-dependent effects from heating that continued to occur.

3.3.3. Optical microscopy

An optical microscope (Leica Microsystems, UK) was used to directly observe particles produced for fluid gels. Differential interference contrast (DIC) was used to increase the contrast of particles. Samples were diluted with either distilled water or appropriate concentrations of acetic acid to maintain the pH of samples. Samples were gently inverted 10 times to mix them. A drop of this diluted sample was placed on a slide and covered with a coverslip. 20× and 40× magnification were used to observe the particles.

3.3.4. Particle sizing

Static light scattering (SLS) measurements were used to investigate particle size distributions. For this a Malvern Mastersizer 2000 with hydro SM manual small volume dispersion unit (Malvern Instruments, UK) was used. Each repeat consisted of three measurements, and three repeats were conducted.

3.3.5. Rheology

3.3.5.1. Viscometry

A 40 mm sand-blasted parallel plate geometry was used for this to minimize slip in these experiments. Slip is expected for suspensions owing to particle depletion at the shear surfaces.

Controlled strain equilibrium shear experiments were used with up to 2 minutes allowed for samples to reach equilibrium at each shear rate 0.1 s^{-1} to 100 s^{-1}. Samples were tested at 25°C with a gap of 1 mm.

3.3.5.2. Amplitude sweeps

A frequency of 1 Hz at 25ºC was used for controlled strain amplitude sweeps. These were obtained using a sand-blasted parallel plate geometry to minimize the effects of slip and repeated three times.

3.3.5.3. Frequency sweeps

Quiescent gels were produced by heating and cooling protein solutions on a cone and plate geometry. A cone and plate geometry was used as it applies an even strain across the sample. Solutions were heated from 40°C to 90°C, held at 90°C and then cooled to 5°C to denature and gel the proteins. These quiescently set gels were then left to stand for 20 minutes before equilibrating to 25°C and frequency sweeps commencing. A strain of 0.05% was used for these, as this was determined to be within the linear viscoelastic region (LVR) of these quiescent gels.

3.3.6. Determination of ζ-potential

For determination of ζ-potential a Zetasizer (Malvern Instruments, UK) was used. Samples were prepared by 10 times dilution in their respective continuous phases to reduce the particle concentration to a measurable range. The samples were diluted in their own continuous phase to maintain the properties of the systems whilst reducing the concentration of the dispersed phase.

3.3.7. Phase volume

The elastic modulus of diluted and concentrated fluid gels was measured to calculate the phase volume of fluid gels produced. Elastic modulus was measured at 1 Hz and 1% strain using a 1 mm gap in a sand-blasted plate geometry. Elastic modulus of suspensions of soft particles is expected to plateau at the maximum packing fraction of particles, and thus from this the phase volume as a function of the maximum packing fraction can be calculated. To reduce the concentration of fluid gels they were diluted in distilled water. To increase the phase volume of fluid gels they were centrifuged and the supernatant removed. Samples were centrifuged at speeds from 500 G to 40,000 G for 20 minutes to achieve this.

This method was used for the determination of phase volume as it has been shown previously for dispersions of plant cells that measurement of water loss is not able to distinguish between particle deformability and phase volume (Lopez-Sanchez *et al.*, 2012). This has previously been resolved by Garrec *et al.* (2013) by comparison of water release through centrifugation of quiescently set gels with fluid gels. However, this was not suitable for the systems discussed in this work as pockets of liquid formed within the quiescently set gels during centrifugation.

3.3.8. Tribology

An MTM2 (Mini Traction Machine, PCS Instruments, UK) tribometer was used for tribology measurements. This consists of a ball rolling on a disk; normal force, speed and slide–roll ratio (SRR) can be controlled.

A mixed sliding and rolling contact was used in this work with an SRR of 50%. SRR can be defined as:

$$SRR = \frac{U_{disc} - U_{ball}}{U} \quad (3.1)$$

where *U* represents the average speed at the contact for each component. A 3N normal force was used. For these experiments, a stainless steel ball–silicone elastomer disk tribopair was used as outlined previously (Mills, 2012). This tribopair and these conditions have been previously shown by Malone *et al*. (2003a) to correlate to mouth feel in the mixed regime of lubrication. In each test, Stribeck curves were measured over a speed range of 1–1,000 mm s^{-1} with ascending and descending runs repeated three times (six curves in total). Tests were performed at 25^{o}C. These tests were repeated three times.

3.4. Results and discussion

3.4.1. Fluid gel preparation

Fluid gels were prepared within the vane geometry of a rheometer by heating and cooling in shear. A rheometer was used for this production so that ordering could be monitored throughout fluid gel preparation. This produced a viscosity profile used to monitor the ordering of proteins through processing, which is shown in Figure 3.1. With increasing ordering of protein molecules, an increase in viscosity will be observed.

Initially there was little change in viscosity observed with increasing temperature. This was followed by a sharp increase in viscosity for all samples except WPI pH 8, and this sharp increase in viscosity during fluid gel production has been observed previously at the gelling temperature (Ellis *et al*., 2017). The observed increase in viscosity has been attributed to protein aggregation (Lazidis *et al*., 2016). Particles are expected to form through a nucleation and growth mechanism, whereby small particles aggregate producing larger particles. The growth of these particles will be limited by break-up in the shear field, and thus final particle size is an

equilibrium between particle growth through aggregation (due to heat-induced gelation) and break-up due to shear (Norton *et al*., 1999).

The temperature at which the sharp increase in viscosity (Figure 3.1) attributed to aggregation occurs in egg was shown to decrease with decreasing pH; however, little change in the temperature of aggregation was found for WPI.

WPI pH 3.5 showed a greater rate of increase in viscosity than WPI pH 8, which can be explained by the difference in the rate of gelation. Gelation rate is controlled by two stages: protein denaturation and protein aggregation. Changes in pH will influence aggregation rates, as net charges and charge distribution of the proteins are altered. This will also be influenced by the differences in structure between the egg and WPI.

For egg at pH 3.5, a reduction in viscosity with increasing temperature was observed after the initial increase in viscosity. This can be explained by the difference in gelation temperature, because these systems were heated to ~40ºC above the gelation temperature. As proteins are further heated above the gelation temperature, further denaturation of proteins is expected to occur. As this happens, protein–protein interactions will be favoured over protein–water interactions.

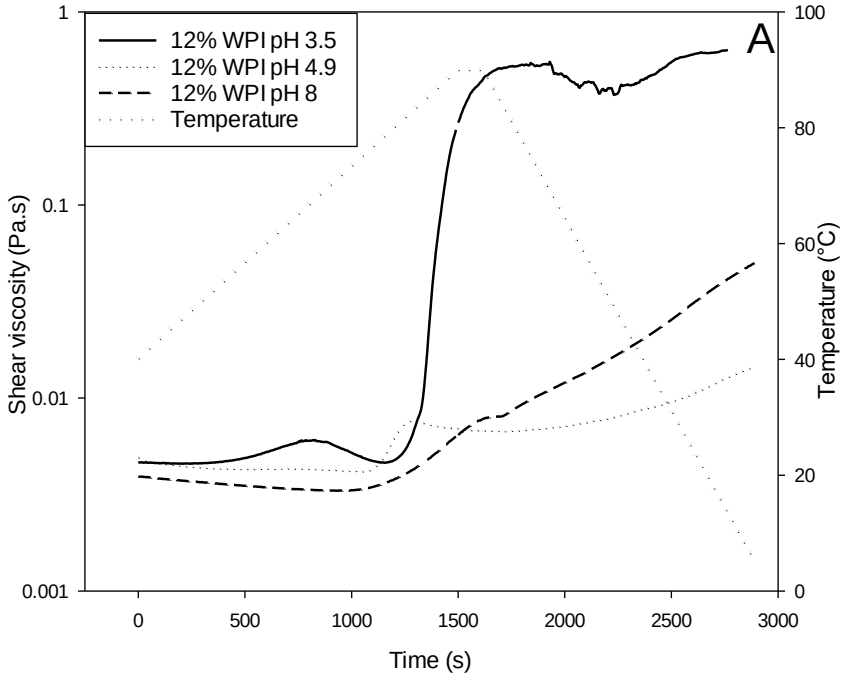

175

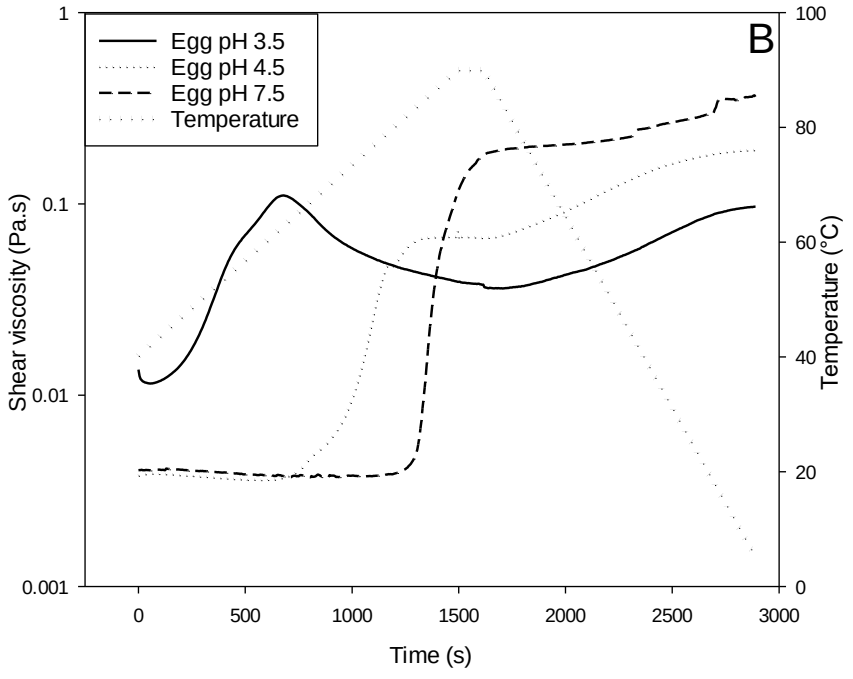

176

177 *Figure 3. 1. Viscosity profiles during protein fluid production showing sheared gelation of A) WPI and*
178 *B) heat-treated egg. Measurements were made using a cup and vane geometry at 500 s^{-1} while a*
179 *heating and cooling profile was applied. A heating rate of 2ºC min^{-1} was applied, followed by a 2-*
180 *minute isothermal step, then a cooling rate of 4ºC min^{-1}. Curves represent an average of three*
181 *repeats; error bars are not shown for clarity.*

Both whey and treated egg white produced fluid gels (suspensions of distinct gelled particles in a non-gelled continuous phase) when heated and cooled under shear. Fluid gels produced at a pH away from the pI for both egg and WPI showed no separation for a month after production. However, those produced at the pI of both proteins sediment out over 48 hours; this is shown in Figure 3.2. In these systems, a clear liquid was observed with an opaque white sediment. This is examined further in the section 'phase volume effects'.

The influence of reducing the pH of egg fluid gels produced at pH 7.5 was investigated to further understand any changes in properties of fluid gels due to changing pH post-production. For this the pH was reduced from pH 7.5 to 4.5 post-production. Within an hour of this pH change, a white sediment formed with a clear liquid above it. This sediment could not be easily dispersed because of the reduced net charge of particles upon reduction of pH to the pI of egg ovalbumin. Two mechanisms may contribute to this: the first is the reduction in net charge of the particles leading to aggregation of particles, and the second is that the structure of the particles is changing with the reduction in pH. Previously for WPI fluid gels Lazidis *et al.* (2016) showed that altering pH post-production did not alter the particle properties. However, the white appearance of the sediment produced supports that the gel structure within the particles was changed to aggregates rather than the fine-stranded structures expected from gels produced at pH 7.5.

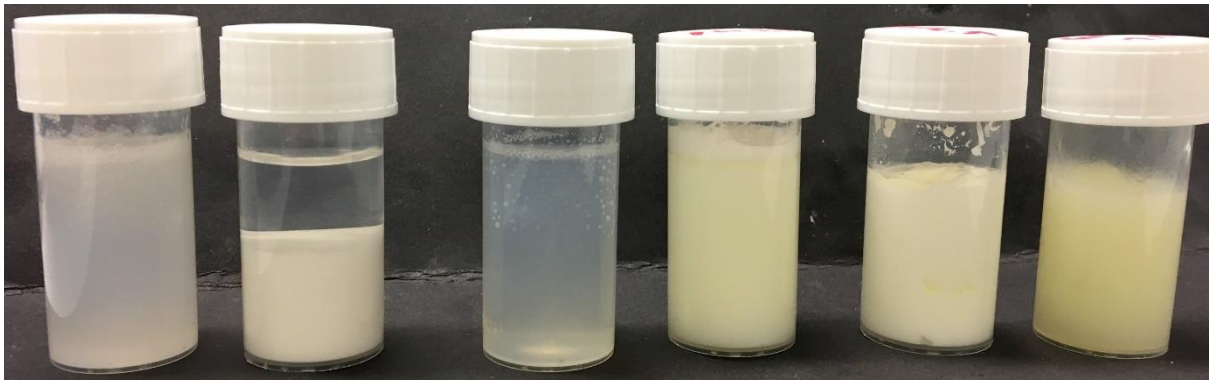

Figure 3. 2. Image of fluid gels produced after 48 hours. From left to right samples are WPI pH 3.5, WPI pH 4.9, WPI pH 8, egg pH 3.5, egg pH 4.5 and egg pH 7.5.

3.4.2. Particle shape and size determination

Light microscopy was used to directly observe particles and to determine particle size and shape (Figure 3.3), as the contribution of particle morphology to rheology has been shown previously by Wolf *et al*. (2001). Samples were diluted between 5× and 20× in the appropriate concentration of acetic acid or distilled water to enable observation of individual particles. Both WPI and egg produced distinct particles at all different pH levels tested.

For both WPI and egg at their respective pI, the particles appeared to have a globular structure that had aggregated together (Figure 3.3). These spherical aggregates agreed with observations of small globular particles produced by Lazidis *et al*. (2016), who showed small individual spherical particles of WPI were produced when fluid gels were prepared at pH 4.9. However, during their production, a dilution step in shear was used to prevent secondary particle aggregation. In the production by Lazidis *et al.* (2016), fluid gels were passed through two pin-stirrers in series; the first heating the protein solution under shear, the second with water being fed in under shear to dilute the fluid gel to achieve the desired final protein concentration. In this thesis, fluid gels were left quiescently overnight before dilution for observation. It would follow that the large aggregates of apparently smaller spherical particles observed here were

produced through secondary aggregation of smaller particles. Lazidis *et al*. (2016) attributed these smaller particles to reduced electrostatic repulsion between the protein molecules during denaturation and aggregation.

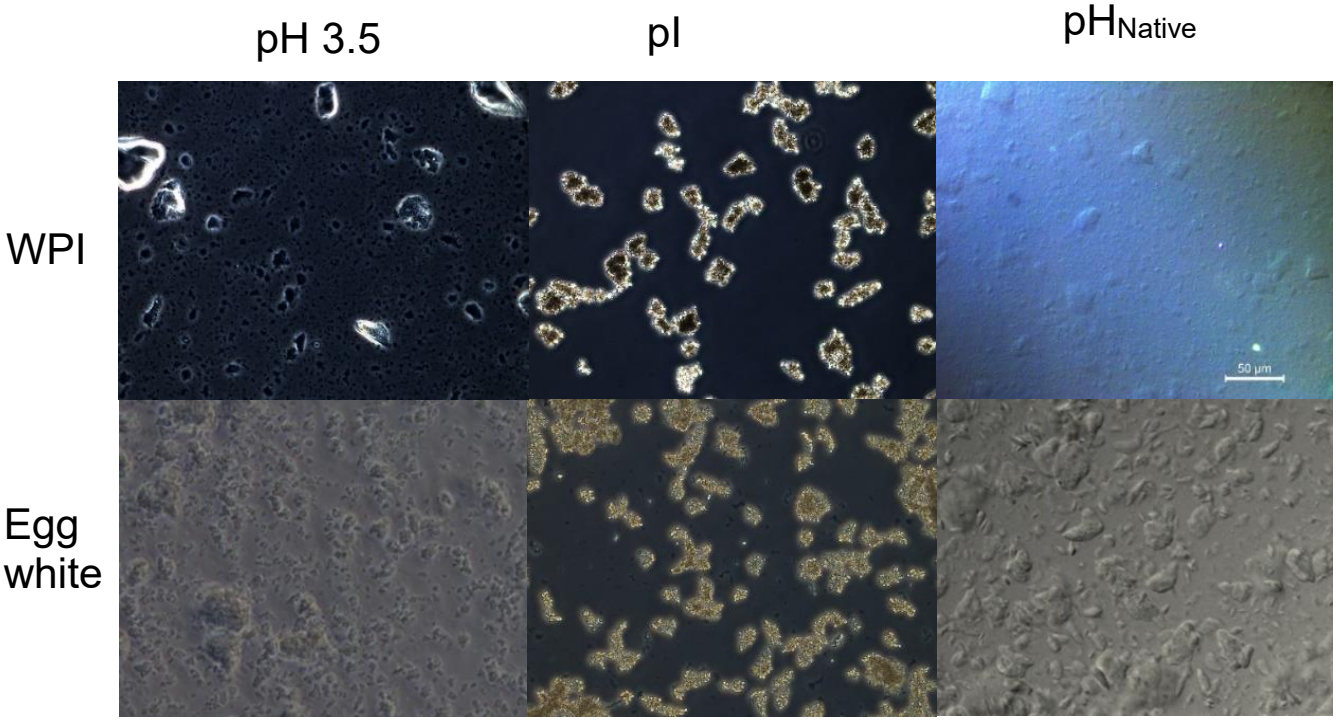

Figure 3. 3. Micrographs at 20× magnification of fluid gel particles of egg and WPI produced at different pH showing fluid gels diluted in distilled water or appropriate concentrations of acetic acid to maintain the appropriate pH. This shows particle shapes and sizes. The scale bar represents 50 µm. For egg, pI = 4.5 and pH_{Native} = 7.5. For WPI, pI = 5 and pH_{Native} = 8.

Owing to the aggregated appearance of particles, SLS measurements were carried out to further investigate primary particle sizes (Figure 3.4). Although these measurements are not directly comparable to the effective particle sizes, they will provide further insight into primary particle sizes. For SLS measurements, particles are dispersed in water with a manual dispersion unit. The shear from this is not expected to break up primary particles but will disrupt aggregation.

For both egg and WPI, fluid gels produced at native pH (pH 7.5 and 8, respectively) produced the largest particles with a broad size distribution and multiple peaks. These multiple peaks

242 can be attributed to inconsistencies in the flow field within the vane geometry. Different shear
243 and flow profiles will be felt at different points within the geometry. For both egg and WPI,
244 particles produced at pH 3.5 were <100 μm. These broad size distributions produced will be
245 contributed to by inconsistencies in the shear field within the vane geometry; increased shear
246 rates could be used to reduce particle sizes produced, but this was not possible with the set-up
247 used owing to foaming issues.

248 Both egg and WPI fluid gels produced at their respective pI showed the smallest particle size,
249 with all particles <10 μm. The smaller particles observed at the pI correlated with a previous
250 suggestion that particles observed at the pI by microscopy are aggregates of smaller particles.

251 For both egg and WPI at their respective pI, bimodal distributions were observed with peaks
252 at 0.2 μm and 0.9 μm. The reduced size of particles produced at the pI of proteins is due to the
253 expected dewatered nature of proteins at their pI where they are expected to have the lowest
254 net charge.

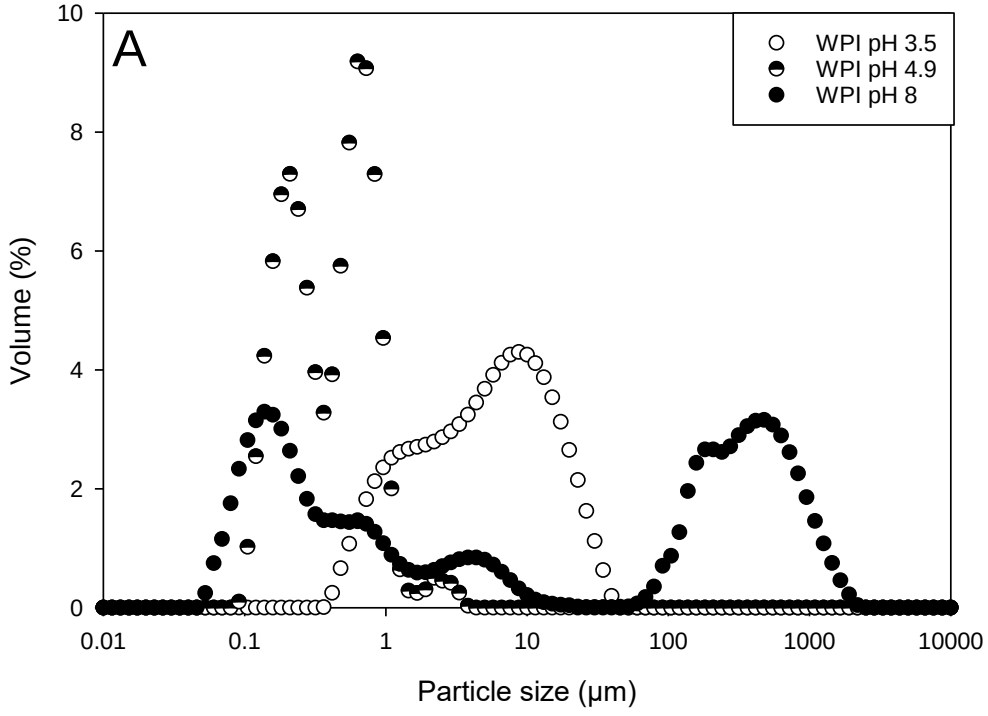

255

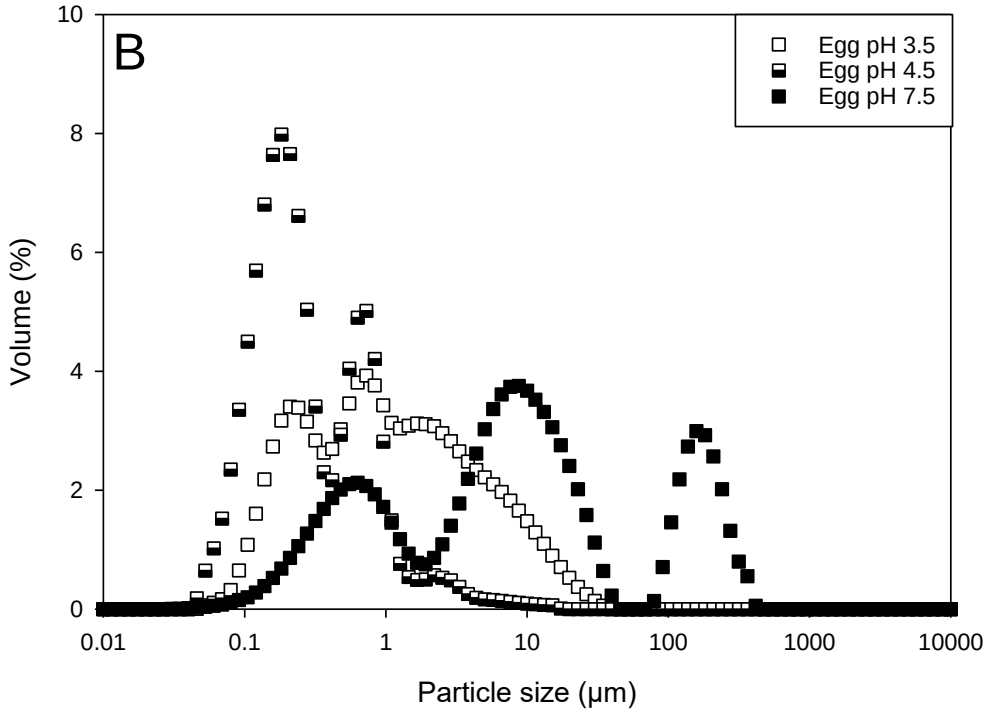

256

257 *Figure 3. 4. Size distribution of protein fluid gel particles produced at different pH. A) WPI. B) Egg.*
258 *Values represent an average of three repeats, each repeat consisting of three measurements. Error*
259 *bars represent +/- 1StD.*

3.4.3. Fluid gel rheology

Shear rate-controlled equilibrium measurements were used to analyse the shear rheology to understand the flow behaviour of these fluid gels (Figure 3.5). Shear thinning behaviour typical of particle suspension rheology was observed in all fluid gels produced here. The shear thinning nature of suspensions is due to ordering of particles in flow (Krieger and Dougherty, 1959a).

WPI fluid gels produced at the pI had a much lower viscosity than those produced above and below the pI. This is in agreement with understanding of WPI gel structures at these pH levels. At the pI, owing to the reduced repulsion between molecules during gelation, aggregation can occur before ordering of the proteins, forming a weaker gel structure. Softer particles will be able to deform and flow past one another more easily than more rigid particles, reducing the viscosity of the system. This rapid aggregation leads to a particulate gel structure with limited water binding. For gels produced away from the pI, a fine-stranded gel structure is expected as protein molecules order into strands owing to the reduced aggregation rate. Particulate gel structures will have a more porous structure with a reduced elastic modulus compared with those with a fine-stranded gel structure.

For egg, a different trend was observed with fluid gels produced at the pI showing a higher viscosity at low shear rates. Fluid gels produced at pH 3.5 showed the lowest viscosity at all shear rates. For egg at pH 3.5, a plateauing of viscosity was observed. Suspensions are expected to transition to a shear thickening regime as particle jamming occurs; this is because at higher shear rates particles do not have time to flow past one another. This observed difference between the behaviour of egg and WPI is likely due to egg fluid gels produced at the pI having a phase volume close to the maximum random packing fraction. This is shown in Figure 3.8. Suspensions with greater phase volumes will have a higher viscosity owing to more particle–particle interactions due to the increased number of particles in the dispersed phase.

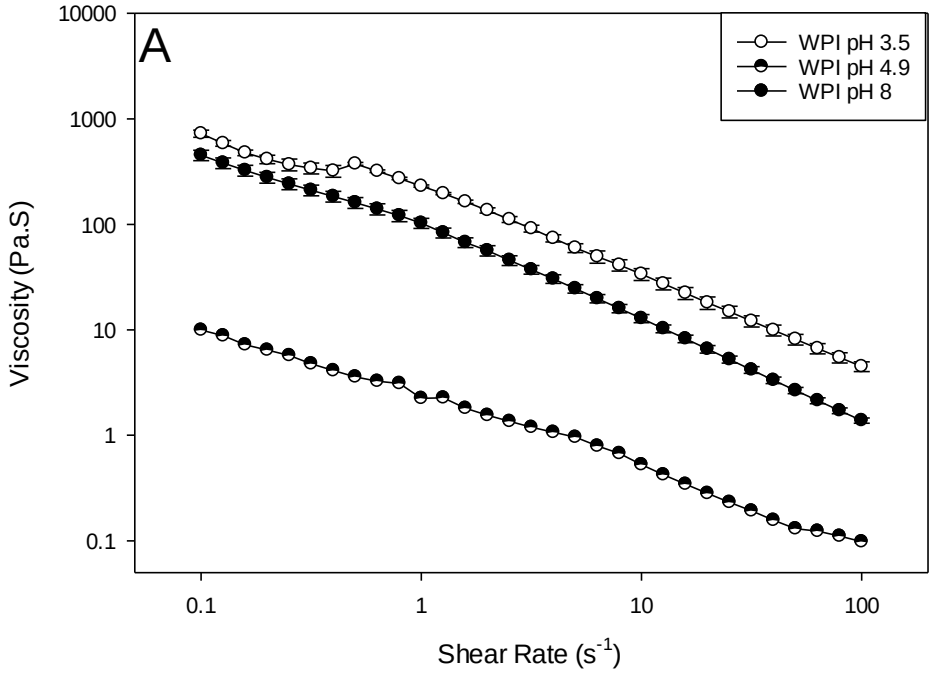

284

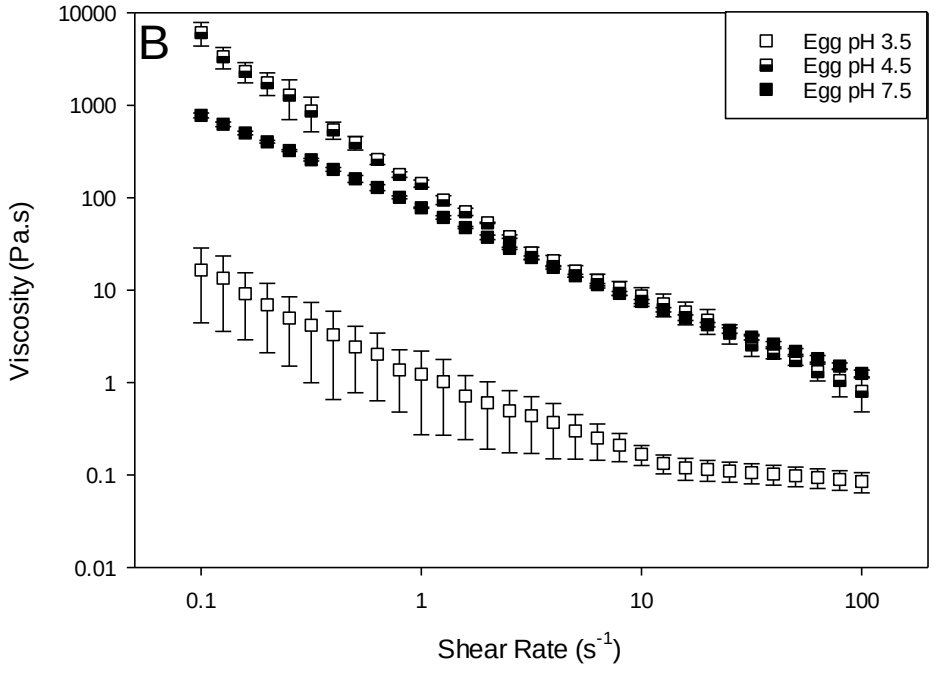

285

286 *Figure 3. 5. Viscosity profiles of protein fluid gels produced at different pH. A) WPI. B) Egg.*
287 *Measurements were taken at least 24 hours after production. A sand-blasted parallel plate geometry*
288 *was used to reduce slip and equilibrium measurements were taken. All measurements were taken at*
289 *25°C. Error bars represent +/- 1StD.*

290 3.4.4. Particle properties

291 Quiescent gel elastic modulus and zeta potential were used to further probe particle properties.
292 Use of quiescently set gel properties to represent particle properties has been shown previously
293 (Garrec *et al*., 2013).

294 Table 3.1 shows the zeta potential of fluid gel particles. This is used to investigate the net
295 surface charge of the particles in the fluid gel systems. The net surface charge of protein
296 molecules is expected to be ~0 at the pI, <0 at pH above the pI and >0 at pH below the pI, which
297 is because of protonation and deprotonation of amino acid groups along the protein.
298 Understanding the net charge of particles is important to understand what electrostatic
299 interactions are occurring. This trend was observed for WPI as would be expected. However,
300 for egg, the zeta potential of the particles at the pI was positive. This can be attributed to the
301 egg consisting of a mixture of proteins with varying pIs. Lysozyme would still be present in
302 small quantities within the mixture of proteins with a pI of 11 (Price *et al*., 1999), and thus
303 lysozyme protein molecules will have a positive charge at all pH levels investigated here.

304 *Table 3. 1. Zeta potential values of fluid gel particles of egg and whey produced at different pH. For*
305 *egg, pI = 4.5 and* pH_{Native} *= 7.5. For WPI, pI = 4.9 and* pH_{Native} *= 8.*

pH	**Egg ζ-potential (mV)**	**WPI ζ-potential (mV)**
3.5	10.604 ± 0.957	11.267 ± 1.320
pI	5.697 ± 1.599	-0.056 ± 0.382
pH_{Native}	-18.550 ± 3.689	-14.950 ± 3.200

306

307 The reduced net charge on the particles may contribute towards the observed sedimentation of
308 fluid gels produced at the pI of the protein, with reduced electrostatic repulsion between the

particles. Although for egg at its pI there was a reduced net charge, this is not the pI of the mixed protein system with a net charge of 5.697. Formation of aggregates of WPI in solution around the pI has been shown (Ju and Kilara, 1998b). This aggregation was attributed to the reduced electrostatic repulsion between protein molecules and the reduced protein affinity for water. This reduced electrostatic repulsion enables hydrophobic interactions to dominate, leading to aggregation. The contribution of particle charge to instability was further supported by the sedimentation of egg fluid gels produced at native pH then adjusted to pH 4.5 post-production. However, the reduced affinity of protein molecules for water at their pI may also lead to a reduced phase volume for fluid gels produced at their pI.

In order to observe inter-particle and particle packing properties of these systems, controlled strain mode amplitude sweeps were performed. This was shown through the elastic and viscous components G´ and G´´, respectively; these are shown in Figure 3.6.

All the fluid gel systems showed a LVR in which G´ and G´´ are independent of strain (Figure 3.7); this was as expected for concentrated suspensions. The observed LVR was typical of solid-like behaviour with G´ ten times greater than G´´ and typical for interconnected structures of concentrated suspensions.

WPI fluid gels produced at pH 3.5 showed a greater G´ in the LVR than whey fluid gels produced at native pH, with G´ values an order of magnitude higher than those for the fluid gel produced at pH 8. WPI fluid gel produced at the pI (pH 4.9) showed lower G´ values, correlating with the lower G´ observed for the quiescent WPI gel produced at pH 4.9. This is because less rigid particles deform more easily.

For egg, a different trend in G´ in the LVR was observed, with fluid gels produced at the pI showing the highest values. Egg fluid gels produced at pH 3.5 showed G´ values three orders

of magnitude lower than those produced at native pH. This is expected because of the difference between the gelation temperature and processing temperature for egg pH 3.5. This favours protein–protein interactions producing dewatered particles, giving a sparser network. The voids in this structure will reduce the elastic response of these suspensions. This trend in G´ for egg fluid gels correlated with G´ values observed for quiescent gels produced at this pH.

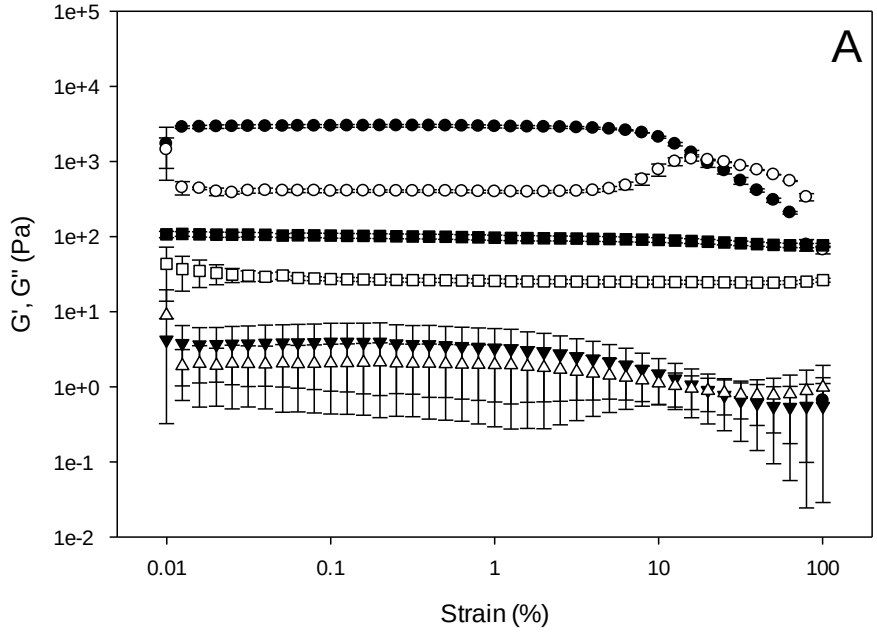

337

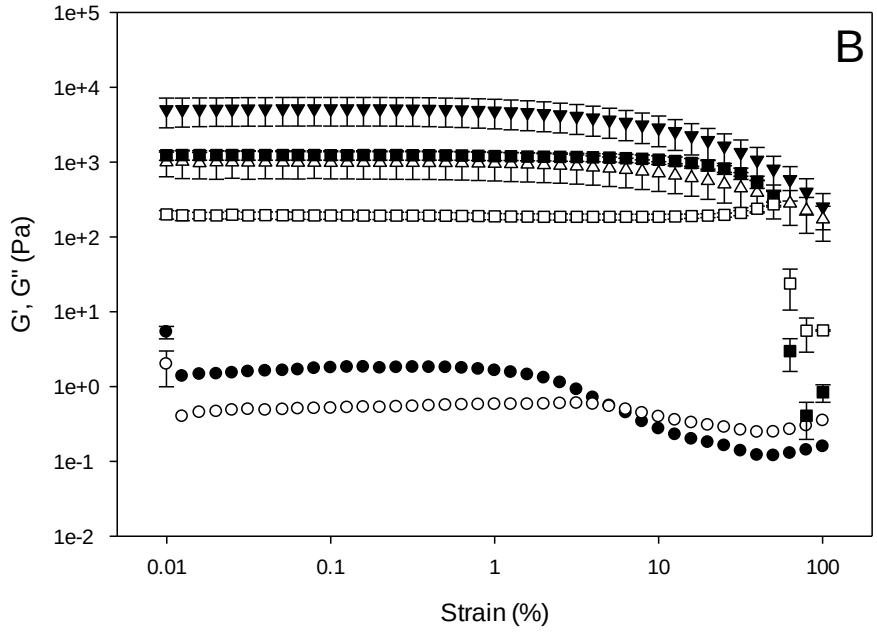

338

339 *Figure 3. 6. Strain-controlled amplitude sweeps for protein fluid gels showing A) WPI (pH 3.5 (G′ ●,*
340 *G′′ ○); pH 4.9 (pI) (G′ ▼, G′′ Δ); pH 8 (G′ □, G′′□)) and B) heat-treated egg (pH 3.5 (G′ ●, G′′ ○);*
341 *pH 4.5 (pI) (G′ ▼, G′′ Δ); pH 7.5 (G′ □, G′′ □)). A sand-blasted parallel plate geometry with a*
342 *frequency of 1 Hz was used to reduce slip. Values represent an average of three repeats; error bars*
343 *show +/- 1StD.*

344 Quiescent gels were used to represent the properties of the particles in the fluid gel systems.

345 Quiescent gels were produced within the cone and plate geometry prior to testing. All gels

346 tested showed a frequency-dependent nature in the frequency range tested. As frequency
347 increased, the time for energy to dissipate through the system was reduced, evidenced by a
348 higher elastic modulus. The structures of these gels were not directly observed here as this has
349 been well documented elsewhere (Katsuta *et al*., 1990; Ould Eleya *et al*., 2004; Ferry, 1948;
350 Gossett *et al*., 1984; Handa *et al*., 1998; Hermansson, 1979; Kiosseoglou, 2003).

351 For egg, little difference was shown in the elastic modulus of the gels produced at pH 7.5 and
352 pH 4.5; however, the gel produced at pH 3.5 had a lower elastic modulus. Egg white gels
353 produced below the pI have been shown to have a more porous structure than gels produced at
354 or above the pI (Handa *et al*., 1998). This porous structure would give a weak structure and thus
355 a reduced elastic modulus.

356 WPI gels produced at pH 3.5 showed the greatest elastic modulus, and those produced at the pI
357 (pH 4.9) showed the lowest elastic modulus. Notably, quiescent gels produced at the pI were
358 cloudy in appearance, which is indicative of an aggregated particulate structure (Verheul and
359 Roefs, 1998). This aggregated particulate structure will be dewatered, whereas for gels
360 produced away from the pI a fine-stranded network is expected. This fine-stranded network
361 orders water, giving a more rigid gel. These differences in gel structure are attributable to the
362 rate of aggregation during gelation. Away from the pI electrostatic repulsion between molecules
363 reduces the aggregation rate, allowing molecules to order into the fine-stranded network;
364 however, at the pI when the net charge of the molecules is 0, aggregation rates are much higher.

365 For both the whey and egg systems, the quiescent gel elastic moduli showed similar trends to
366 those of their fluid gels, validating the use of quiescent gel modulus to represent particle moduli.

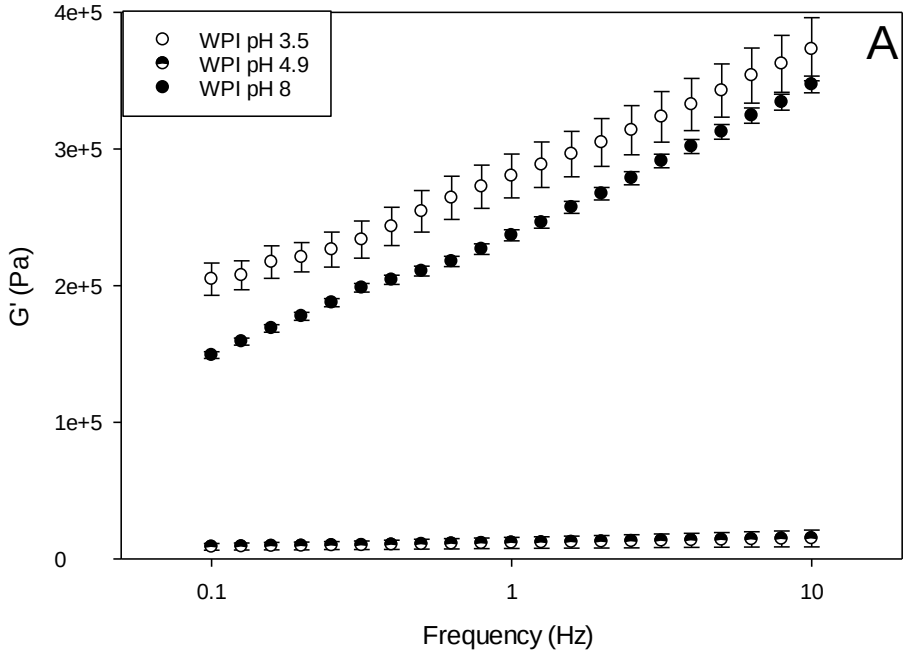

367

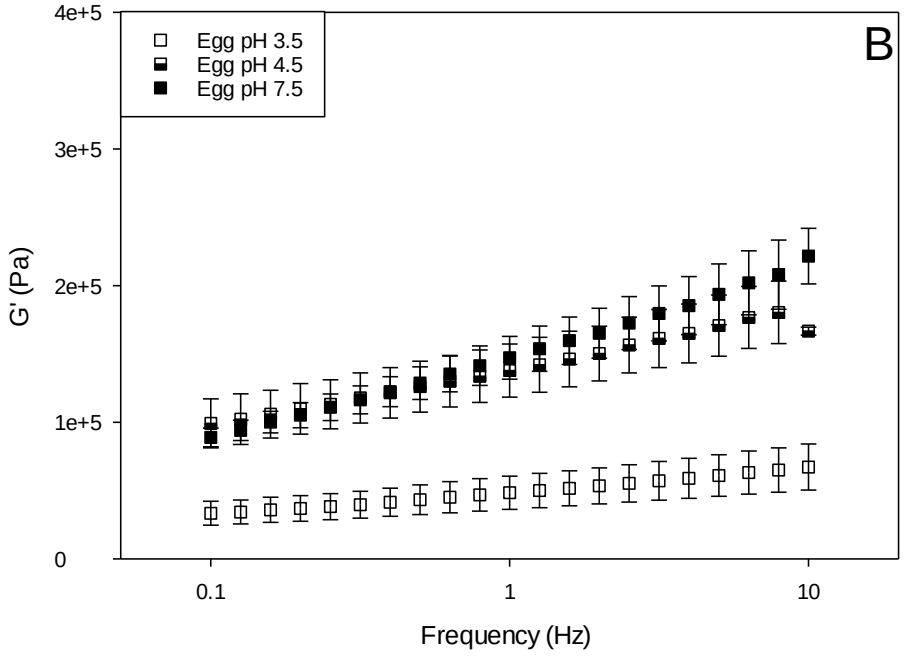

368

369 *Figure 3. 7. Frequency sweeps of quiescently set protein gels at different pH used to represent particle*
370 *properties of fluid gels at different pH. A) WPI. B) Egg. Quiescent gels were set within a cone and*
371 *plate geometry before the frequency sweeps commenced. 0.05% strain shown to be in the LVR for*
372 *these gels was used. Values represent three repeats with error bars showing +/- 1StD.*

3.4.5. Phase volume effects

Small amplitude oscillatory measurements were used to observe elastic modulus, with changing dispersed phase concentration in order to understand potential contributions of phase volume to the observed properties of fluid gels. Gels produced at the pI of the protein are expected to produce more dewatered particles, thus occupying a lower phase volume.

Figure 3.8 shows elastic modulus of samples. The concentration has been normalized. A concentration of 1 is the concentration of the fluid gels when produced with no diluting or concentrating. For all samples, as concentration increased, elastic modulus increased up to a crucial concentration at which elastic modulus plateaued. This has been previously observed for fluid gel particles produced from WPI and agarose (Frith *et al*., 2002; Moakes *et al*., 2015b). Adams *et al*. (2004) explained this plateau as being a result of elastic modulus being dominated by particle modulus once the maximum random packing fraction is reached. For monodisperse hard spheres, the maximum random packing fraction is 0.64 (Einstein, 1906).

Egg fluid gels produced at the pI and native pH were approximately at the maximum random packing fraction, as shown by increasing G´ up to 1.0 and plateauing at higher concentrations. For egg fluid gels produced below the pI, the concentration was below the maximum packing fraction with no plateau observed in G´ over the concentration range observed. This reduced phase volume for egg fluid gels below the pI is explained as being because of the reduced gelation temperature at pH 3.5 of the egg system. As the egg is heated above the gelation temperature, further protein denaturation will lead to the favouring of protein–protein interactions over protein–water interactions, reducing the water binding of the gel particles. This will produce particles with a more dewatered gel structure.

WPI fluid gels produced at the pI were approximately at the maximum packing fraction, and those produced below the pI were above the maximum packing fraction with a phase volume of Φ/Φ_{max} ~1.05. For suspensions of gelled particles, the maximum random packing fraction can be exceeded as particles are deformable. WPI fluid gels produced at the pI did not plateau over the range of concentrations observed. This reduced phase volume of fluid gels produced at the pI can be explained by the reduced affinity of the protein molecules for water at the pI.

A difference was observed in the effect of pH on the phase volume of fluid gels between egg and WPI. For WPI, the lowest phase volume was observed at the pI as a result of the reduced intermolecular repulsion during gelation giving particles a more dewatered particle structure. For egg white fluid gels produced at the pI of egg ovalbumin, however, as shown in Table 3.1, egg particles have a net charge at this pH, attributed to the mix of proteins present in the egg white. This charge will shift the gel structure away from the aggregated structure when there is no net charge towards the fine-stranded gel structure. However, these fluid gels still have an opaque appearance indicating a mixed structure of aggregates and strands.

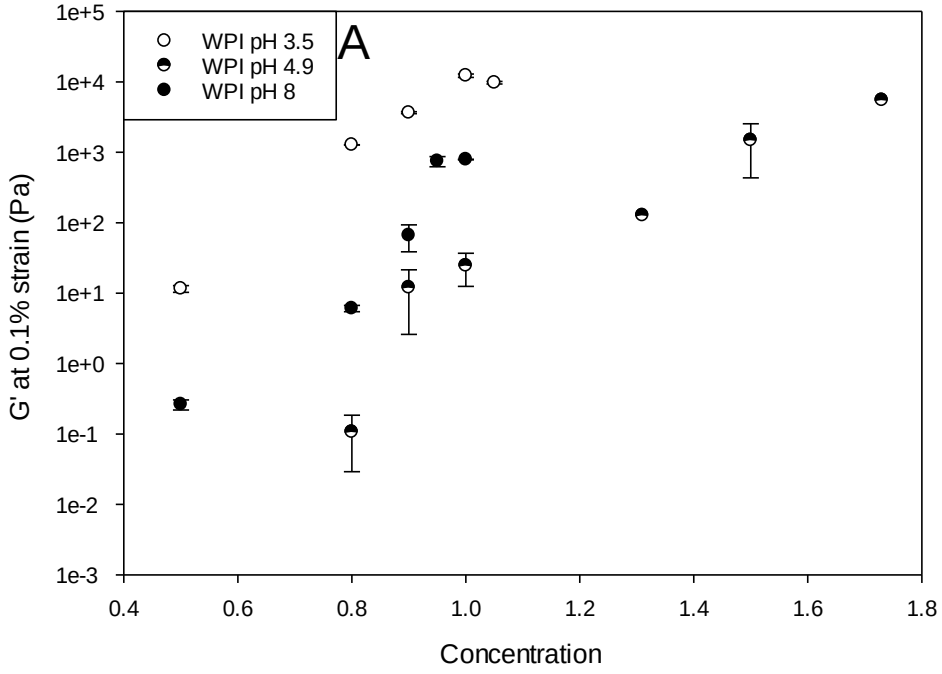

409

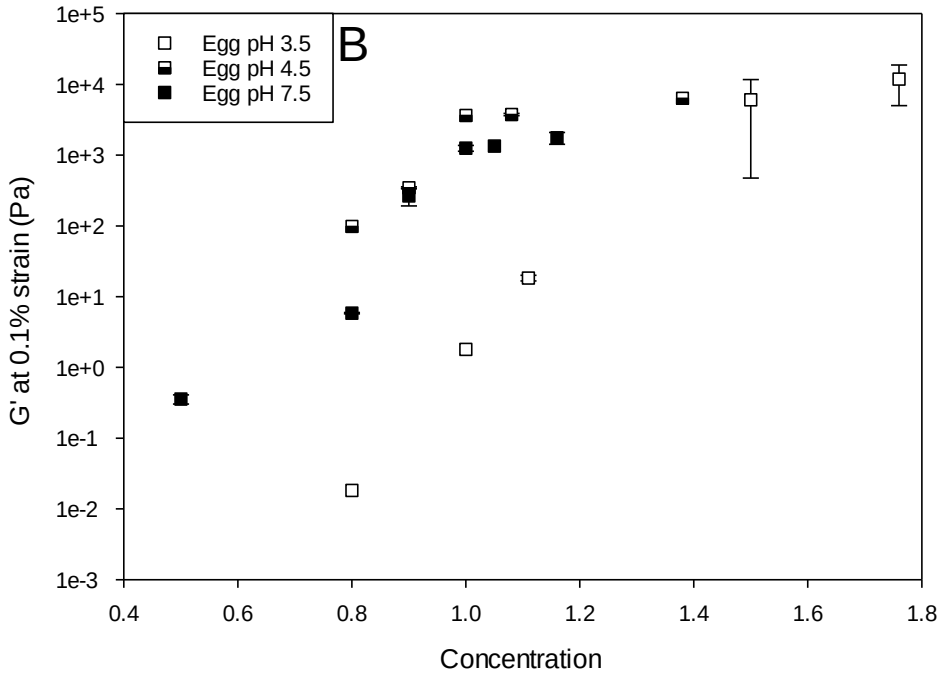

410

411 *Figure 3. 8. Elastic modulus versus concentration for protein fluid gels produced at different pH. A)*
412 *WPI. B) Egg. A concentration of 1 is defined as the concentration of fluid gels post-production. For*
413 *concentrations below 1, fluid gels were diluted with the appropriate concentration of distilled water or*
414 *acetic acid. For concentrations above 1, samples were centrifuged to remove liquid from the*
415 *continuous phase. Values represent an average of three measurements, with error bars representing*
416 *+/- 1StD. 0.1% strain was used; this was shown to be within the LVR at a frequency of 1 Hz.*

3.4.6. Tribology

The friction and lubrication properties of the fluid gel systems were examined (Figure 3.9). Tribology was used to evaluate the potential performance of these fluid gel systems for the use in food systems.

WPI fluid gels produced at pH 3.5 were shown to be the most lubricating fluid gel system examined over the speed range tested (Figure 3.9). For this system, the mixed lubrication regime was observed with friction coefficient decreasing with increasing entrainment speed. For WPI at both pH 3.5 and 8, typical Stribeck behaviour was observed. However, for particles produced at the pI, a peak in friction coefficient was observed between speeds of 1 mm s^{-1} and 10 mm s^{-1}. Once maximum friction was observed at 5 mm s^{-1}, particles entered the mixed regime and friction decreased rapidly as speed was increased. Above 100 mm s^{-1}, friction behaviour was similar to that of particles produced at pH 3.5 and 8.

For egg fluid gels produced at pH 3.5 and 7.5, a peak in friction was observed, but at an entrainment speed of approximately 2 mm s^{-1}. At speeds above 2 mm s^{-1}, friction coefficient decreased with increasing speed typical of the mixed regime and tends to similar values of friction coefficient to WPI fluid gels. As with WPI suspensions produced at the pI, a different behaviour was found in egg fluid gels produced at pH 4.5. From 1 mm s^{-1}, friction coefficient increased as speed increased. A maximum was observed at a similar point to WPI at a speed of approximately 5 mm s^{-1}, with a similar friction coefficient value of ~0.5. As speed increased above 5 mm s^{-1}, friction coefficient decreased at a slower rate than for WPI fluid gels. At 1000 mm s^{-1}, all fluid gels showed similar friction values.

For particles produced at the pI for WPI and egg at pH 4.5, different lubrication was observed to those produced at other pH levels. This peak in friction as lubrication transitions from the

boundary to the mixed regime has been shown previously for agarose fluid gels of particle size ~100 μm greater than the roughness of the surfaces used. This peak may be due to the entrainment of the particles when the gap is smaller than the observed particle size (Gabriele *et al*., 2010). The aggregation of particles shown in Figure 3.3 will lead to a greater effective particle size. This greater effective particle size will increase friction as these particles pass through the contact as greater deformation of particles and surfaces will occur as these particles are entrained through the contact.

WPI particles were shown to be more rigid than those of egg (Figure 3.8). Greater lubrication by more rigid particles has been shown previously in κ-carrageenan, agar and alginate fluid gel systems (Fernández Farrés *et al*., 2013; Gabriele *et al*., 2010; Garrec and Norton, 2013). This is because more rigid particles can support the gap and are deformed less in the contact, reducing the area of contact. This is only true when the particles are softer than the surface, as wear will occur within the contact when particle hardness is comparable to the surface.

Particle rigidity can also explain the difference observed between egg and WPI for fluid gels produced away from the pI. WPI fluid gels produced below the pI were shown to have a greater elastic modulus than those produced above the pI. However, for egg, the opposite trend of particle modulus was observed, with particles produced above the pI having a greater elastic modulus.

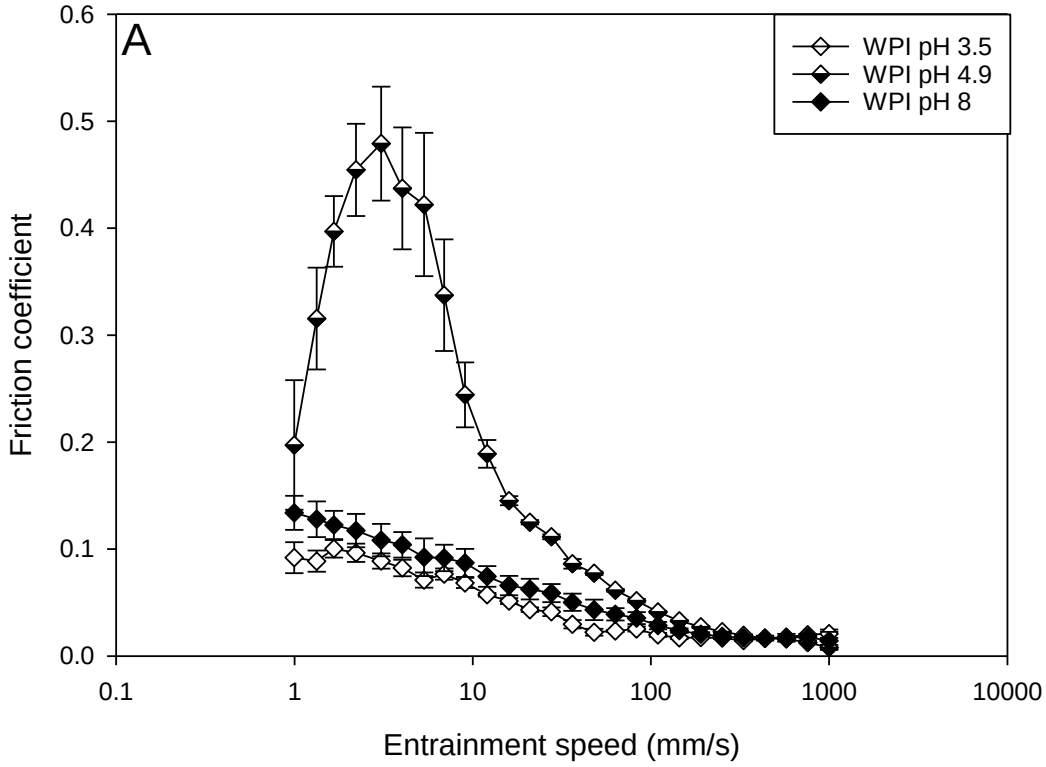

458

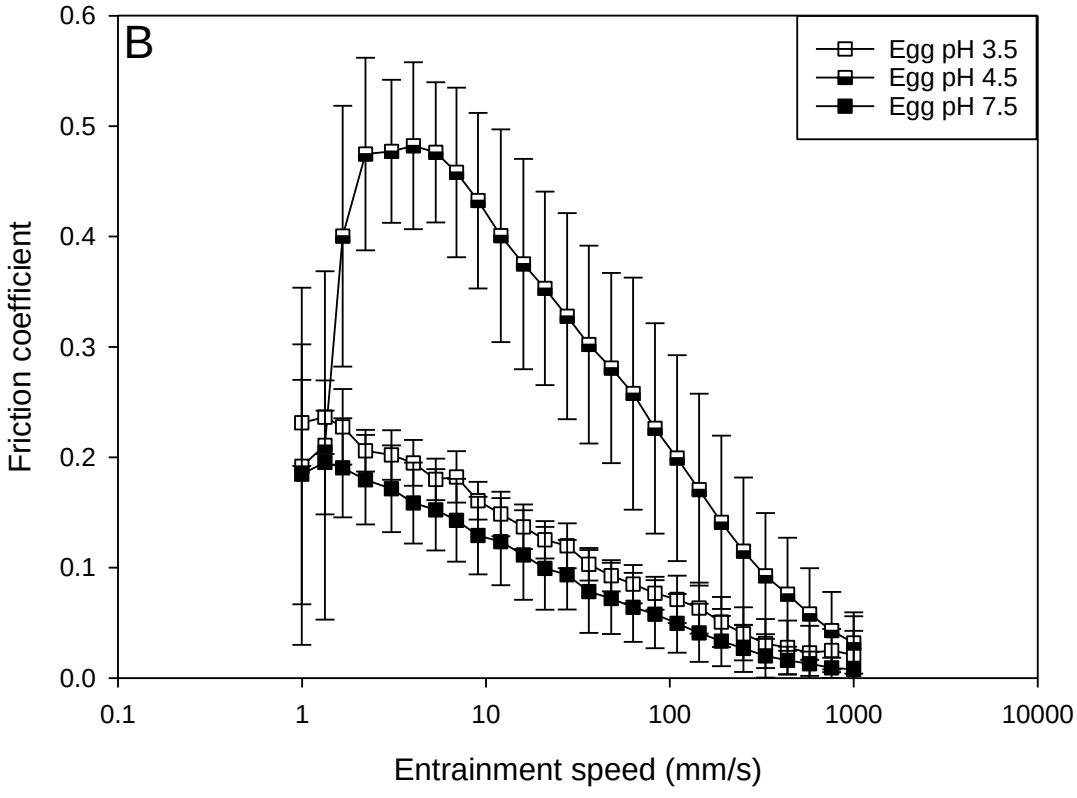

459

460 *Figure 3. 9. Stribeck curves for A) WPI and B) egg. Fluid gels produced at different pH using a*
461 *stainless steel ball–silicone elastomer disk tribopair at 50% SRR. Error bars show +/- 1 StD.*

3.5. Conclusion

Fluid gels showed potential for the reduction of fat content in emulsion-based foods while maintaining the desirable textural properties of their full fat counterparts. Egg white fluid gels have been presented for the first time. Egg showed potential as an ingredient for the production of fluid gels, showing high viscosities and good lubricating properties when produced at pH 7.5. Egg fluid gels offer an option for the replacement of fat in mayonnaises without adding additional ingredients, as egg is already used in these products. WPI fluid gels showed high viscosity and good lubricating properties when produced at pH 3.5 and pH 8. WPI fluid gels produced at the pI were found to have a poor lubrication. This same poor lubrication was shown for egg white fluid gels produced at the pI of ovoalbumin. This was explained by the aggregation of particles leading to increased effective particle size for fluid gels at their pI. Protein fluid gels offer a nutritionally beneficial functional ingredient with potential for thickening of products whilst contributing nutritionally.

3.6. References

ADAMS, S., FRITH, W. J. & STOKES, J. R. 2004. Influence of particle modulus on the rheological properties of agar microgel suspensions. *Journal of Rheology,* 48**,** 1195-1213.

CROGUENNEC, T., NAU, F. & BRULÉ, G. 2002. Influence of pH and Salts on Egg White Gelation. *Journal of Food Science,* 67**,** 608-614.

DEMETRIADES, K., J.N., C. & MCCLEMENTS, D. J. 1997. Physicochemical Properties of Whey Protein-Stabilized Emulsions as affected by Heating and Ionic Strength. *Journal of Food Science,* 62**,** 462-467.

EINSTEIN, A. 1906. A new determination of molecular dimensions. *Ann. Phys.,* 19**,** 289-306.

ELLIS, A. L., NORTON, A. B., MILLS, T. B. & NORTON, I. T. 2017. Stabilisation of foams by agar gel particles. *Food Hydrocolloids,* 73**,** 222-228.

EVANS, I. D. & HAISMAN, D. R. 1980. RHEOLOGY OF GELATINISED STARCH SUSPENSIONS. *Journal of Texture Studies,* 10**,** 347-370.

FERNÁNDEZ FARRÉS, I., DOUAIRE, M. & NORTON, I. T. 2013. Rheology and tribological properties of Ca-alginate fluid gels produced by diffusion-controlled method. *Food Hydrocolloids,* 32**,** 115-122.

FERRY, J. D. 1948. Protein Gels11Supported in part by the Research Committee of the Graduate School of the University of Wisconsin from funds supplied by the Wisconsin Alumni Research Foundation. *In:* ANSON, M. L. & EDSALL, J. T. (eds.) *Advances in Protein Chemistry.* Academic Press.

FRITH, W., GARIJO, X., FOSTER, T. & NORTON, I. 2002. Microstructural origins of the rheology of fluid gels. *Special Publication-royal Society of Chemistry,* 278**,** 95-103.

GABRIELE, A., SPYROPOULOS, F. & NORTON, I. 2010. A conceptual model for fluid gel lubrication. *Soft Matter,* 6**,** 4205-4213.

GARREC, D. A., GUTHRIE, B. & NORTON, I. T. 2013. Kappa carrageenan fluid gel material properties. Part 1: Rheology. *Food Hydrocolloids,* 33**,** 151-159.

GARREC, D. A. & NORTON, I. T. 2013. Kappa carrageenan fluid gel material properties. Part 2: Tribology. *Food Hydrocolloids,* 33**,** 160-167.

GOSSETT, P. W., RIZVI, S. & BAKER, R. 1984. Quantitative analysis of gelation in egg protein systems. *Food Technology,* 38**,** 67-96.

HANDA, A., TAKAHASHI, K., KURODA, N. & FRONING, G. W. 1998. Heat-induced Egg White Gels as Affected by pH. *Journal of Food Science,* 63**,** 403-407.

HERMANSSON, A. M. 1979. Aggregation and Denaturation Involved in Gel Formation. *Functionality and Protein Structure.* AMERICAN CHEMICAL SOCIETY.

HOLLAND, S., TUCK, C. & FOSTER, T. J. F. B. 2018. Fluid Gels: a New Feedstock for High Viscosity Jetting. 13**,** 175-185.

JU, Z. Y. & KILARA, A. 1998. Gelation of pH-Aggregated Whey Protein Isolate Solution Induced by Heat, Protease, Calcium Salt, and Acidulant. *Journal of Agricultural and Food Chemistry,* 46**,** 1830-1835.

KATSUTA, K., RECTOR, D. & KINSELLA, J. E. 1990. Viscoelastic Properties of Whey Protein Gels: Mechanical Model and Effects of Protein Concentration on Creep. *Journal of Food Science,* 55**,** 516-521.

KIOSSEOGLOU, V. 2003. Egg yolk protein gels and emulsions. *Current Opinion in Colloid & Interface Science,* 8**,** 365-370.

KOKINI, J. L. 1987. The physical basis of liquid food texture and texture-taste interactions. *Journal of Food Engineering,* 6**,** 51-81.

KRIEGER, I. M. & DOUGHERTY, T. J. 1959. A mechanism for non-Newtonian flow in suspensions of rigid spheres. *Transactions of the Society of Rheology,* 3**,** 137-152.

LAZIDIS, A., HANCOCKS, R. D., SPYROPOULOS, F., KREUß, M., BERROCAL, R. & NORTON, I. T. 2016. Whey protein fluid gels for the stabilisation of foams. *Food Hydrocolloids,* 53**,** 209-217.

LIU, R., ZHAO, S.-M., LIU, Y.-M., YANG, H., XIONG, S.-B., XIE, B.-J. & QIN, L.-H. 2010. Effect of pH on the gel properties and secondary structure of fish myosin. *Food Chemistry,* 121**,** 196-202.

LOPEZ-SANCHEZ, P., CHAPARA, V., SCHUMM, S. and FARR, R., Shear elastic deformation and particle packing in plant cell dispersions. Food Biophysics. 2012 Mar 1;7(1):1-4.

MALONE, M. E., APPELQVIST, I. A. M. & NORTON, I. T. 2003. Oral behaviour of food hydrocolloids and emulsions. Part 1. Lubrication and deposition considerations. *Food Hydrocolloids,* 17**,** 763-773.

MILLS, T. B. 2012. *Development of in-vitro mouth methods for studying oral phenomena.* University of Birmingham.

MOAKES, R. J. A., SULLO, A. & NORTON, I. T. 2015a. Preparation and characterisation of whey protein fluid gels: The effects of shear and thermal history. *Food Hydrocolloids,* 45**,** 227-235.

MOAKES, R. J. A., SULLO, A. & NORTON, I. T. 2015b. Preparation and rheological properties of whey protein emulsion fluid gels. *RSC Advances,* 5**,** 60786-60795.

MUDGAL, P., DAUBERT, C. R. & FOEGEDING, E. A. 2011. Kinetic study of β-lactoglobulin thermal aggregation at low pH. *Journal of Food Engineering,* 106**,** 159-165.

NORTON, I. T., JARVIS, D. A. & FOSTER, T. J. 1999. A molecular model for the formation and properties of fluid gels. *International Journal of Biological Macromolecules,* 26**,** 255-261.

OULD ELEYA, M. M., KO, S. & GUNASEKARAN, S. 2004. Scaling and fractal analysis of viscoelastic properties of heat-induced protein gels. *Food Hydrocolloids,* 18**,** 315-323.

PRICE, W. S., TSUCHIYA, F. & ARATA, Y. 1999. Lysozyme Aggregation and Solution Properties Studied Using PGSE NMR Diffusion Measurements. *Journal of the American Chemical Society,* 121**,** 11503-11512.

RAIKOS, V., CAMPBELL, L. & EUSTON, S. R. 2007. Rheology and texture of hen's egg protein heat-set gels as affected by pH and the addition of sugar and/or salt. *Food Hydrocolloids,* 21**,** 237-244.

ROSS, J. R. 1991. Practical handbook of biochemistry and molecular biology; Edited by G D Fasman. pp 601. CRC Press, Boca Raton, Florida, USA. 1989. $00 ISBN 0-8493-3705-4. *Biochemical Education,* 19**,** 95-96.

SHAMA, F. & SHERMAN, P. 1973. Identification of stimuli controlling the sensory evaluation of viscosity II. Oral methods. *Journal of texture studies,* 4**,** 111-118.

SINGER, N. S. & DUNN, J. M. 1990. Protein microparticulation: the principle and the process. *Journal of the American College of Nutrition,* 9**,** 388-397.

STEVENS, L. 1991. Egg white proteins. *Comparative Biochemistry and Physiology Part B: Comparative Biochemistry,* 100**,** 1-9.

VERHEUL, M. & ROEFS, S. P. F. M. 1998. Structure of Particulate Whey Protein Gels: Effect of NaCl Concentration, pH, Heating Temperature, and Protein Composition. *Journal of Agricultural and Food Chemistry,* 46**,** 4909-4916.

569 WOLF, B., FRITH, W. J., SINGLETON, S., TASSIERI, M. & NORTON, I. T. 2001. Shear
570 behaviour of biopolymer suspensions with spheroidal and cylindrical particles.
571 *Rheologica Acta,* 40**,** 238-247.

CHAPTER 4.
Development of a spray drying method for the production of dispersible protein particles

4.1. Introduction

Protein fluid gels demonstrated potential in the previous chapter for use in reduced fat mayonnaises. However, there are challenges with the scale-up potential of these production methods, with challenges incorporating these into current production facilities. If these particles could be produced as a powder, this powder has the potential to be used in current production facilities without the need to invest in equipment for sheared gelation. WPI was chosen because of the properties of fluid gels produced at pH 3.5. WPI is a less variable source of protein than egg. This chapter investigates the potential for a method of producing dry protein particles for dispersion from WPI using spray drying.

4.2. Materials and methods

4.2.1. Solution preparation

The WPI used in this chapter was sourced from Muller, Germany, not Davisco as used in Chapter 3; as a result of this, the native pH of these samples is 6.5 as opposed to 8.

WPI solutions were prepared by dispersing WPI (Muller, Germany) powder at 15% W/W in reverse osmosis water. 0.01% sodium azide was added to inhibit bacterial growth. This was dispersed by means of an overhead stirrer for 12 hours and then stored in a fridge until required.

pH of this stock solution was adjusted with 2 M acetic acid and appropriate salts added prior to use. The resulting solution was then diluted to a final WPI concentration of 12% W/W with reverse osmosis water.

4.2.2. Spray drying

Samples were maintained at 65ºC on a stirred hotplate throughout the spray drying process. A Buchi B-290 Mini-spray dryer was used with a 0.8 mm nozzle. An inlet temperature of 180ºC

was used, giving an outlet temperature of 63–68ºC. A 95% aspirator was used with the feed pump set at 20%. Spray drying is traditionally used as a low temperature method for the drying of heat-labile systems; however, in this work, the protein is deliberately denatured throughout the drying process.

Solutions were heated to the 65ºC temperature in a stirred water bath for 1 hour.

These solutions were then spray dried, and the temperature was maintained between 60ºC and 65ºC during spray drying using a stirred hot plate.

Powders were stored at 25ºC in a dark airtight container.

4.2.3. Dispersion preparation

Dispersions were produced by dispersing the powder produced in water or salt solutions at room temperature. This was achieved by stirring with a magnetic stirrer for 2 hours at a speed of approximately 200 RPM unless otherwise stated. Samples were degassed at -100 mbar for 20 minutes. Samples were then stored at 5ºC overnight before measurements.

4.2.4. Solubility measurements

UV absorbance spectroscopy was used to quantify the soluble protein content of samples. A standard curve at 280 nm was prepared from WPI dispersed at increasing concentrations. From this curve, an extinction coefficient of 8.71 was determined.

For determination of soluble protein content of samples, samples were centrifuged at 2400 G for 1 hour. The supernatant of samples was weighed to determine the volume of supernatant. The supernatant of these samples was then diluted 100 times to give absorbance readings within the effective range of the equipment. Absorbance measurements were then taken to

calculate the concentration of protein in the supernatant. From this, loss of solubility was calculated as per Equation 4.1.

$$\frac{Concentration\ of\ protein\ in\ supernatant\ x\ supernatant\ volume}{Total\ protein\ concentration} = soluble\ protein\ content \quad (4.1a)$$

$$Loss\ of\ protein\ solubility = 1 - soluble\ protein\ content \quad (4.1b)$$

4.2.5. Optical microscopy

An optical microscope (Leica Microsystems, UK) was used to directly observe particles produced. Phase contrast was used to increase the contrast of particles. Samples were diluted with distilled water to a final WPI concentration of 5%. A drop of this diluted sample was placed on a slide and covered with a coverslip.

4.2.6. Particle sizing

Particle size distributions were determined by SLS using a Malvern Mastersizer with a hydro SM manual small volume dispersion attachment (Malvern Instruments, UK). Samples were diluted to 1% (w/w) and three repeats were used with each repeat consisting of three measurements. A refractive index of 1.456 was used for these measurements.

4.2.7. Shear rheology

To investigate the effects of shear on particle ordering in flow, flow curves were obtained for suspensions. A 40 mm sand-blasted parallel plate geometry was used to minimize slip. Equilibrium shear experiments were used with up to 2 minutes allowed for samples to reach equilibrium at each shear rate. Samples were tested at 25°C using a 1 mm gap.

4.2.8. FTIR

Fourier transform infrared (FTIR) spectroscopy was used to look at the structures of proteins. FTIR is suitable for investigating protein secondary and tertiary structures of protein solutions, protein aggregates in solution and dry protein powders. It is also capable of measuring both wet and dry samples, and thus structuring in the drying phase can be investigated. A resolution of 4 cm^{-1} was used, with each test consisting of 64 measurements. Three repeats were taken for each sample.

4.2.9. Curve fitting

Curve fitting of the amide I region was used to investigate the secondary structure of proteins. Fityk curve fitting software was used for this. Second order derivatives of baseline-corrected absorbance spectra of the amide I region (1600–1700 cm^{-1}) were carried out. Deconvolution analysis was also carried out on the baseline-corrected spectra. Only peaks that were present on the deconvoluted spectra that corresponded to troughs on the second order derivative spectra were fitted.

4.2.10. NMR

T_2 relaxation times were measured using an mq20 minispec nuclear magnetic resonance (NMR) instrument (Bruker, USA). The temperature was held at 25ºC throughout NMR measurements. A pulse sequence was used with a pulse separation of 0.25 ms, and three dummy echoes were used followed by a collection. From this a T_2 relaxation time was calculated as the exponent of the decay function.

4.2.11. Tribology

An MTM2 (Mini Traction Machine, PCS Instruments, UK) tribometer was used for tribology measurements. This consists of a ball rolling on a disk; normal force, speed and SRR can be controlled.

A mixed sliding and rolling contact was used in this work with an SRR of 50%. SRR can be defined as:

$$SRR = \frac{U_{disc} - U_{ball}}{U} \quad (4.2)$$

where U represents the average speed at the contact for each component. A 3N normal force was used. For these experiments, a stainless steel ball–silicone elastomer disk tribopair was used as outlined previously (Mills, 2012). This tribopair and these conditions have been previously shown by Malone *et al*. (2003a) to correlate to mouth feel in the mixed regime of lubrication. In each test, Stribeck curves were measured over a speed range of 1–1000 mm s^{-1} with ascending and descending runs repeated three times (six curves in total). Tests were performed at 25ºC. These tests were repeated three times.

4.3. Results and discussion

4.3.1. Influence of pH on spray drying of heat-denatured WPI

4.3.1.1. Particle properties

The influence of pH throughout heat treatment at 65ºC and spray drying were investigated as a method for the production of dry fluid gel-like particles. Particles were dispersed in deionized water at a concentration of 12%. Sizes of aggregates produced at three different pH levels were investigated. These pH levels were used because of the different net charge of the protein above, below and at the pI. The WPI used in this chapter is from a different source to that used in Chapter 3, and as such the native pH of this WPI dispersed in diwater is pH 6.5. Suspension preparation is summarized in Figure 4.1.

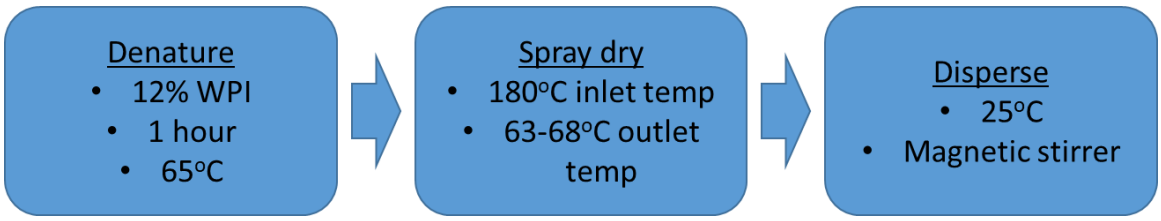

Figure 4. 1. Flow diagram summarizing protein suspension preparation.

Figure 4.2 shows SLS size measurements of particles produced by spray drying heated WPI solutions at different pH levels. WPI solutions were dispersed overnight to ensure proteins were fully hydrated. The pH of this solution was then adjusted and made up to a final concentration of 12% (w/v). These solutions were heated in a stirred water bath at 65ºC for 1 hour before commencing spray drying. Throughout the spray-drying process, the temperature of the feed was maintained between 60 and 65ºC on a stirred hot plate. Spray-dried particles were dispersed in water at room temperature (25ºC) with a magnetic stirrer for 1 hour and left at 25ºC overnight before measurements were taken.

WPI particles spray dried at pH 6.5 showed an average size (D [4, 3]) of 97.2 (±2.5) μm, with a wide distribution of particle size covering two orders of magnitude. Particles produced at pH 3.5 showed an average size of 22.9 (±2.0) μm, with a narrower distribution than that shown for pH 6.5. Particles produced at pH 5, the pI of WPI, showed a bimodal distribution with peaks at 10 μm and 1 μm. This reduced particle size produced at the pI of the protein was observed in the previous body of work for protein fluid gels and is consistent with the literature. This is attributed to the reduced charge on protein molecules at their pI leading to smaller, more dewatered particles being produced, as a result of aggregation being favoured that gives a less ordered gel network.

The production of smaller particles at the pI is in line with what has been observed previously for the production of fluid gels, both in Chapter 3 of this thesis and by Lazidis *et al*. (2016). Owing to the net neutral charge of protein molecules at the pI, aggregation rates are highest at this pH, favouring production of smaller more dewatered particles.

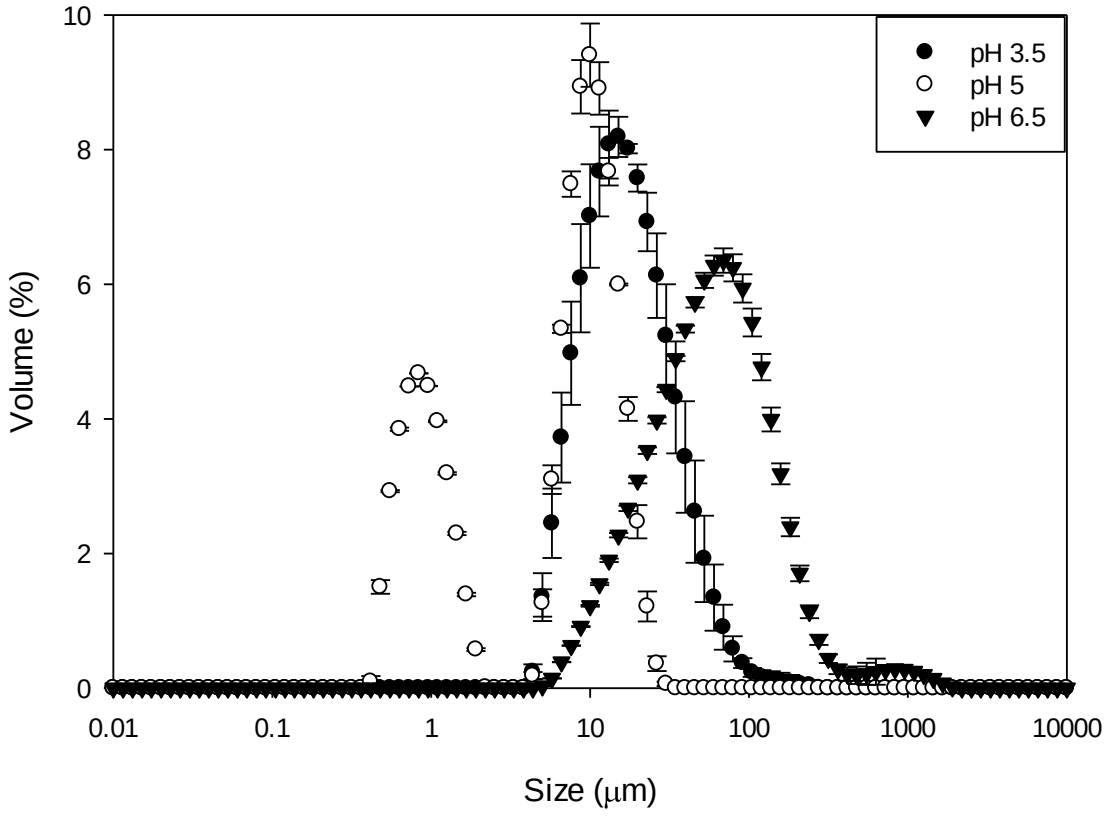

Figure 4. 2. Sizes of particles dispersed after heat treatment at 65ºC and spray drying at pH 3.5, 5 and 6.5. Values represent three repeats, each repeat consisting of three measurements. Error bars represent +/- 1 StD.

Loss of protein solubility was measured to understand the extent of particle formation. Suspensions were centrifuged and a volume-corrected concentration of WPI in the supernatant was determined by UV spectroscopy. This loss of solubility can be attributed to the formation of particles (Table 4.1). It can be seen that the loss of solubility increases with decreasing pH across the three pH levels tested. At pH 6.5, only a 3.15% loss of solubility was observed, which showed that few particles were being produced. At pH 3.5, a 72.9% loss of solubility was observed. From this it can be concluded that 72.9% of the protein present formed particles.

NMR was used to look at the ordering of water by these particles. This was done to investigate whether particles had gel-like water ordering properties similar to those of fluid gels, or whether they had properties of dewatered aggregates. The T2 relaxation of water was calculated from relaxation measurements, with greater values of T2 relaxation representing a more mobile environment of water molecules. For reference, the T2 relaxation time for water is ~2000 ms and for ice it is ~0.001 ms. The lowest T2 relaxation was observed for WPI suspensions at pH 3.5, with the largest T2 for those produced at pH 5. This increased T2 relaxation for suspensions showed water to be in a more mobile environment for these systems. It was proposed that this higher T2 observed for WPI at pH 5 is due to dewatered WPI particles, leading to increased mobility of water being observed in the continuous phase. An increase in loss of solubility was observed between pH 6.5 and pH 5; thus, the ordering of water by particles would be expected to be greater at pH 5. This explanation of dewatered particles being formed fits with the particle sizes observed and the explanation offered for this.

Dewatering of protein gels produced at the pI has been observed previously, with gels having a more porous structure owing to favouring of protein–protein interactions over protein–solvent interactions (Langton and Hermansson, 1992). This is further shown through the use of isoelectric precipitation in which pH is adjusted to the surface pI of proteins to induce hydrophobic aggregation (Vilg and Undeland, 2017).

Figure 4.3 shows a light micrograph of particles produced at pH 3.5 dispersed in water at room temperature. This was carried out to investigate the shapes of particles produced and to verify SLS size measurements. From this it can be seen that anisotropic particles are produced. These particles appear to aggregate together, with some larger aggregates being

observed that appear to be made up of smaller aggregates. The sizing from this micrograph is in good agreement with the SLS measurements in Figure 4.2.

Table 4. 1. Loss of solubility of WPI through heat treatment and spray drying, and T2 relaxation representing the environment of water within the suspensions.

pH	**Loss of solubility (%)**	**T2 relaxation (ms)**
3.5	72.9 ± 0.04	203.8 ± 0.23
5	35.4 ± 0.17	440.5 ± 1.5
6.5	3.15 ± 0.24	307.7 ± 3.6

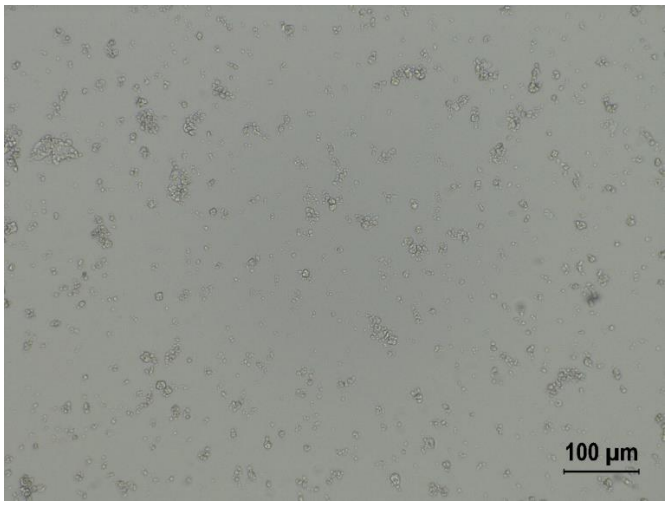

Figure 4. 3. Light micrograph of particles produced through heating and spray drying at pH 3.5 dispersed in water with a magnetic stirrer.

4.3.1.2. Protein structure

To further understand the effects of pH on protein structure through denaturation and spray drying, FTIR spectroscopy was studied. FTIR has been widely used to observe structural changes in proteins as conformational changes of proteins result in changes in absorbance (Arrondo et al., 1993; Mantsch, 1995; Haris and Chapman, 1994). The spectra are presented in Figure 4.4, which shows a full transmission spectrum and an absorbance spectrum focusing on the amide I–III regions.

The amide I–III regions are of specific interest because of the changes in protein secondary and tertiary structure being prevalent in these regions owing to bond stretching. The amide I (1600–1700 cm^{-1}) absorbance is directly related to the secondary structure of the protein, with absorbance being predominantly due to stretching vibration of the C=O bond. This region is particularly useful for investigating secondary structure of proteins as the oxygen in the C=O is involved in the hydrogen bonding that is responsible for protein secondary structure (Barth, 2000). With each secondary structure having a defined hydrogen bonding structure, the amide I region can be used to predict secondary structure of proteins (Jilie and Shaoning, 2007). Absorbance in the amide II region (1510–1590 cm^{-1}) is related to secondary structure. The amide II absorbance is attributed to both N–H bond bending and C–N stretching vibrations. Amide II absorbance is conformationally sensitive.

All three pH values show the typical amide absorbance peaks expected of polypeptides with the amide I peak (1600–1700 cm^{-1}) greater than the amide II peak (1510–1590 cm^{-1}). A large peak is observed at 3000–3600 cm^{-1}, which is attributed to the O–H stretch vibrations. The main distinguishable features of this peak can be attributed to water, owing to the high concentration of water and the number of O–H bonds within the water molecules relative to those present on protein.

Little difference was observed between the spectra of WPI spray dried at pH 5 and pH 6.5, with peaks in the amide I and II regions having similar amplitudes. However, for particles produced at pH 3.5, a change in shape of the peak at 3300 cm^{-1} was observed. A peak at 2980 cm^{-1} was present in the pH 3.5 system, which was not observed at either of the other pH levels. An increase in absorbance in the amide I, II and III peaks was also observed at pH 3.5. These differences in the absorbance spectra showed changes in the protein structure for particles prepared at pH 3.5. These changes will be caused by a degree of unfolding in the

protein through processing. The amide II peak is influenced by a combination of secondary and tertiary structure changes; this change could be due to movement of folded domains within the protein, potentially owing to a molten globule state occurring during processing. These structural changes were investigated in further detail in section 4.3.3.1.

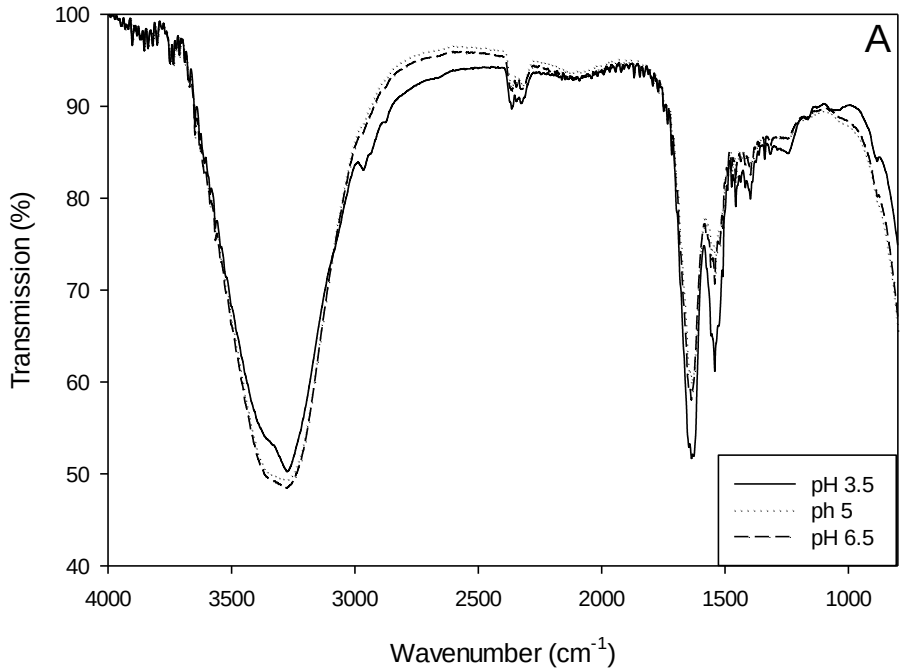

210

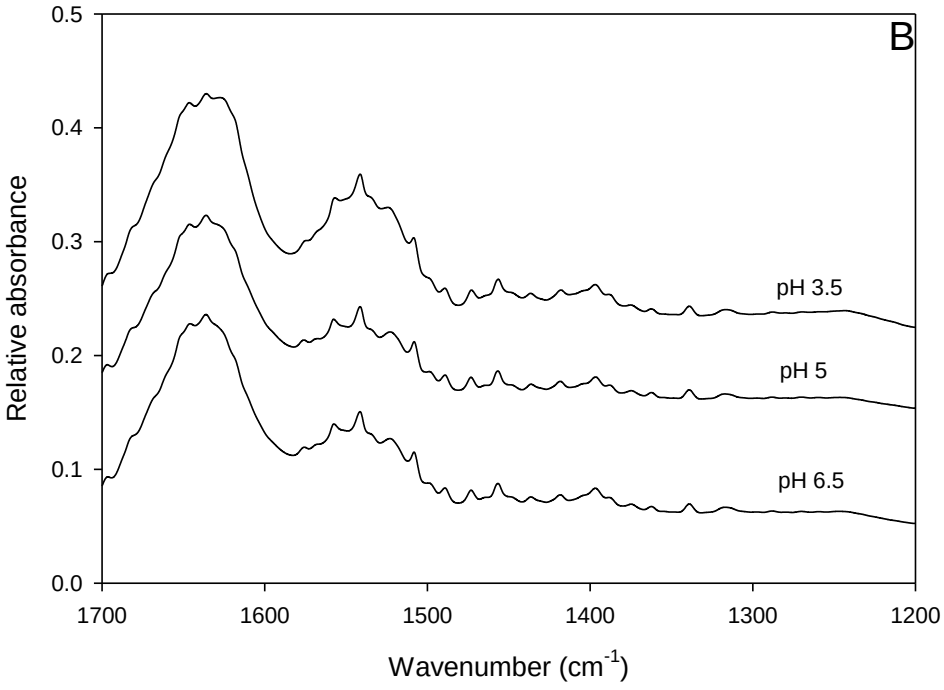

211

212 *Figure 4. 4. A) FTIR transmission spectra and B) absorbance spectra of amide I–III region of WPI*
213 *heat treated and spray dried at pH 3.5, 5 and 6.5, dispersed at 12% (w/w) in water. Each plot is an*
214 *average of 5 tests, each consisting of 64 measurements.*

4.3.1.3. Suspension rheology

To investigate the thickening properties of these particles, increasing concentrations of powder were dispersed in water at room temperature and viscometries were taken. The thickening properties of WPI produced at pH 5 and 6.5 were not investigated owing to the low loss of solubility observed (Table 4.1), inferring minimal particle production. At all concentrations, the shear thinning nature typical of suspensions is observed (Krieger and Dougherty, 1959a) (Figure 4.5). With increasing concentration of WPI from 5% to 20%, viscosity increases. Above 20% there is little change in the viscosity profile observed with increasing concentration.

Increasing viscosity with increasing particle concentration is expected, as with increasing dispersed phase concentration there will be more inter-particle interactions with the increased number of particles. This indicates that the maximum random packing fraction has been reached by 20% concentration. Up to the maximum random packing fraction, interactions between particles are expected to dominate viscosity; with increasing concentration an increase in the number of interactions will occur. However, once the maximum packing fraction of particles has been reached, viscosity will be dominated by particle modulus (Moakes *et al*., 2015b). For suspensions of gel-like particles, it is possible for increased phase volumes as particles deform.

Once the maximum random packing fraction has been reached, it is expected that shear thickening will be observed at higher shear rates; however, this was not observed (Hoffman, 1998). Shear rates used were not high enough for shear thickening to be observed due to the soft nature of these particles.

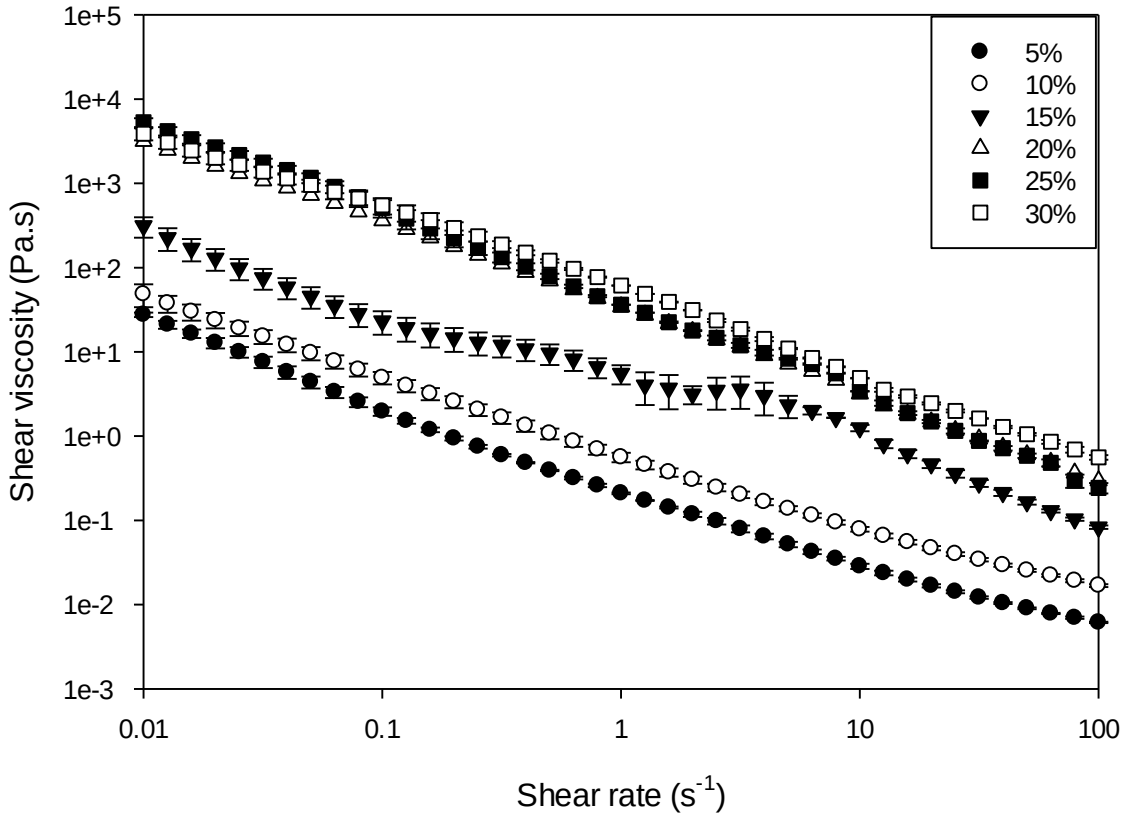

Figure 4. 5. Viscosity profiles of WPI particles produced at pH 3.5 dispersed at different concentrations. Samples were heat treated at 65ºC and spray dried before dispersion in water. Error bars represent +/- 1 StD.

4.3.2. Processing

12% WPI solution was heat treated at 65ºC for 1 hour. Spray-dried solutions were then passed through a Buchi lab scale spray dryer with an inlet temperature of 180ºC, pump speed of 20% and aspirator rate of 95%. This gave an outlet temperature of ~64ºC. Non-spray-dried samples were left to cool at room temperature. Before testing, dry samples were dispersed at 25ºC and left for 24 hours to rehydrate.

To understand the influence of spray drying as a processing technique in the production of protein particles, the effects of heat treatment and heat treatment with spray drying were compared. Figure 4.6 shows the particle size difference between the samples spray dried and

dispersed compared with those that were heat treated without spray drying. The heat-treated and spray-dried sample shows a monomodal distribution peaking at approximately 10 μm. The heat-treated-only samples showed a bimodal distribution with peaks at 25 μm and 300 μm.

Particles are larger for heat-treated-only samples, with a wider size distribution than those that have been spray dried. Heat-treated-only particles have a more irregular shape than those that have been spray dried.

Increased particle size of non-spray-dried samples is a result of a combination of break-up of aggregates in the shear field of the atomizer and inhibited aggregation during cooling. Shear rates in the region of 10,000–100,000 s^{-1} have been estimated through mathematical modelling of the atomization process (Ameri and Maa, 2006). Break-up of aggregates formed during the heat treatment step will be reduced by break-up in shear (Schröder *et al*., 2011; Maa and Hsu, 1996). Further aggregation of WPI occurs during cooling. This aggregation of protein during cooling as well as heating has been observed previously (Van Kleef, 1986). Spray drying of the solution while hot inhibits this aggregation, as the sample cools in its powdered state no longer in suspension.

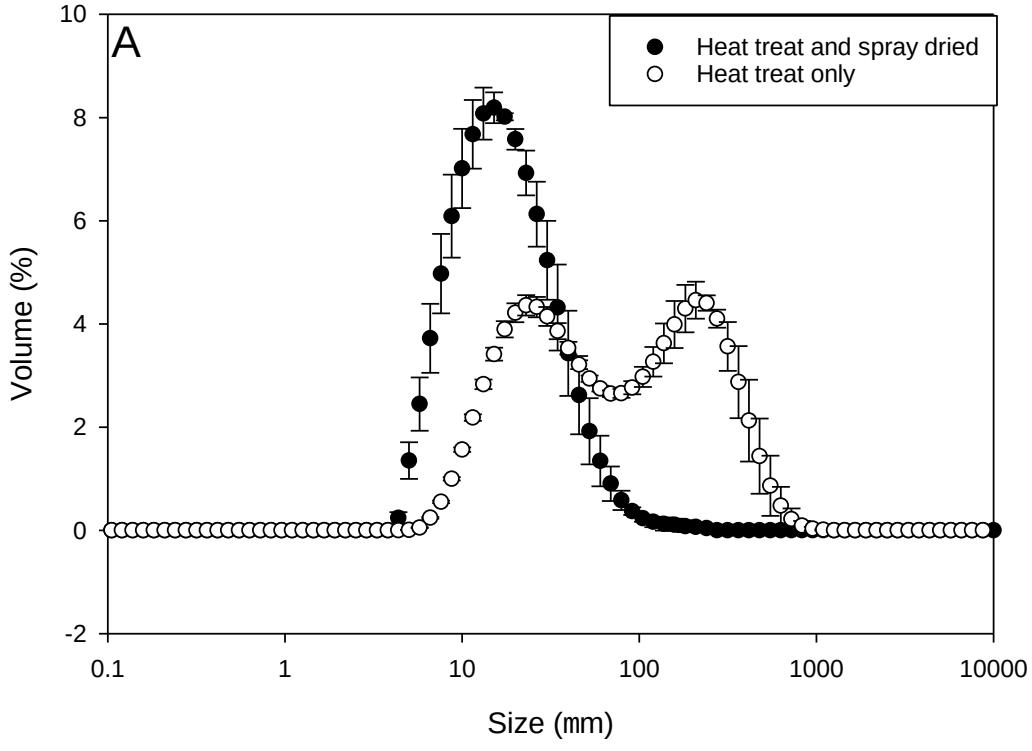

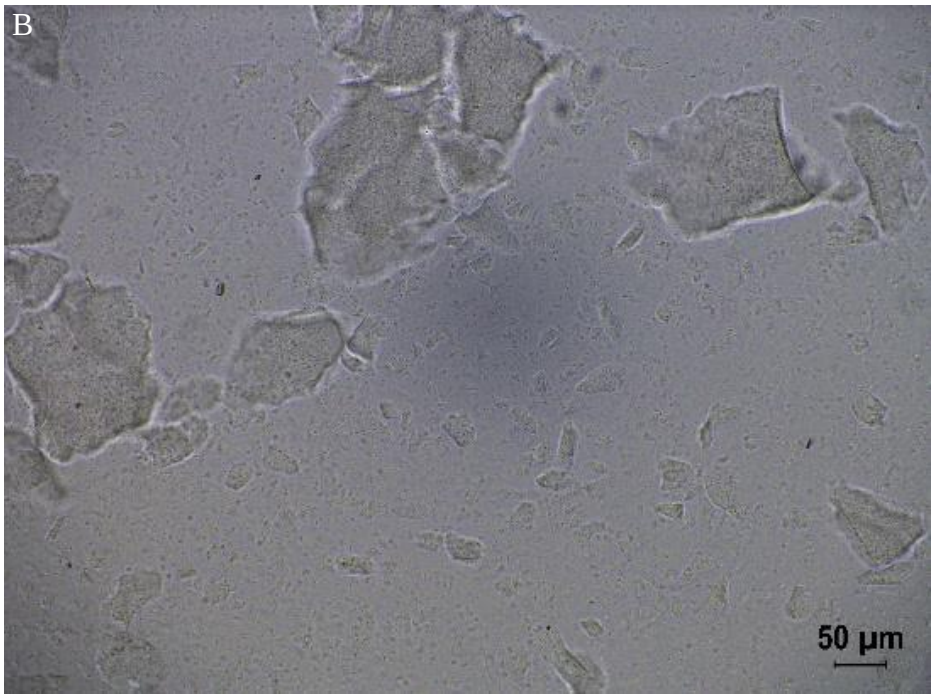

Figure 4. 6. A) Size distribution of WPI particles produced at pH 3.5. B) Micrograph of heat-treat-only sample.

Table 4.2 shows that there was a negligible loss of solubility through spray drying of the heat-treated samples, which suggests that no further aggregation and/or denaturation of proteins occurs during the spray drying. However, the T2 relaxation of water is lower for samples that were spray dried than for those that were not. This shows water to be in a less mobile environment in the spray-dried systems. This greater ordering of water by spray-dried particles suggests structural changes to particles through spray drying. This structural change was further investigated in Figure 4.8.

Table 4. 2. Comparing properties of WPI at pH 3.5 heat treated and spray dried with samples that were only heat treated.

Sample	**Loss of solubility (%)**	**T2 relaxation (ms)**
Heat treat only	72.7 ± 0.03	228.1 ± 2.74
Heat treat and spray dry	72.9 ± 0.04	203.8 ± 0.23

Both spray-dried and non-spray-dried samples showed a shear thinning nature that is expected of particulate systems (Figure 4.7) (Krieger and Dougherty, 1959a). Below 0.5 s^{-1}, very similar viscosity profiles are shown for the heat-treat-only sample and the heat-treat and spray-dried sample. However, above 0.5 s^{-1} there is a reduced shear thinning shown for the heat-treat-only sample. This appears to be a regime change, as at low shear rates inter-particle interactions will dominate viscosity. At higher shear rates, particles are in flow and their properties, such as size distribution, shape and rigidity, dominate viscosity. This difference in observed flow of these two samples is attributed to the larger size distribution with larger particles shown in Figure 4.6.

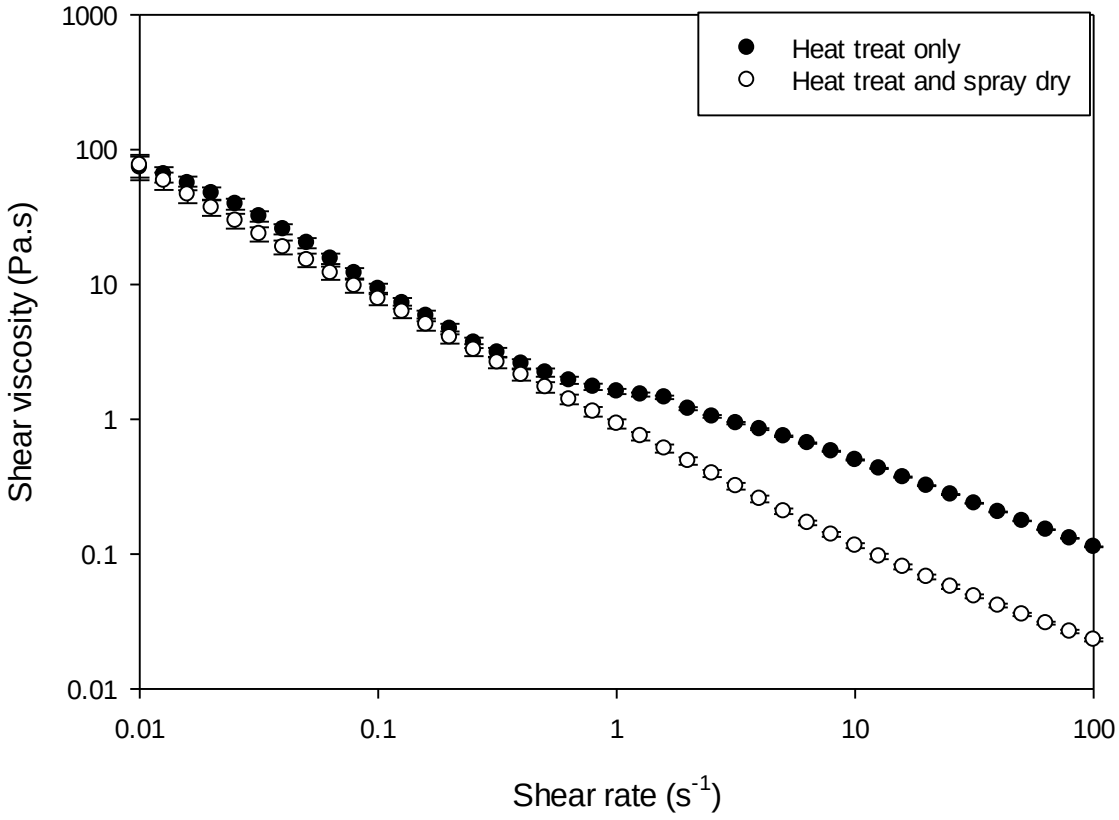

289

290 *Figure 4. 7. Viscosity profiles of 12% WPI at pH 3.5 after heat treatment or heat treatment and spray*
291 *drying. Error bars show +/- 1StD.*

292 4.3.3. Structure determination

293 Figure 4.8 shows FTIR absorbance spectra of WPI through different stages of processing and
294 focuses on the amide I and II regions of the spectra. Similar spectra are observed for the WPI
295 solution and heat-treat-only samples, with broad peaks being observed in the amide I and II
296 regions. Heat treat only shows a slightly broader amide I peak than the WPI solution (1600–
297 1700 cm^{-1}) and a larger amide II peak (1520–1580 cm^{-1}). Again, similar trends were shown in
298 the amide III (1450–1300 cm^{-1}) region, where a broad weak absorbance was shown.

299 For the spray-dried powder, a narrower amide I peak exhibiting a shoulder was observed; the
300 shape of these amide I peaks is looked at in greater detail in the next section (Figure 4.9). A
301 much larger peak in the amide II region was observed for the dry powder. This peak was of

similar intensity to the amide I peak and there were distinct narrower peaks observed within this peak. In the amide III region, there were more individual peaks present in the spray-dried powder than in the solution or heat-treat-only samples.

The dispersed powder showed a decrease in intensity of the amide II band relative to the amide I band. Shoulders are apparent at approximately 1696, 1681 and 1668 cm^{-1}. Narrow peaks are also evident at approximately 1636 and 1645 cm^{-1}. This change in shape of the amide I band is discussed more in the next section. The amide II band decreased in intensity relative to the amide I band compared with that for dry powder. However, the amide I:II ratio was lower for the dispersed powder than for the heat-treat-only samples. This shows that some of the structuring observed through the drying is maintained upon rehydration of the particles. Some narrow peaks appeared in the amide II band for the dispersed powder with distinct peaks at 1506, 1540 and 1555 cm^{-1}. Trends observed for the amide III region of the dispersed powder were similar to that for the amide II region, with the intensity of peaks decreasing and narrow distinct peaks becoming apparent.

This change in structure shown through spray drying is in accordance with findings by Mauerer and Lee (2006), who worked with poly-L-lysine. In this work, an increase in β-sheet content was observed through spray drying. The nature of the structural changes observed is now further investigated.

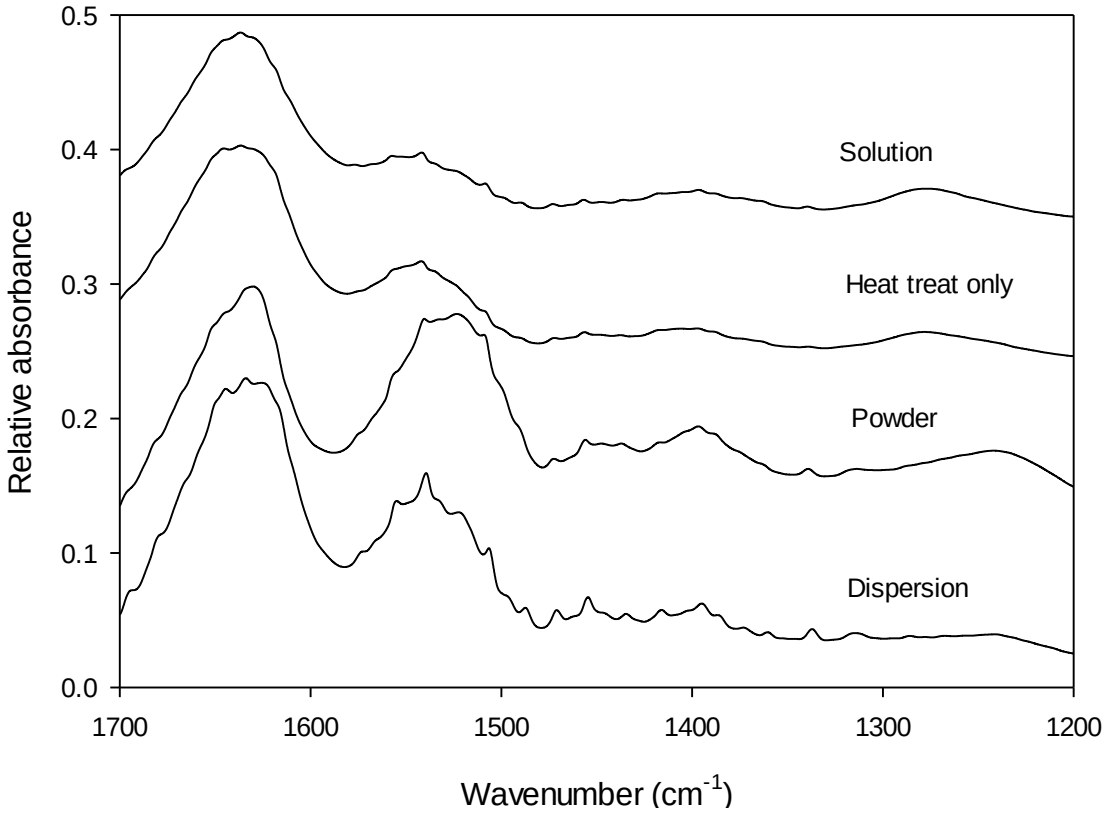

Figure 4. 8. FTIR absorbance spectra of 12% WPI at pH 3.5 at different steps of processing showing the amide I–III regions.

4.3.3.1. Curve fitting for prediction of secondary structure

To further understand the nature of the changes to protein structure through processing, secondary structures were predicted by curve fitting in the amide I region. The amide I region is mainly contributed to by the C=O bond of the proteins, with the O being involved in hydrogen bonding of secondary structures owing to its two lone pairs of electrons. The observed peak is a sum of peaks; these component peaks have been attributed to specific secondary structures. Curve fitting of the amide I region was used to further investigate the observed changes in the shape of the amide I peaks. Second order derivatives and curve deconvolution were used to determine locations of peaks for curve fitting. Only peaks present on both of these were fitted.

The relative areas of these peaks are shown in Table 4.3. The relative areas represent the estimated proportions of the respective secondary structures as the absorbance of a bond is proportional to the number of said bond present.

All samples showed ten component peaks. The position of these peaks showed little variation (within 1 cm^{-1}) for all samples except for the dry powder; for the dry powder, a shift in the position of three peaks was observed (highlighted in Table 4.3). The shifting of these absorbance peaks is likely because of solvation effects, as in the dry powder water will not form hydrogen bonds with amino acid residues of the protein. Shift in absorbance of the low frequency band of β-sheets has been observed previously with solvation effects (Jansen *et al*., 2006).

The only changes in peak areas were observed for the dry powder, in which a loss of intermolecular β-sheets was observed and an increase in β-structure. However, the attribution of structure to dry powder presents challenges owing to peak shifts observed related to solvation of the structures (Gilmanshin *et al*., 1997; Reisdorf and Krimm, 1996; Parrish and Blout, 1972; Manas *et al*., 2000; Walsh *et al*., 2003).

The secondary structure not being broken down through processing is consistent with literature regarding the temperatures used. The maximum temperature the protein is expected to have reached is 65ºC during the heat treatment (refer to Figure 2.1. for prediction of droplet temperature profile), as the outlet temperature in the spray drying process was <65ºC. At these temperatures, the secondary structure of WPI is not expected to break down (Nicolai *et al*., 2011; Geara, 1999). From this, it can be concluded that the changes in the amide I:II ratio observed through spray drying are due to changes in the tertiary structure of WPI. This change in tertiary structure may be linked to the increased ordering of water observed in Table

4.2 for particles spray dried compared with those that were only heat treated. This change in structure is likely due to a lobe of the protein unfolding, which changes the tertiary structure whilst the secondary structure of these lobes remains intact. This correlates with what has been shown previously for egg albumen by Barbu *et al*. (1954). This work showed the mechanism of globular protein gelation to be one of globular protein polymerization not total protein denaturation.

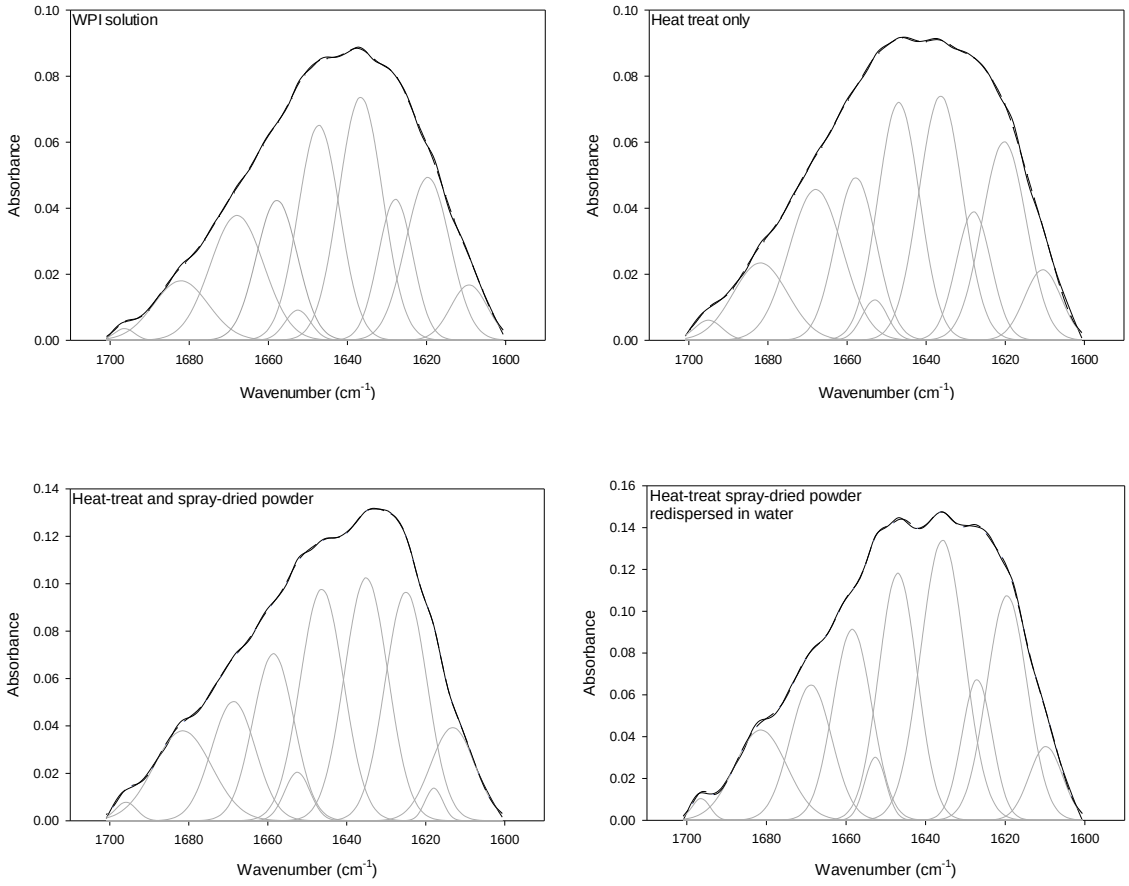

Figure 4. 9. Curve fitting of amide I peaks for WPI at pH 3.5. Grey curves are component peaks, black solid lines are experimental data and black dashed lines show the sum of component peaks fit.

Table 4. 3. Peak parameters for curve fitting of amide I band in WPI at different stages of processing.

Solution		**Heat treat only**		**Powder**		**Re-dispersed**		**Secondary structure assignment**
Centre (cm^{-1})	**Area (%)**	**Centre (cm^{-1})**	**Area (%)**	**Centre (cm^{-1})**	**Area (%)**	**Centre (cm^{-1})**	**Area (%)**	
1696.39	0.994	1695.06	1.51	1695.91	1.46	1696.45	1.49	β-sheet
1682.1	5.02	1681.92	5.8	1681.53	7.06	1681.43	6.15	Intermolecular β-sheet
1667.92	10.54	1667.92	11.33	1668.69	9.37	1668.81	9.22	β-turn
1657.83	11.82	1657.8	12.22	1658.58	13.13	1658.44	13.01	α-helix
1652.55	2.55	1653	3.03	1652.52	3.81	1652.64	4.29	Random coil
1647.24	18.17	1646.93	17.87	1646.31	18.20	1646.97	16.83	Random coil
1636.64	20.55	1636.31	18.36	1635.08	19.09	1635.75	19.08	Intramolecular β-sheet
1627.84	11.91	1628	9.65	1624.97*	17.98	1627.07	9.59	β-structure
1619.67	13.77	1620.26	14.52	1617.92*	2.56	1619.54	15.30	Intermolecular β-sheet
1609.24	4.68	1610.5	5.30	1613.16*	7.32	1609.79	5.03	Side chain vibration

**Highlighted values show the shift in the position of three peaks for the dry powder.*

4.3.4. Influence of salts on the dispersion of protein particle powder

The effects of salts on the dispersion of protein particle powders were investigated. For other hydrocolloid powders, ions have been shown to influence hydration kinetics, and this hydration has been shown to affect microstructures of these systems (Norton, 2016). Understanding of the effects of salts on fat replacers is important, as salts are present in many emulsion-based products.

WPI was dispersed in salt solutions with magnetic stirring as was successfully used for dispersion in diwater. Figure 4.10 shows particle size distributions of spray-dried WPI

particles dispersed in 100 mmol salt solutions. All samples had a single size distribution. WPI dispersed in KCl and NaCl solutions showed a small decrease in size relative to those dispersed in water, with a narrower size distribution. Particles dispersed in $CaCl_2$ showed a wider size distribution with a higher average size, which suggests aggregation was promoted by $CaCl_2$. $CaCl_2$ has been shown previously to bind to denatured WPI, increasing aggregation rates (Ju and Kilara, 1998a). Increased aggregate size has been observed with increasing calcium concentration by Kennel (1994); this increased aggregate size was attributed to intermolecular calcium bridging. Inter-particle calcium bridging may be responsible for the larger particles observed for WPI particles dispersed in $CaCl_2$ solutions.

Figure 4.10B shows the size distributions of spray-dried WPI dispersed in $CaCl_2$ at two different stirrer speeds. This increased stirrer speed was used to further investigate the aggregation observed. This shows that the particle size decreases when the powder is dispersed at a higher stirrer speed. This size was then monitored over time after this higher speed dispersion to investigate the nature of the aggregation. Little change in size was observed over 14 days after dispersion at 800 RPM, showing no secondary aggregation. This supports the fact that the larger particle size observed was due to aggregation of particles in solution of $CaCl_2$. These particles were shown not to re-aggregate over 14 days once broken up.

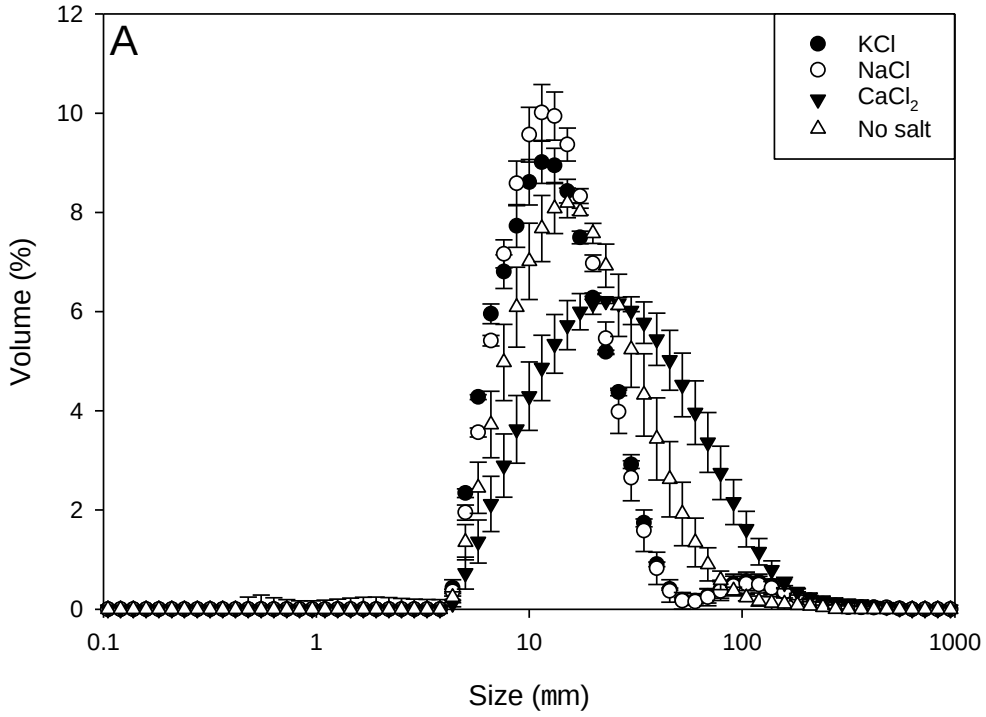

394

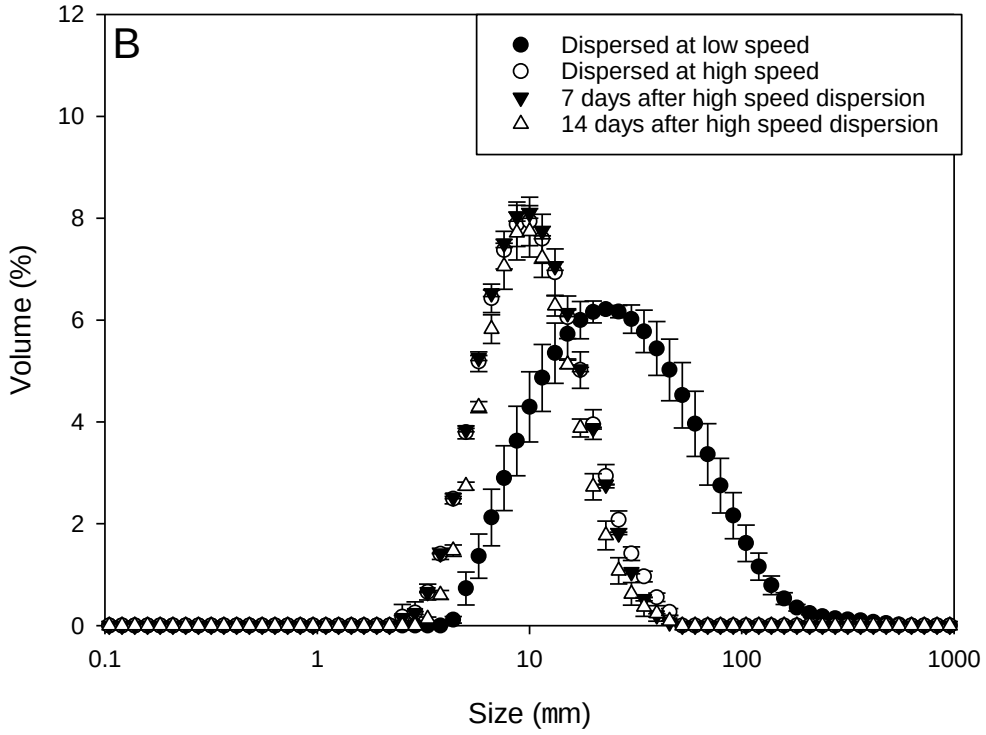

395

396 *Figure 4. 10. Size distribution of protein powder prepared at pH 3.5 heat treated at 65ºC with a spray-*
397 *dried inlet temperature of 180ºC dispersed in salt solutions. A) Dispersed by a magnetic stirrer at 200*
398 *RPM. B) Dispersed in $CaCl_2$ solution by a magnetic stirrer at 200 RPM (low speed) and at 800 RPM*
399 *(high speed). Error bars show +/- 1StD.*

WPI dispersed in salt solutions showed similar shear thinning to particles dispersed in water. The type of salt and concentrations 10–100 mmol had no effect on the observed shear rheology of suspensions (Figure 4.11).

Particles of comparable sizes produced through dispersion of spray-dried WPI in salt solutions and distilled water support that particles are produced through the heat-treatment and spray-drying steps. Thus, particle formation has occurred during the powder preparation. This is further supported by the shear rheology of these suspensions being unaffected by dispersion in salt solutions, showing particle properties to have been determined before dispersion.

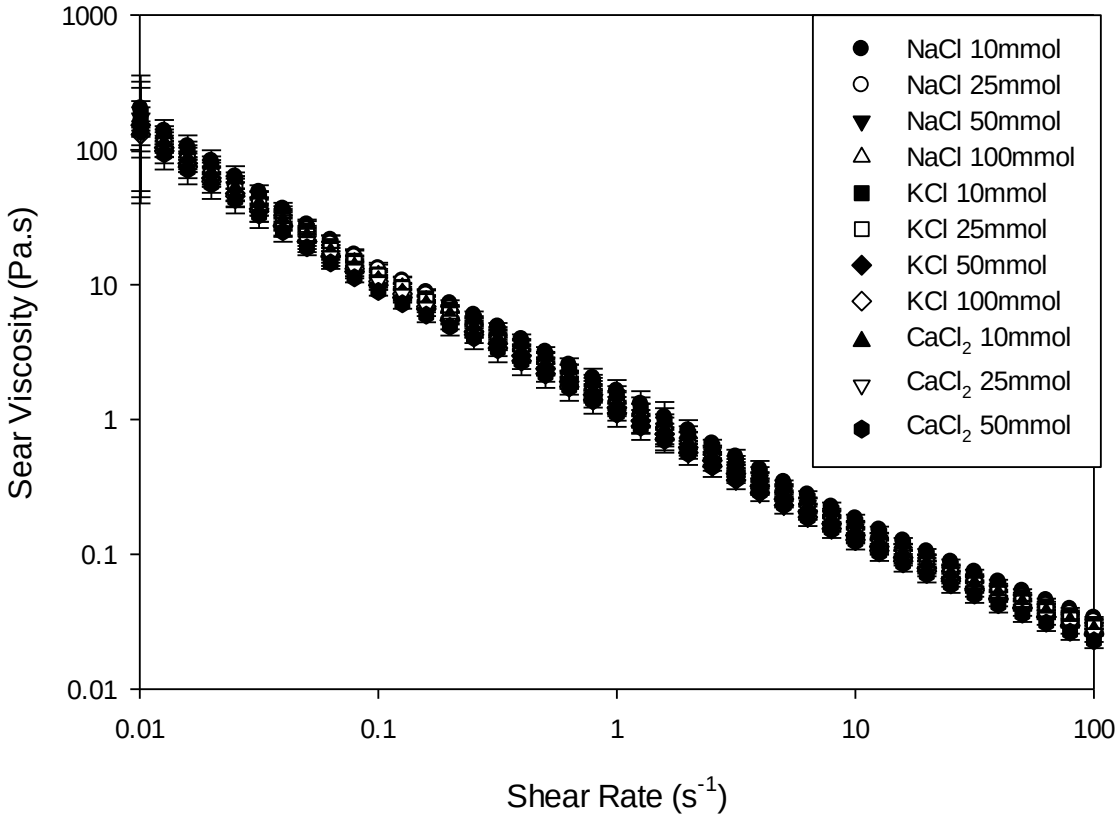

Figure 4. 11. Viscosity profiles of spray-dried WPI particles dispersed in salt solutions 12% w/w. Error bars show +/- 1 STD.

4.3.5. Effect of salts on spray drying and heat treatment

The effects of salts through the heat-treatment and spray-drying process were investigated. This was performed to look at how properties of the same formulations are influenced by processing parameters.

Particles produced with all three salts used showed a bimodal distribution with a larger volume around 10 μm and a smaller volume peak at 1 μm (Figure 4.12). For NaCl and KCl, both monovalent cations, a very similar size distribution was observed. For $CaCl_2$, a divalent cation, a larger modal size for the larger peak was observed and a decrease in volume of smaller particles. All particles produced in salt solutions showed a smaller average size than those produced without salt.

The bimodal size distribution with peaks at 1 μm and 10 μm is similar to that observed in Figure 4.2 for particles produced at the pI of WPI. The production of these smaller particles may be due to reduced electrostatic repulsion between molecules favouring aggregation. The effect of electrostatic repulsion will reduce in the presence of ions, as electrostatic shielding will occur. WPI has been shown previously to favour aggregation in salt solutions (Verheul and Roefs, 1998; Nicolai *et al*., 2011).

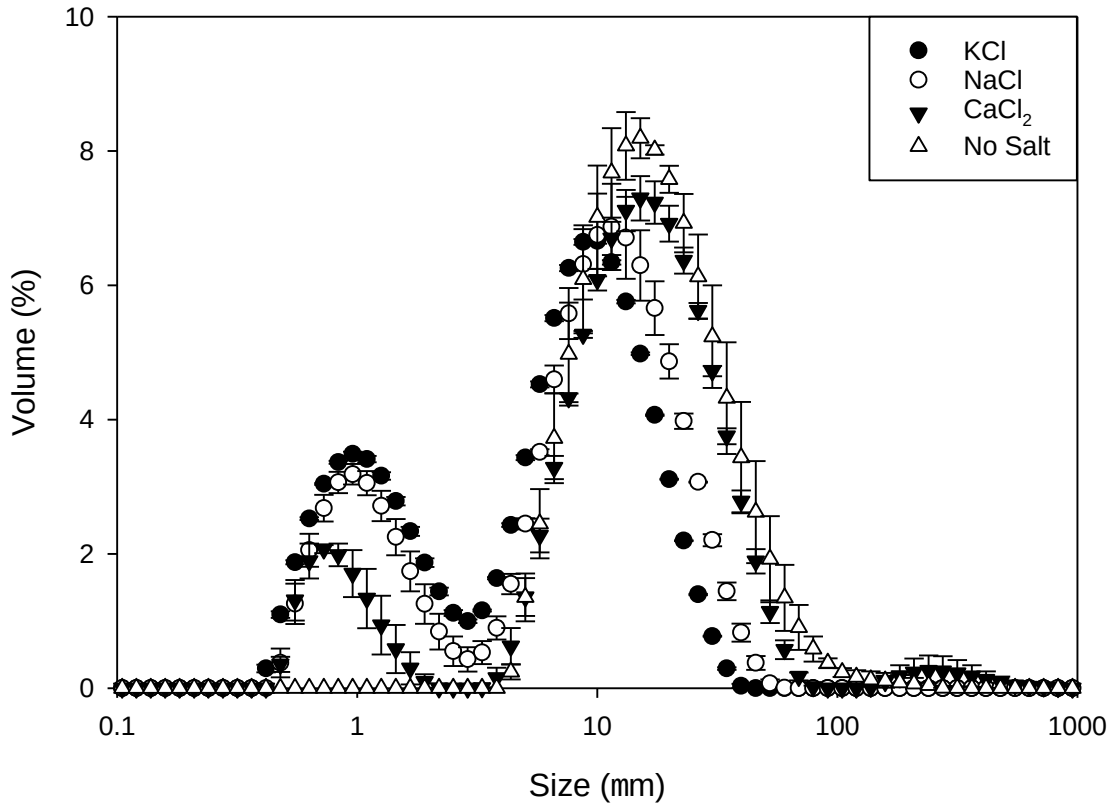

Figure 4. 22. Size distribution of WPI powders dispersed in water that were prepared by heat treatment and spray drying at pH 3.5 and 100 mmol of KCl, NaCl or $CaCl_2$. Error bars show +/- 1 StD.

4.3.5.1. FTIR

Figure 4.13 shows FTIR absorbance spectra of WPI heated at 65ºC for 1 hour then spray dried at pH 3.5 in 100 mmol of the appropriate salt. This was used to probe the effects of salts on the structure of the proteins. For all samples, the classic amide I–III peaks expected of a protein were observed. Little change in the spectra between no salt and KCl was observed. For NaCl, there was a decrease in amplitude of the amide II band (1510–1590 cm^{-1}), with distinct narrow peaks at 1506, 1540 and 1555 cm^{-1}. Narrower peaks are observed in the amide III region also. However, the overall absorbance spectrum for NaCl was similar to that for KCl and no salt. This suggests that these observed changes are due to band narrowing as a result of small alterations in the environment of structures. For $CaCl_2$, fewer distinct peaks

were present within the broad amide I and II peaks. Shoulders at the same wavenumbers indicate that these structures were still present.

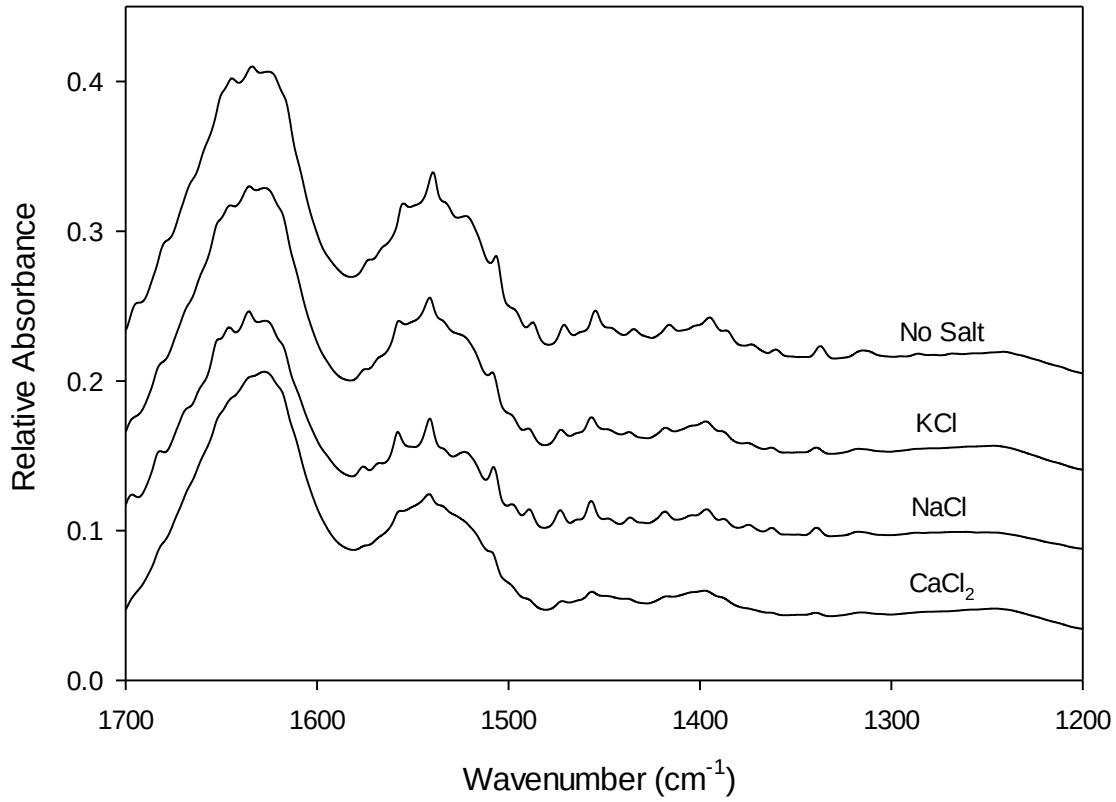

Figure 4. 13. FTIR absorbance spectra showing the amide I–III regions for dispersions of WPI heat treated and spray dried at pH 3.5 in 100 mmol of KCl, NaCl or $CaCl_2$. Each plot is an average of 3 repeats, each repeat consisting of 64 measurements.

4.3.5.2. Shear rheology

Figure 4.14 shows the influence of concentration on shear viscosity of WPI suspensions spray dried in salts. All samples showed a shear thinning nature similar to that observed in Figure 4.5. For all samples, viscosity increased with increasing concentration between 5% and 20%. However, for the samples spray dried without salt, viscosity plateaued at 20%, showing no further increase between 20% and 30%. For WPI particles produced with no salt, a concentration >30% could not be achieved as the powder did not fully disperse. For all samples spray dried in 100 mmol of salt, no plateau was observed.

The plateau observed for particles produced with no salt was explained previously as being caused by the maximum random packing fraction of these particles being reached. The lack of plateau for samples produced in salt suggests that this maximum random packing fraction has not been reached. This is explained by the bimodal particle size distribution observed for particles produced in salts. Because small particles can fit in the gaps between larger particles, the maximum packing fraction is expected to be a higher phase volume than for a monomodal distribution. Thus, larger concentrations of WPI are required to reach this maximum packing fraction.

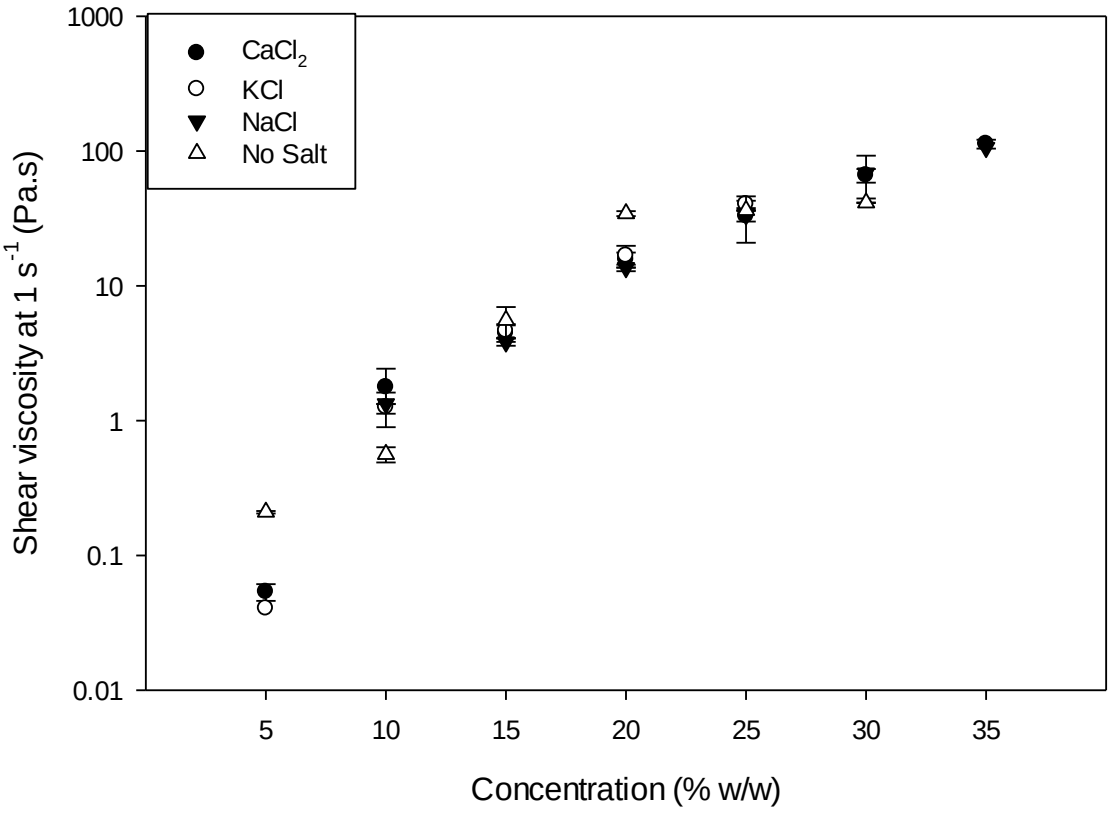

Figure 4. 34. Viscosity at 1 s^{-1} of WPI heat treated at 65ºC and spray dried at pH 3.5 in 100 mmol of KCl, NaCl or $CaCl_2$. Error bars show +/- 1 StD.

4.3.6. Tribology

Figure 4.15A shows Stribeck curves for increasing concentrations of spray-dried WPI. As concentration increased, friction in the boundary regime decreased. For concentrations up to 15%, however, there was an overlap of error bars in this region. This observed decrease in boundary friction with increasing particle phase volume has been observed previously by Garrec and Norton (2013). As speed increases, lubrication transitions into the mixed regime of lubrication. For concentrations up to 15%, similar lubricating properties were shown. For these concentrations, the hydrodynamic regime of lubrication was not observed. At the speeds tested, 20% and 25% spray-dried WPI showed all three regimes of lubrication. This agrees with the changes in viscosity observed with an increase in viscosity at 20%. Increased viscosity is expected to decrease the entrainment speed at which a system will transition to the boundary and elasto-hydrodynamic lubrication (EHL) regimes of lubrication (Stribeck, 1902).

No difference in the friction profiles was observed between ramping up and ramping down (Figure 4.15B). For agarose and alginate fluid gels, a peak in friction in the mixed regime was observed as the speed ramped up, with no peak observed as the speed ramped down (Fernández Farrés *et al*., 2013; Fernández Farrés, 2015). This observed difference has been attributed to the entrainment of particles into the contact as the gap between the ball and disc is comparable to the particle size, leading to a rolling–sliding contact in which the surfaces are supported by the particles. The explanation for this phenomenon only being observed as speed was ramped up was because of the contact starting as a dry contact on the up ramp. However, on the ramp down, particles are already present within the gap, supporting the surfaces. No difference being observed between the up and down ramps suggests that particles are not being obstructed from entering the contact as the entrainment speed ramps up.

In the literature in which these phenomena have been investigated previously, the phase volume of systems used was not documented; thus, the effect of particle concentration in previous cases was not discussed. However, it has been observed in agarose fluid gels that with increasing concentration of agarose used for fluid gel production, there was a reduction in the observed difference between the friction values of ramping up and ramping down.

Figure 4.15C shows Stribeck curves of spray-dried WPI, a WPI solution and water; this was carried out to investigate whether soluble WPI had a surface effect and to further investigate the presence of particles in the contact. Surface effects have been observed previously for anisotropic systems owing to the hydrophobic nature of the polydimethylsiloxane (PDMS) surface used. The spray-dried WPI dispersion showed increased friction values in the boundary regime of lubrication compared with the WPI solution. This suggests that at these low speeds there are particles present in the contacts. This increased friction as particles are entrained while the gap is smaller than particle size has been observed previously (Fernández Farrés and Norton, 2015). This increased friction is due to the deformation of the surfaces and particles to squeeze them through the contact. If there are particles present in the contact at 10% concentration of particles, there will be particles present in the contact at all speeds for 15% spray-dried WPI. This observation of particles being entrained at all speeds has been shown by Fernández Farrés and Norton (2015) for agar particles >100 μm.

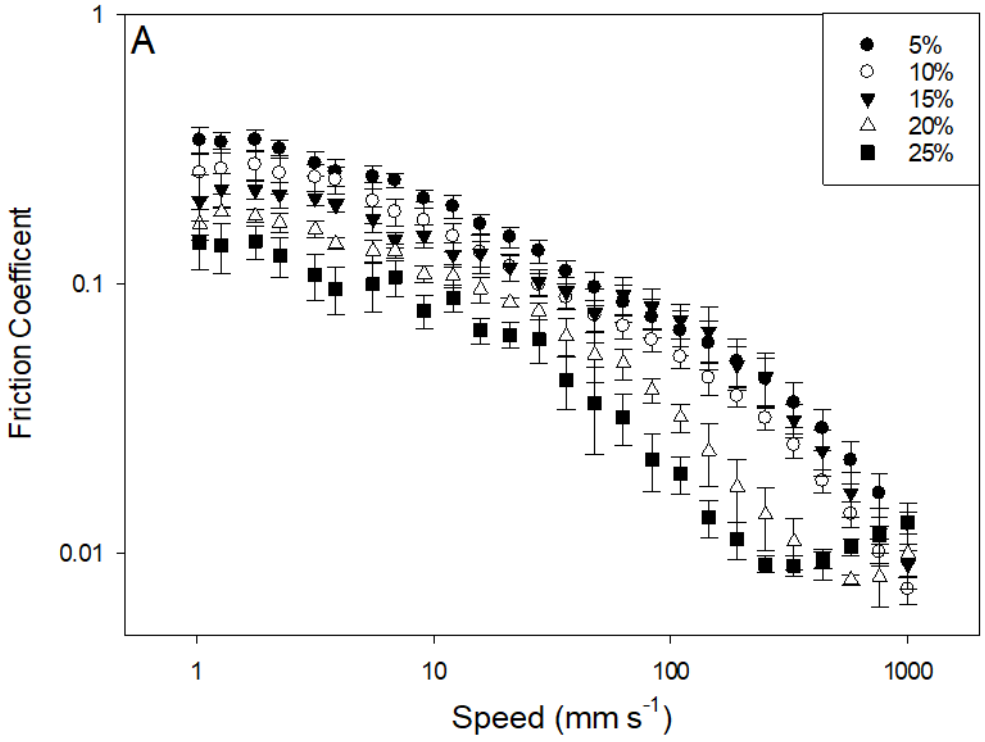
A
5%
10%
15%
20%
25%
Friction Coefficent
1
0.1
0.01
1
10
100
1000
Speed (mm s-1)

510

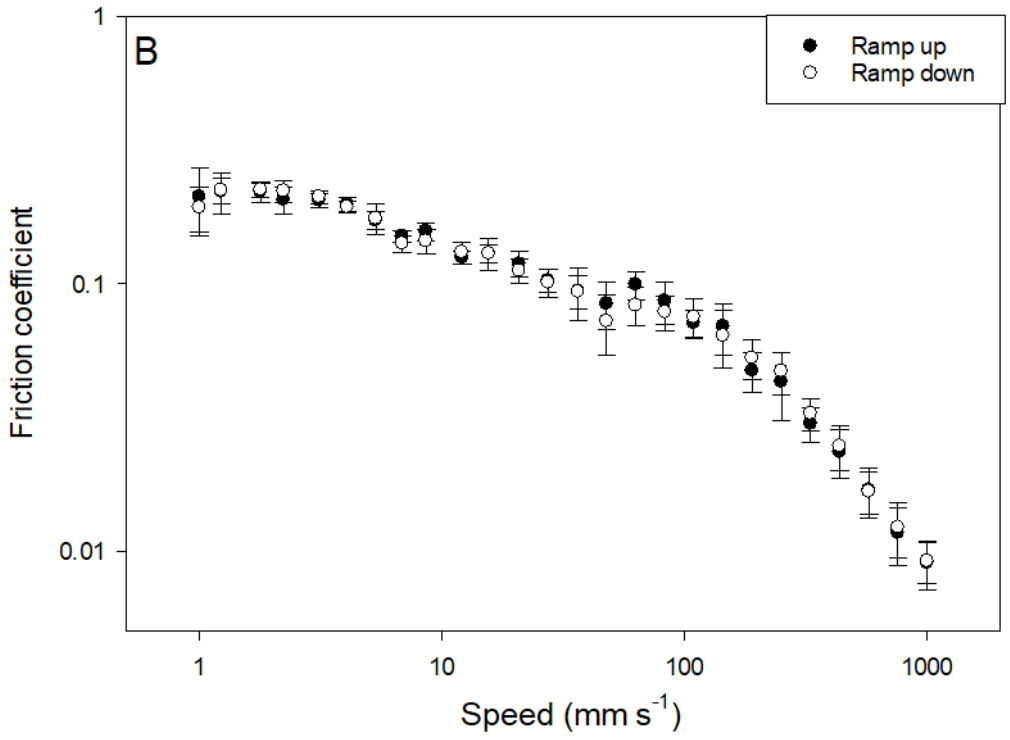
B
Ramp up
Ramp down
Friction coefficient
1
0.1
0.01
1
10
100
1000
Speed (mm s-1)

511

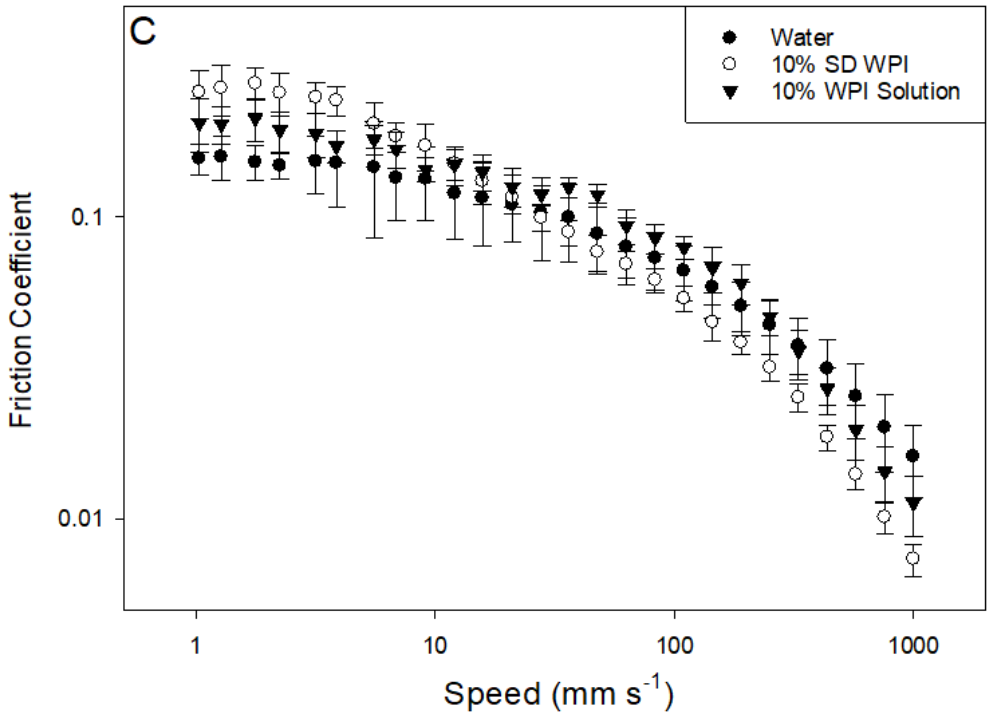

Figure 4. 15. Tribology measurements of WPI prepared by a spray-drying method using a stainless steel ball–elastomer disc tribopair. A) Dispersed at increasing concentration. B) Dispersed at 15% showing the up and down ramps. C) Comparing WPI that has been spray dried with water and a non-spray-dried WPI solution. Error bars show +/- 1 StD.

The suspensions produced from spray drying WPI appear to have similar bulk properties to WPI fluid gels produced at pH 3.5; however, a higher concentration of protein is required for this. 15% spray-dried WPI was less viscous than the 12% WPI fluid gel (Figure 3.5). The tribology shown for 20% WPI produced by the spray-drying method was similar to that shown in Figure 3.9 for 12% WPI fluid gels produced at pH 3.5. This shows that the properties of fluid gels can be recreated with dry powder produced by the spray-drying method presented here.

4.4. Conclusions

A novel method for the production of dry protein fluid gel particles has been presented. Spray drying of heated WPI solution can successfully produce dispersible particles at pH 3.5. These

particles showed thickening at protein concentrations of 20% w/w. This novel processing technique using the spray dryer as the shearing step provides scale-up potential, removing the requirement for the rapid heat exchange at large scales that is required for traditional fluid gel production methods. The rheology of these suspensions was shown to be stable with salts, showing no change when dispersed in salt solutions. This demonstrates the potential use of these suspensions in salt-containing products.

4.5. References

AMERI, M. & MAA, Y.-F. 2006. Spray Drying of Biopharmaceuticals: Stability and Process Considerations. Drying Technology, 24, 763-768.

ANANDHARAMAKRISHNAN, C. 2015. *Spray drying techniques for food ingredient encapsulation*, John Wiley & Sons.

ANANDHARAMAKRISHNAN, C., RIELLY, C. D. & STAPLEY, A. G. F. 2008. Loss of solubility of α-lactalbumin and β-lactoglobulin during the spray drying of whey proteins. *LWT - Food Science and Technology,* 41**,** 270-277.

ARRONDO, J. L. R., MUGA, A., CASTRESANA, J. & GOÑI, F. M. 1993. Quantitative studies of the structure of proteins in solution by fourier-transform infrared spectroscopy. *Progress in Biophysics and Molecular Biology,* 59**,** 23-56.

BARTH, A. 2000. The infrared absorption of amino acid side chains. *Progress in Biophysics and Molecular Biology,* 74**,** 141-173.

BECKTEL, W. J. & SCHELLMAN, J. A. 1987. Protein stability curves. *Biopolymers,* 26**,** 1859-1877.

BOYE, J. I., AKSAY, S., ROUFIK, S., RIBÉREAU, S., MONDOR, M., FARNWORTH, E. & RAJAMOHAMED, S. H. 2010. Comparison of the functional properties of pea, chickpea and lentil protein concentrates processed using ultrafiltration and isoelectric precipitation techniques. *Food Research International,* 43**,** 537-546.

CARPENTER, J. F. & CROWE, J. H. 1989. An infrared spectroscopic study of the interactions of carbohydrates with dried proteins. *Biochemistry,* 28**,** 3916-3922.

CHI, E. Y., KRISHNAN, S., KENDRICK, B. S., CHANG, B. S., CARPENTER, J. F. & RANDOLPH, T. W. 2003a. Roles of conformational stability and colloidal stability in

the aggregation of recombinant human granulocyte colony-stimulating factor. *Protein Science,* 12**,** 903-913.

CHI, E. Y., KRISHNAN, S., RANDOLPH, T. W. & CARPENTER, J. F. 2003b. Physical Stability of Proteins in Aqueous Solution: Mechanism and Driving Forces in Nonnative Protein Aggregation. *Pharmaceutical Research,* 20**,** 1325-1336.

CONWAY, B. E. & AYRANCI, E. 1999. Effective Ionic Radii and Hydration Volumes for Evaluation of Solution Properties and Ionic Adsorption. *Journal of Solution Chemistry,* 28**,** 163-192.

DE WIT, J. 1989. The milk protein system, Functional properties of whey proteins. *Developments in Dairy Chemistry-4*.

DEBYE, P. & HÜCKEL, E. 1923. De la theorie des electrolytes. I. abaissement du point de congelation et phenomenes associes. *Physikalische Zeitschrift,* 24**,** 185-206.

DILL, K. A. 1990. Dominant forces in protein folding. *Biochemistry,* 29**,** 7133-7155.

FARID, M. 2003. A new approach to modelling of single droplet drying. *Chemical Engineering Science,* 58**,** 2985-2993.

G. MULKERRIN, M. & WETZEL, R. 1989. *pH dependence of the reversible and irreversible thermal denaturation of γ interferons*.

GANEA, C., BABES, A., LÜPFERT, C., GRELL, E., FENDLER, K. & CLARKE, R. J. 1999. Hofmeister Effects of Anions on the Kinetics of Partial Reactions of the Na+,K+-ATPase. *Biophysical Journal,* 77**,** 267-281.

GEARA, C. 1999. *Study of the gelation of whey protein isolate by FTIR spectroscopy and rheological measurements.* McGill University.

GIDLEY, M. J. & HEDGES, N. D. 1998. Suspensions of gelled biopolymers. Google Patents.

GILMANSHIN, R., WILLIAMS, S., CALLENDER, R. H., WOODRUFF, W. H. & DYER, R. B. 1997. Fast Events in Protein Folding: Relaxation Dynamics and Structure of the I Form of Apomyoglobin. *Biochemistry,* 36**,** 15006-15012.

GRIMSLEY, G. 1999. *Increasing protein stability by altering long-range coulombic interactions*.

HALL, G. M. 1996. *Methods of testing protein functionality*, Springer Science & Business Media.

HARIS, P. I. & CHAPMAN, D. 1994. Analysis of Polypeptide and Protein Structures Using Fourier Transform Infrared Spectroscopy. *In:* JONES, C., MULLOY, B. & THOMAS, A. H. (eds.) *Microscopy, Optical Spectroscopy, and Macroscopic Techniques.* Totowa, NJ: Humana Press.

HOFFMAN, R. L. 1998. Explanations for the cause of shear thickening in concentrated colloidal suspensions. Journal of Rheology, 42, 111-123.

HOFMEISTER, F. 1888. Zur lehre von der wirkung der salze. *Archiv für experimentelle Pathologie und Pharmakologie*, 25**,** 1-30.

IP, A., ARAKAWA, T., SILVERS, H., M. RANSONE, C. & W. NIVEN, R. 1995. *Stability of recombinant consensus interferon to air-jet and ultrasonic nebulization.*

JANSEN, T. L. C., DIJKSTRA, A. G., WATSON, T. M., HIRST, J. D. & KNOESTER, J. 2006. Modeling the amide I bands of small peptides. *The Journal of Chemical Physics*, 125**,** 044312.

JILIE, K. & SHAONING, Y. 2007. Fourier Transform Infrared Spectroscopic Analysis of Protein Secondary Structures. *Acta Biochimica et Biophysica Sinica,* 39**,** 549-559.

JORDAN, I. K., KONDRASHOV, F. A., ADZHUBEI, I. A., WOLF, Y. I., KOONIN, E. V., KONDRASHOV, A. S. & SUNYAEV, S. 2005. A universal trend of amino acid gain and loss in protein evolution. *Nature,* 433**,** 633.

JU, Z. Y. & KILARA, A. 1998. Aggregation Induced by Calcium Chloride and Subsequent Thermal Gelation of Whey Protein Isolate. *Journal of Dairy Science,* 81**,** 925-931.

KAKALIS, L. T. & REGENSTEIN, J. M. 1986. Effect of pH and salts on the solubility of egg white protein. *Journal of Food Science,* 51**,** 1445-1447.

KARACA, A. C., LOW, N. & NICKERSON, M. 2011. Emulsifying properties of chickpea, faba bean, lentil and pea proteins produced by isoelectric precipitation and salt extraction. *Food Research International,* 44**,** 2742-2750.

KENNEL, R. 1994. *Hitzeinduzierte Aggregatbildung von Molkenproteinen.* PhD thesis, Technische Universität München.

KRIEGER, I. M. & DOUGHERTY, T. J. 1959. A mechanism for non-Newtonian flow in suspensions of rigid spheres. *Transactions of the Society of Rheology,* 3**,** 137-152.

KUHN, P. R. & FOEGEDING, E. A. 1991. Factors Influencing Whey Protein Gel Rheology: Dialysis and Calcium Chelation. *Journal of Food Science,* 56**,** 789-791.

LANGTON, M. & HERMANSSON, A.-M. 1992. Fine-stranded and particulate gels of β-lactoglobulin and whey protein at varying pH. *Food Hydrocolloids,* 5**,** 523-539.

MAA, Y.-F. & HSU, C. C. 1996. Effect of high shear on proteins. *Biotechnology and Bioengineering,* 51**,** 458-465.

MANAS, E. S., GETAHUN, Z., WRIGHT, W. W., DEGRADO, W. F. & VANDERKOOI, J. M. 2000. Infrared Spectra of Amide Groups in α-Helical Proteins: Evidence for Hydrogen Bonding between Helices and Water. *Journal of the American Chemical Society,* 122**,** 9883-9890.

MANN, B. & MALIK, R. 1996. Studies on some functional characteristics of whey protein-polysaccharide complex.

MANTSCH, H. H. 1995. The Use and Misuse of FTIR Spectroscopy in the Determination of Protein Structure AU - Jackson, Michael. *Critical Reviews in Biochemistry and Molecular Biology,* 30**,** 95-120.

MASTERS, G. M. & ELA, W. P. 1991. *Introduction to environmental engineering and science*, Prentice Hall Englewood Cliffs, NJ.

MAUERER, A. & LEE, G. 2006. Changes in the amide I FT-IR bands of poly-l-lysine on spray-drying from α-helix, β-sheet or random coil conformations. *European Journal of Pharmaceutics and Biopharmaceutics,* 62**,** 131-142.

MOAKES, R. J. A., SULLO, A. & NORTON, I. T. 2015. Preparation and rheological properties of whey protein emulsion fluid gels. *RSC Advances,* 5**,** 60786-60795.

NICOLAI, T., BRITTEN, M. & SCHMITT, C. 2011. β-Lactoglobulin and WPI aggregates: Formation, structure and applications. *Food Hydrocolloids,* 25**,** 1945-1962.

NORTON, A. B. 2016. *Microstructural understanding of hydrocolloid and mixed hydrocolloid systems for biomedical applications.* University of Birmingham.

NUCCI, N. V. & VANDERKOOI, J. M. 2008. Effects of Salts of the Hofmeister Series on the Hydrogen Bond Network of Water. *Journal of molecular liquids,* 143**,** 160-170.

PACE, C. N., GRIMSLEY, G. R. & SCHOLTZ, J. M. 2009. Protein ionizable groups: pK values and their contribution to protein stability and solubility. *Journal of Biological Chemistry,* 284**,** 13285-13289.

PARRISH, J. R. & BLOUT, E. R. 1972. The conformation fo poly-L-alanine in hexafluoroisopropanol. *Biopolymers,* 11**,** 1001-1020.

PELEGRINE, D. H. G. & GASPARETTO, C. A. 2005. Whey proteins solubility as function of temperature and pH. *LWT - Food Science and Technology,* 38**,** 77-80.

REISDORF, W. C. & KRIMM, S. 1996. Infrared Amide I‘ Band of the Coiled Coil. *Biochemistry,* 35**,** 1383-1386.

SCHRÖDER, J., LEDERER, M., GAUKEL, V. & SCHUCHMANN, H. Effect of atomizer geometry and rheological properties on effervescent atomization of aqueous polyvinylpyrrolidone solutions. ILASS–Europe 24rd Annual Conference on Liquid Atomization and Spray Systems, Estoril, Portugal, 2011.

SHAH, S. M. & LUKSAS, A. J. 1980. Food composition containing whey colloidal precipitate. Google Patents.

STRIOLO, A., BRATKO, D., WU, J. Z., ELVASSORE, N., BLANCH, H. W. & PRAUSNITZ, J. M. 2002. Forces between aqueous nonuniformly charged colloids from molecular simulation. *The Journal of Chemical Physics,* 116**,** 7733-7743.

STROP, P. & MAYO, S. L. 2000. Contribution of Surface Salt Bridges to Protein Stability. *Biochemistry,* 39**,** 1251-1255.

TANFORD, C. & KIRKWOOD, J. G. 1957. Theory of Protein Titration Curves. I. General Equations for Impenetrable Spheres. *Journal of the American Chemical Society,* 79**,** 5333-5339.

TOLLINGER, M., CROWHURST, K. A., KAY, L. E. & FORMAN-KAY, J. D. 2003. Site-specific contributions to the pH dependence of protein stability. *Proceedings of the National Academy of Sciences,* 100**,** 4545-4550.

TSAI, A. M., VAN ZANTEN, J. H. & BETENBAUGH, M. J. 1998. II. Electrostatic effect in the aggregation of heat-denatured RNase A and implications for protein additive design. *Biotechnology and Bioengineering,* 59**,** 281-285.

672 VAN KLEEF, F. S. M. 1986. Thermally induced protein gelation: Gelation and rheological
673 characterization of highly concentrated ovalbumin and soybean protein gels.
674 *Biopolymers,* 25**,** 31-59.
675 VERHEUL, M. & ROEFS, S. P. F. M. 1998. Structure of Particulate Whey Protein Gels:
676 Effect of NaCl Concentration, pH, Heating Temperature, and Protein Composition.
677 *Journal of Agricultural and Food Chemistry,* 46**,** 4909-4916.
678 VILG, J. V. & UNDELAND, I. 2017. pH-driven solubilization and isoelectric precipitation of
679 proteins from the brown seaweed Saccharina latissima-effects of osmotic shock, water
680 volume and temperature. *Journal of applied phycology,* 29**,** 585-593.
681 WALSH, S. T. R., CHENG, R. P., WRIGHT, W. W., ALONSO, D. O. V., DAGGETT, V.,
682 VANDERKOOI, J. M. & DEGRADO, W. F. 2003. The hydration of amides in
683 helices; a comprehensive picture from molecular dynamics, IR, and NMR. *Protein*
684 *science : a publication of the Protein Society,* 12**,** 520-531.
685 WONG, D. W., CAMIRAND, W. M., PAVLATH, A. E., PARRIS, N. & FRIEDMAN, M.
686 1996. Structures and functionalities of milk proteins. *Critical Reviews in Food Science*
687 *& Nutrition,* 36**,** 807-844.
688 ZHU, H. & DAMODARAN, S. 1994. Effects of calcium and magnesium ions on aggregation
689 of whey protein isolate and its effect on foaming properties. *Journal of Agricultural*
690 *and Food Chemistry,* 42**,** 856-862.

CHAPTER 5.
Particle-stabilized emulsions

5.1. Introduction

To further understand the potential for these protein particles in reduced fat products the properties of emulsions containing these particles must be investigated. The dry WPI particles were chosen to be investigated. These dry protein particles offer advantages over fluid gel particles as they can be manufactured and shipped into current production facilities. This chapter investigates the properties of emulsions stabilized by the WPI particles produced by the spray-drying method. Understanding the interactions of oil droplets with the suspensions for fat replacement is important, as some fat needs to be present in reduced fat products to maintain a desirable flavour profile.

5.2. Materials and methods

5.2.1. WPI powder preparation

The spray-dried WPI powder was prepared as follows. WPI powder was dispersed at 15% W/W in reverse osmosis water to produce WPI solutions. 0.01% sodium azide was added to inhibit bacterial growth. This was dispersed by means of an overhead stirrer for 12 hours and then stored at 4ºC until required. The pH of this stock solution was adjusted to pH 3.5 with 2 M acetic acid. The resulting solution was then diluted to a final WPI concentration of 12% W/W.

Samples were heated to 65ºC in a stirred water bath for 60 minutes immediately before spray drying. Samples were transferred to a stirred hot plate to maintain the temperature of the sample at 65ºC throughout spray drying. A Buchi B-290 mini-spray dryer was used with a 0.8 mm nozzle. An inlet temperature of 180ºC was used, giving an outlet temperature of ~64ºC. A 95% aspirator was used with the feed pump set at 20%.

The pH of the WPI solution was adjusted before solutions were heated to 65ºC in a stirred water bath for 1 hour.

These solutions were then spray dried, and the temperature was maintained during spray drying using a stirred hot plate.

Powders were stored at 25ºC in a dark, airtight container.

5.2.2. Dispersion preparation

Dispersions were produced by dispersing the WPI powder produced in reverse osmosis water at room temperature. This was achieved by stirring with a magnetic stirrer for 2 hours at a speed of approximately 200 RPM unless otherwise stated. Samples were degassed at -100 mbar for 20 minutes. Samples were then stored at 5ºC overnight before measurements.

5.2.3. Emulsion preparation

Emulsions were prepared using an overhead mixer because of foaming issues with higher shear production methods. Sunflower oil was purchased from a supermarket (Tesco) and stored in the dark at 25ºC. The WPI particle powder and oil were added slowly to the water during mixing. Samples were then mixed for 1 hour with an overhead mixer.

5.2.4. Interfacial tension

Interfacial tension measurements were performed using a K100 Tensiometer (Kruss GmbH). This was performed using a Wilhelmy plate geometry, with a 10-second sampling interval. For interfacial tension measurements, the interfacial tension between the oil and water with no protein was tested as well as the whole protein powder, dispersed phase and continuous phase. The dispersed phase and continuous phase were prepared individually to understand

contribution to surface activity of the phases; this preparation is presented in sections 5.2.4.1 and 5.2.4.2.

5.2.4.1. Continuous phase preparation

The spray-dried powder was dispersed in distilled water to a concentration of 5% by agitation using a magnetic stirrer. The suspension was left at 5ºC overnight and then centrifuged at 2400 G for 20 minutes. The supernatant was then diluted with distilled water to make it up to the original volume of suspension; this is presented in Figure 5.1.

5.2.4.2. Dispersed phase preparation

The spray-dried powder was dispersed in distilled water to a concentration of 5% by agitation using a magnetic stirrer. This suspension was left at 5ºC overnight. This suspension was then centrifuged at 2,400 G for 20 minutes. The supernatant was removed, and particles were dispersed in distilled water with a pipette followed by mixing with a vortex mixer for 60 s. This was repeated five times to remove all soluble protein. The particles were then dispersed in distilled water made up to the original suspension volume.

5.2.5. Rheology

5.2.5.1. Viscometry

A 40 mm sand-blasted parallel plate geometry was used to minimize slip in these experiments. Slip is expected for suspensions because of particle depletion at the shear surfaces. Equilibrium shear experiments were used with up to 2 minutes allowed for samples to reach equilibrium at each shear rate ($0.1\ s^{-1}$–$100\ s^{-1}$). Samples were tested at 25ºC with a gap of 1 mm.

5.2.5.2. Thixotropic loop

A 40 mm sand-blasted plate was used to minimize the effects of slip. Two tables of shear rates ramping up from $0.1\ s^{-1}$ to $100\ s^{-1}$ followed immediately by a table of shear rates

ramping down from 100 s^{-1} to 0.1 s^{-1} was undertaken. This was followed by a 10-minute rest period with no shear. The tables of shear rates up and down were then repeated.

5.2.5.3. Amplitude sweeps

Strain-controlled amplitude sweeps were performed at strain 0.1–100%. A frequency of 1 Hz at 25ºC was used for amplitude sweeps. These were obtained using a sand-blasted parallel plate geometry to minimize the effects of slip and repeated three times.

5.2.6. Droplet sizing

SLS measurements were used to investigate oil droplet size distributions. A Malvern Mastersizer 2000 with hydro SM manual small volume dispersion unit (Malvern Instruments, UK) was used. Each repeat consisted of three measurements, and three repeats were conducted.

5.2.7. Light microscopy

An optical light microscope (Leica Microsystems, UK) was used to directly observe particles and oil droplets. Samples were diluted with distilled water. A drop of this diluted sample was placed on a slide and covered with a coverslip. 20× magnification was used for visualization.

5.2.8. Tribology

An MTM2 (Mini Traction Machine, PCS Instruments, UK) tribometer was used for tribology measurements. This consists of a ball rolling on a disk; normal force, speed and SRR can be controlled.

A mixed sliding and rolling contact was used in this work with an SRR of 50%. SRR can be defined as:

$$SRR = \frac{U_{disc} - U_{ball}}{U} \quad (5.1)$$

where U represents the average speed at the contact for each component. A 3N normal force was used. For these experiments, a stainless steel ball–silicone elastomer disk tribopair was used as outlined previously (Mills, 2012). This tribopair and these conditions have been previously shown by Malone *et al*. (2003a) to correlate to mouth feel in the mixed regime of lubrication. In each test, Stribeck curves were measured over a speed range of 1–1,000 mm s^{-1} with ascending and descending runs repeated three times (six curves in total). Tests were performed at 25ºC. These tests were repeated three times.

5.3. Results and discussion

5.3.1. Surface activity of suspensions

Interfacial tension measurements were used to investigate the surface activity of suspension of WPI particles produced by spray drying. The potential for these spray-dried particles to stabilize emulsions is useful if this system is to be used in reduced fat emulsion-based products, offering the potential to remove current emulsifying agents. Surface activity of these particles was determined by taking interfacial tension measurements of these suspensions. The continuous phase and the dispersed phase in distilled water are presented in Figure 5.1. This was observed to understand the contribution of soluble protein and protein particles at oil–water interfaces. This is important to understand, as it was shown in the previous chapter that ~28% of the WPI remains in a soluble form. The whole protein suspension showed the lowest interfacial tension, with the suspension containing no protein showing the greatest interfacial tension. This shows that both the soluble and insoluble protein contribute to the reduction in interfacial tension observed.

Spray-dried particles are expected to be surface active because of the amphiphilic nature of their component proteins (Dickinson, 2015). The surface activity of 'gel-like' particles is not due to contact angle of the particle as is true for traditional Pickering particles (Wu *et al*., 2014). The porous nature of these gel particles means there is no distinct interface between the particles and their surroundings (Schmidt *et al*., 2011). Owing to the soft nature of these particles, there is potential for some conformational changes once the particles have adsorbed to the interface as is the case for native proteins (Deshmukh *et al*., 2015).

Protein fluid gels have been used previously to stabilize foams. It was proposed that the soluble protein was responsible for reduction of surface tension in these systems, with the role

of particles in foam stabilization being mechanical owing to controlling flow during drainage (Lazidis *et al*., 2016). However, it was shown that particles produced through spray drying have surface activity.

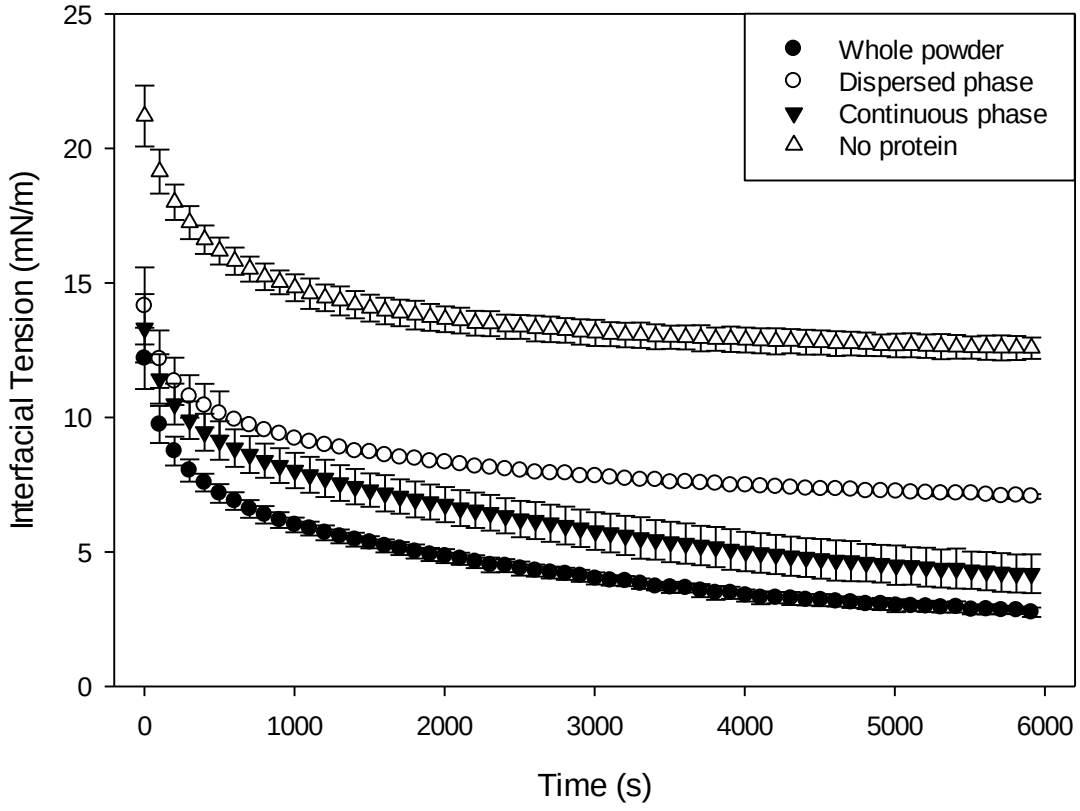

Figure 5. 1. Dynamic interfacial tension measurements between sunflower oil and distilled water stabilized by different components of the spray-dried WPI suspension. Error bars show +/- 1StD.

5.3.2. Properties of emulsions

5.3.2.1. Particle concentration

Oil concentration remained the same at 20%; WPI concentration in the continuous phase was changed.

Particle sizing for sunflower oil and water emulsions stabilized by increasing concentrations of spray-dried WPI are shown in Figure 5.2. For 5% and 10% WPI-stabilized emulsions, some oiling off was observed after 24 hours. For 15% WPI and above, no oiling off was

observed over 60 days. For all concentrations of WPI used, a broad size distribution was observed, with sizes ranging from 2 µm to 400 µm. Both protein particles and oil droplets will contribute to the sizes observed here. This overlaps with the size of the protein particles present in the system, with protein particle sizes ranging from 5 µm to 100 µm (Figure 4.1).

Light microscopy was used to further understand the structuring of WPI particles at the interface of oil droplets. Emulsions were diluted to enable clear observation of individual oil droplets (Figure 5.3). Spherical oil droplets were observed as well as anisotropic protein particles. Particles can be observed free in the solution not associated to oil droplets. The oil droplets appear to have an irregular layer around them. This ordering of the particles around oil droplets supports interfacial tension data showing the particles to be surface active.

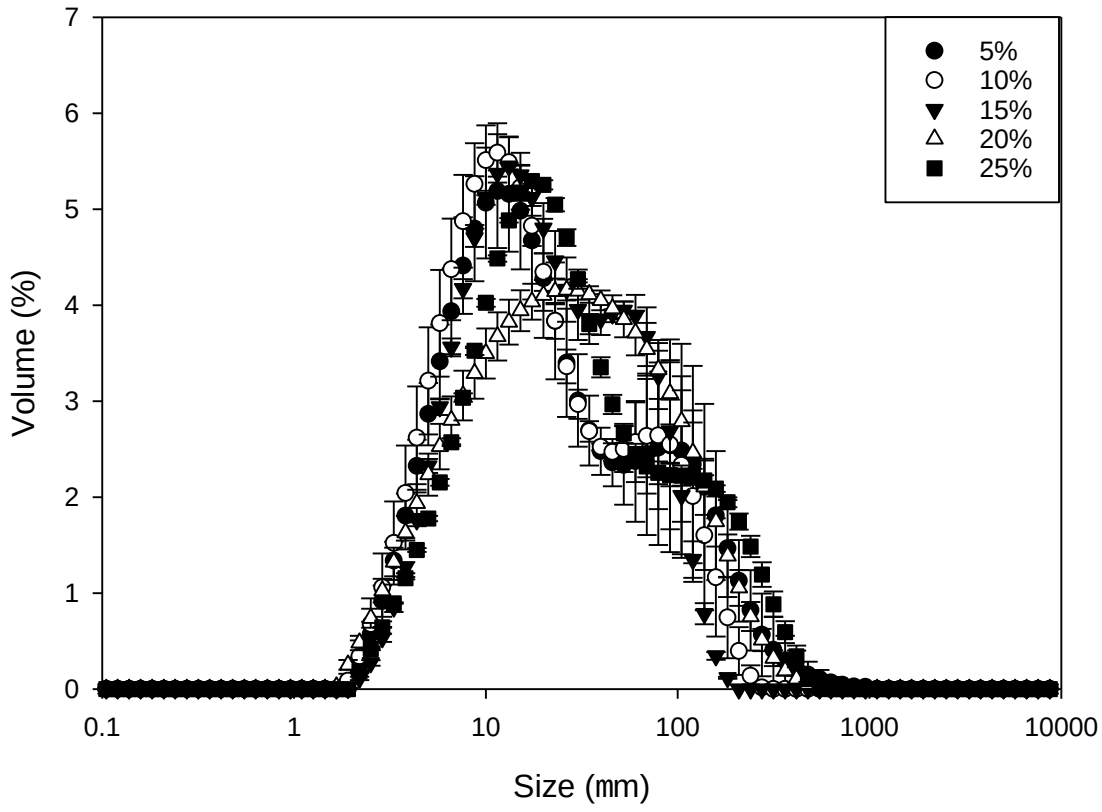

Figure 5. 2. Oil droplet sizing for sunflower oil and water emulsions stabilized by increasing concentrations of spray-dried WPI. Error bars show +/- 1StD.

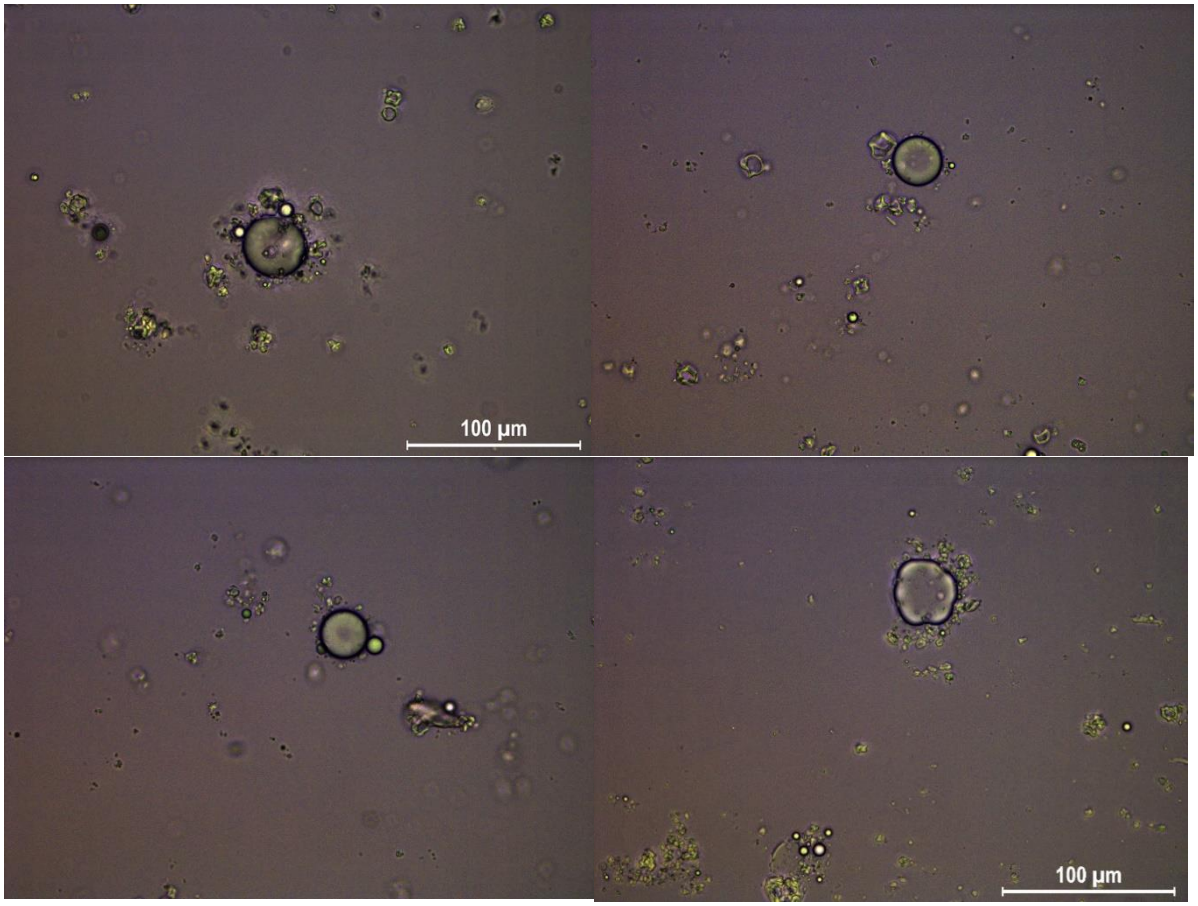

Figure 5. 3. Light micrographs of WPI-stabilized emulsions diluted in deionized water for observation. Scale bars represent 100 µm.

5.3.2.2. Rheology

Rheology of WPI particle-stabilized emulsions was investigated to understand the flow and yield stress behaviours of these systems (Figure 5.4). This was done to further understand the interactions of protein particles with oil droplets.

All concentrations of WPI showed a shear thinning nature, with viscosity increasing with increasing WPI concentration. This continued up to 20% WPI; above 20% WPI, no further increase in viscosity was observed. This was observed for WPI suspensions without oil and was explained as a result of particles reaching the maximum packing fraction at 20% WPI. Below the maximum packing fraction, viscosity is dominated by inter-particle interactions; above the maximum packing fraction, particle properties dominate (Ellis *et al*., 2017).

158 Amplitude sweeps were used to understand the viscoelastic properties of these systems. At all
159 concentrations, an LVR is observed at low strains. With increasing WPI concentration, G´ in
160 the LVR increases at all concentrations observed. This increase is explained by the increased
161 density of the network formed.

162 Unlike viscosity, elastic modulus continues to increase with increasing concentration above
163 20% WPI. This has been observed previously in agar fluid gels by Ellis *et al*. (2017) and was
164 explained as being caused by the increased density of the network with increasing
165 concentration, as particles are forced into closer contact with each other.

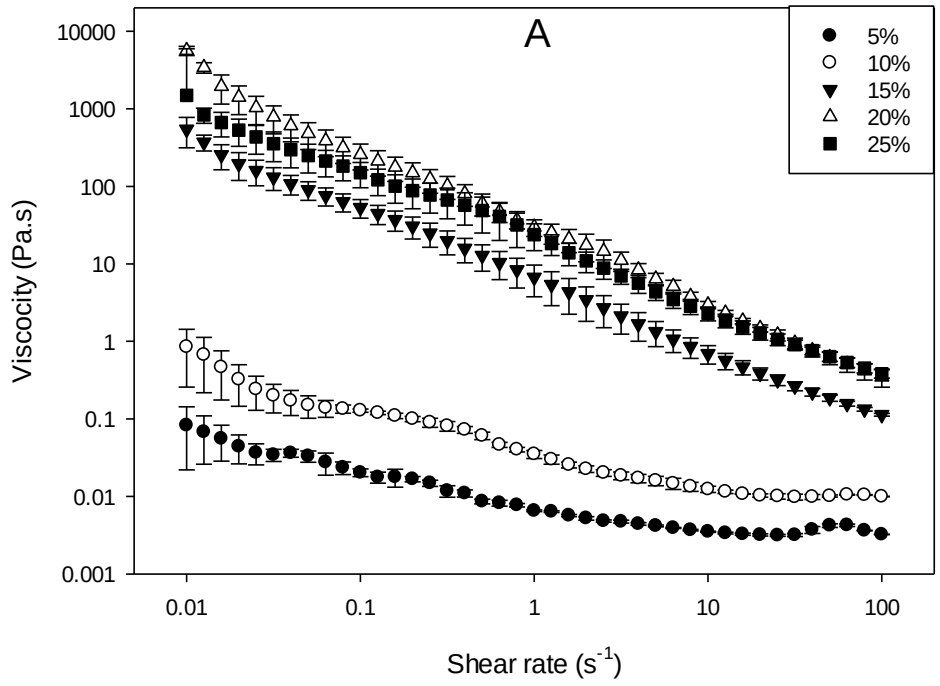

166

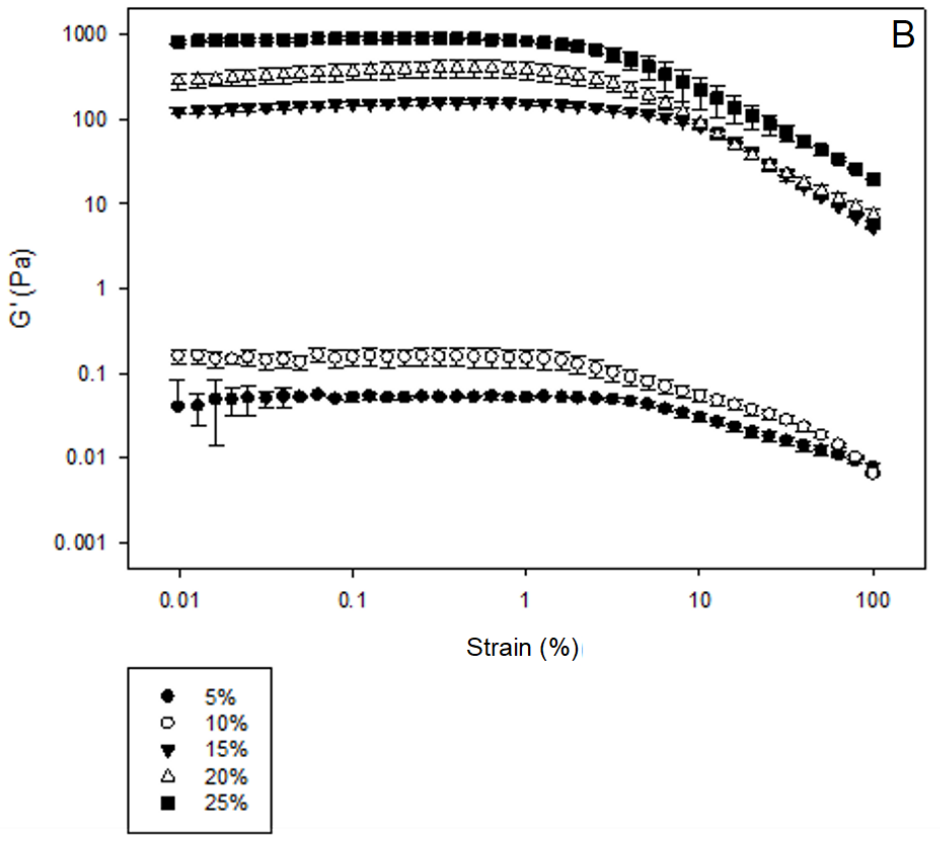

167

168 *Figure 5. 4. A) Viscosity profiles and B) amplitude sweeps of spray-dried WPI-stabilized emulsions*
169 *with 20% oil and increasing WPI concentrations. Error bars show +/- 1StD.*

5.3.2.3. Tribology

The contribution of particles in an emulsion was investigated by maintaining an oil concentration of 20% and increasing WPI concentration in the aqueous phase (Figure 5.5). For WPI concentrations increasing from 5% to 15%, little change in the lubrication was observed, with friction starting in the boundary regime and decreasing in the mixed regime of lubrication from 5 mm s^{-1} entrainment speed up to 1,000 mm s^{-1}. For 20% WPI, lower friction was observed than for concentrations <20% in the boundary regime of lubrication. A further reduction in friction in the boundary regime was observed for 25% WPI. For 20% and 25% WPI, there was overlap of error in the mixed regime. However, 25% WPI transitions into the EHL regime of lubrication at a lower speed than 20% WPI.

This trend of WPI concentrations up to 15% showing little change in lubricating properties agrees with that observed for WPI suspensions with no oil (Figure 5.1). This also agrees with the rheology shown in the previous chapter, as at 20% WPI the WPI is expected to be at maximum packing fraction and thus particles will be forced through the contact. These shifts in lubricating properties with increasing phase volume have been shown previously by Garrec (2013) in the boundary regime of lubrication. A difference was observed between 20% and 25% WPI-stabilized emulsions because there is an increased number of particles in the contact supporting the contacts separately at lower entrainment speeds.

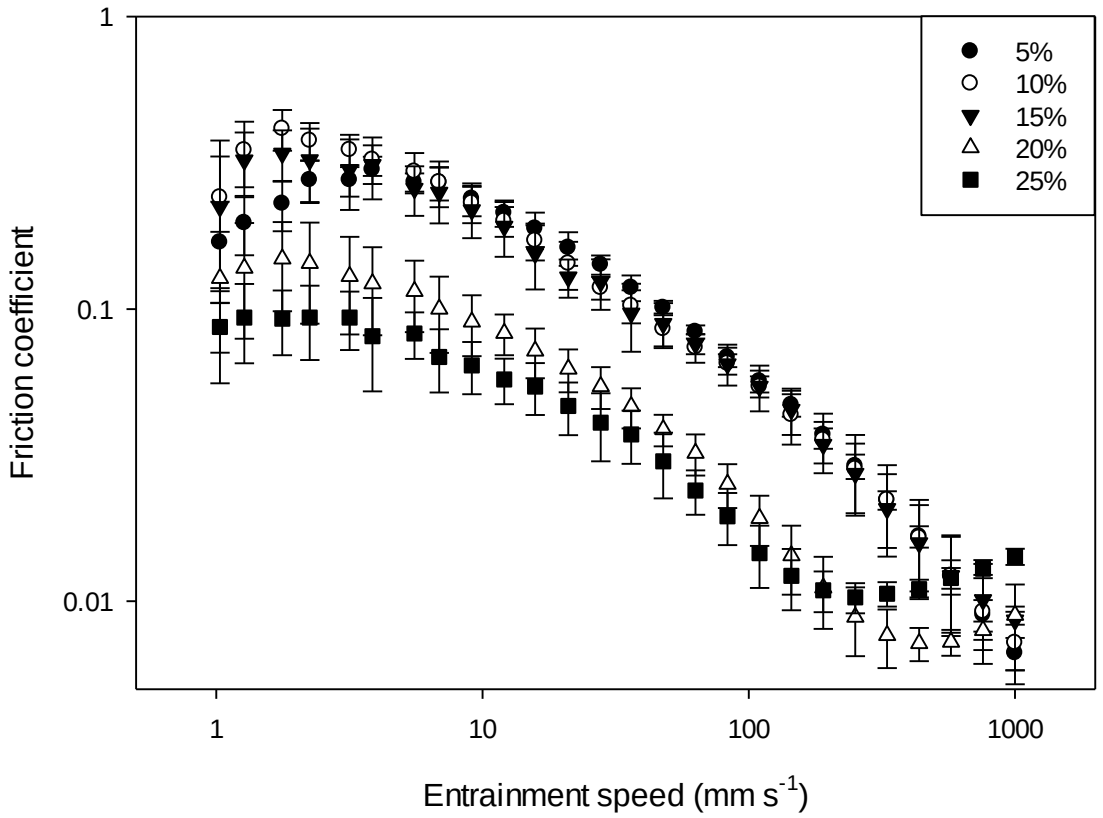

Figure 5. 5. Stribeck curves of 20% oil emulsions stabilized by different concentrations of spray-dried WPI in the aqueous phase. Measurements use a stainless steel ball–silicone elastomer disk tribopair at 3N normal force with a 50% SRR. Error bars show +/- 1StD.

5.3.3. Oil concentration

The contribution of oil droplets to the microstructure of these suspensions was further investigated by looking at the influence of oil concentration on rheology and soft tribology. WPI concentration was kept constant in the aqueous phase at 20%, and these emulsions were prepared with an overhead mixer. Understanding the effect of oil concentration on emulsion properties is important for low fat and reduced fat products, as different concentrations of oil are required to maintain desirable flavour profiles in reduced fat products

5.3.3.1. Rheology

Flow profiles of emulsions stabilized by 20% WPI in the aqueous phase are presented in Figure 5.6. All emulsions produced showed a shear thinning nature over the range of shear rates observed. For increasing oil concentrations from 0% to 20%, no change in flow profiles was observed. At 40% oil, a relative shear thickening was observed at shear rates greater than 10 s^{-1}. This similarity in shear rheology of emulsions with increasing oil concentration shows that the oil droplets contribute to the structure of the suspension, acting as an 'active' filler (Dickinson *et al*., 1999). Oil droplets can act as inactive or active fillers within systems; as active fillers they contribute to structuring and as inactive fillers they disrupt structuring. The lack of change in viscosity with increasing oil concentration shows that the oil droplets contribute to the structure of the suspensions.

For 50% oil systems, a viscosity nearly two orders of magnitude lower was observed at 0.01 s^{-1}. It was proposed that this observed decrease in viscosity is a result of phase inversion to a W/O emulsion. This was confirmed with conductivity measurements: emulsions at 50% produced a conductivity value orders of magnitude lower than the 40% oil emulsion.

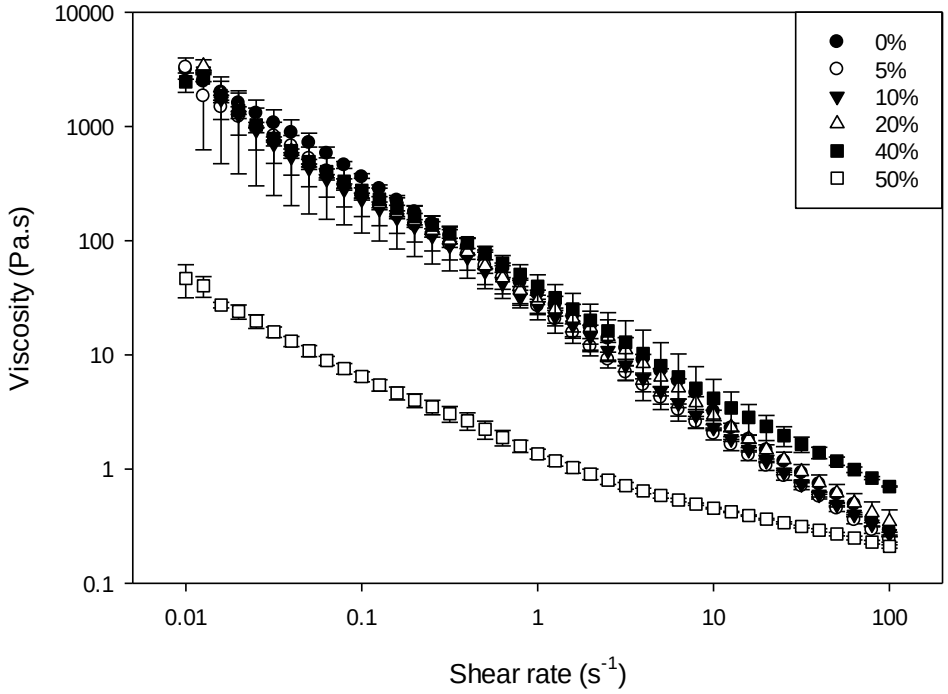

Figure 5. 6. Viscosity profiles for spray-dried WPI-stabilized emulsions, with a WPI concentration of 20% in the aqueous phase. Error bars show +/- 1 StD.

This phase transition at 50% oil concentration is not normally observed until higher oil concentrations for WPI-stabilized emulsions because of the high HLB of WPI favouring water as the continuous phase (Boyd *et al*., 1972; Frenkel *et al*., 1983). This phase inversion at lower oil concentrations than would be expected for WPI is because of the thickening of the aqueous phase, and thus in the flow field during emulsion production it is favourable for oil as the less viscous phase to be the continuous phase. The mechanism of flow-induced phase inversion with increasing oil concentration has been well documented (Brooks *et al.,* 1998). As the concentration of oil increases, the dispersed phase volume fraction gets above the phase inversion concentration, and at this concentration a bicontinuous phase will form, as indicated in Figure 5.7B. As the concentration of oil further increases, a W/O emulsion will

be formed. Figure 5.7 shows a schematic for the mechanism of phase inversion of W/O emulsions with increasing water concentration.

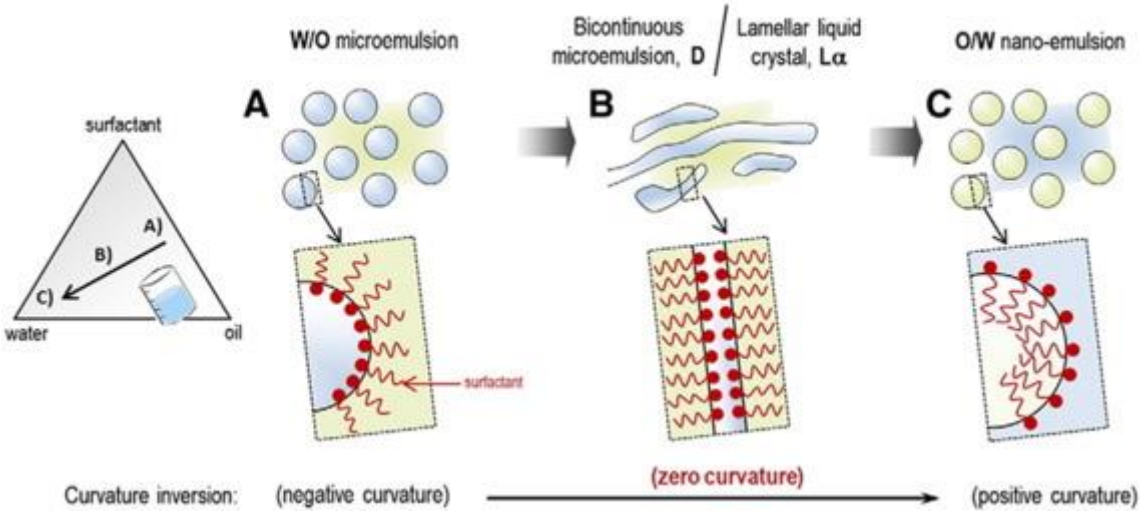

Figure 5. 7. Schematic of the mechanism of flow-induced phase inversion of emulsions. Taken from Perazzo et al. (2015).

Amplitude sweeps were used to investigate the influence of increasing oil concentration on the yield stress behaviour of the WPI suspensions (Figure 5.8). No change in elastic modulus in the LVR was observed with oil concentration increasing from 5% to 40%. At 50% oil concentration, a decrease in G´ in the LVR was observed. As seen for viscosity profiles, this reduced G´ was attributed to the phase transition to an O/W emulsion at 50% oil. The yield strain for emulsions up to 40% oil did not change with increasing oil concentration as shown by the yielding of G´. For 50% oil emulsions, a lower yield strain was observed. This is expected as there will be no structuring in the continuous phase for the oil continuous emulsions, as protein particles will reside in and structure the aqueous phase.

The limited change in shear viscosity and oscillatory rheology of these emulsions with oil concentrations up to 40% suggests that oil droplets contribute to the structure as ‘active’ fillers (McClements, 2015), with droplets contributing to the structuring of the suspension (Dickinson and Chen, 1999). This contribution of oil droplets to structuring has previously

been related to the size of oil droplets relative to pores within the network of particles. Sizes of oil droplets are presented in Figure 5.9 (McClements *et al*., 1993).

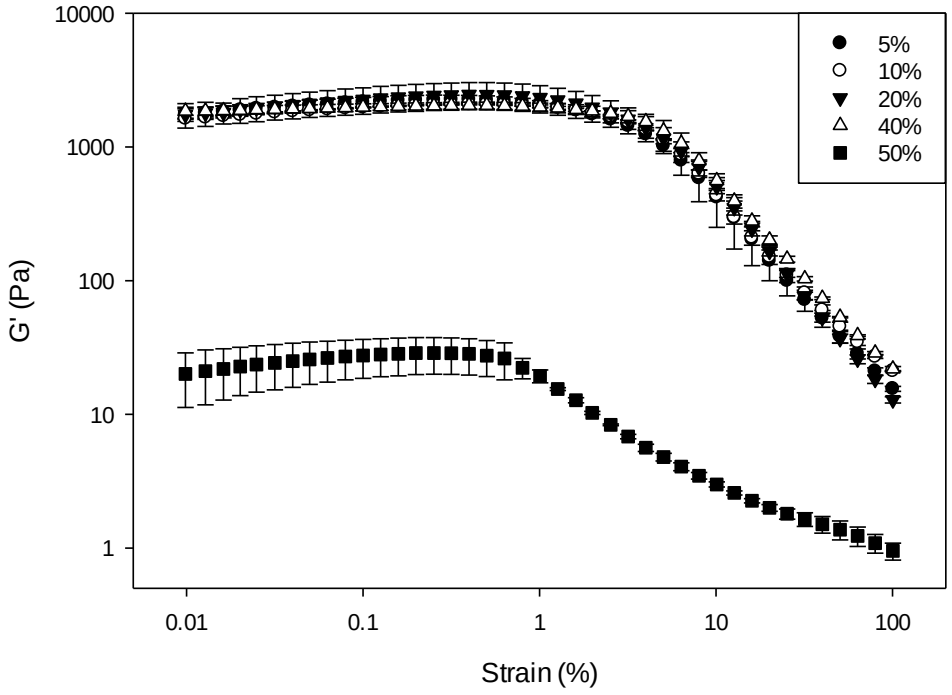

Figure 5. 8. Strain-controlled amplitude sweeps showing the elastic modulus of spray-dried WPI-stabilized emulsions, with a WPI concentration of 20% in the aqueous phase. This was used to observe the yield stress behaviour of these emulsions. Error bars show +/- 1 StD.

Particle size will contribute to the structuring of the system protein particles and droplets will contribute to these measurements. Particle sizes overlap for all oil concentrations with the sizes of the protein particles, as shown in Figure 4.1. The size distribution observed will include a contribution from protein particles and oil droplets.

A Sauter mean particle size for all oil concentrations varied between 11 μm and 18 μm. A volume weighted mean (D(4,3)) between 50 μm and 67 μm was observed for these emulsions. No trend in average droplet diameter with increasing oil concentration was observed. For all oil concentrations, a broad droplet size distribution was observed. This is expected because of the low shear production method used to prepare these emulsions.

The sizes of oil droplets overlap fully with those of the WPI particles. Thus, there are droplets of comparable size to the WPI particles. However, the average sizes for oil droplets were higher than for the WPI particles, with a broader size distribution. The observed overlap of protein particle size and droplet size contributes to the observed lack of change in rheology of emulsions stabilized by these suspensions from oil concentrations of 0–20%. Oil droplets have a similar size to the protein particles displacing them within the network.

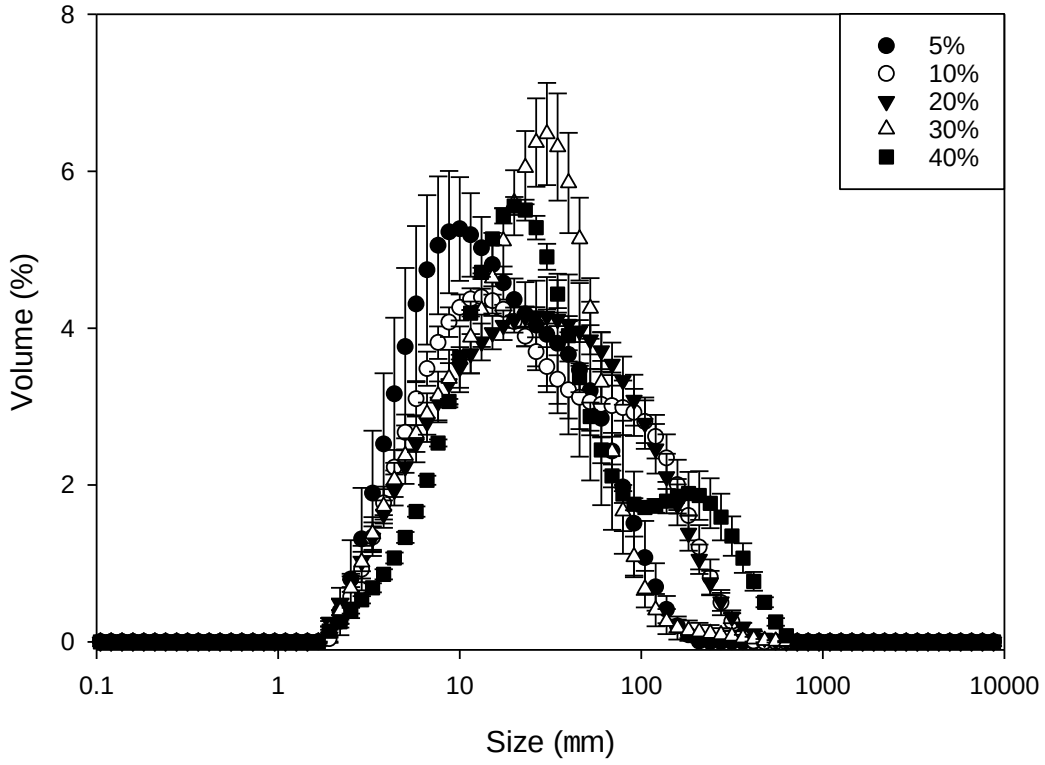

Figure 5. 9. Particle size of emulsions stabilized by 20% spray-dried WPI in the aqueous phase. Error bars show +/- 1 StD.

5.3.3.2. Thixotropy

In Figure 5.7, it was shown that little change was observed in viscosity profiles with increasing oil concentration. To further understand how oil contributes to structuring, thixotropy was investigated to show how interactions recovered. This was performed by increasing shear rate up and down followed by a 10-minute break and repeating this.

Recovery is important in mayonnaise products as they are expected to flow under stress during spreading and spooning and then recover to solid-like behaviour at rest.

With increasing oil concentration, a reduction in hysteresis between the two up ramps was observed. For no oil, hysteresis is shown between the two up ramps at shear rates below 0.5 s^{-1}, suggesting inter-particle interactions are not recovered in the 10-minute relaxation. For 20% oil, less hysteresis was observed between the two up ramps, with little hysteresis shown for 40% oil. For no oil and 20% oil, there was an overlap between the first down ramp and the second up ramp. This shows that the interactions at play at these lower shear rates are not recovering during the 10 minutes at rest. Prior to the first ramp, the sample had been stored at rest for 24 hours. During this time inter-particle structures can occur, and once broken down these interactions require longer than ten minutes to recover. However, for the interactions responsible for viscosity at shear rates >0.5 s^{-1}, these recover in the 10-minute rest period.

This observed decrease in thixotropy with increasing oil concentration shows that the oil droplets contribute to the reformation of flocs after break-up. In flocculated systems, the recovery of structure is controlled by the balance of break-up and reformation of flocs. Recovery hydrophobic interactions between oil droplets and protein particles may be responsible for this recovery, with the oil droplets promoting the formation of flocs (Barnes, 1997).

Spatial ordering of particles in shear will also contribute to the recovery. If the oil droplets are treated as particles, they behave as a second dispersed phase. With increasing oil concentration, the number of larger particles will increase, increasing the polydispersity. More polydisperse samples will be less susceptible to shear banding in which the particles orientate in line with flow. Shear banding is the phenomenon of particles ordering and aligning with

297 flow. Ordering of particles into layers in line with the flow is less likely to form in a sample
298 with a wider particle size distribution. This reduced shear banding also explains the reduced
299 shear thinning shown for higher oil concentration samples, as discussed in Figure 5.10.

300 This recovery of viscosity is important in mayonnaises as they are expected to flow under
301 shear then hold their shape once shearing stops during spooning and spreading.

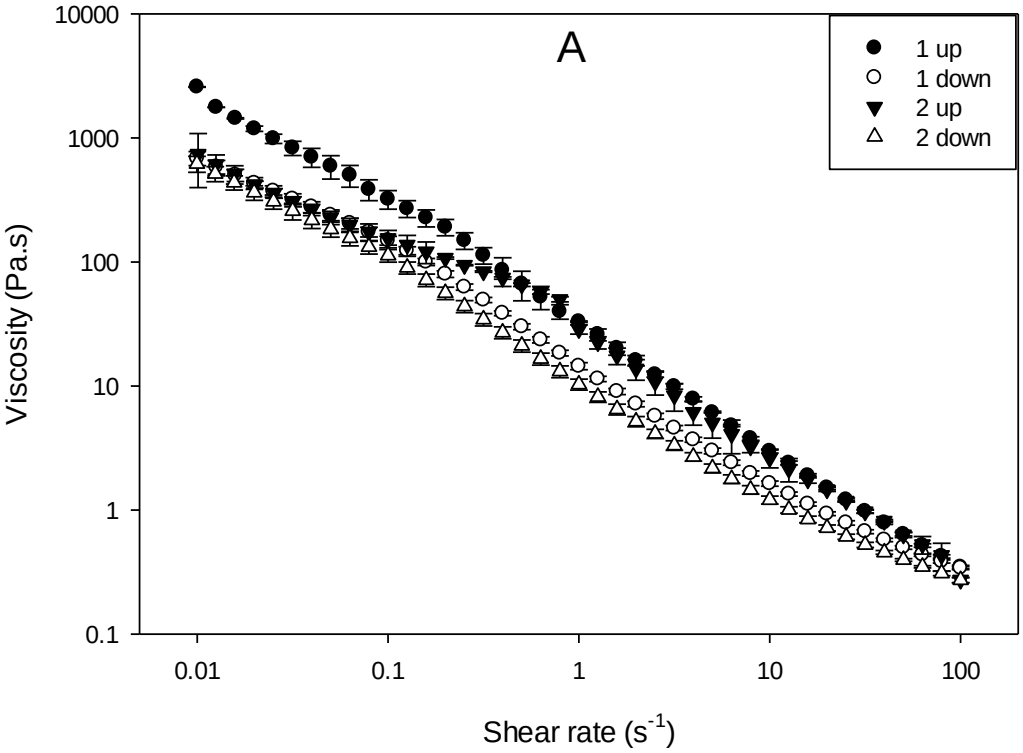
A
1 up
1 down
2 up
2 down
Viscosity (Pa.s)
10000
1000
100
10
1
0.1
0.01
0.1
1
10
100
Shear rate (s-1)

302

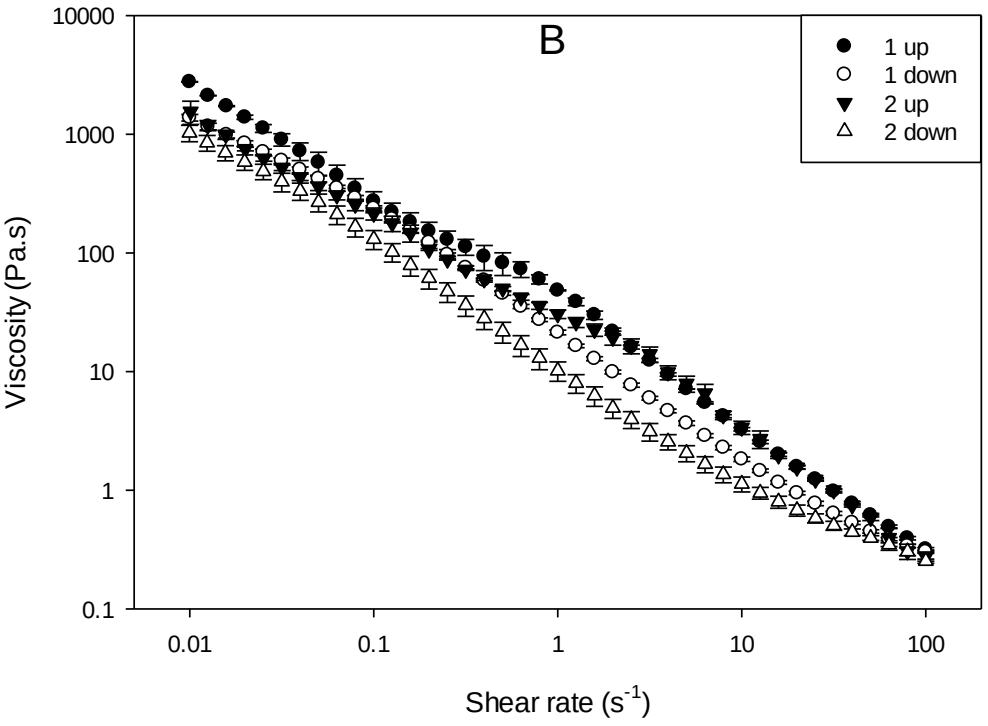
B
1 up
1 down
2 up
2 down
Viscosity (Pa.s)
10000
1000
100
10
1
0.1
0.01
0.1
1
10
100
Shear rate (s-1)

303

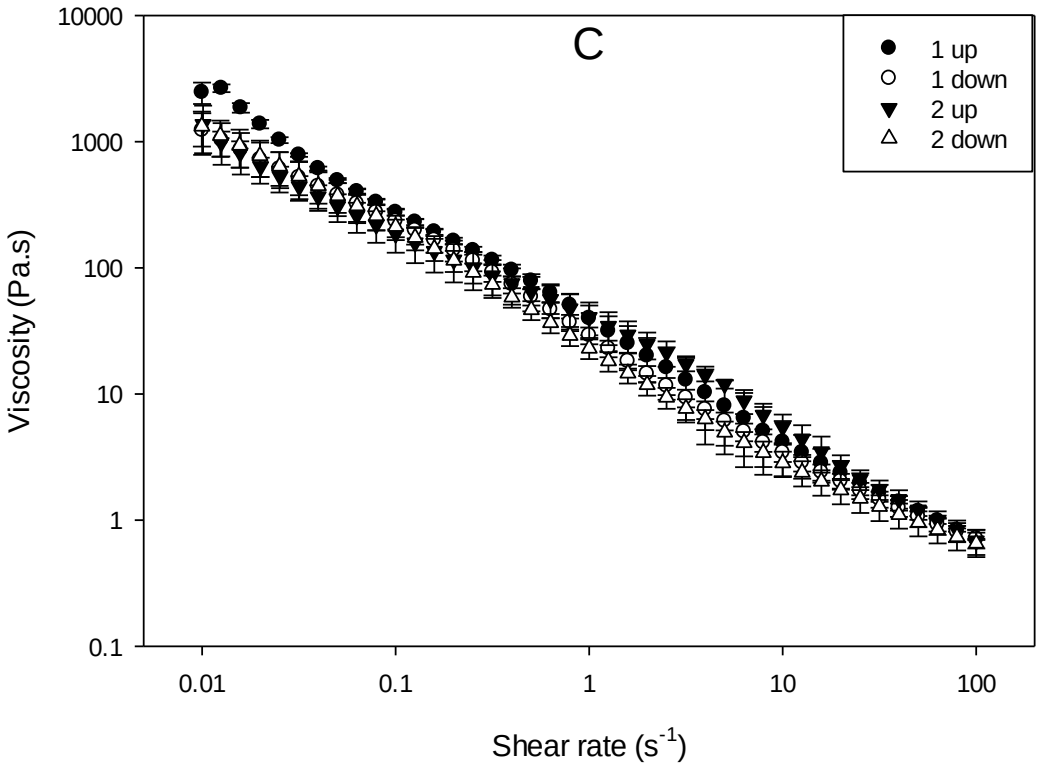

Figure 5. 20. Thixotropic loops showing shear rate ramps up and down followed by a 10-minute rest and another shear rate ramp up and down for A) 20% WPI suspension, B) 20% oil emulsion with 20% WPI in the aqueous phase and C) 40% oil emulsion with 20% WPI in the aqueous phase. Error bars show +/- 1 StD.

5.3.4. Emulsion tribology

Soft tribology of these emulsions with increasing oil content was investigated to understand the contribution of oil droplets to the lubricating properties of these systems (Figure 5.11). All three regimes of lubrication appeared to be present over the speed range investigated for all oil concentrations. The friction coefficient started as a plateau in the boundary regime, in which friction coefficient is independent of speed. This progressed into the mixed regime, in which friction coefficient decreased with increasing speed, and then into the EHL regime, in which friction increased with increasing speed.

Little change in tribology was observed for oil concentrations between 5% and 20%. In the boundary regime of lubrication, no difference was observed between 0% and 20% oil;

however, in the mixed regime of lubrication, lower friction coefficients were observed for 5% oil than for 0% oil. The speed at which lubrication transitions from the mixed regime of lubrication to the EHL regime as indicated by the minimum in friction, the entrainment speed at which this is observed is lower for 5% oil than for 0% oil.

Lower friction coefficients were observed in the boundary regime for 40% oil than for lower oil concentrations. This trend continued through the mixed regime of lubrication. The speed at which the transition from the mixed to EHL regime of lubrication occurred was lower for 40% oil than for oil concentrations lower than 40%. The 40% oil emulsion showed similar friction coefficients to pure oil in the boundary and mixed regimes of lubrication. However, 40% oil transitioned to the EHL regime at lower entrainment speeds than pure oil.

It was proposed that this shift in behaviour at 40% oil was because of instability of the emulsion in the contact, leading to a phase inversion. Thus, owing to the viscosity of the aqueous phase in the squeezing flow of the contact, a phase transition to oil continuous occurred. This agrees with the similarity observed between pure sunflower oil and the 40% emulsion.

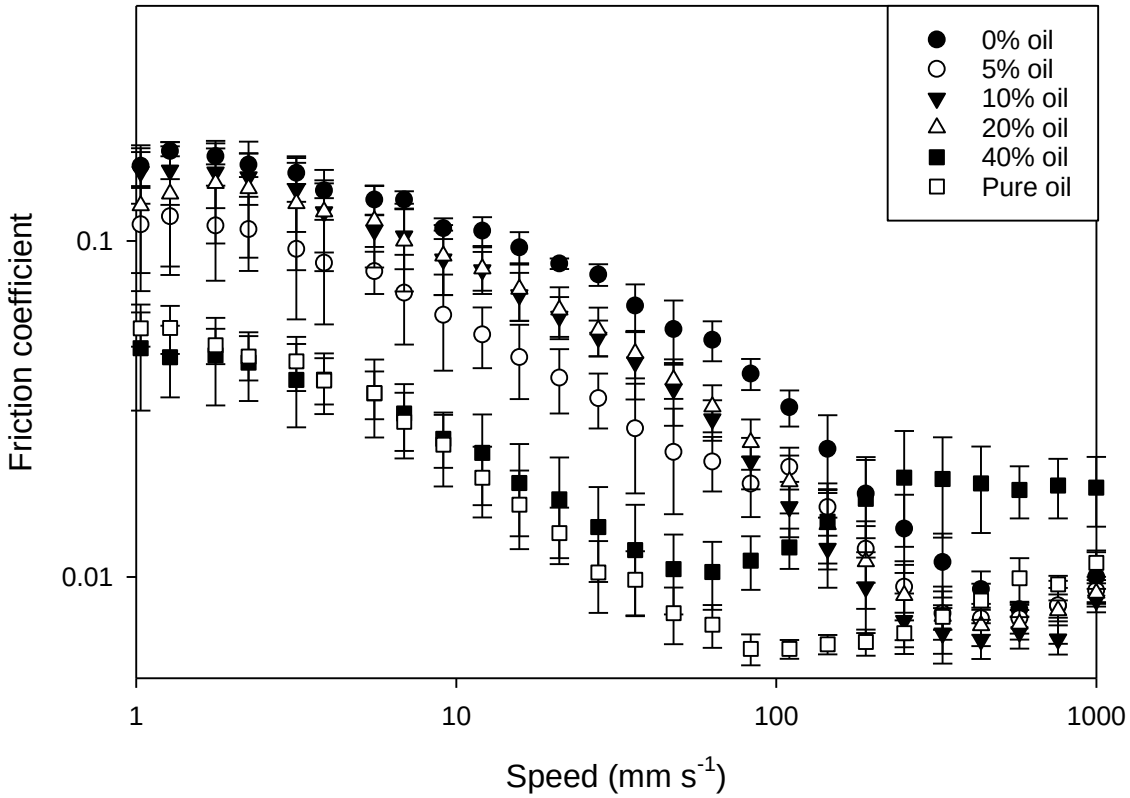

Figure 5. 31. Tribology of spray-dried WPI-stabilized emulsions with increasing oil concentration. WPI concentration was 20% in the aqueous phase. Error bars show +/- 1 StD.

5.3.5. Simplesse® comparison

Emulsions produced from spray-dried WPI were compared with those stabilized by the commercially available WPI powder Simplesse®. The flow profiles and Stribeck curves comparing 20% oil emulsions stabilized with 20% WPI in the aqueous phase are shown in Figure 5.12.

Both emulsions stabilized by Simplesse® and emulsions stabilized by spray-dried WPI showed a shear thinning nature, as expected for suspensions. At 0.01 s^{-1}, suspensions stabilized by spray-dried WPI showed a viscosity four orders of magnitude higher than those stabilized by Simplesse®. The rate of shear thinning for emulsions stabilized by spray-dried WPI was greater than that for the Simplesse®-stabilized emulsions. This can be explained by

the structure of the particles and the influence of this on the phase volume. Simplesse® is dewatered protein particles, whereas those prepared through spray drying bear more resemblance to the soft gelled particles of fluid gels. Thus, for the same concentration of WPI, a higher phase volume is occupied as the particles hydrate, ordering water. It was shown in the previous chapter that these particles order water.

Emulsions stabilized by the two different WPI particles showed different lubricating properties. For Simplesse®-stabilized emulsions, the transition to the EHL regime was not observed. For emulsions stabilized by spray-dried WPI, all three regimes of lubrication were observed. In the boundary regime, similar lubrication was observed for both types of WPI. However, as the emulsions progressed into the mixed regime of lubrication, lower friction coefficients were observed for emulsions stabilized by spray-dried WPI than those stabilized by Simplesse®.

These observed differences in lubrication are contributed to by the viscosity difference observed. On master Stribeck curves for Newtonian fluids, entrainment speed is corrected for viscosity; however, this is more challenging for non-Newtonian fluids. Entrainment is corrected for as more viscous samples will be forced into the contact at lower speeds owing to their increased viscosity. There will also be a microstructural contribution; owing to the higher phase volume occupied by the spray-dried particles, they are more likely to enter the contact. Particle size and rigidity will also contribute to the entrainment of particles, with smaller particles more easily entrained and softer particles more easily entrained. Simplesse® particles are <3 μm in size but are expected to be hard particles compared with the larger ‘soft’ spray-dried particles.

The WPI particles produced by spray drying are more similar to fluid gel particles than the particles of Simplesse®. This is expected because of the lower temperatures during production allowing particles to remain hydrated during the heating step. For Simplesse® production, the solution is heated rapidly to 120ºC (Singer *et al*., 1988), WPI is heated above the denaturation temperature, high shear is used also (Verheul and Roefs, 1998). At higher temperatures, a courser gel structure is produced as a result of aggregates being more dewatered and favouring protein–protein interactions over protein–solvent interactions (Hoffmann *et al*., 1996). This is a result of the kinetics of gelation: at lower temperatures, denaturation is the rate-limiting factor, but at higher temperatures this shifts to aggregation being the rate-limiting factor (Hermansson, 1986).

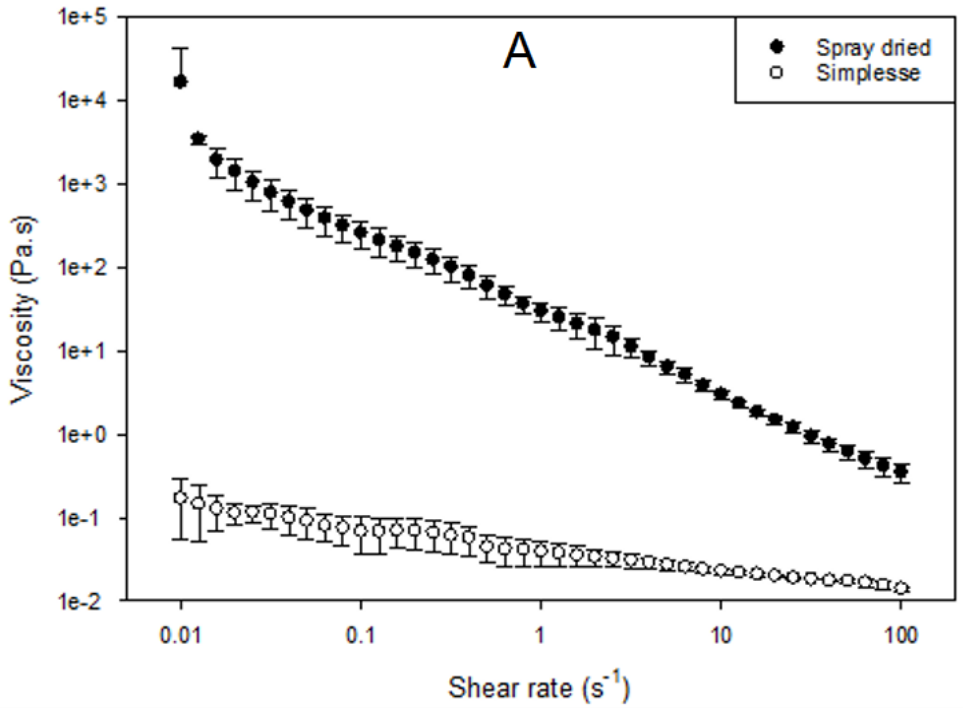

379

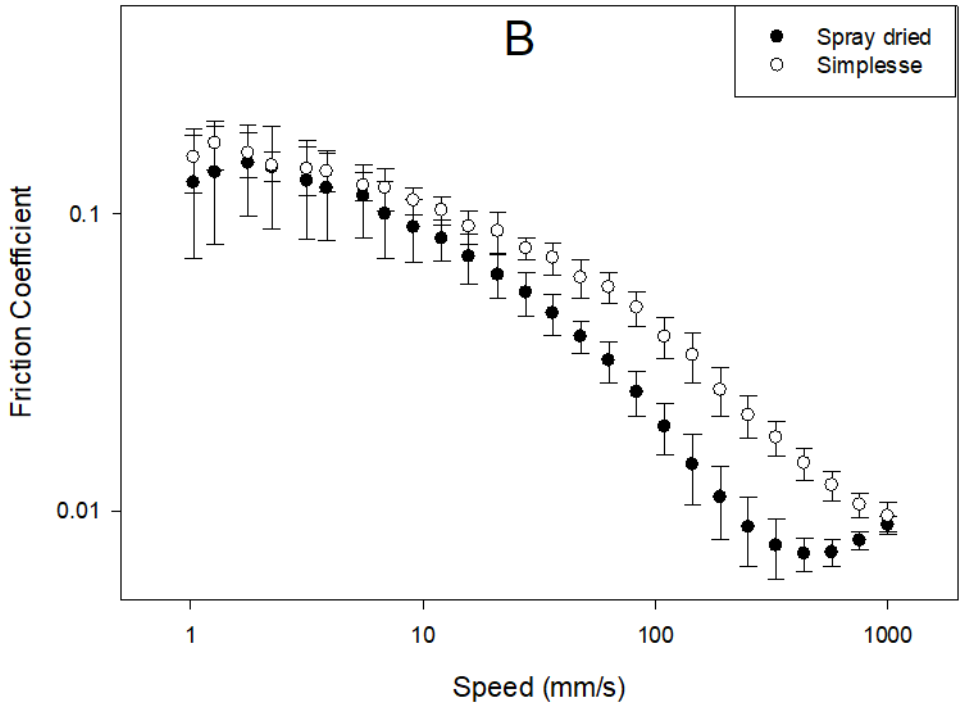

380

381 *Figure 5. 42. A) Viscosity profile and B) tribology of a 20% oil stabilized with 20% WPI either spray*
382 *dried or commercially available Simplesse®. Error bars show +/- 1 StD.*

5.3.6. Comparison with full fat mayonnaise

Rheology of 5% oil emulsions stabilized by 20% WPI in the aqueous phase was compared with a full fat mayonnaise sample. The full fat mayonnaise used was 72.5% oil. An oil concentration of 5% was used for the reduced fat emulsion, as this has previously been shown to be the required oil content for the flavour profile to be maintained in margarines (Malone *et al.*, 2003b). Reduction of fat content in cheeses and dressings has been shown to increase bitter flavours previously by Shamil *et al*. (1991). Bitter flavours have a hydrophobic nature, and thus reside in the oil phase of products. When the volume of oil is reduced, the concentration of bitter flavour compounds in the oil increases. This increased concentration of bitter flavour compounds leads to a more bitter flavour.

Both the 5% emulsion and the full fat mayonnaise showed a shear thinning nature as expected (Figure 5.13). At shear rates below 0.9 s^{-1}, both systems had comparable viscosities. As shear rate increased above this, greater shear thinning was observed for the 5% emulsion than for the full fat emulsion. This observed difference is explained by the difference in particle properties, which is represented schematically in Figure 5.14. At low shear rates, the particles/droplets are expected to be in contact with one another in relaxed shapes. As shear increases, particles will deform whilst remaining in contact. As shear further increases, the inter-particle forces will break down as disruption of the structure begins; this will progress as particles flow at increased shear rates. The WPI particles contributing to the structure of the 5% oil emulsion will be more rigid than the oil droplets of the full fat mayonnaise. These more rigid particles begin to disrupt at lower shear rates than the oil droplets as they are less deformable, shown previously by Garrec *et al*. (2013). This partial disruption of structure explains the greater rate of shear thinning for the 5% emulsion. The plateau at low shear rates

406 shown in Figure 5.14 was not observed in these measurements as shear rate-controlled
407 measurements were used.

408 This is further supported by amplitude sweeps (Figure 5.13B). For both the full fat emulsion
409 and the 5% emulsion, an LVR was observed in which G´ was independent of strain. In the
410 LVR, G´ for the 5% emulsion was higher than for full fat mayonnaise, supporting that the
411 WPI particles are more rigid than the oil droplets. This is because in the LVR no flow will
412 occur and thus particle properties will dominate G´. As G´ begins to decrease, the systems are
413 yielding (Shao *et al.*, 2013). This yielding indicates the beginning of structure breakdown.
414 The yield strain of the 5% emulsion was lower than for the full fat mayonnaise. This agrees
415 with the previous explanation as more rigid particles deform less before favouring breakdown
416 of structure and thus yielding.

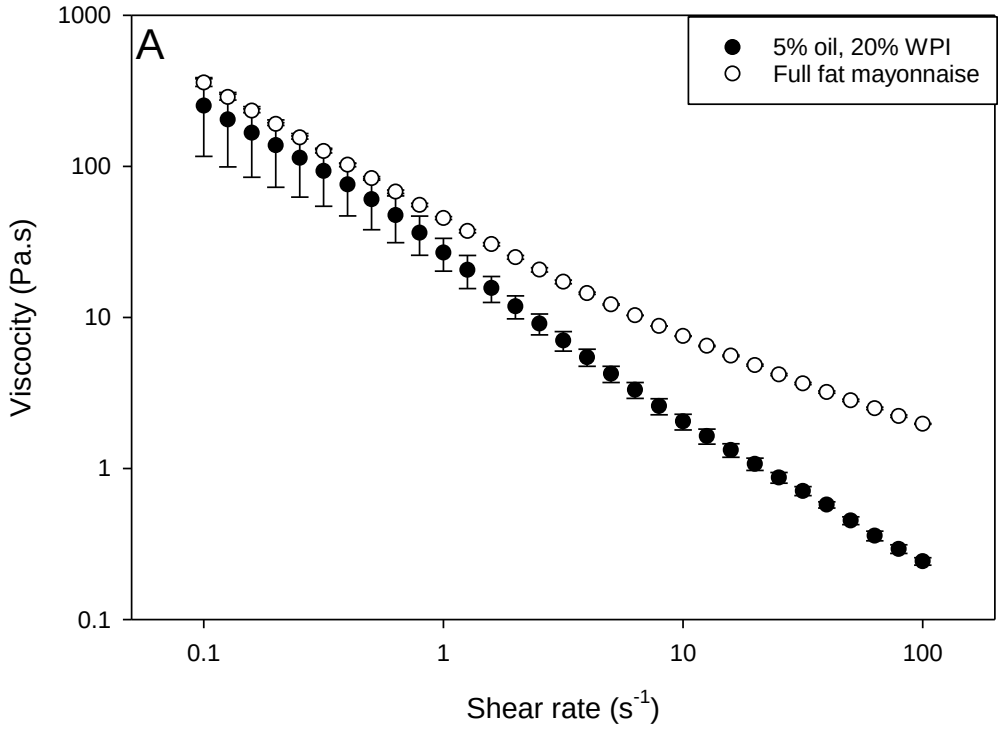

417

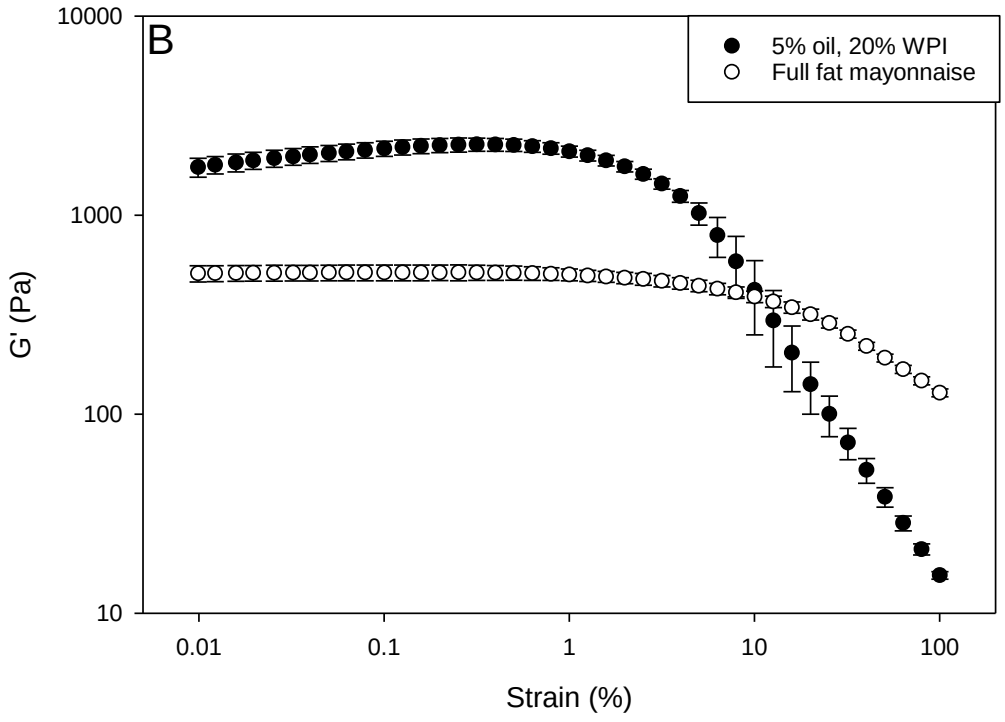

418

419 *Figure 5. 13. Graphs comparing 5% oil emulsions stabilized by 20% WPI in the continuous phase and*
420 *a full fat mayonnaise: A) viscocity profiles and B) amplitude sweeps. Error bars show +/- 1 StD.*

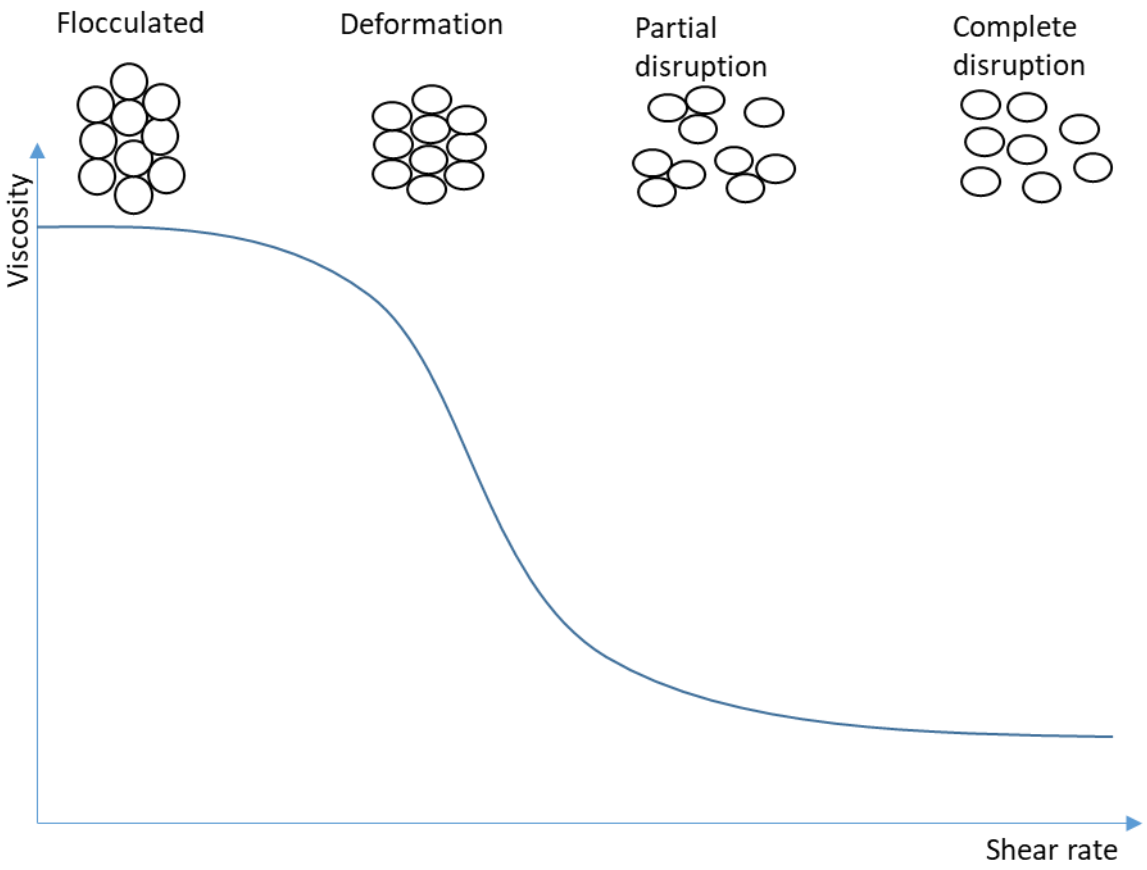

Figure 5. 54. Schematic diagram of the structuring of particles in flow. Adapted from McClements (2015).

To further understand how the 5% emulsion stabilized by spray-dried particles compared with a full fat mayonnaise texturally, the lubricating properties of the emulsion were investigated using soft tribology. This is used for mayonnaise systems to understand how they will perform in the later stages of oral processing as they are perceived in thin films between the tongue and the palate. Figure 5.15 compares the soft tribology of these systems.

For both systems, all three regimes of lubrication appear to be observed over the investigated speeds. The full fat mayonnaise showed greater lubrication in the boundary regime of lubrication indicated by the initial region in which friction coefficient is independent of speed. Both systems then transitioned into the mixed regime of lubrication, in which friction coefficient decreases with increasing speed. Through the boundary and mixed regimes of

lubrication, the full fat mayonnaise showed lower friction coefficients than the 5% fat emulsion. However, the full fat mayonnaise transitioned to the EHL regime at a lower speed than the 5% emulsion. This may be related to the observed difference in viscosity shown in Figure 5.13A. For the 5% emulsion, the friction coefficient continued to decrease to a lower minimum than for the full fat mayonnaise, transitioning to the EHL regime at a higher speed.

Traditionally for master Stribeck curves, the x axis is corrected for viscosity in Newtonian fluids to negate the effects of viscosity difference. This is more challenging for non-Newtonian fluids. Figure 5.15B shows the same data presented in 5.15A with the speed adjusted to investigate whether these curves overlay if speed is adjusted. For this, the shear rate at which the best overlap between the two samples in the mixed regime of lubrication was determined. It was determined that the best overlap of the two was achieved by correcting entrainment speed for viscosity at a shear rate of 15.8 s^{-1}. It was shown that the full fat mayonnaise and the 5% emulsion can be overlapped in the mixed regime of lubrication by adjusting the entrainment speed, which is known to be influenced by viscosity. In this figure, both the full fat mayonnaise and the 5% emulsion overlay each other for the majority of the mixed regime of lubrication.

Further investigation and ultimately sensory tests are required to truly determine mouth feel. However, the mixed regime of lubrication has previously been shown to correlate with sensory data for Guar solutions and has been used as a model for semi-liquid foods (Malone *et al*., 2003a). For these systems, the mixed regime of lubrication fell into the 40–250 mm s^{-1} entrainment speed.

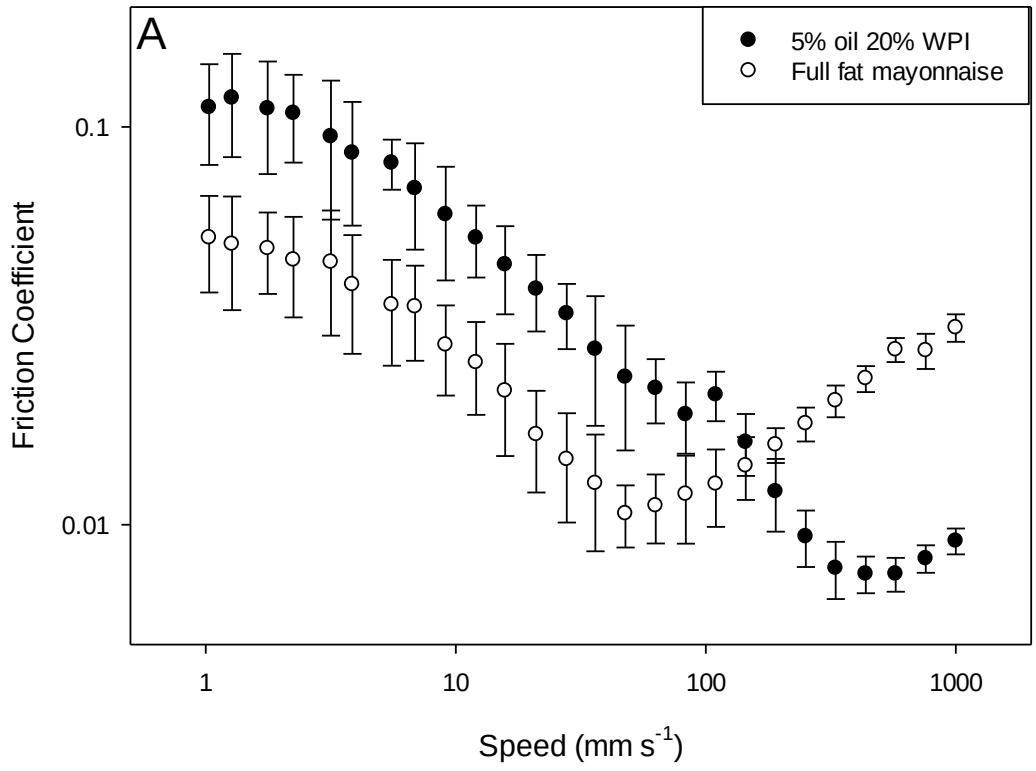

455

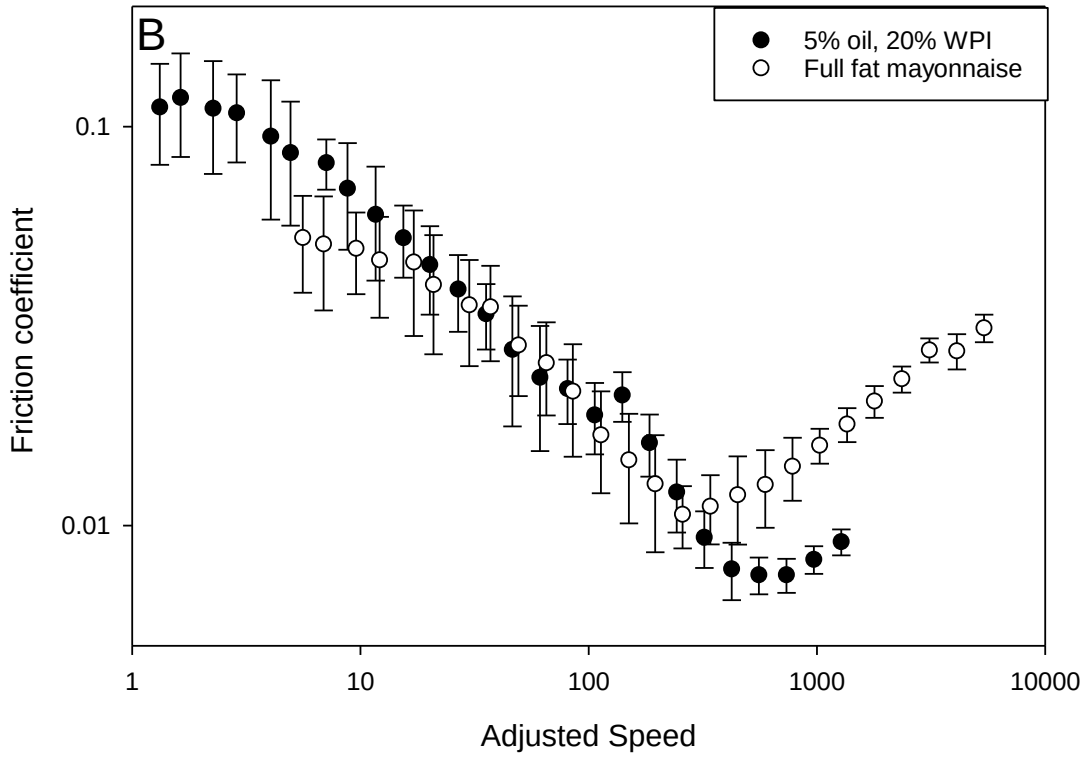

456

457 *Figure 5. 15. Stribeck curves comparing WPI-stabilized 5% oil emulsions and a full fat mayonnaise.*
458 *A) Stribeck curves. B) Stribeck curves with entrainment speed adjusted. Error bars show +/- 1StD.*

These WPI particles produced showed similar rheology to fluid gels produced from hydrocolloids (Garrec *et al*., 2013). However, they showed greater recovery than κ-carrageenan and WPI fluid gels produced previously (Garrec *et al*., 2013; Moakes *et al*., 2015). Previous studies used shear rate ramps as opposed to the table of shear rates used in this work. Recovery is essential in mayonnaise products as they are required to flow under shear when spreading and spooning but must then hold their shape.

Proteins offer advantages over hydrocolloids as structuring components in reduced fat products because of their surface activity. Surface-active particles contribute to emulsion stability. Greater quantities of raw materials are required for proteins to achieve the equivalent fluid gels to those produced with hydrocolloids. Greater quantities of protein are also required for protein particles produced by the spray-drying method; however, further optimization of this process may improve this. This is outside the scope of this project.

Particles produced by the method presented here are more fluid-gel like than those produced by alternative methods involving high shear rates, salts or high temperatures, which produce protein particles with a more dewatered structure.

5.4. Conclusions

The potential for soft gel-like particles of WPI produced through spray drying to stabilize emulsions has been presented. These gelled particles have been shown for the first time to be surface active, combining with soluble protein to stabilize the oil–water interface. Their properties have been compared with commercially available WPI particles and full fat emulsions, showing comparable textural properties with rheology and soft tribology. Emulsion viscosity was shown to increase with increasing WPI concentration. No change in rheology was observed for 0–40% oil emulsions stabilized by 20% WPI in the aqueous phase;

these oil droplets are incorporated into the network of particles. WPI particles produced have properties closer to those of fluid gel particles than to those of commercially available Simplesse®. This means the protein particles produced have potential to be used at lower protein concentrations than Simplesse®. This reduced protein concentration could further reduce the calorie content of reduced fat mayonnaises and reduce the raw material costs. 5% oil emulsion stabilized by 20% WPI particles showed similar rheology and lubricating properties to full fat mayonnaise containing 72.5% oil.

5.5. References

AVEYARD, R., BINKS, B. P., CLINT, J. H. J. A. I. C. & SCIENCE, I. 2003. Emulsions stabilised solely by colloidal particles. 100**,** 503-546.

BAIER, S. K., MCCLEMENTS, D. J. J. C. R. I. F. S. & SAFETY, F. 2005. Influence of cosolvent systems on the gelation mechanism of globular protein: thermodynamic, kinetic, and structural aspects of globular protein gelation. 4**,** 43-54.

BARNES, H. A. 1994. Rheology of emulsions — a review. *Colloids and Surfaces A: Physicochemical and Engineering Aspects,* 91**,** 89-95.

BARNES, H. A. 1997. Thixotropy—a review. *Journal of Non-Newtonian Fluid Mechanics,* 70**,** 1-33.

BELITZ, H.-D., GROSCH, W. & SCHIEBERLE, P. J. F. C. 2009. Food additives. 429-466.

BINKS, B. & LUMSDON, S. J. P. C. C. P. 1999. Stability of oil-in-water emulsions stabilised by silica particles. 1**,** 3007-3016.

BINKS, B. P. & FLETCHER, P. D. I. 2001. Particles Adsorbed at the Oil−Water Interface: A Theoretical Comparison between Spheres of Uniform Wettability and "Janus" Particles. *Langmuir,* 17**,** 4708-4710.

BOHIN, M. C., VINCKEN, J.-P., VAN DER HIJDEN, H. T., GRUPPEN, H. J. J. O. A. & CHEMISTRY, F. 2012. Efficacy of food proteins as carriers for flavonoids. 60**,** 4136-4143.

BOYD, J., PARKINSON, C., SHERMAN, P. J. J. O. C. & SCIENCE, I. 1972. Factors affecting emulsion stability, and the HLB concept. 41**,** 359-370.

Brooks, B.W., Richmond, H.N. and Zerfa, M., 1998. Phase inversion and drop formation in agitated liquid–liquid dispersions in the presence of nonionic surfactants. In Modern Aspects of Emulsion Science (pp. 175-204).

513 BRUGGER, B., ROSEN, B. A. & RICHTERING, W. J. L. 2008. Microgels as stimuli-
514 responsive stabilizers for emulsions. 24**,** 12202-12208.
515 CHONG, J. S., CHRISTIANSEN, E. B. & BAER, A. D. 1971. Rheology of concentrated
516 suspensions. 15**,** 2007-2021.
517 DAMODARAN, S. J. F. S. F. C. 2008. Amino acids, peptides and proteins. 4**,** 217-329.
518 DAVIS, H. T. 1994. Factors determining emulsion type: Hydrophile—lipophile balance and
519 beyond. *Colloids and Surfaces A: Physicochemical and Engineering Aspects,* 91**,** 9-
520 24.
521 DE FOLTER, J. W., VAN RUIJVEN, M. W. & VELIKOV, K. P. 2012. Oil-in-water
522 Pickering emulsions stabilized by colloidal particles from the water-insoluble protein
523 zein. *Soft Matter,* 8**,** 6807-6815.
524 DE WIJK, R. A. & PRINZ, J. F. 2005. The role of friction in perceived oral texture. *Food*
525 *Quality and Preference,* 16**,** 121-129.
526 DEPREE, J. A. & SAVAGE, G. P. 2001. Physical and flavour stability of mayonnaise.
527 *Trends in Food Science & Technology,* 12**,** 157-163.
528 DERKACH, S. R. 2009. Rheology of emulsions. *Advances in Colloid and Interface Science,*
529 151**,** 1-23.
530 DESHMUKH, O. S., VAN DEN ENDE, D., STUART, M. C., MUGELE, F. & DUITS, M.
531 H. G. 2015. Hard and soft colloids at fluid interfaces: Adsorption, interactions,
532 assembly & rheology. Advances in Colloid and Interface Science, 222, 215-227.
533 DESTRIBATS, M., ROUVET, M., GEHIN-DELVAL, C., SCHMITT, C. & BINKS, B. P. J.
534 S. M. 2014. Emulsions stabilised by whey protein microgel particles: towards food-
535 grade Pickering emulsions. 10**,** 6941-6954.
536 DICKINSON, E. 1992. *Introduction to food colloids*, Oxford University Press.

DICKINSON, E. 2015. Microgels — An alternative colloidal ingredient for stabilization of food emulsions. Trends in Food Science & Technology, 43, 178-188.

DICKINSON, E. & CHEN, J. 1999. HEAT-SET WHEY PROTEIN EMULSION GELS: ROLE OF ACTIVE AND INACTIVE FILLER PARTICLES. *Journal of Dispersion Science and Technology,* 20**,** 197-213.

DICKINSON, E., CHEN, J. J. J. O. D. S. & TECHNOLOGY 1999. Heat-set whey protein emulsion gels: role of active and inactive filler particles. 20**,** 197-213.

DICKINSON, E. & PARKINSON, E. L. 2004. Heat-induced aggregation of milk protein-stabilized emulsions: sensitivity to processing and composition. *International Dairy Journal,* 14**,** 635-645.

DICKINSON, E. 2011. Double emulsions stabilized by food biopolymers. 6**,** 1-11.

DICKINSON, E. 2003. Hydrocolloids at interfaces and the influence on the properties of dispersed systems. 17**,** 25-39.

EINSTEIN, A. J. A. D. P. 1911. Berichtigung zu meiner Arbeit:„Eine neue Bestimmung der Moleküldimensionen" . 339**,** 591-592.

ELLIS, A. L., NORTON, A. B., MILLS, T. B. & NORTON, I. T. 2017. Stabilisation of foams by agar gel particles. *Food Hydrocolloids,* 73**,** 222-228.

FERNÁNDEZ FARRÉS, I. 2015. *Fluid gel production and tribological behaviour of alginate and agar*. University of Birmingham.

FERNÁNDEZ FARRÉS, I., DOUAIRE, M. & NORTON, I. T. 2013. Rheology and tribological properties of Ca-alginate fluid gels produced by diffusion-controlled method. *Food Hydrocolloids,* 32**,** 115-122.

FERNÁNDEZ FARRÉS, I. & NORTON, I. T. 2015. The influence of co-solutes on tribology of agar fluid gels. *Food Hydrocolloids,* 45**,** 186-195.

561 FOEGEDING, E. A. & DAVIS, J. P. J. F. H. 2011. Food protein functionality: A
562 comprehensive approach. 25**,** 1853-1864.
563 FRENKEL, M., SHWARTZ, R., GARTI, N. J. J. O. C. & SCIENCE, I. 1983. Multiple
564 emulsions: I. Stability: Inversion, apparent and weighted HLB. 94**,** 174-178.
565 GABRIELE, A., SPYROPOULOS, F. & NORTON, I. 2010. A conceptual model for fluid gel
566 lubrication. *Soft Matter,* 6**,** 4205-4213.
567 GARREC, D. 2013. *Understanding fluid gels and hydrocolloid tribology.* University of
568 Birmingham.
569 GARREC, D. A., GUTHRIE, B. & NORTON, I. T. 2013. Kappa carrageenan fluid gel
570 material properties. Part 1: Rheology. *Food Hydrocolloids,* 33**,** 151-159.
571 GARREC, D. A. & NORTON, I. T. 2013. Kappa carrageenan fluid gel material properties.
572 Part 2: Tribology. *Food Hydrocolloids,* 33**,** 160-167.
573 GRIFFIN, W. C. J. J. S. C. C. 1949. Classification of surface-active agents by" HLB". 1**,** 311-
574 326.
575 HERMANSSON, A. M. 1986. Soy protein gelation. Journal of the American Oil Chemists
576 Society, 63, 658-666.
577 HODGE, S. & ROUSSEAU, D. 2005. Continuous-phase fat crystals strongly influence water-
578 in-oil emulsion stability. *Journal of the American Oil Chemists' Society,* 82**,** 159-164.
579 HOFFMANN, M. A., ROEFS, S. P., VERHEUL, M., VAN MIL, P. J. & DE KRUIF, K. G.
580 1996. Aggregation of β-lactoglobulin studied by in situ light scattering. Journal of
581 Dairy Research, 63, 423-440.
582 HUNTER, T. N., PUGH, R. J., FRANKS, G. V., JAMESON, G. J. J. A. I. C. & SCIENCE, I.
583 2008. The role of particles in stabilising foams and emulsions. 137**,** 57-81.

584 JIAO, B., SHI, A., WANG, Q. & BINKS, B. P. 2018. High-Internal-Phase Pickering
585 Emulsions Stabilized Solely by Peanut-Protein-Isolate Microgel Particles with
586 Multiple Potential Applications. 57**,** 9274-9278.
587 JOSHI, M., ADHIKARI, B., ALDRED, P., PANOZZO, J., KASAPIS, S. & BARROW, C. J.
588 F. C. 2012. Interfacial and emulsifying properties of lentil protein isolate. 134**,** 1343-
589 1353.
590 KALASHNIKOVA, I., BIZOT, H., CATHALA, B. & CAPRON, I. 2011. New Pickering
591 emulsions stabilized by bacterial cellulose nanocrystals. *Langmuir*, 27**,** 7471-7479.
592 KARACA, A. C., LOW, N. & NICKERSON, M. J. F. R. I. 2011. Emulsifying properties of
593 chickpea, faba bean, lentil and pea proteins produced by isoelectric precipitation and
594 salt extraction. 44**,** 2742-2750.
595 KARGAR, M., FAYAZMANESH, K., ALAVI, M., SPYROPOULOS, F. & NORTON, I. T.
596 2012. Investigation into the potential ability of Pickering emulsions (food-grade
597 particles) to enhance the oxidative stability of oil-in-water emulsions. *Journal of*
598 *colloid and interface science*, 366**,** 209-215.
599 KIM, H., DECKER, E. & MCCLEMENTS, D. J. L. 2005. Influence of protein concentration
600 and order of addition on thermal stability of β-lactoglobulin stabilized n-hexadecane
601 oil-in-water emulsions at neutral pH. 21**,** 134-139.
602 KOKINI, J. L. 1987. The physical basis of liquid food texture and texture-taste interactions.
603 *Journal of Food Engineering*, 6**,** 51-81.
604 KRALCHEVSKY, P., IVANOV, I., ANANTHAPADMANABHAN, K. & LIPS, A. J. L.
605 2005. On the thermodynamics of particle-stabilized emulsions: curvature effects and
606 catastrophic phase inversion. 21**,** 50-63.

KRALOVA, I., SJÖBLOM, J. J. J. O. D. S. & TECHNOLOGY 2009. Surfactants used in food industry: a review. 30**,** 1363-1383.

KRIEGER, I. M. & DOUGHERTY, T. J. J. T. O. T. S. O. R. 1959. A mechanism for non-Newtonian flow in suspensions of rigid spheres. 3**,** 137-152.

LAM, R. S. & NICKERSON, M. T. J. F. C. 2013. Food proteins: a review on their emulsifying properties using a structure–function approach. 141**,** 975-984.

LAZIDIS, A., HANCOCKS, R. D., SPYROPOULOS, F., KREUß, M., BERROCAL, R. & NORTON, I. T. 2016. Whey protein fluid gels for the stabilisation of foams. *Food Hydrocolloids,* 53**,** 209-217.

LIU, F. & TANG, C.-H. 2016a. Soy glycinin as food-grade Pickering stabilizers: Part. II. Improvement of emulsification and interfacial adsorption by electrostatic screening. *Food Hydrocolloids,* 60**,** 620-630.

LIU, F. & TANG, C.-H. 2016b. Soy glycinin as food-grade Pickering stabilizers: Part. III. Fabrication of gel-like emulsions and their potential as sustained-release delivery systems for β-carotene. *Food Hydrocolloids,* 56**,** 434-444.

LIU, F., TANG, C.-H. J. J. O. A. & CHEMISTRY, F. 2013. Soy protein nanoparticle aggregates as Pickering stabilizers for oil-in-water emulsions. 61**,** 8888-8898.

LUO, Z., MURRAY, B. S., ROSS, A.-L., POVEY, M. J. W., MORGAN, M. R. A. & DAY, A. J. 2012. Effects of pH on the ability of flavonoids to act as Pickering emulsion stabilizers. *Colloids and Surfaces B: Biointerfaces,* 92**,** 84-90.

LUO, Z., MURRAY, B. S., YUSOFF, A., MORGAN, M. R. A., POVEY, M. J. W. & DAY, A. J. 2011. Particle-Stabilizing Effects of Flavonoids at the Oil−Water Interface. *Journal of Agricultural and Food Chemistry,* 59**,** 2636-2645.

630 MA, Z., BOYE, J. I. J. F. & TECHNOLOGY, B. 2013. Advances in the design and
631 production of reduced-fat and reduced-cholesterol salad dressing and mayonnaise: a
632 review. 6**,** 648-670.
633 MACKIE, A. R., RIDOUT, M. J., MOATES, G., HUSBAND, F. A., WILDE, P. J. J. J. O. A.
634 & CHEMISTRY, F. 2007. Effect of the interfacial layer composition on the properties
635 of emulsion creams. 55**,** 5611-5619.
636 MADIVALA, B., FRANSAER, J. & VERMANT, J. J. L. 2009a. Self-assembly and rheology
637 of ellipsoidal particles at interfaces. 25**,** 2718-2728.
638 MADIVALA, B., VANDEBRIL, S., FRANSAER, J. & VERMANT, J. J. S. M. 2009b.
639 Exploiting particle shape in solid stabilized emulsions. 5**,** 1717-1727.
640 MAGDASSI, S. 1996. *Surface activity of proteins: chemical and physicochemical*
641 *modifications*, Crc Press.
642 MALMSTEN, M. 1998. *Biopolymers at interfaces*, CRC Press.
643 MALONE, M. E., APPELQVIST, I. A. M. & NORTON, I. T. 2003a. Oral behaviour of food
644 hydrocolloids and emulsions. Part 1. Lubrication and deposition considerations. *Food*
645 *Hydrocolloids,* 17**,** 763-773.
646 MALONE, M. E., APPELQVIST, I. A. M. & NORTON, I. T. 2003b. Oral behaviour of food
647 hydrocolloids and emulsions. Part 2. Taste and aroma release. *Food Hydrocolloids,*
648 17**,** 775-784.
649 MCCLEMENTS, D. Food Emulsions: Principles, Practice, and Techniques. CRC series in
650 contemporary food science. 2005. Boca Raton: CRC Press.
651 MCCLEMENTS, D. J. 2015. *Food emulsions: principles, practices, and techniques*, CRC
652 press.

MCCLEMENTS, D. J., MONAHAN, F. J. & KINSELLA, J. E. 1993. EFFECT OF EMULSION DROPLETS ON THE RHEOLOGY OF WHEY PROTEIN ISOLATE GELS. 24**,** 411-422.

MELZER, E., KREUTER, J. & DANIELS, R. 2003. Ethylcellulose: a new type of emulsion stabilizer. *European Journal of Pharmaceutics and Biopharmaceutics,* 56**,** 23-27.

MILLS, T. B. 2012. *Development of in-vitro mouth methods for studying oral phenomena.* University of Birmingham.

MOAKES, R. J. A., SULLO, A. & NORTON, I. T. 2015. Preparation and characterisation of whey protein fluid gels: The effects of shear and thermal history. Food Hydrocolloids, 45, 227-235.

NAJBAR, L. V., CONSIDINE, R. F. & DRUMMOND, C. J. J. L. 2003. Heat-induced aggregation of a globular egg-white protein in aqueous solution: investigation by atomic force microscope imaging and surface force mapping modalities. 19**,** 2880-2887.

NGAI, T., AUWETER, H. & BEHRENS, S. H. J. M. 2006. Environmental responsiveness of microgel particles and particle-stabilized emulsions. 39**,** 8171-8177.

NIKNAFS, N., SPYROPOULOS, F. & NORTON, I. T. J. J. O. F. E. 2011. Development of a new reflectance technique to investigate the mechanism of emulsification. 104**,** 603-611.

PAL, R. J. C. O. I. C. & SCIENCE, I. 2011. Rheology of simple and multiple emulsions. 16**,** 41-60.

PASQUALI, R. C., TAUROZZI, M. P. & BREGNI, C. J. I. J. O. P. 2008. Some considerations about the hydrophilic–lipophilic balance system. 356**,** 44-51.

PAUNOV, V. N., CAYRE, O. J., NOBLE, P. F., STOYANOV, S. D., VELIKOV, K. P. & GOLDING, M. 2007. Emulsions stabilised by food colloid particles: Role of particle adsorption and wettability at the liquid interface. *Journal of colloid and interface science,* 312**,** 381-389.

PERAZZO, A., PREZIOSI, V. and GUIDO, S., 2015. Phase inversion emulsification: Current understanding and applications. Advances in colloid and interface science, 222, pp.581-599.

PICHOT, R., SPYROPOULOS, F., NORTON, I. J. J. O. C. & SCIENCE, I. 2009. Mixed-emulsifier stabilised emulsions: Investigation of the effect of monoolein and hydrophilic silica particle mixtures on the stability against coalescence. 329**,** 284-291.

PICKERING, S. U. 1907. CXCVI.-Emulsions. *Journal of the Chemical Society, Transactions,* 91**,** 2001-2021.

QUEMADA, D., BERLI, C. J. A. I. C. & SCIENCE, I. 2002. Energy of interaction in colloids and its implications in rheological modeling. 98**,** 51-85.

RAMSDEN, W. J. P. O. T. R. S. O. L. 1904. Separation of solids in the surface-layers of solutions and 'suspensions'(observations on surface-membranes, bubbles, emulsions, and mechanical coagulation).—Preliminary account. 72**,** 156-164.

RAYNER, M., TIMGREN, A., SJÖÖ, M. & DEJMEK, P. 2012. Quinoa starch granules: a candidate for stabilising food-grade Pickering emulsions. *Journal of the Science of Food and Agriculture,* 92**,** 1841-1847.

RICHMOND, J. 1990. *Cationic surfactants: organic chemistry*, CRC Press.

ROMERO, A., BEAUMAL, V., DAVID-BRIAND, E., CORDOBÉS, F., ANTON, M., GUERRERO, A. J. L.-F. S. & TECHNOLOGY 2011. Interfacial and emulsifying behaviour of crayfish protein isolate. 44**,** 1603-1610.

ROSEN, M. J. & KUNJAPPU, J. T. 2012. *Surfactants and interfacial phenomena*, John Wiley & Sons.

ROSS-MURPHY, S. B. 1994. Rheological characterization of polymer gels and networks. *Polymer Gels and Networks,* 2**,** 229-237.

SCHMIDT, S., LIU, T., RÜTTEN, S., PHAN, K.-H., MÖLLER, M. & RICHTERING, W. 2011. Influence of microgel architecture and oil polarity on stabilization of emulsions by stimuli-sensitive core–shell poly (n-isopropylacrylamide-co-methacrylic acid) microgels: Mickering versus pickering behavior? Langmuir, 27, 9801-9806.

SCHMITT, V., DESTRIBATS, M. & BACKOV, R. J. C. R. P. 2014. Colloidal particles as liquid dispersion stabilizer: Pickering emulsions and materials thereof. 15**,** 761-774.

SHAMIL, S., WYETH, L. J., KILCAST, D. J. F. Q. & PREFERENCE 1991. Flavour release and perception in reduced-fat foods. 3**,** 51-60.

SHAO, Y. & TANG, C.-H. 2016. Gel-like pea protein Pickering emulsions at pH3.0 as a potential intestine-targeted and sustained-release delivery system for β-carotene. *Food Research International,* 79**,** 64-72.

SHAO, Z., NEGI, A. S. & OSUJI, C. O. J. S. M. 2013. Role of interparticle attraction in the yielding response of microgel suspensions. 9**,** 5492-5500.

SHIMIZU, M., NAKANE, Y. J. B., BIOTECHNOLOGY, & BIOCHEMISTRY 1995. Encapsulation of biologically active proteins in a multiple emulsion. 59**,** 492-496.

SIKORA, M., BADRIE, N., DEISINGH, A. K., KOWALSKI, S. J. C. R. I. F. S. & NUTRITION 2008. Sauces and dressings: a review of properties and applications. 48**,** 50-77.

SINGER, N. S., YAMAMOTO, S. & LATELLA, J. 1988. Protein product base. Google Patents.

724 SJOBLOM, J. 2001. *Encyclopedic handbook of emulsion technology*, CRC press.
725 STICKEL, J. J. & POWELL, R. L. J. A. R. F. M. 2005. Fluid mechanics and rheology of
726 dense suspensions. 37**,** 129-149.
727 STRIBECK, R. 1902. Die wesentlichen eigenschaften der gleit-und rollenlager. *Zeitschrift*
728 *des Vereines Deutscher Ingenieure,* 46**,** 1341-1348, 1432-1438, 1463-1470.
729 TAMBE, D. E., SHARMA, M. M. J. A. I. C. & SCIENCE, I. 1994. The effect of colloidal
730 particles on fluid-fluid interfacial properties and emulsion stability. 52**,** 1-63.
731 TCHOLAKOVA, S., DENKOV, N. D., IVANOV, I. B., CAMPBELL, B. J. A. I. C. &
732 SCIENCE, I. 2006. Coalescence stability of emulsions containing globular milk
733 proteins. 123**,** 259-293.
734 TIMGREN, A., RAYNER, M., SJÖÖ, M. & DEJMEK, P. 2011. Starch particles for food
735 based Pickering emulsions. *Procedia Food Science,* 1**,** 95-103.
736 VELLA, D., AUSSILLOUS, P. & MAHADEVAN, L. J. E. 2004. Elasticity of an interfacial
737 particle raft. 68**,** 212.
738 VERHEUL, M. & ROEFS, S. P. F. M. 1998. Structure of Particulate Whey Protein Gels:
739 Effect of NaCl Concentration, pH, Heating Temperature, and Protein Composition.
740 Journal of Agricultural and Food Chemistry, 46, 4909-4916.
741 WALSTRA, P. 2002. *Physical chemistry of foods*, CRC Press.
742 WU, J., SHI, M., LI, W., ZHAO, L., WANG, Z., YAN, X., NORDE, W. & LI, Y. 2015.
743 Pickering emulsions stabilized by whey protein nanoparticles prepared by thermal
744 cross-linking. *Colloids and Surfaces B: Biointerfaces,* 127**,** 96-104.
745 WU, Y., WIESE, S., BALACEANU, A., RICHTERING, W. & PICH, A. 2014. Behavior of
746 Temperature-Responsive Copolymer Microgels at the Oil/Water Interface. Langmuir,
747 30, 7660-7669.

YUSOFF, A. & MURRAY, B. S. 2011. Modified starch granules as particle-stabilizers of oil-in-water emulsions. *Food Hydrocolloids,* 25**,** 42-55.

CHAPTER 6.
Scale up

6.1. Introduction

A key inhibitor in progression from food research to industry is the potential for scale up of processing. In this chapter, the potential for alternative methods and larger-scale systems for the production of protein particles was investigated, comparing particles produced from a benchtop spray dryer and a pilot scale spray dryer. For egg white fluid gels, the batch method of production in the rheometer is compared with a continuous throughput method using pin-stirrers.

6.2. Materials and methods

6.2.1. Egg white solutions

Eggs were sourced from a supermarket (Tesco) and separated by hand to obtain the egg white. Fresh eggs were used as these eggs will not have been treated in a manner that may influence protein functionality

6.2.1.1. Whole egg white solutions

Whole eggs whites were used for fluid gels produced by the pin-stirrer method. These separated egg whites were stirred gently for 15 minutes and then passed through a 1 mm sieve. This was to remove ovomucin aggregates. This was then diluted to a final concentration of 75% with reverse osmosis water. The concentration of 75% was used as it was determined to be an appropriate concentration for treated egg white fluid gel production within the vane geometry of a rheometer in Chapter 3. This solution was stored at 4ºC for no longer than 48 hours prior to use.

6.2.1.2. Treated egg white solutions

Treated egg white solutions were used for fluid gel production using a rheometer, as discussed in Chapter 3. For production of egg white fluid gels in the rheometer, the egg whites were

treated to remove the ovotransferrin. Eggs were purchased from a supermarket (Tesco) and separated by hand to obtain the egg whites. These egg whites were heated at 65ºC for 10 minutes and then passed through a 1 mm sieve. This treated egg white was then diluted to 75% with diwater.

6.2.2. WPI solution

WPI solutions were prepared to a final concentration of 12%. This was achieved by producing a stock solution at 15% prior to pH adjustment then further dilution. WPI solutions were prepared by dispersing this powder at 15% W/W in reverse osmosis water. 0.01% sodium azide was added to inhibit bacterial growth. This was dispersed by means of an overhead stirrer for 12 hours and then stored in a fridge until required for a maximum of 14 days.

The pH of this stock solution was adjusted with 2 M acetic acid to a final pH of 3.5. The resulting solution was then diluted to a final WPI concentration of 12% W/W.

6.2.3. Spray drying

Prior to spray drying, WPI samples were heated to 65ºC for 1 hour in a stirred water bath.

6.2.3.1. Lab scale

A Buchi B-290 Mini-spray dryer was used with a 0.8 mm nozzle, an inlet temperature of 180ºC, an aspirator rate of 95% and a feed rate of 20%. This corresponded to an outlet temperature of 63–68ºC.

Samples were stored in an airtight container at 18ºC and were used within 3 months of production.

6.2.3.2. Pilot scale

An Armfield FT80 Tall form pilot scale spray dryer was used with a 2.4 mm nozzle, an inlet temperature of 180ºC, an inlet fan frequency of 30 Hz and an outlet fan frequency of 34 Hz. A feed rate of 25 Hz was used. This corresponded to an outlet temperature of 68–71ºC.

6.2.4. Fluid gel production

6.2.4.1. Rheometer

A Malvern Kinexus rheometer was used with a vane and cup geometry to heat and cool the solution in shear. Solutions were degassed in a vacuum at 100 mbar for 5 minutes prior to commencement of fluid gel preparation. This was to reduce any foaming through production. A constant shear rate of 500 s^{-1} was applied throughout the heating and cooling processes. Samples were heated from 40ºC to 90ºC at a rate of 2ºC min^{-1} and then held at 90ºC for 2 minutes. The samples were then cooled from 90ºC to 5ºC at a rate of 4ºC min^{-1}.

6.2.4.2. Pin-stirrer

For continuous production of egg fluid gels, two jacketed pin-stirrers were used in series. The first heated and the second cooled the egg. The whole egg white solution was degassed at 100 mbar for 5 minutes then heated to 40ºC using a stirred hotplate. This preheated solution was passed through two pin-stirrers in series. The first pin-stirrer had a jacket temperature of 90ºC, and the second had a jacket temperature of 5ºC. This gave an outlet temperature of the first pin-stirrer of >87ºC and an outlet temperature of the second pin-stirrer of <6ºC. Samples were stored at 5ºC for less than a week prior to use.

A flow rate of 7 ml min^{-1} was used. This gave an average heating rate of ≈2.5ºC min^{-1} and a cooling rate of ≈4.5ºC min^{-1}.

6.2.5. Dispersion preparation

Dispersions were produced by dispersing the powder produced in reverse osmosis water at room temperature. WPI was dispersed at 20% W/W. This was achieved by stirring with a magnetic stirrer for 1 hour at a speed of approximately 200 RPM. Samples were degassed at -100 mbar for 20 minutes. Samples were then stored at 5ºC overnight before measurements.

6.2.6. Light microscopy

An optical microscope (Leica Microsystems, UK) was used to directly observe particles. Samples were diluted with distilled water. A drop of this diluted sample was placed on a slide and covered with a coverslip. 20× magnification was used to observe the particles.

6.2.7. Particle sizing

Particle size distributions were determined by SLS using a Malvern Mastersizer with a hydro SM manual small volume dispersion attachment (Malvern Instruments, UK). Samples were diluted down to 1% (w/w), and three repeats were used with each repeat consisting of three measurements.

6.2.8. Shear rheology

To investigate the effects of shear on particle ordering in flow, flow curves were obtained for suspensions. A 40 mm sand-blasted parallel plate geometry was used to minimize slip. Equilibrium shear experiments were used with up to 2 minutes allowed for samples to reach equilibrium at each shear rate. Samples were tested at 25ºC using a 1 mm gap.

6.3. Results and discussion

6.3.1. Spray-dried WPI particles

Spray drying offers scale-up potential; however, this does not come without its challenges. Atomization with increased liquid feed rates presents challenges. It is important in order for the spray drying to be effective that the droplets produced are small and consistent in size. The increased fall time and changes in drying chamber size influence the drying time of the particles, and subsequently outlet humidity is also influenced. These conditions influence the drying kinetics and temperature profile experienced by droplets throughout the spray dryer. This investigation of scale-up potential was undertaken to understand whether the production method was robust or was sensitive to the conditions specific to those found in the lab scale spray dryer. For the lab scale spray dryer, a feed rate of 320 ml h^{-1} was used; for the pilot scale spray dryer, a feed rate of 2.5 l h^{-1} was used.

A size comparison of WPI particles spray dried after heat treatment at pH 3.5 produced in a lab scale and pilot scale spray dryer is presented in Figure 6.1. The lab scale sample had an average particle size of 22.9 (± 2.0) μm and the pilot scale sample had an average particle size of 29.0 (± 5.2) μm. Both samples showed a similar size distribution ranging from 4 μm to 200 μm, with a peak at 15 μm. Pilot scale samples showed a broader distribution, with larger volumes of particles >35 μm present. Little difference was observed between the size of particles produced from the lab scale spray dryer and the pilot scale spray dryer. For both lab scale and pilot scale spray dryers, the highest pressure of atomization possible with the set-up was used in both cases (~5 bar). Increased atomization pressure will give higher shear rates during atomization. Higher shear rates will lead to greater break-up of particles, in turn producing smaller particles. The pilot scale spray dryer has a larger diameter nozzle than the

lab scale spray dryer (2.4 mm and 0.8 mm, respectively). Thus, lower shear rates were expected throughout atomization in the pilot scale spray dryer, but similar sized particles were produced. Production of droplets of comparative sizes in nozzles of varying size has been observed previously.

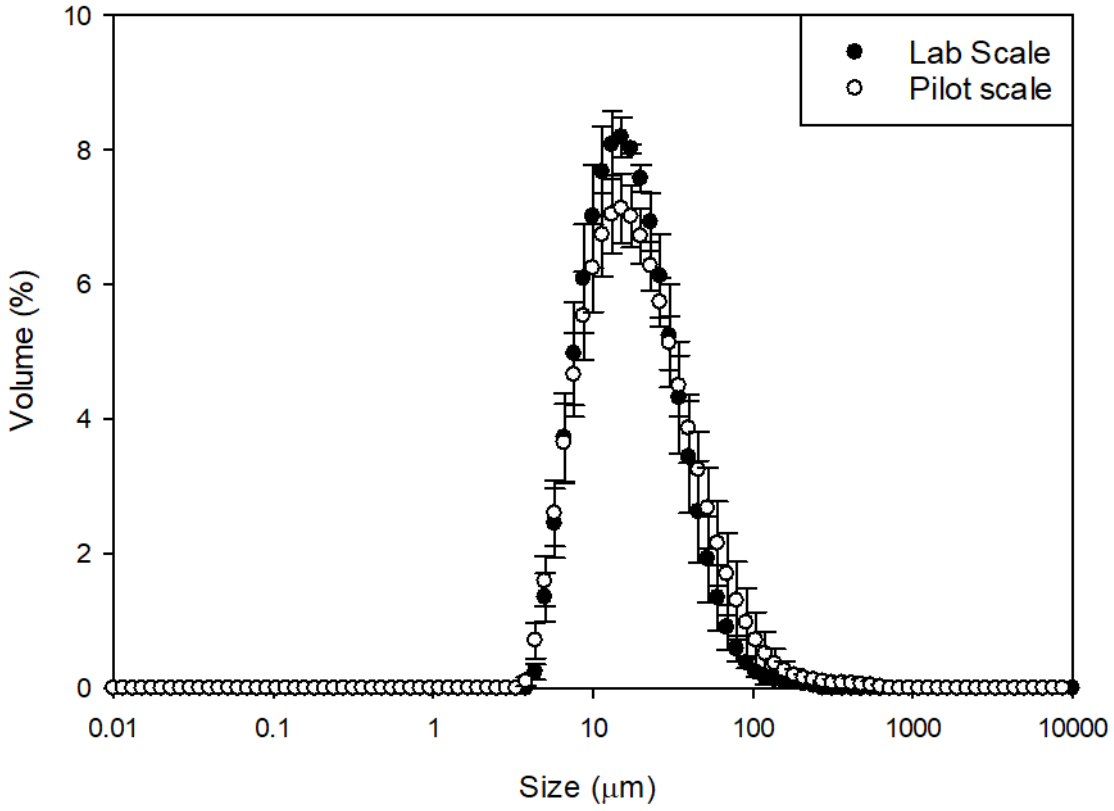

Figure 6. 1. WPI particle sizing for particles produced in a Buchi lab scale spray dryer and an Armfield tall form spray dryer (pilot scale). Points represent averages of three measurements, error bars show +/- 1StD.

It has been shown previously by Thybo *et al*. (2008) that at a high enough atomization gas–liquid–mass ratio (ALR) nozzle diameter does not influence droplet sizes during spray drying. At low ALR, smaller droplets are produced by smaller diameter nozzles.

Figure 6.2 shows micrographs of the particles produced from both spray dryers dispersed in water. For both spray dryers, anisotropic particles were produced. The sizes of these particles

observed is in good agreement with SLS measurements, with particles ranging from 1 μm to 20 μm.

The similarity in particle size and shape observed supports that these systems can be produced through higher throughput nozzles with little change to particle size.

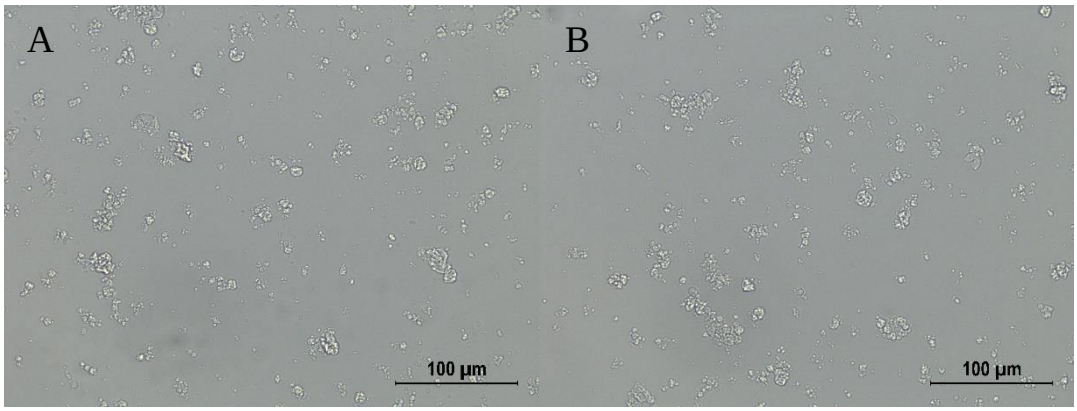

Figure 6. 2. Micrographs of WPI spray dried after heat treatment at 65ºC for 60 minutes at pH 3.5. Samples were spray dried on A) a lab scale spray dryer or B) a pilot scale spray dryer.

The flow properties of suspensions of the WPI particles produced through spray drying with the lab scale and pilot scale spray dryers were investigated. This is presented in Figure 6.3, which compares the flow properties of 20% suspensions of WPI particles. Both suspensions showed very similar flow properties. This agrees with sizing data that there is little change in functionality of these particles produced in a higher throughput spray dryer. The similarity in the rheology of suspensions suggests similar properties of the particles produced, which concurs with sizing and microscopy. However, this further supports that the higher temperatures experienced by particles during pilot scale production has not hindered the ability of these particles to hydrate. Particles produced in the pilot scale spray dryer will have experienced a different temperature profile owing to the greater drying chamber size and increased fall time.

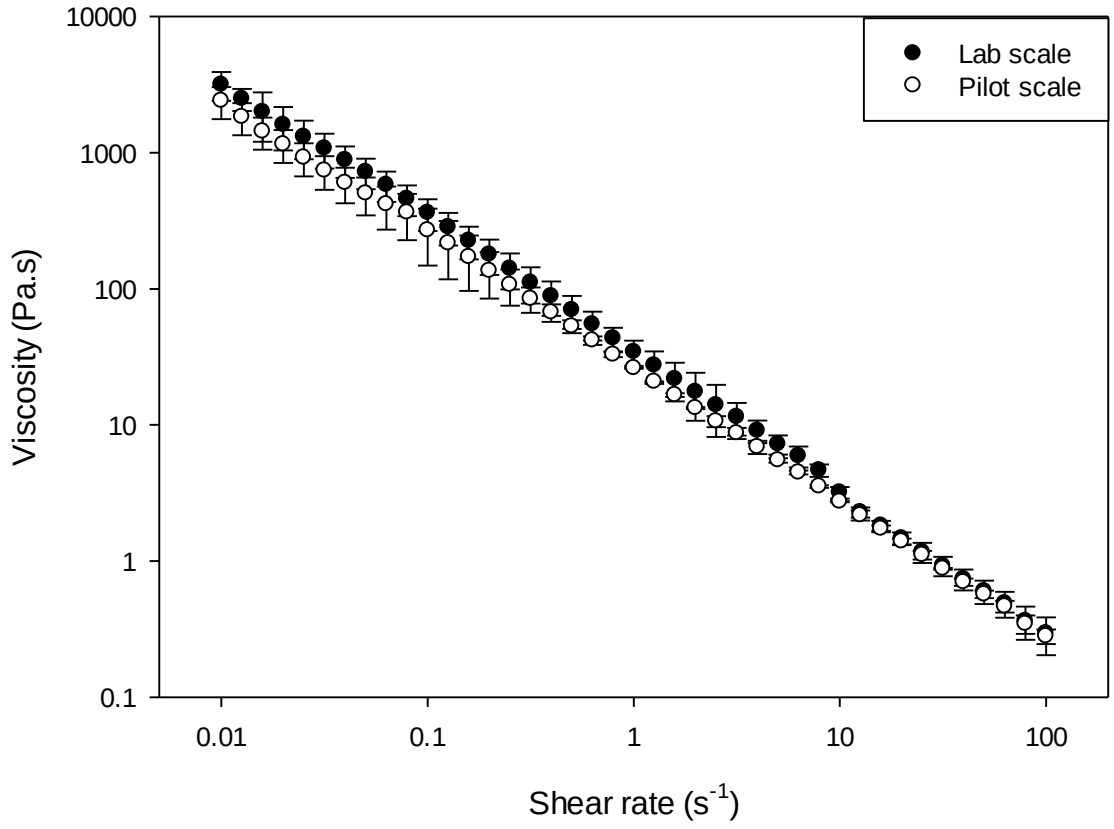

Figure 6. 3. Viscosity profile of 20% WPI particles produced by spray drying of heat-treated WPI at pH 3.5 in lab scale and pilot scale spray dryers. Error bars show +/- 1StD.

6.3.2. Egg white fluid gels

Egg white fluid gels were produced from whole egg white using two pin-stirrers in series. Pin-stirrers are continuous throughput jacketed shear devices. Two pin-stirrers were used in series with one heating to 90ºC and the second cooling to 5ºC. This was done to confirm whether this continuous throughput method could be used for the production of protein fluid gels. It was also used to investigate whether whole egg white could be used in the pin-stirrer as the pin-stirrer has a different shear field relative to the vane geometry. A flow rate of 7 ml min^{-1} was used in the pin-stirrer, which was a compromise between rate of production and average heating rate. Lower average heating rates should produce smaller particles as the equilibrium between aggregation and break-up of particles should shift with reduced

aggregation rates. A shaft speed of 2000 RPM was used as this is the maximum possible on the pin-stirrer used; increasing shaft speed will increase shear rate, increasing break-up of particles.

The size distribution of particles produced from whole egg white through pin-stirrers were compared with treated egg white fluid gels produced in a vane geometry. The size distribution of particles produced is presented in in Figure 6.4. Fluid gels produced in the rheometer had a size distribution from 0.1 μm to 400 μm; for fluid gels produced in a pin-stirrer, sizes ranged from 5 μm to 600 μm. Three peaks are observed at 0.5 μm, 8 μm and 150 μm for fluid gels produced in a rheometer, whereas fluid gels produced in the pin-stirrer had a distribution of particle sizes with a peak at 100 μm. The average particle sizes were 161 (±26) μm for those produced in the pin-stirrers and 8 (±4) μm for those produced in the rheometer.

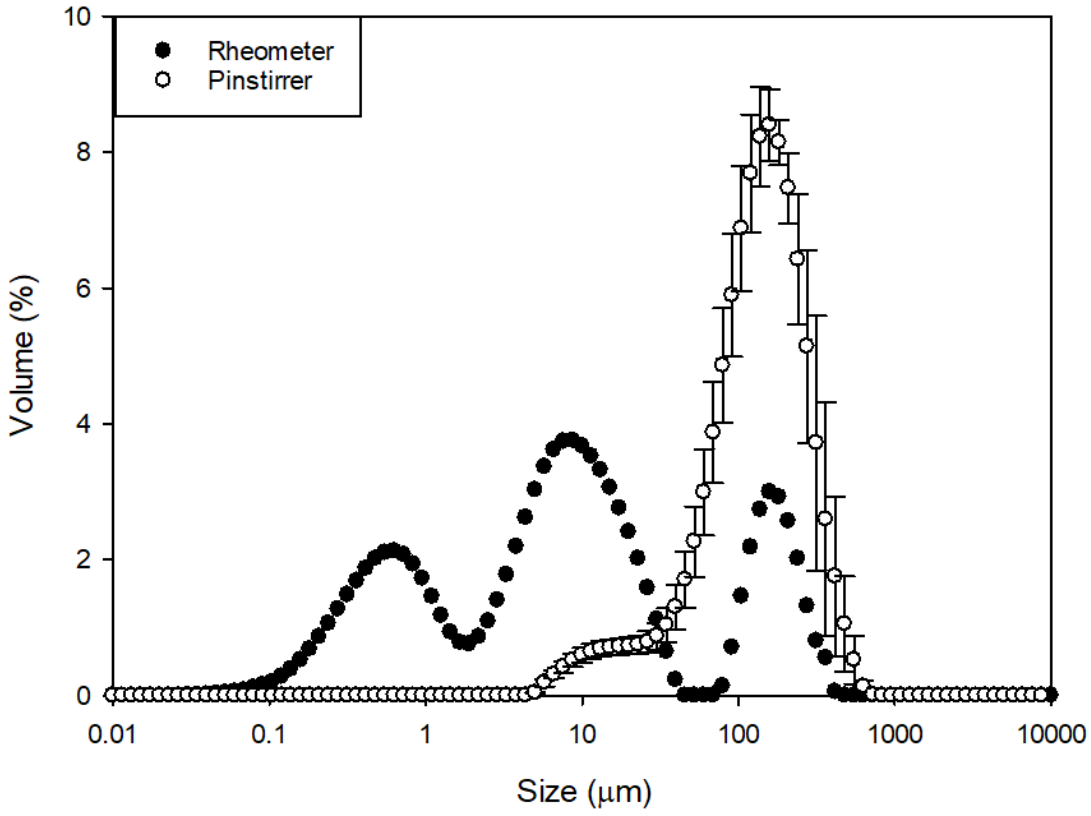

Figure 6. 4. Particle sizes for egg white fluid gels produced from treated egg white in the vane geometry of a rheometer and whole egg using pin-stirrers. Error bars show +/- 1StD.

Several factors may contribute to the increased particle size observed for fluid gels produced in the pin-stirrer. The first is the shear field in the pin-stirrer; previous research using positron emission particle tracking showed a shaft speed of 2000 RPM to give a shear rate ≈200 s^{-1} (Gabriele, 2011). During particle formation, the size of particles will be controlled by the equilibrium between particle aggregation and particle break-up. Particle break-up will be influenced by the shear environment. The aggregation rate is controlled by the gelation kinetics of the protein and the rate of heating. With the lower shear rates observed in the pin-stirrer, larger particles will be expected owing to reduced particle break-up (Garrec and Norton, 2012).

The whole egg white used for fluid gels produced from the pin-stirrer contains the ovotransferrin protein. This protein was shown in preliminary work presented in Chapter 3 to prevent fluid gel formation in rheometer methods of production.

The heating profile experienced by the egg in the pin-stirrer must also be considered. Whilst the flow rate through the pin-stirrer corresponded to an average heating rate of 2.5ºC min^{-1}, this increased heating rate relative to the 2ºC min^{-1} average heating rate in rheometer production. Increased heating rate will increase particle size as the rate of aggregation will increase. Final particle size is controlled by the equilibrium between the rate of aggregation and the rate of break-up. As well as the difference in average heating rate, the temperature profile experienced will not be linear for fluid gels produced in the pin-stirrer as it was for those produced within the rheometer in which heating rate was controlled. If a more rapid heating rate is experienced as gelation occurs, the equilibrium of particle aggregation and break-up will shift towards aggregation, producing larger particles (Garrec *et al*., 2013).

Light microscopy was used to further understand the particle properties of these fluid gels and is presented in Figure 6.5. Here, the difference in size distributions was evident. The particles produced through the pin-stirrer are large and anisotropic, resembling a quiescently set gel that has been broken up with sharp edges. Particles produced in the rheometer are also anisotropic, but they have more rounded edges.

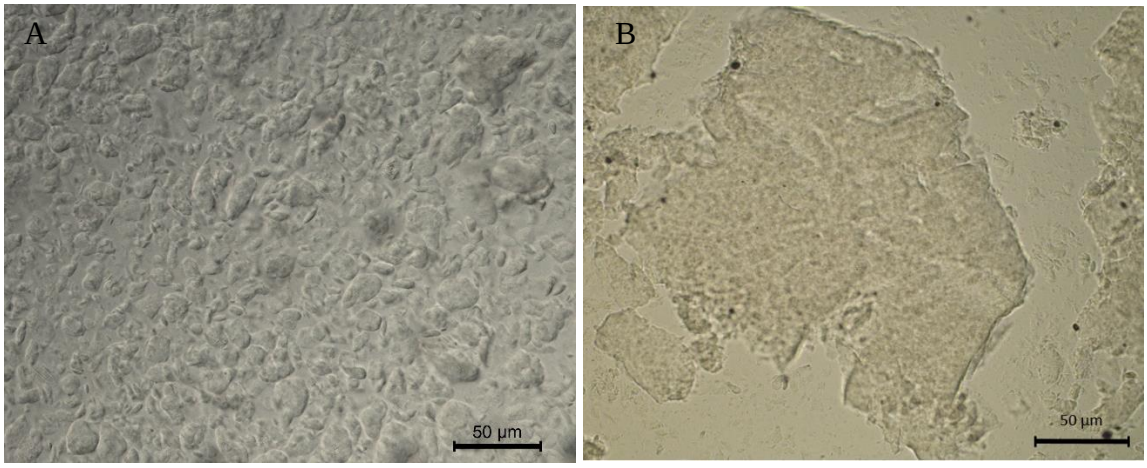

Figure 6. 5. Light micrographs of egg fluid gel particles A) produced in a rheometer and B) produced in a pin-stirrer.

How production method influences the flow properties of egg white fluid gels was investigated and is shown in Figure 6.6. Egg fluid gels produced by both methods showed the shear thinning nature expected for suspensions. At shear rates below $1s^{-1}$, the same viscosities were observed, with error bars overlapping. At shear rates above $1s^{-1}$, fluid gels produced in the rheometer showed a higher viscosity with a reduced degree of shear thinning.

At lower shear rates viscosity will be dominated by particle modulus, as flow in this regime is through deformation. However, as shear rate increases, this transitions into the disruption phase as particles begin to move past one another whilst remaining in flocs. In this regime, particles size and shape will be important, as can be seen in Figure 6.5. Fluid gels produced in the pin-stirrer have a more jagged shape than the smooth, more rounded shape of particles produced in the rheometer. These more rounded particles will break up more easily than the jagged-shaped particles, which will interpenetrate.

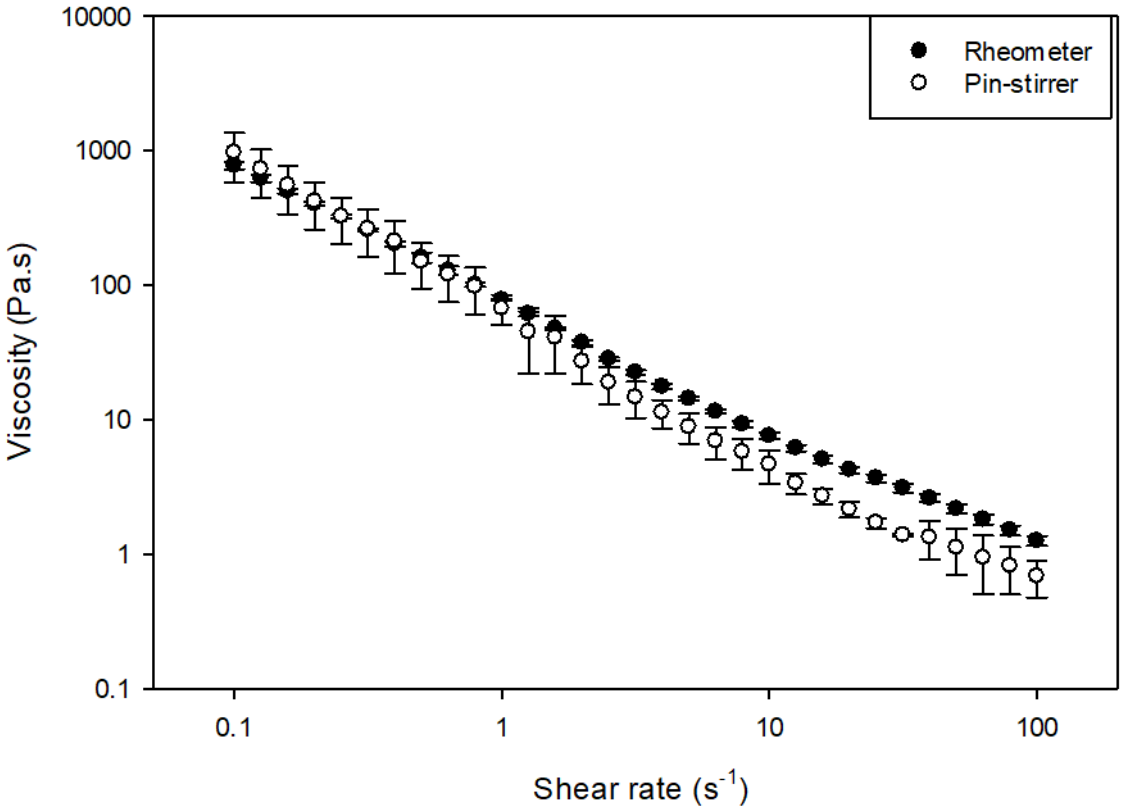

Figure 6. 6. Viscometry flow profiles of egg white fluid gels produced from whole egg white in a pin-stirrer compared with treated egg white fluid gels produced in the vane geometry of a rheometer. Points represent an average of three repeats, error bars show +/- 1StD.

Egg white fluid gels produced from whole egg white in pin-stirrers showed potential with suitable rheological properties for use in a reduced fat mayonnaise. However, the particle sizes produced here are potentially large enough to be sensed within the mouth. There is potential, however, to develop processing parameters to reduce the size of particles produced through reducing the heating rate within the pin-stirrers or increasing the shear rate.

6.4. Conclusions

Production of WPI particles for redispersion through spray drying of heat-denatured protein produced on a pilot scale spray dryer has been shown to produce particles of similar properties to those produced at lab scale. Conditions were kept as similar as possible between

the two processes, with inlet temperature being kept constant, feed rate and aspirator controlled to produce a dry powder with an outlet temperature comparable to that from lab scale production. This was achieved allowing a fourfold increase in the rate of production. The production of egg fluid gels from whole egg white using a continuous throughout pin-stirrer device showed potential also for the scale up of sheared gelation for the production of egg white fluid gels. Use of whole egg white makes this a more viable and efficient option for production of fluid gels.

6.5 References

GABRIELE, A. 2011. Fluid Gels: formation, production and lubrication. University of Birmingham.

GARREC, D. A. & NORTON, I. T. 2012. Understanding fluid gel formation and properties. Journal of Food Engineering, 112, 175-182.

GARREC, D. A. & NORTON, I. T. 2013. Kappa carrageenan fluid gel material properties. Part 2: Tribology. Food Hydrocolloids, 33, 160-167.

THYBO, P., HOVGAARD, L., ANDERSEN, S. K. & LINDELØV, J. S. 2008. Droplet Size Measurements for Spray Dryer Scale-Up. Pharmaceutical Development and Technology, 13, 93-104.

CHAPTER 7.
Conclusions and future work

This thesis aimed to develop understanding of protein fluid gel production and their properties. Rheology and tribology were used to characterize these. Tribology was used as it has previously been related to perception of creamy textures associated with full-fat products. Proteins are seen as desirable ingredients in foods, thus replacement of fat with proteins is of benefit to Bakkavor offering reduced fat alternatives.

This was achieved by production of fluid gels from egg white and WPI. Egg white and WPI fluid gels produced by sheared gelation were used to investigate the influence of pH on fluid gel properties. WPI was then used to investigate a new method of producing a dry powder of protein fluid gel particles with influence of pH and salts on properties of these particles investigated. Properties of emulsions stabilized by protein particles produced by spray drying was investigated to further understand the potential of these particles for use in reduced fat products. The properties of these were compared with a full fat mayonnaise and commercially available Simplesse™.

7.1. Conclusions

- **Egg white can be used as a feedstock for preparation of protein fluid gels.**
  Egg white fluid gels have been produced from sheared gelation in the cup and vane geometry of a rheometer; as well as a continuous through-put pin-stirrer. Fluid gels were produced by heating and cooling of egg white solutions under shear. For both the batch and continuous through-put production suspensions of gelled particles in a non-gelled continuous phase was produced. These fluid gels showed shear thinning rheology. Egg white fluid gels had anisotropic particles with a broad size distribution <500µm produced at native pH.

- **pH of production influences stability of egg white and WPI fluid gels.**

  For WPI fluid gels produced at pI showed sedimentation of particles within 24 hours of production. For egg white fluid gels produced at pH 4.5 some sedimentation was observed over 24 hours post production. For both egg and WPI no sedimentation was observed for fluid gels produced at pH 3.5 or pH_{native}. This sedimentation is contributed to by the reduced electrostatic charge of particles produced at these pH this leads to a reduction in inter-particle electrostatic repulsion.

- **pH of egg white and WPI fluid gel production influences particle size.**

  Fluid gels produced at pI for WPI and pH 4.5 for egg white produce the smallest particle size of the three pH tested with a bimodal size distribution with peaks at 0.2 µm and 0.9 µm. Due to reduced electrostatic repulsion between protein molecules at these pH. The Size distribution of particles produced at thes pH was narrower than for fluid gels at the other pH tested.

- **Particles produced at pI of WPI aggregate giving a greater effective particle size.**

  Particles produced at the pI for WPI and pH 4.5 for egg were shown to aggregate. These particles had the smallest primary particle size of the pH tested, however these were shown by light microscopy to aggregate into larger particles. This is due to reduced electrostatic repulsion between particles at these pH.

- **Viscosity of protein fluid gels correlates with Quiescent gel elastic modulus**

  Quiescent gel elastic modulus was used to represent the relative properties of particles in fluid gels. From this it was shown that viscosity of fluid gels correlated with the elastic modulus of the quiescent gels. Increased particle modulus increases the force required to deform particles as the flow past one another.

- **Particle aggregation increases friction in the mixed regime of lubrication.**

  Increased friction in the mixed and boundary regimes of lubrication were shown for egg and WPI fluid gel particles that were shown to aggregate into Both egg and WPI fluid gels showed much greater friction values in the boundary and mixed regimes of lubrication. This is due to the increased effective particle size due to aggregation of particles. As these larger particles are entrained into the contact greater deformation of the particle and disc is required increasing friction. .

- **pH influences degree of WPI aggregation through denaturation and spray-drying process.**

  With increasing pH increased loss of soluble protein content was shown for WPI through processing for the three pH tested. This loss of solubility is attributed to particle production, thus with decreasing pH and increase in particle production is shown through denaturation and spray drying.

- **pH influences WPI particle size produced through denaturation and spray-drying process.**

  WPI particles produced by spray drying at [H 6.5 had a modal size of 100 µm, with those produced at pH 5 (pI) having a bimodal size distribution with peaks at 1 µm and 10 µm. Those produced at pH 3.5 had an average size of 22.9 µm.

- **pH through processing influences protein tertiary structure.**

  FTIR measurements showed that pH of processing influenced the tertiary structure of WPI through processing. This explains the differences in particle size and loss of solubility observed through processing with changing pH.

- **Particle size distribution is influenced by $CaCl_2$, NaCl or KCl through processing.**

A Bimodal size distribution of particles is produced in the presence of these salts at 100mmol, compared to the mono-modal size distribution for particles processed in diwater. Electrostatic shielding by the salts producing smaller particles as the aggregation rate is increased as there is reduced intermolecular repulsion.

- **The Dispersion of WPI particles in salt solutions does not influence suspension rheology.**

When WPI particles produced by denaturation and spray drying are dispersed in solutions of KCl, NaCl or $CaCl_2$ at concentrations <100mmol no change in suspension viscosity is observed. This shows that particle properties are set during the spray drying process, not during dispersion. This is promising for their use in hard water areas and foods containing salts.

- **Both protein particles and soluble protein are surface active.**

Both the dispersed phase and continuous phase of fluid gels produced by spray drying were shown to reduce the interfacial tension between water and sunflower oil. The whole system with continuous phase and dispersed phase was shown to reduce the interfacial tension more than either of the individual components.

- **When WPI concentration is maintained at 20% in the aqueous phase no change in viscosity is observed with increasing oil concentration up to 40% oil.**

WPI particle stabilized emulsions show no change in viscosity with increasing oil concentrations 5-40%, this shows the particles to be contributing to structure in a

similar way to oil droplets. Particles will displace oil droplets in the structure with oil droplet size and WPI particle size overlapping.

- **Emulsion stabilized by spray dried particles have a higher viscosity than those stabilized by Simplesse at 20%.**

Emulsions stabilized by spray dried WPI particles showed greater thickening than the commercially available simplesse^{TM}. At $0.1s^{-1}$ the viscosity of 20% oil emulsions stabilized by 20% spray dried WPI were 4 orders of magnitude higher than for those stabilized by 20% Simplesse. This difference in viscosity is due to the increased effective phase volume of the particles produced by spray drying. Spray dried particles behave as gel-like particles structuring water within the particles. Whereas simplesse particles are dewatered reducing their effective phase volume. This increased viscosity of WPI particle produced in this thesis is beneficial as it means reduced quantities of protein are required to give the desired texture, saving on raw materials.

- **5% oil emulsions stabilized by SD-WPI are comparable with a full- fat mayonnaise.**

A 72.5% oil full fat mayonnaise was used to understand how reduced fat emulsions stabilized by particles produced compare. Emulsions with 5% oil and 20% SD-WPI in the aqueous phase showed good lubricating properties similar to that of the full fat mayonnaise. However, this requires further confirmation with sensory tests.

7.2. Future work

- **Investigate the potential for weak gels/flowable gels.**

  There is currently little work in the literature covering the potential for low concentration gels that flow under shear gels as a functional ingredient. By this I mean weak quiescently set gels that flow under shear stress. There is a gap in the literature around the use of weak gels to thicken reduced fat products. The recovery of viscosity in such systems requires research as the structure of a quiescent gel will be broke down under shear and is unlikely to recover in the timescales relevant for spooning and spreading of products.

- **Further look at how processing parameters will influence properties of fluid gels at individual pH.**

  Throughout this thesis processing parameters were kept constant changing only pH to give a direct comparison. However, further research into how the processing parameters can be manipulated to optimize particle and suspension properties requires further investigation. Especially for egg fluid gels produced at pH 3.5 with overheating potentially contributing to the observed low phase volume. For WPI particles produced through heat denaturation and spray drying, influence of changing protein concentration spray dried was not investigated however if this follows similar trends to fluid gel production this will enable manipulation of particle properties.

- **Sensory studies to back up the analytical findings.**

  This work requires sensory work for the systems used within this project to confirm that the correlation previously observed for soft tribology and rheology is observed for these systems.

- **Potential for use of this technique with alternative proteins? Potential for use to spray dry egg white. Alternative proteins.**

This technique for production of soft gelled protein particles has been shown to be successful with WPI, however its potential for alternative protein sources has not been investigated. Further work should include investigating the potential of this method to produce functional proteins from other sources. This could include egg proteins, which would enable the incorporation of a texturizing agent to mayonnaises without changing the ingredients present in the product, also the potential for vegetable or legume particles for use in vegetarian and vegan products to cater for the changing demands of consumers.

- **Interactions of these systems with other ingredients in more complex foods.**

Another important factor that requires further research is the interactions of these particles with other ingredients in more complex systems. This is important if these systems are to be used in real food products as most food products are complex mixtures of ingredients. Ingredients that may present issues include onions as these will leach proteases into the products. Proteases are enzymes that work to break down proteins. The resistance of these particle to breakdown by proteases will be essential if they are to work in coleslaws and similar foods.

- **Confirm these results can be replicated using different acids.**

Further work should include work to confirm that these same methods for the production of WPI particles can be achieved using alternative acids. If this can be achieved then this method of production will have a wider scope for uses of the end products. This is due to the strong vinegar flavour of acetic acid. Using acetic acid to

adjust the pH while useful for production in mayonnaises which typically contain vinegar will impart undesirable flavours on foods which do not contain vinegar. Producing the same particles with alternative acids opens up the potential for these particles to be used in products like reduced fat yoghurts, thickened drinks and more.

- **Start with native WPI direct from cheese production, remove need to dry twice**

It would be of merit to further investigate the production of these particles starting with raw WPI instead of starting with a dry powder as has been shown in this thesis. The capability of this would remove excess processing from the production of these particles. Enabling their production to only add a pH adjustment and heating step into the current methods used for the production of WPI powder.